THE THERMAL PERFORMANCE OF COURTYARD HOUSES

A Study of the Relationship between
Built Form and Solar Radiation
in the Climate of Egypt

MORAD ABDEL KADER A. MOHSEN

B.Sc. (Arch.) Cairo
M.Sc. (Arch.) Cairo

Ph.D. THESIS

Department of Architecture
University of Edinburgh

1978

DECLARATION

This thesis has been composed entirely by myself and the work reported is my own.

Morad Abdel Kader A. Mohsen

CONTENTS

PART TWO : THE MODEL

PART THREE : THE INVESTIGATION

ACKNOWLEDGEMENTS

I would like to express my gratitude to Professor C B Wilson, Professor of Architectural Science in the Department of Architecture, University of Edinburgh, for his supervision, guidance and support throughout the study.

My thanks are due to Dr F Smith, Post Doctoral Research Fellow in the Department of Architecture, for his help in reading part of the manuscript and for his useful comments.

I am grateful to my fellow research students in the Department for their helpful discussions and suggestions.

I am also grateful to the advisory of the Edinburgh Regional Computing Centre for the assistance I received during developing and operating the computer programs.

My deep thanks are due to Mrs L Halstead for her expert typing.

My sincere gratitude to my wife who shared my years of study in Edinburgh.

ABSTRACT

This thesis is concerned with the study of aspects of the thermal performance of the courtyard house form in hot dry climates. It attempts to establish the relationships between the variation of the parameters of the form and its corresponding thermal performance. Solar radiation is considered the main source of thermal excitation in the physical model upon which the study is based. The parameters of the form which are included in the model are : geometrical (proportions, size and orientation) and physical (reflectivity of its surfaces).

The investigation is carried out by developing a mathematical model which simulates the interactions taking place in the physical model at the external surfaces of the courtyard's envelope. It enables the generation of detailed data of the irradiation load on the surfaces. Using Cairo as an example of a typical hot dry region, the model is implemented on a computer and used to systematically evaluate the initial and final irradiation load on the form's surfaces.

The analysis of the investigation leads to an identification of the effect of each of the geometrical and physical parameters on the irradiation load and of the ranges within which these parameters significantly affect the irradiation load. Satisfactory thermal design for hot dry climates calls for minimizing the irradiation load in summer and maximizing it in winter. On this basis, a systematic assessment of the consequences of changing any parameter on the departure from the optimum form can be carried out.

NOTATION

Symbol		Units
	Form's Geometry	
A_i	Area of surface i	m^2
A_T	Area of the top opening of the courtyard form	m^2
A_G	Area of the ground surface of the courtyard form	m^2
H	Height of the courtyard form	m
P	Perimeter of the courtyard form	m
L	Length of the courtyard form	m
W	Width of the courtyard form	m
R_1	Ratio of the perimeter to the height of the form = $\frac{P}{H}$	dimensionless
R_2	Ratio of the width to the length of the form = $\frac{W}{L}$	dimensionless
R_3	Ratio of the area of the top opening to the area of the ground surface of the form = $\frac{A_T}{A_G}$	dimensionless
ϕ	Angle of orientation of the form (angle between the longitudinal axis of the form and the east direction measured anticlockwise)	degrees
	Sun's Position and Times	
a, b and c	Direction cosines of the sun's rays	
$\vec{l}$, $\vec{m}$ and $\vec{n}$	Unit vectors in the x, y, and z directions respectively	
$\vec{s}$	Unit vector parallel to the sun's rays	

Symbol		Units
ψ_1, ψ_2 and ψ_3	Angles between a sun's ray and the positive directions of x, y and z respectively	degrees
d	Solar declination angle	degrees
ξ	Sun's zenith angle	degrees
θ	Sun's altitude angle	degrees
l	Latitude of the locality	degrees
h	Hour angle	degrees
h'	Hour angle	radians
h_a	Absolute value of hour angle	radians
h_R	Hour angle at sunrise	radians
h_S	Hour angle at sunset	radians
h_{sa}	Absolute value of hour angle at sunset	radians
h_N	Absolute value of hour angle at noon	radians
e_t	Equation of time	minutes
t_L	Longitude correction	minutes
t_c	Clock time	hours
t_a	Absolute value of time measured from noon	hours
t_{la}	Local apparent time	hours
t_R	Time of sunrise measured from midnight (local apparent time)	hours
t_S	Time of sunset measured from midnight (local apparent time)	hours
t_{sa}	Absolute value of sunset time measured from noon	hours

Symbol		Units
	Solar Radiation	
I	Intensity of solar radiation	W/m^2
I_{sc}	Solar constant (1395 W/m^2)	W/m^2
I_{as}	Apparent solar constant = 0.85 r I_{sc}	W/m^2
r	Ratio of solar radiation intensity outside the earth's atmosphere to the solar constant = $\frac{I_{on}}{I_{sc}}$	dimensionless
I_{on}	Intensity of solar radiation at normal incidence outside the earth's atmosphere	W/m^2
I_{oh}	Intensity of solar radiation incident upon a horizontal surface outside the earth's atmosphere	W/m^2
I_{Dn}	Intensity of direct radiation at normal incidence	W/m^2
I_{Dh}	Intensity of direct radiation incident upon a horizontal surface	W/m^2
I_{dh}	Intensity of diffuse radiation on a horizontal surface	W/m^2
I_{Dv}	Intensity of direct radiation on a vertical surface	W/m^2
I_{dv}	Intensity of diffuse radiation on a vertical surface	W/m^2
I_{Th}	Intensity of total radiation incident upon a horizontal surface	W/m^2
T_{oh}	Daily total solar radiation on a horizontal surface outside the atmosphere	W/m^2

Symbol		Units
$\overline{T_{oh}}$	Monthly average of daily total solar radiation on a horizontal surface outside the atmosphere	W/m^2
T_h	Daily total solar radiation received on a horizontal surface at the earth's surface	W/m^2
$\overline{T_h}$	Monthly average of daily total solar radiation received on a horizontal surface at the earth's surface	W/m^2
D_h	Daily direct radiation received on a horizontal surface at the earth's surface	W/m^2
$\overline{D_h}$	Monthly average of daily direct radiation on a horizontal surface at the earth's surface	W/m^2
d_h	Daily diffuse radiation on a horizontal surface at the earth's surface	W/m^2
$\overline{d_h}$	Monthly average of daily diffuse radiation on a horizontal surface at the earth's surface	W/m^2
$\overline{K}$	Monthly value of cloudiness index = $\frac{\overline{T_h}}{\overline{T_{oh}}}$	dimensionless
f_d	Ratio of diffuse to total radiation on a horizontal surface = $\frac{\overline{d_h}}{\overline{T_h}}$	dimensionless
τ_D	Transmission coefficient for direct solar radiation = $\frac{I_{Dh}}{I_{oh}}$	dimensionless
τ_d	Transmission coefficient for diffuse solar radiation = $\frac{I_{dh}}{I_{oh}}$	dimensionless
A	Atmospheric extinction coefficient	dimensionless

Symbol		Units
B	Ratio of instantaneous diffuse radiation on a horizontal surface to the instantaneous direct normal solar radiation = $\frac{I_{dh}}{I_{Dn}}$	dimensionless
m	Air mass = cosecant of the angle of solar altitude θ	dimensionless

Radiant Exchanges

F_{ij}	Configuration factor from surface i to surface j	
F_{GW}	Configuration factor from the ground surface to the walls' surfaces of the form	
F_{WG}	Configuration factor from the walls' surfaces to the ground surface of the form	
F_{GR}	Configuration factor from the ground surface to the hypothetical roof of the courtyard form	dimensionless
B_{ij}	Absorption factor at the surface j to energy received from surface i	dimensionless
B_{GW}	Absorption factor at the walls' surfaces to energy received from the ground surface	dimensionless
B_{WW}	Absorption factor at the walls' surfaces to energy received from the walls' surfaces	dimensionless
ρ_i	Reflectivity of the surface i to the short-wave radiation	dimensionless

INTRODUCTION

The courtyard house is a characteristic traditional domestic building in many countries in hot dry regions (Dunham, 1960). Examples of the traditional courtyard house in Arab countries show that house design was conditioned by the integration of social, cultural, technical and environmental factors. Variations of designs were introduced to meet successive changes of some of the factors, nevertheless, the underlying concept of arranging a house's spaces around an open space to solve climatic problems was continuously maintained for centuries.

At present, courtyard houses are still being built in some Arab countries, like Tunisia and Lybia, but, as a contemporary form, it has almost disappeared from urban areas in Egypt (El-Dars and Said, 1972). A turning point in its evolution in Egypt took place at the beginning of the nineteenth century, when adoption of western concepts was considered the ideal solution for problems created by contact with western culture (Fathy, 1972). Since then, a complete disregard for local climatic conditions has often been reflected in buildings. Some of the socio-cultural factors have also been weakening: with continuing urbanization, land has become scarce, and consequently, the sizes of houses have been greatly influenced.

The suitability of the courtyard house for the climate of hot dry regions suggests the desirability of reintroducing it in the urban areas from which it has disappeared though perhaps in modified form. The present work concentrates on the thermal performance of courtyard house forms. Its objective is to obtain precise understanding of the climatic implications for design as a prerequisite for systematizing the process of designing courtyard houses.

The main concern is directed towards establishing an approach which allows detailed investigations to be carried out into the effect of the geometrical and physical parameters of the form on the irradiation load on its surfaces. It is seen as a subsystem of a physical system which describes the interaction between the external climatic conditions and the thermal environment of the indoor space passing through the envelope of the courtyard.

In order to carry out the investigation, a mathematical model is constructed to simulate the interaction between solar radiation and the geometrical and physical parameters of the form. The input of the model includes a wide range of combinations of the form's parameters and the data of the sun's geometry and solar radiation. The outcome of the model is a systematic evaluation of the irradiation load on the form's surfaces. In order to carry out the lengthy computations which are involved, the mathematical model is implemented on a computer.

The thesis defines the effect of the geometrical and physical parameters of the form and identifies the ranges within which the irradiation load is significantly influenced by the changes of these parameters. Its aim is to illustrate the effect of manipulating the geometrical and physical parameters of the form on the control of the irradiation load on its surfaces. The results of the study of the relationships between geometry and radiation are used to generate a range of alternative satisfactory solutions which correspond to an acceptable range of thermal performance.

The thesis is divided into four parts : in Part One, an introductory chapter furnishes background material, describes the problem and suggests the approach. The second chapter provides a descriptive account of the processes involved in the thermal performance of courtyard house form. It is concluded by some considerations that have guided the investigation.

Part Two is concerned with developing a mathematical model for assessing the irradiation of courtyard's surfaces. Chapter III discusses the geometrical description of both the sun's position in the sky and the courtyard's geometry. The two sets of descriptors are related together to determine the exposure of the surfaces to the sun. In Chapter IV a method is developed to derive from the available data, information about solar radiation intensities that are used in assessing irradiation loads on surfaces. Chapter V deals with the computer programs:

description of the programs accompanied by flow charts are included.

In Part Three, Chapter VI is an analysis of the results concerning the first stage of the model which deals with the initial irradiation load on surfaces. Chapter VII is devoted to the study of further aspects of thermal performance. Thermal exchanges at the outside surfaces of the courtyard's envelope are examined and the final irradiation load on surfaces is discussed.

Part Four is a concluding one that discusses the outcome of the work and suggests its application.

The thesis is supplemented with three appendices: one includes some mathematical expressions complementary to the text, another concerns the climatic data of the region under consideration. Appendix 3 is a historical review of the courtyard form's application in domestic architecture in Egypt.

PART ONE : THE PROBLEM

CHAPTER I

BACKGROUND OF THE STUDY

I.1 General Introduction

Built forms are human products intended to provide multifunctional frames for human activities. The functions which are to be performed by such frames are conditioned by environmental, spatial, technical and socio-cultural considerations. Environmentally a built form may be viewed as an intermediate object between environment and man, its function being to control the former in favour of the latter. Thermal, atmospheric, sonic and luminous factors are the main aspects of physical environment. They are to some extent interrelated, yet for the purpose of analysis, each of them can be considered separately. The present study is focused on the thermal performance of built forms in the context of housing design in hot dry regions with Egypt taken as an example.

People in hot dry regions have, over the centuries, attempted to exploit the local resources within the means at their disposal in order to solve the thermal problems facing them. Successive processes of trial and error over long periods of time have resulted in the development of some concepts concerning the thermal performance of built forms. These evolving concepts were influenced by changes in people's requirements induced by changes gradually taking place in their societies.

The progress in means of communications has helped in the exchange of ideas between people of different backgrounds. Over the years, the influence of western culture has grown in the less developed countries; people of these countries, impressed by new technology, have tended to admire imported ideas and methods and to discard their own (Fathy, 1972). The effect on architecture has been profound; design problems have been approached with ideas and concepts which were originally formulated by European and American architects in entirely different contexts (Cornell, 1957). The potentials of traditional solutions have been neglected and no attention has been paid towards developing them to cope with the rapidly changing requirements of the era.

The concept of the courtyard house has been developed in hot dry regions. The potential of this traditional concept to solve climatic problems is evidently manifested in the examples of domestic architecture of these regions. It is not intended in this study to examine the few existing examples of courtyard houses in Egypt, analysing how their designs had met socio-cultural and climatic requirements within available technology then. However, a description of the traditional courtyard houses in Egypt is given in Appendix 3. The present study concentrates on investigating the thermal performance of the form with the ultimate objective of incorporating

systematically the thermal aspect with other aspects of design. A review of the existing material concerning climatic considerations in courtyard house design is needed to initiate the study.

1.2 Climatic Considerations in Courtyard House Design : Review of Existing Material

The principal problem confronting a designer in hot dry regions, is how to reduce heat loads imposed on the internal spaces of built forms. Discussions of ways and means of solving such a problem often refer to the potentials of the concept of courtyard form for providing a satisfactory basis for house design in such a climate (Saini, 1962). Some references tend to list, in fairly general terms, principles of design in hot dry climates concerning both the geometrical properties of built forms, and the qualities of materials which ought to be selected (Atkinson, 1952, 1953, Cornell, 1957, Van Straaten, 1964, U.N., 1971 and Saini, 1973), others discuss the subject at some length (Oakley, 1961, Olgyay, 1963, Tropical Advisory Service, 1966, Lippsmeier, 1969 and Givoni, 1969).

Regarding the geometrical properties of a built form, recommendations have been directed towards how to protect the form's surfaces and its surroundings from intense solar radiation and hot dusty winds; the effect of shading is to bring surfaces temperatures much closer to that of air (Saini, 1973). A discussion of these recommendations is presented in the following paragraphs.

The minimization of a built form's surfaces exposed to solar radiation and hot air, can be achieved by using compact structures that accommodate under one roof as many spaces as possible. Internal courtyards and a compact layout for a group of forms would provide mutual shading between surfaces with the consequence of reducing the thermal load on them (Tropical Advisory Service, 1966). In a monograph on "Climate and House Design" (U.N., 1971), compact courtyard planning is advocated on the ground that if the courtyard's size is kept small enough to achieve shade during the day, it will allow less thermal impact and more heat dissipation from surrounding indoor spaces. In general, it is suggested that the courtyard's dimensions in plan should not exceed its height (Tropical Advisory Service, 1966).

In a study of the impact of the external thermal forces on built forms, Olgyay (1963) considered boxlike forms having the same volume and type of construction. His aim was to find, for a particular climatic setting, the optimum form which loses the minimum amount of heat in winter and gains the least amount

in summer. This condition is seen to be satisfied when there is an inverse relationship between thermal impacts and the sizes of the form's sides. In a hot dry climate he has shown that the optimum form is a rectangle in plan having a proportion of 1:1.3, the length being in the east-west direction. He concluded :

> " In the hot arid regions under winter conditions the house could have an elongated form but it is returned to a squarish shape by strong summer stresses. However by cutting one part of the cube and filling the hole with shade (walls, trees, trellis) and with cooled air (evaporative cooling, lawn, trees, pool, fountain effect), the environment is changed for the better ..... Accordingly the basic plan changes here to an inward looking scheme."
>
> (Olgyay, 1963)

At the scale of town structure he recommended closely grouped houses around a courtyard. His study illustrates how far built forms are influenced by thermal forces; however, since it was not intended in his study to investigate specific forms, the courtyard form was mentioned just as a device for improving thermal conditions, no quantitative evaluation concerning the effect of changing courtyard's geometrical properties being discussed. Some information of this sort has been presented in a report on climatic design in Islamabad (Tropical Advisory Service, 1966). Comparison

between solar penetration in four courtyards having different sizes revealed that the courtyard's height is the most important factor: for a given courtyard, increasing the height from one storey to two causes a decrease of two or three hours of solar penetration. It is recommended that overhead shading devices are required in courtyards over 18 m^2 in area for improving their thermal performance. Such devices might take one of three forms: fixed vertical louvers, closable louvers and removable shadings. Spacing in the first one should be designed to allow the night radiation from the courtyard's surfaces. Closable louvers are more effective in cutting down the sun's rays but give a consequent reduction in lighting levels. The third type allows full solar penetration in winter (Tropical Advisory Service, 1966). It is suggested that the roof of the courtyard house should be surrounded by a parapet at the outer edges to restrict heating the air layer above the roof by warmer external air; and the roof should slope towards the courtyard to channel the air cooled by night into the courtyard space.

Orientation of built forms with respect to solar radiation is an important factor in controlling heat gain. Some studies have been directed towards recommending an optimum orientation that allows for lowest heat load to be received by a built form's surfaces (Buchberg and Naruishi, 1967, Olgyay, 1967 and Danby, 1973). Buchberg and Naruishi (1967) have

indicated with detailed calculations that, for latitude 37°N, the orientation in which the long walls of a boxlike built form are perpendicular to the north-south axis realizes the minimum solar irradiation input in summer and the maximum in winter. Olgyay (1967) has found that for latitude 40°N, the optimum case of orientation applies when the longitudinal axis of a built form lies at about 18° east of south. Danby (1973) refers to the work done by Kuba in which he has shown that a deviation of twenty degrees off a recommended east-west axis does not produce a corresponding increase in the total solar heat load.

Need for ventilation is not so critical in deciding upon orienting built forms because of the hot air during day time, nevertheless, ventilation during evening and night requires the consideration of orientation in order to improve ventilation conditions while satisfying the primary consideration of radiation (Givoni, 1969). The effect of orientation of the courtyard's surfaces on the mutual shading taking place between them has not been studied.

Since windows are critical elements in the process of heat flow to indoor spaces even when shaded against radiation and closed against hot air, it has been stressed that careful attention must be paid to determining their size (U.N., 1971). Ventilation conditions depend mostly on the windows' location: if some windows are placed at low level and others at high

level, air movement can be induced. Therefore, it is desirable to locate small windows properly so as to maintain efficient ventilation when opened, yet Givoni (1969) advises connecting indoor spaces to courtyard space through large openings protected by movable shutters so that by opening them, the interior might be cooled rapidly.

The second set of recommendations concerns the control of heat flow through the structure of the built form in order to keep the inside temperature as near as possible to the minimum outdoor air temperature and not allow it rise to the maximum outdoor air temperature in the afternoon (Atkinson, 1950). Colours of external surfaces exposed to the sun affect the absorption of incoming solar radiation; dark colours should be avoided. White painted surfaces cause a considerable reduction in heat gain (Givoni, 1969), on the other hand they may cause undesirable glare.

Heavyweight construction has a great advantage in a hot dry climate owing to its relatively high heat-storage capacity. Experiments have shown an inverse relationship between the range of diurnal variation in indoor air temperature and the product of heat capacity and overall resistance of external walls (Richards, 1957). The time elapsing between the occurrence of maximum temperature in and out depends on the thickness and density of the material used. Relationship between time lag, thickness and densities of materials is represented in a chart (U.N., 1971) which enables a choice of

the values of the materials' properties that produce a specific value of time lag. Determination of the required value of time lag depends on the time of occupation of indoor space and on daily variations in outdoor air temperature and in exposure to solar radiation. It is recommended that spaces used in day time should have a minimum of 8 hours and a maximum of 14 hours time lag (U.N., 1971). An extra improvement could be achieved if these spaces were helped to cool off rapidly at night through a suitable ventilation arrangement (Richards, 1957). For spaces used at night, less heavy construction is more desirable. Investigation undertaken by Givoni (1969) has shown the effectiveness of applying a layer of insulating material on the external side of heavy-weight structures.

Studies concerning the properties of building materials and their thermal performance constitute most of the work that has been done in the field of building research in a hot dry climate. The established detailed knowledge in this field is of great help in studying the thermal performance of built forms. Regarding geometrical properties, it is clear from the foregoing review that the courtyard house form, although being described as a suitable solution in hot dry regions, has not been investigated to an extent which would clarify the interaction between its geometrical properties and the prevailing climatic conditions. There is a need, therefore, for a study which thoroughly examines such interactions in

order to establish the relationship between a courtyard form and its corresponding thermal performance.

I.3 Formulation of the Problem under Consideration

I.3.1 Thermal design objectives and criteria

The theme of the present work is a study of the thermal performance of courtyard houses under specific climatic conditions. The context of such study is viewed with regard to the presumption that one of the main tasks of any built form is to transform environmental conditions, which are often unsuitable for human life, to others more beneficial. Therefore, assessing a building's thermal performance requires the application of a criterion based on man's responses to the thermal stresses of his environment. A necessary but by no means a sufficient criterion is to maintain thermal equilibrium in man's body, i.e., a condition where heat lost to the environment must - on average - be equal to bodily heat production so as to maintain a certain range of temperature within which man's body can function. Owing to the flexibility of the body's metabolic and perceptual mechanisms, such a condition can be fulfilled when man is exposed to fairly wide variations of environmental conditions. However, it is only within a relatively narrow range that he feels thermally comfortable.

Thermal comfort is designated, according to ASHRAE (1968), as that condition of mind which expresses satisfaction with the thermal environment. Hence, the criterion adopted here for assessing the thermal performance of buildings is to reduce thermal stresses to such a level that strain in man is kept within the limits that enable human activities to be performed efficiently. In the following, some points regarding the concept of comfort are mentioned to help define the problem under consideration.

First : The sensation of comfort is affected by a combination of thermal factors: ambient air temperature, radiant temperature of the surrounding surfaces, air movement and moisture content of air. It is also influenced by the level of activity, since it affects bodily heat production and the type of clothing, since clothing modulates the effect of environmental stress. Besides,it is noticed that people acclimatize themselves to their environments so that those who are living in hot regions, for example, would prefer thermal conditions different from those required by others living in cold regions (Fanger, 1973), sex and age are also influencing factors in determining comfort sensation.

Second : Human beings are capable of tolerating a degree of flexibility in environmental conditions, so there is no point in trying to maintain a constant level of conditions in space or time claiming that it is the optimum level. On the contrary, studies have shown that a changing environment seems

to be essential for human satisfaction (Heron, 1957) since it produces a stimulating effect which would be missing in the case of monotonous environments.

Third : There is no way of measuring comfort sensation directly, but it is possible to employ a rating scale for judging the degree of comfort in a space (Hopkinson, 1964). Such judgements are subjectively based on each person's sensation, therefore, some form of statistical analysis must be applied in order to express environmental conditions preferred by a group of people.

I.3.2 Definition of the problem

From the foregoing, it is clear that precise determination of thermal comfort standards is neither possible nor even required, nevertheless, it is a first premise to acquire some information about the zone of thermal comfort so that the climate under consideration could be classified in terms of length, nature and severity of its seasons (Mahoney, 1969). In such a classification, the combined effect of climatic elements, namely, air temperature, solar radiation, longwave radiation, wind and moisture content of air should be considered. All these elements can be regarded as random variables since they are influenced by random factors such as cloud cover, cloud type, extent of air pollution, topography, height above sea level, proximity to water bodies, etc.

We shall consider a system consisting of outdoor climate on the one hand, a desirable indoor climate on the other, and a built form which is intended to transform the first to the second. It has been seen that the two ends of the system are only statistically predictable, therefore, it is not worth trying to quantify a built form's thermal performance precisely. It is more significant from the designer's point of view to study relationships between variations in built forms and their corresponding thermal performance. The present work will concentrate on this area of research. The aim is to illustrate these relationships in such a way that designers are helped in incorporating the climatic implications for design with other considerations which have to be accounted for in solving total architectural problems. Because of the complexity of the requirements to which built forms ought to respond, it is believed that the form of the outcome of this work should allow designers as much flexibility as possible in making their decisions.

I.3.3 The approach to the problem

Differentiation between cold and hot periods is essential for studying the thermal performance of built forms. Such differentiation would be made possible by testing some form of climatic data against some sort of indicator of human thermal comfort. Climatic data published by meteorological

stations are prepared from readings of instruments located away from any topographical features, since they have been intended to represent the general climatic conditions of the region they serve. Local climatic conditions often differ from regional data but the differences - although having some implications for final designs in each locality - are rarely significant as far as the preliminary assessment of climate is concerned.

The climate of Egypt is characterized by large diurnal variations in both air temperature and solar radiation intensity, consequently built forms are subjected to a marked periodic flow of heat in and out. Therefore, concerning differentiation between cold and hot periods, it is more realistic to consider the whole daily fluctuation of air temperature and solar radiation intensities rather than to distinguish between hot and cold parts of a single day. Daily values need to be chosen to represent each climatic element but the extreme recorded values are of no practical use because of their rare occurrence. As mentioned above in section I.3.2, the choice should be statistically based; that is by finding the probabilities that similar or worse conditions will occur on relatively few occasions during the period of observation, in addition, data should be selected from coincident values of the climatic elements (Van Deventer, 1971).

In view of the unavailability of such statistical analyses of climatic data for Egypt, the monthly mean of daily maximum and of daily minimum are chosen as two representative values for the whole month. For each month, an indication of the thermal stress can be obtained by comparing these two values with the comfort range prepared by Mahoney (U.N., 1971). He presents a table for comfort limits based on a consideration of three categories of annual mean temperature and four groups of relative humidities, which include the upper and lower limits for both day and night. Applying data for Cairo, a distinction is made between a hot season which includes May, June, July, August, September and October; and a cold season which includes December, January and February.

In the following study, investigations of thermal performance are undertaken for these two seasons. In the hot season the objective is to minimize heat load on built form, and in the cold one the objective is to maximize it. In order to carry out the investigations, it is required to determine the parameters of the form that influence thermal performance. As a preliminary to this, a qualitative study of the processes involved in the form's thermal performance is made.

CHAPTER II

DESCRIPTION OF THE THERMAL PERFORMANCE OF THE COURTYARD HOUSE FORM

II.1 General

A description of the processes involved in the thermal performance of the courtyard house form is given in this chapter in order to identify the parameters of the form upon which such processes depend.

First, it is useful to point out the characteristic qualities of the courtyard house form which distinguish it from boxlike forms. It encloses a void within it, an inner envelope composed of the courtyard's walls screens the sheltered house space from the open space of the courtyard. Its outer envelope (external walls and roof), like that of other built forms, constitutes the boundary for the house space and screens it from the open space outside the form. The total area of the two envelopes is greater than that of the outer envelope of a boxlike form having the same floor area. Most of the openings are located in the inner envelope and the form does not depend on the outer envelope for obtaining light and air. Accordingly, the clustering of forms is achieved by both retaining minimum spaces between them as streets and open spaces and by attaching them to each other on some sides. The attached sides are no longer outer envelopes, they are considered as internal partitions that separate between spaces in the collective form (figure II.1).

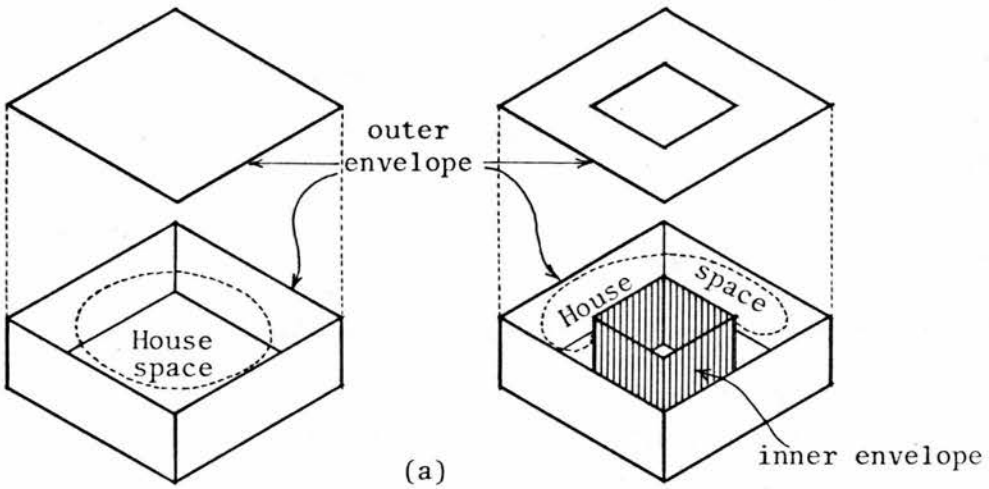

(a)

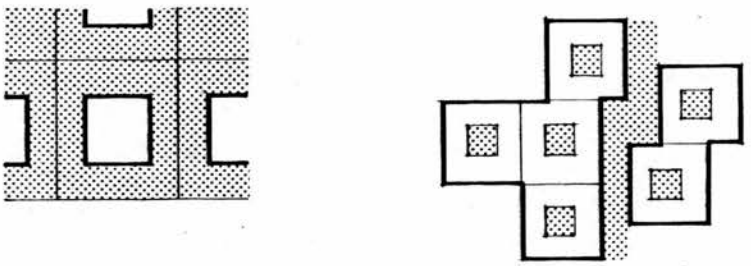

(b)

Figure II.1 Comparison between courtyard form and boxlike form

A cluster of courtyard houses comprises different kinds of spaces (figure II.2) that vary in the degree of closure : (a) indoor space is bounded by the inner envelope from one side and by the outer envelope from the other, it is covered by a roof, (b) internal open space (courtyard space) is surrounded by the inner envelope and is open to the sky. A part of it may be roofed forming a covered terrace, and (c) external open spaces are formed by the outer envelopes of the houses and open to the sky. They are more loosely defined than the internal courtyards and are joined together by streets.

Consider a site where a cluster of courtyard houses is to be built. The local climate is composed of various climatic fields such as temperature, radiation, wind, humidity and precipitation. After it is built, various degrees of modifications of such fields would take place in the previously mentioned kinds of spaces. Each space will possess a certain set of climatic fields that constitute its thermal environment. The following section illustrates the continuous thermal exchanges that take place in these environments (figure II.3).

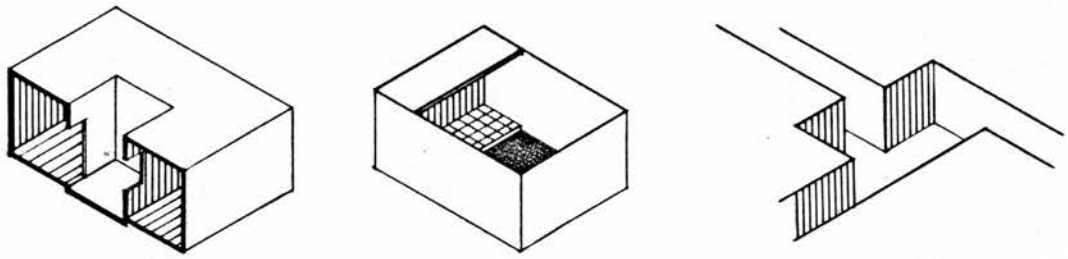

Figure II.2 The different kinds of spaces in a cluster of courtyard houses

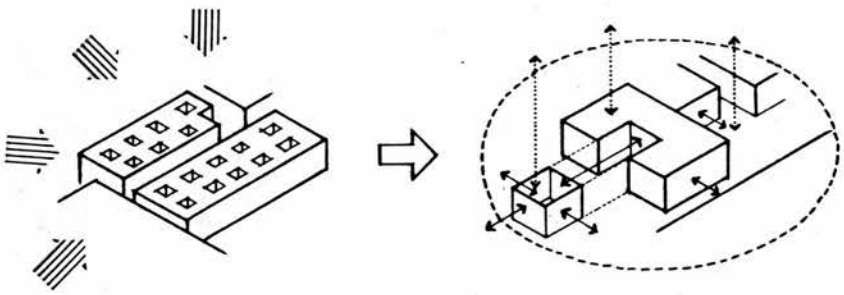

Figure II.3 The interaction among the thermal environments in a courtyard housing development

II.2 Description of the Interaction among the Thermal Environments in a Courtyard Housing Development

II.2.1 At day

In the early morning before sunrise, the outer surfaces of built forms are at their minimum temperature owing to the continuous emittance of long-wave radiation taking place all through the night to the sky. The outside air temperature too is at its minimum value. It is usual for the indoor temperature to be higher than the outside air temperature and in consequence, heat is flowing outwards. Just after sunrise, the rays make a small angle with the horizon, the effect on the surface of the ground is still minimal, consequently the rise in the outside air temperature is small and the outward flow of heat continues.

As the sun moves upwards in the sky, the intensity of its radiation becomes greater. The exposure of built forms to solar radiation varies with time, the sunlit surfaces are heated up, hence the flow of heat starts reversing its direction and heat flows inward. The outdoor temperature gradually rises above indoor temperature. It reaches a maximum in the early afternoon. Heat flows inward from shaded surfaces too. As far as the incidence of the sun's rays are concerned,the geometry of the courtyard house form comprises three kinds of planes :

1. The roof is a horizontal plane which receives solar radiation irrespective of the geometry of the form - provided that the surrounding forms are of uniform height - as follows :

(a) It starts receiving radiation in the early morning both directly from the sun and in diffuse form from the sky. Part of the radiation is reflected and the rest is absorbed by the surface.

(b) As the cold surface receives more and more radiation, the absorbed component causes its temperature to rise approaching the temperature of the adjacent air layer, and eventually exceeding it. Such an increase is dependent upon the absorption coefficient of the surface and the material of the roof.

(c) The recently heated surface exchanges heat in two directions: one with the external environment in the form of convective heat flow to the adjacent layer of air and in the form of long-wave radiation emitted to the sky (figure II.4). The convective flow depends on the instantaneous difference between the air temperature and the surface's temperature. It is augmented by air movement over the roof. The radiative flow depends on the surface's temperature and the sky's temperature, so its effect is not noticeable during the day. The other direction of heat flow is through the materials of the

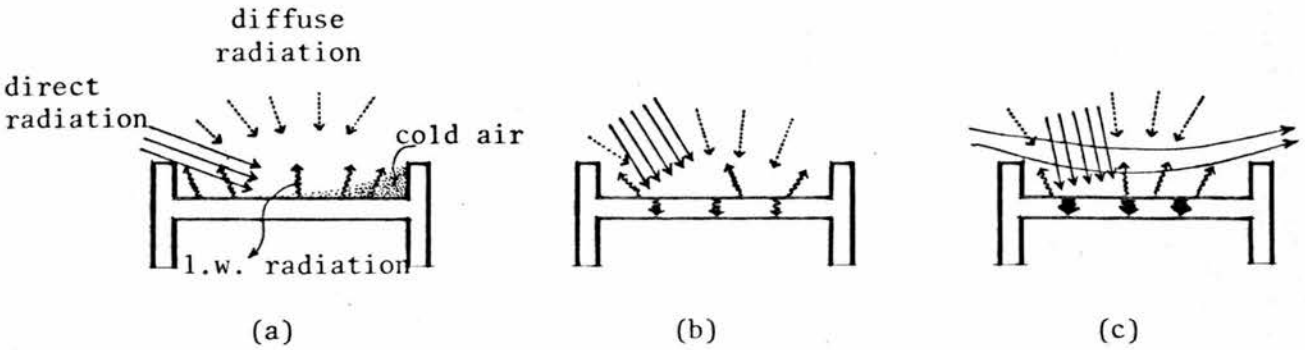

Figure II.4 Thermal exchanges taking place at the surface of a roof

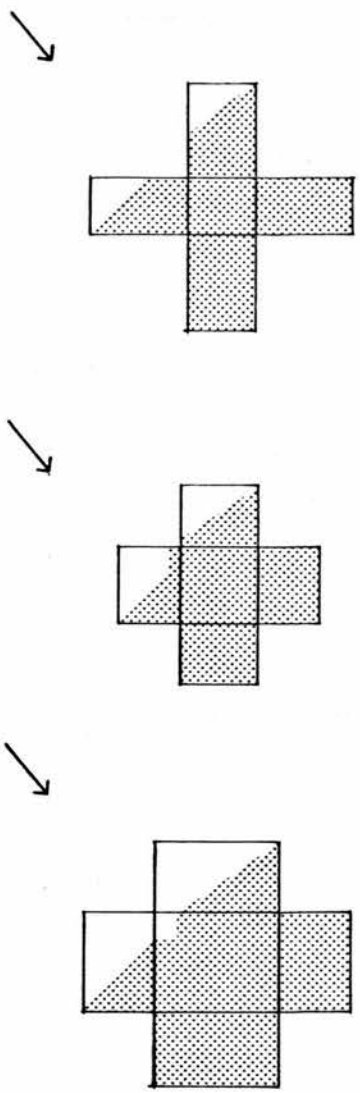

Figure II.5 The exposure of walls to the sun varies with the geometry of the form

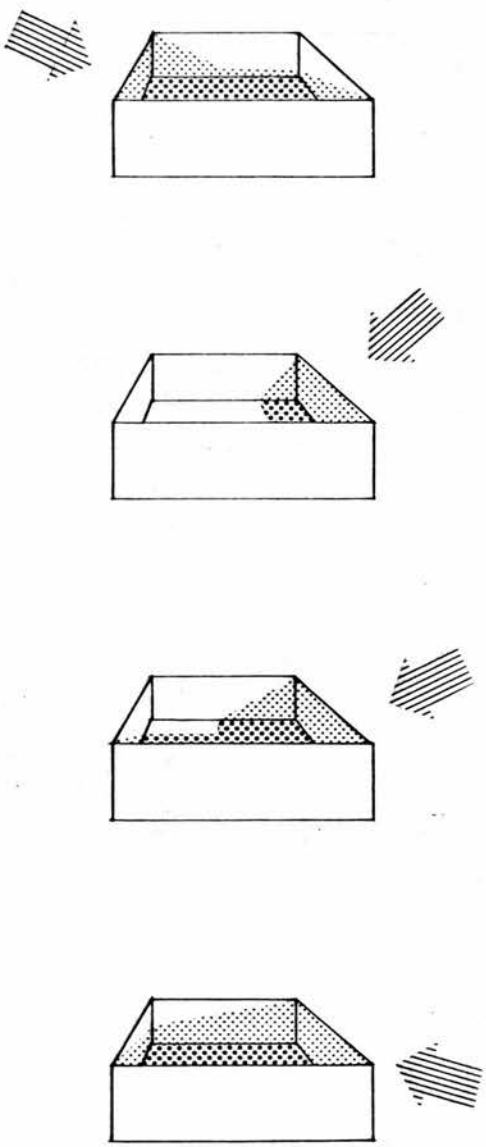

Figure II.6 The exposure of each wall changes with the movement of the sun

roof. This flow is influenced by the thermal capacities, thermal resistivities and thicknesses of the materials.

2. The walls surrounding the courtyard

The instantaneous exposure to the sun varies from one wall to another according to the geometry of the courtyard (figure II.5). The exposure of each wall changes with the movement of the sun. Some walls are probably in shade in the morning but are exposed to intensive radiation for a long period in the afternoon. Others receive most of the radiation in the morning and are protected afterwards (figure II.6). The wall surfaces exposed to solar radiation react differently as follows :

(a) Opaque surfaces absorb part of the incident direct radiation and diffusely reflect the rest according to the reflective coefficient of the surface which is a function of its colour and texture. Some of the radiation reflected by one wall is received by the others. Diffuse radiation coming from the sky contributes to the total radiation received by the walls. The amount of radiation absorbed by the surface of a wall elevates its temperature above the relatively low temperature of the air inside a courtyard. The heated surface loses some of its gained heat in one direction to the material of the wall; in the other direction the convective currents and the emission of long-wave radiation

to the colder surfaces and to the sky are the two channels of heat exchange (figure II.7). The flow of heat through a wall depends on its thickness and on the thermal capacities and resistivities of its materials.

(b) Transparent surfaces (Glass) allow a considerable portion of short-wave radiation to be transmitted to indoor space, another portion is absorbed and the rest is reflected. Transmission depends on the angle of incidence of the rays and the composition of the glass. Transmitted radiation elevates the temperature of indoor surfaces which in turn start emitting long-wave radiation. Owing to the glass's property of selective transmission, such radiation is not allowed to dissipate outwards. The accumulated heat causes the indoor temperature to rise. Heat gain can be considerably affected by the application of shading devices; when they are applied from outside some of the radiation is intercepted before striking the glass, part of it is reflected outwards and another part inwards while the rest is absorbed in the shading device. The absorbed component is dissipated both by long-wave emittance - without affecting the glass - and by convection with little effect on the glass. Eventually, a small fraction of the impinging radiation penetrates to the indoor space. When the temperature of the air inside a courtyard rises above

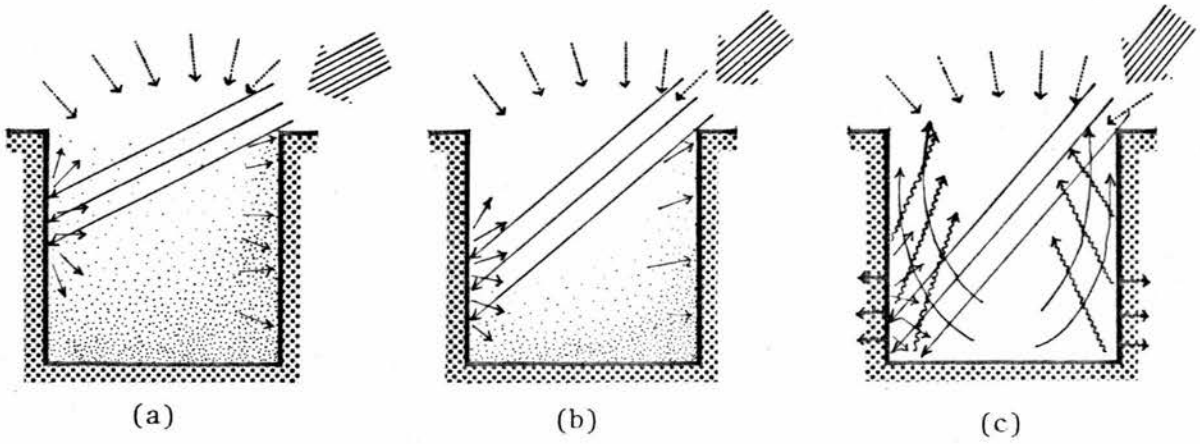

Figure II.7 Thermal exchanges taking place at the opaque surfaces of the courtyard form's walls

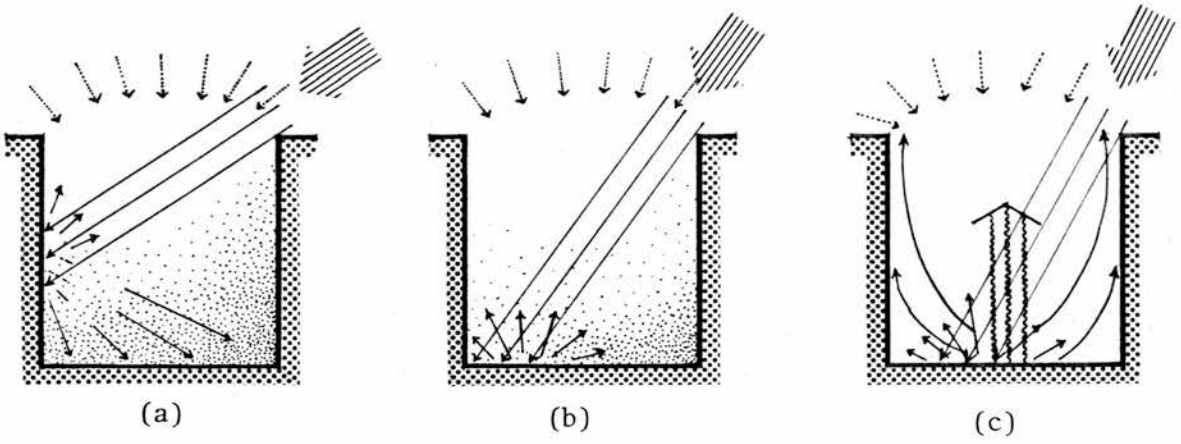

Figure II.8 Thermal exchanges taking place at the ground surface of the courtyard form

that of the indoor air, heat is conducted through the glass. The main parameter affecting the heat flow through the glass from air to air is its surface resistance which is low compared with solid walls. Opening the windows and the doors onto the courtyard during day time causes a flow of hot air to the indoor space and allows the penetration of solar radiation.

3. The ground

In the early morning the ground of a courtyard receives the diffuse radiation coming from the sky and from the surrounding walls by reflection. As the sun rises, the ground surface is more likely to receive direct radiation. This radiation is partially absorbed according to the properties of the surface: the lighter the surface's colour, the higher is its reflectivity and the greater the amount of radiation that might be reflected to the surrounding walls adding to their total amount of heat gain. The heated surface of the ground loses heat to the adjacent cold air layer. The rising heated air is replaced by relatively colder air until the temperature of the air inside the courtyard reaches that of the outisde air. The surface loses heat also by emitting long-wave radiation to the surrounding colder walls (figure II.8).

The duration of the ground's exposure to intense radiation is greater than that of any vertical wall, this accounts for the criticality of the treatment of its surface.

Planting of the ground plays two roles in the heat exchange processes taking place within the courtyard space. Green plants have low reflectivity compared with sand or paved ground. They absorb a great amount of radiation, and at the same time, give off water vapour during the process of transpiration. Consequently, they keep cool and assist in preserving the low temperature of the adjacent air. Pools and water bodies are also of great help in this regard; during the day,water evaporates causing a gradual increase in the relative humidity of the air, and a decrease in its temperature (figure II.9).

II.2.2 At night

After sunset and during the night the sky becomes much colder than the surfaces of the courtyard. Being exposed to the sky, these surfaces get rid of the previously absorbed heat through the emittance of long-wave radiation. Since there is no radiation coming from the sky at the time, the rate of net heat loss is greater than that during the day. Because of the relatively more intensive radiation received by the surfaces of roof and ground during day time, their contribution to heat loss is more significant. As the surfaces lose heat, the temperature of the adjacent layer of air gradually decreases. The cold air being denser than the relatively warm air in the courtyard tends to sink down; this process continues all through the night, and

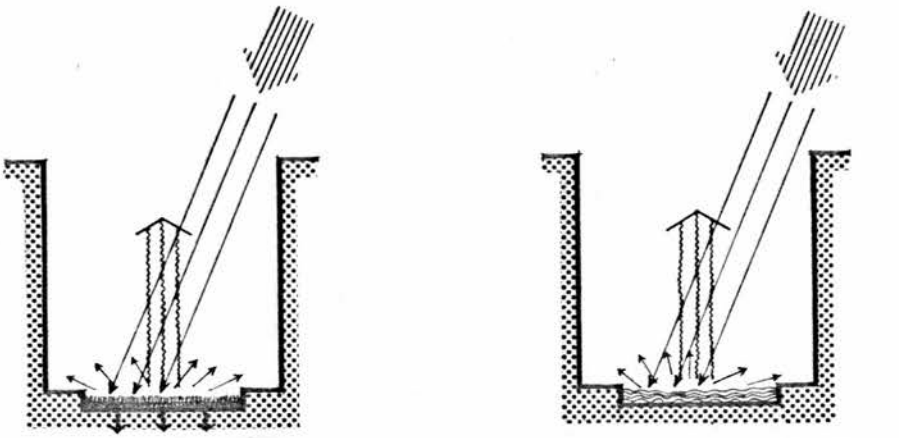

Figure II.9 The effect of different treatments for the ground surface

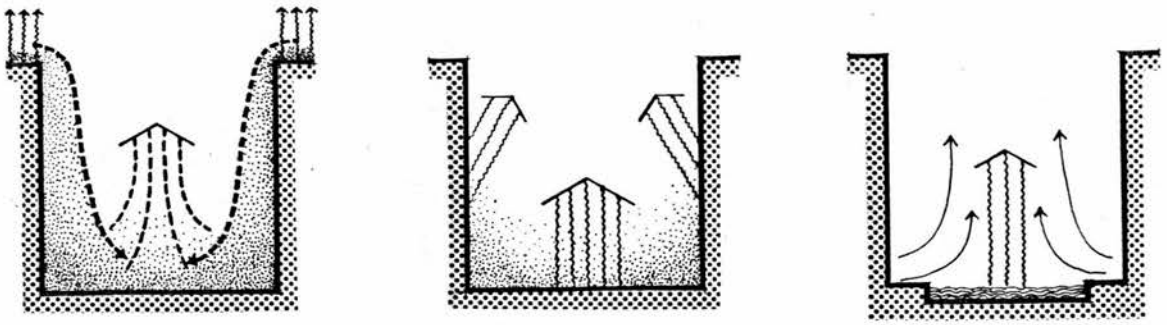

Figure II.10 Thermal exchanges at night

the cold air is collected inside the courtyard (figure II.10). Exchange between this cold air and the warmer indoor air takes place through the openings in the surrounding walls. Another aspect of thermal exchange that takes place during the night is the outward heat flow through the materials of the walls and roof. Such a process starts when the outer layer of the material reaches a thermal balance and the direction of heat flow to the inside is reversed.

II.3 Guidelines for the Present Study

The foregoing discussion reveals the following points which will be used as guidelines for the present investigation.

1. The thermal performance of the courtyard house comprises heat exchange processes taking place among the environments of three interrelated spaces : the indoor space, the courtyard space and the external open spaces between houses.

2. Concerning the indoor thermal environment, heat is exchanged through : (a) the inner envelope (courtyard walls) and (b) the outer envelope (external walls and roof).

3. The different surfaces of the two envelopes are constantly exposed to the outside air temperature, however, their exposure to solar radiation varies with time. This emphasizes the importance of

studying means of controlling the exposure to solar radiation. In such control, the inner envelope is more critical since most of the openings are located there.

4. Regarding the physical system which represents the impact of solar radiation upon the indoor space passing through the inner envelope, two subsystems are identified. The external subsystem deals with :

   (a) The insolation of the courtyard surfaces which is a joint function of the sun's geometry and the courtyard's geometry; and

   (b) The thermal balance of the surfaces as affected by the incident radiation.

   The internal subsystem deals with the heat flow taking place through the opaque as well as the transparent materials of the envelope. The scope of the present work is restricted to study the external subsystem. The parameters of the form which influence the two steps of this subsystem must be included in the model upon which the study is based (see figure II.11).

5. Regarding the first step, the geometrical parameters of the form are the proportions, size and orientation. The proportions are the ratiosbetween the dimensions of

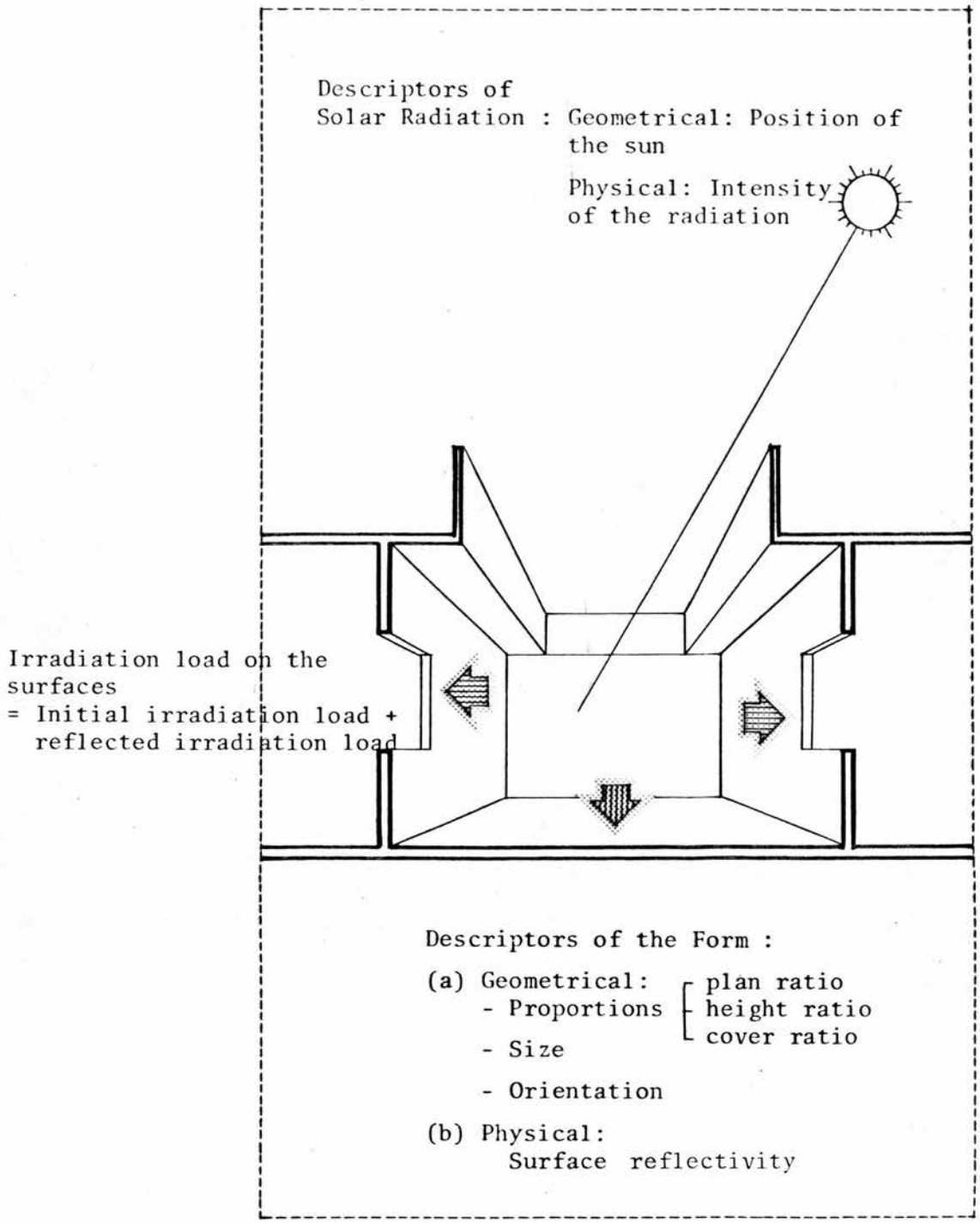

Figure II.11 A representation of the external subsystem

the surfaces defining the form : the plan ratio, the height ratio and the cover ratio. Detailed discussion is needed to define the measures of each one.

6. The physical parameter of the form which influence the second step of the subsystem is the reflectivity of the surfaces of the form.

7. The solar radiation is described in the model in terms of : geometrical descriptors which deal with specifying the position of the sun and physical descriptors which deal with assessing the intensity of radiation.

PART TWO : THE MODEL

CHAPTER III

STUDY OF THE INTERACTION BETWEEN THE SUN AND THE GEOMETRY OF THE COURTYARD FORM

III.1 Introduction

This chapter discusses the interaction between solar geometry and the geometry of the courtyard form, and describes an approach for assessing the insolation of the envelope of the form. The approach which is described includes the necessary mathematical expressions for : (a) specifying the position of the sun as observed from any specific point on the earth's surface, and (b) determining the insolated areas of the form's envelope. It is believed that such an approach is more appropriate, for the present study, than either experimental models or graphic methods, since it leads to the establishment of an extremely flexible model. The investigation of the mathematical model is carried out using computer techniques which make it feasible to carry out lengthy computations which would be both difficult and tedious to perform manually.

In Chapter IV, another segment of the mathematical model is presented, it concerns the derivation of the intensity of solar radiation from the available data. The implementation of the model on the computer is discussed in Chapter V.

III.2 Calculation of the Sun's Position in Relation to a Specific Place on the Earth

In order to determine the sun's position in relation to any point on the earth, it is necessary to specify both the position of the sun in the sky and the location of the point on the earth. The first task may be done by imagining a celestial sphere surrounding the earth and concentric with it, and by defining a suitable co-ordinate system on this sphere as shown in figure III.1.

The imaginary path of the sun round the earth is diagramatically represented by a great circle on the celestial sphere making an angle of approximately 23.45^{o} to the equatorial plane; it is called the ecliptic. A vector parallel to the sun's rays and reaching the earth's centre cuts the ecliptic at a point s', the location of which is defined in a similar way to that used in defining the location of a point on the earth's surface. In this system, the basic circles are the celestial equator and the hour circle. The former is a great circle perpendicular to the earth's axis, and the latter is a great circle passing through the point s' and the celestial poles (Robinson, 1966). The angle made by the line s'o with the equatorial plane is called the solar declination d. It is measured in degrees, positively if s' is north of the equator and negatively if it is south of the equator; it is analogous to the terrestial latitude.

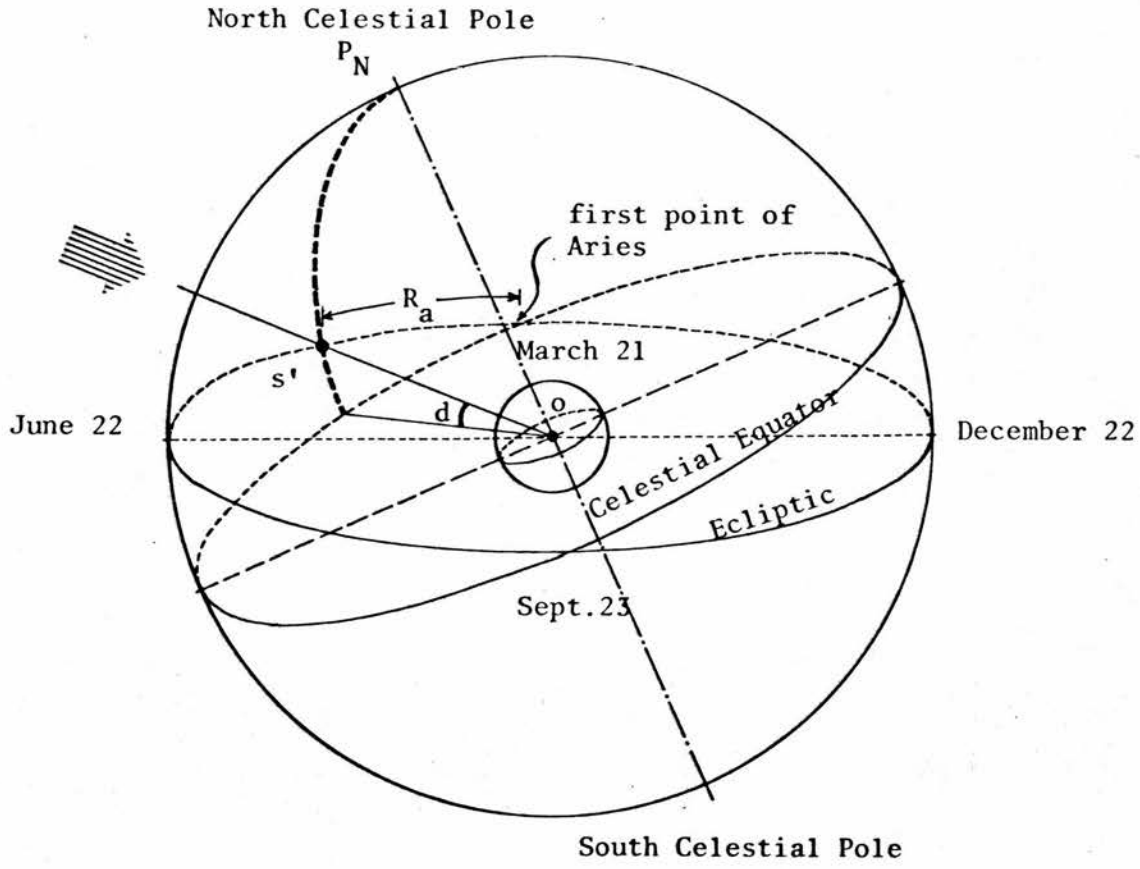

Figure III.1 The celestial sphere and the description of the sun's position

Variations of the value of the solar declination are caused by the tilt of the earth's axis with respect to the plane of the ecliptic and the earth's movement around the sun. At the equinoxes, the sun's rays are parallel to the equatorial plane and hence the angle of solar declination equals zero. In the northern hemisphere it varies from $+23.45^{o}$ in the midsummer to -23.45^{o} in the midwinter.

The second co-ordinate which describes the position of the sun in the sky is the right ascension, R_a, defined as the angular distance the hour circle of the point s' makes with the meridian of the first point of Aries which is considered as a datum line and is represented by the great circle which passes the point of intersection of the celestial equator and the ecliptic when solar declination changes from south to north (Spencer, 1965a). The right ascension is expressed either in degrees from 0^{o} to 360^{o} or in hours from 0 to 24. Both solar declination and right ascension specify the position of the sun in the sky independently from the point of observation.

In order to relate the position of the sun to a particular locality on the earth, the locality is described in terms of latitude and longitude. The term hour angle, h, will be used instead of the right ascension, to describe the apparent daily movement of the sun. It is defined as the angular distance between the meridian of the point s' and the meridian

of a point s'_n that corresponds to the solar noon at the locality. It is measured in degrees, negatively in the afternoon and positively before noon. Each longitude degree is equivalent to four minutes of time.

In order to study the geometrical relationships between the sun's position and the geometry of the courtyard form, it is necessary to derive expressions that relate all of these parameters, (namely, solar declination, hour angle, latitude and longitude) to a three-dimensional Cartesian system.

Consider a system of three mutually perpendicular Cartesian co-ordinates x, y and z, such that the positive x-direction points to the East, the positive y-direction points to the North and the z-direction points vertically upwards as shown in figure III.2. In such a system the direction of a line, S, representing the sun's rays is specified by the angles (ψ_1, ψ_2 and ψ_3) the line makes with the positive directions of the three co-ordinates. Let $\vec{s}$ be a unit vector lying in the direction of the line S and let a, b and c be its direction cosines with respect to the (x, y, z) co-ordinate system. They are equal to the cosines of the angles ψ_1, ψ_2 and ψ_3 and are related to the basic parameters of the sun's position as follows :

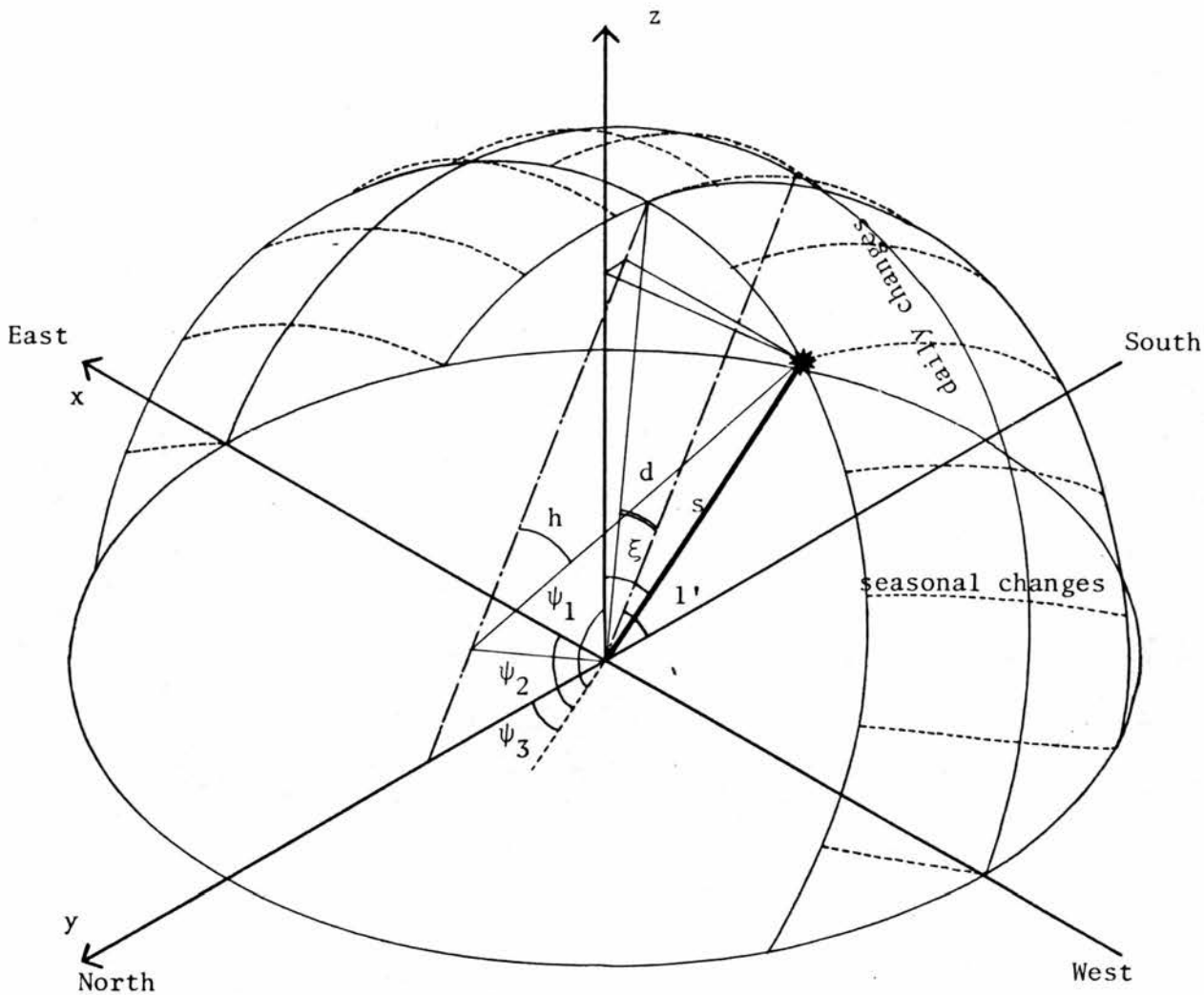

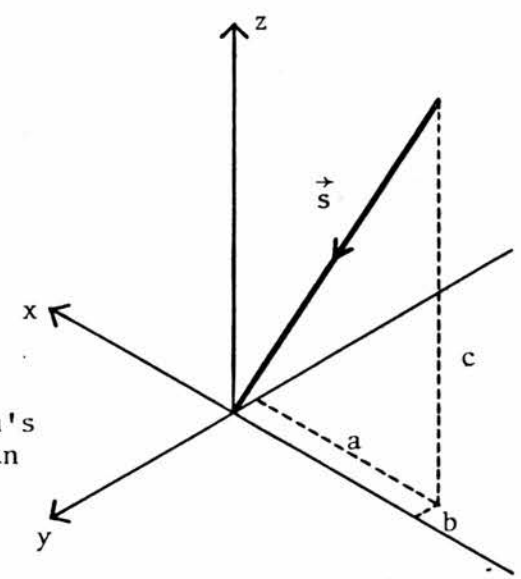

Figure III.2 Description of the sun's position in a Cartesian co-ordinates

$\vec{s} = (\vec{a1}, \vec{bm}, \vec{cn})$

where 1, m and n are unit vectors in the x, y and z directions respectively

$$\cos \psi_1 = -\cos \xi$$

where ξ is the sun's zenith angle

$$= -(\cos l \cos d \cos h + \sin l \sin d)$$

$\therefore$ Direction cosine $\quad c = -(\cos l \cos d \cos h + \sin l \sin d)$ III.1

$$\cos \psi_2 = -\cos d \sin h$$

$\therefore$ Direction cosine $\quad a = -\cos d \sin h$ III.2

$$\cos \psi_3 = \sin l \cos d \cos h - \cos l \sin d$$

$\therefore$ Direction cosine $\quad b = \sin l \cos d \cos h - \cos l \sin d$ III.3

For a particular locality (i.e., given latitude and longitude), the fundamental parameters needed for using equations III.1-3 are solar declination, d, and hour angle, h. Daily values of solar declination are tabulated in the Nautical Almanac (British Admiralty, 1957).

Values of hour angle may be obtained from the corresponding values of the local apparent time, since by definition, the hour angle corresponds to the apparent motion of the sun. Therefore, the clock time needs to be corrected by means of two factors. A longitude correction counts

for any difference between the meridian of the locality and the standard meridian of the whole country or zone; and each degree of longitude counts for a difference of four minutes of time. The second correction is applied to overcome the non-uniformity of the earth's orbital speed, it is known as equation of time, e_t.

Thus : Local apparent time t_{la} = clock time t_c + equation of time e_t + longitude correction t_l.

Values of equation of time are tabulated in the Nautical Almanac (British Admiralty, 1957). They range from about -10 to +15 minutes. Such a degree of accuracy seems unnecessary for the type of investigation undertaken in this study. However, bearing in mind that the calculations were to be performed on a computer, it was decided to include the various correction factors.

It will be observed from equation III.1 that the direction cosine c is negative during daylight hours whilst the reverse is true during the hours of darkness. The times of sunrise and sunset may be obtained by substituting c = 0 in equation III.1, thus :

$$\cos l \cos d \cos h_R + \sin l \sin d = 0$$

$$\cos h_R = \frac{-\sin l \sin d}{\cos l \cos d}$$

$$= -\tan l \tan d$$

$$\therefore \quad h_R = \cos^{-1}(-\tan l \tan d) \qquad \text{III.4}$$

$$h_S = -h_R \qquad \text{III.5}$$

where h_R and h_S are the sunrise and sunset hour angles respectively, measured in radians.

$$t_R = 12 - \frac{12}{\pi} h_R \qquad \text{III.6}$$

$$t_S = 12 - \frac{12}{\pi} h_S \qquad \text{III.7}$$

where t_R and t_S are the times of sunrise and sunset respectively, measured from midnight (local apparent time).

By subtracting the quantity $\frac{e_t + t_l}{60}$ from the expressions in equations III.6 and III.7 the times of sunrise and sunset are obtained in clock time.

A computer subroutine SOLGEO was developed to determine times of sunrise and sunset for any day according to equations III.4 - 7. The time interval between sunrise and sunset (day time) was divided into small intervals, for each midinterval the direction cosines a, b and c were calculated using equations III.1 - 3. The calculated values were arranged in tables showing the date of day, times of sunrise and sunset, length of day time, the times of midintervals and the corresponding direction cosines. An example is shown in table III.1, and a graphical representation is given in

LATITUDE 30,0N, LONGITUDE 31,0E,

195 15/ 7 DECLINATION 21,67DEG, EQ,OF TIME -5,7MIN,

	STD,TIME	L,A,TIME	A	B	C
SUNRISE AT	5,14	5,12	-0,905	-0,426	-0,000
	5,41	5,38	-0,917	-0,395	-0,055
	5,94	5,91	-0,929	-0,331	-0,166
	6,47	6,44	-0,923	-0,266	-0,277
	7,00	6,97	-0,900	-0,203	-0,387
	7,53	7,50	-0,859	-0,142	-0,492
	8,06	8,03	-0,801	-0,084	-0,592
	8,59	8,56	-0,729	-0,031	-0,684
	9,12	9,09	-0,642	0,016	-0,767
	9,65	9,62	-0,543	0,057	-0,838
	10,18	10,15	-0,433	0,091	-0,897
	10,71	10,68	-0,316	0,117	-0,942
	11,23	11,21	-0,192	0,135	-0,972
	11,76	11,74	-0,064	0,144	-0,988
	12,29	12,26	0,064	0,144	-0,988
	12,82	12,79	0,192	0,135	-0,972
	13,35	13,32	0,316	0,117	-0,942
	13,88	13,85	0,433	0,091	-0,897
	14,41	14,38	0,543	0,057	-0,838
	14,94	14,91	0,642	0,016	-0,767
	15,47	15,44	0,729	-0,031	-0,684
	16,00	15,97	0,801	-0,084	-0,592
	16,53	16,50	0,859	-0,142	-0,492
	17,06	17,03	0,900	-0,203	-0,387
	17,59	17,56	0,923	-0,266	-0,277
	18,12	18,09	0,929	-0,331	-0,166
	18,65	18,62	0,917	-0,395	-0,055
SUNSET AT	18,91	18,88	0,905	-0,426	-0,000

DAY TIME =13,77 HOURS
INTERVAL = 0,53 HOURS

Table III.1 Direction cosines of the sun's rays at the 15th of July
(A sample of the tables produced by subroutine SOLGEO)

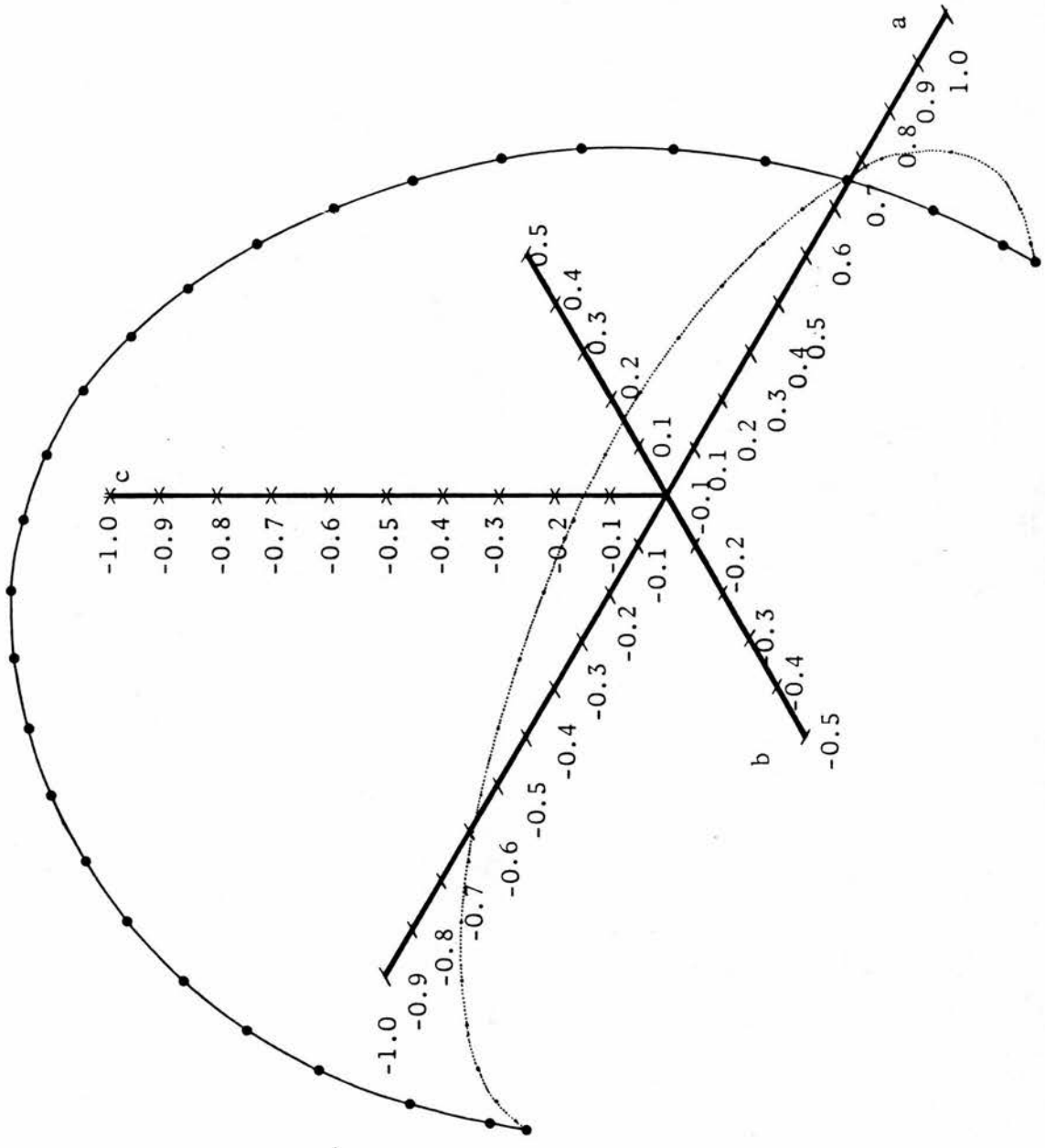

Figure III.3 Representation of the values of the direction cosines given in Table III.1

figure III.3. The use of such tables for studying the exposure of the surfaces of a courtyard to the sun is discussed in the following section.

III.3 The Use of the Descriptors of the Position of the Sun for Determining the Insolation of the Courtyard Form

Whether a surface of a courtyard form is shaded, exposed to the sun or partially shaded is a joint function of the position of the sun in the sky and the geometry of the form under consideration. The determination of the former has been discussed in section III.3 and a discussion of the latter will follow in the next section. The present section describes the use of the descriptors of the sun's position for determining the conditions of shading for the four surfaces of the courtyard's envelope as well as for the ground surface.

Consider a courtyard form whose edges are parallel to the directions x, y and z shown in figure III.4.

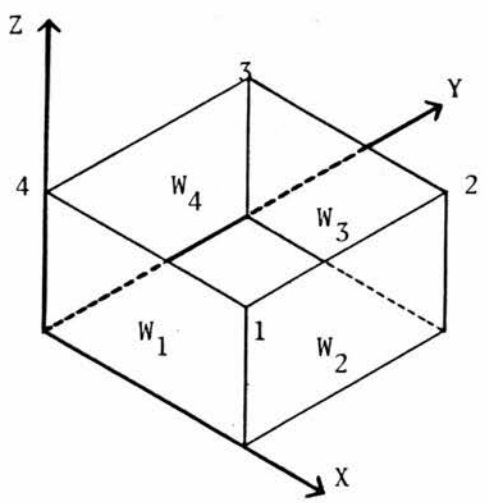

Figure III.4 A courtyard form parallel to the cardinal directions

The components, a, b and c of a unit vector parallel to the sun's rays may be determined, at any specified time, as described in section III.2.

In cases when c has negative values, i.e., the sun is above the horizon, the values of a and b should be examined in order to determine which of the form's top corners is closer to the sun :

if $a \leq 0$ and $b > 0$ then

$n = 1$

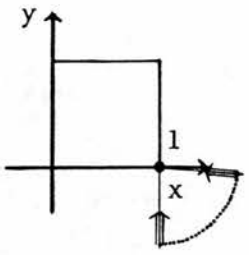

if $a < 0$ and $b \leq 0$ then

$n = 2$

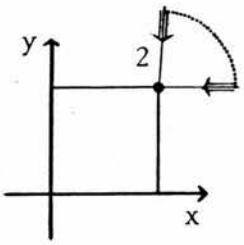

if $a \geq 0$ and $b < 0$ then

$n = 3$

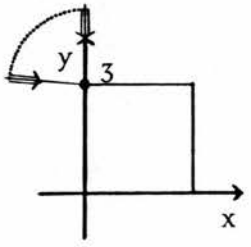

if $a > 0$ and $b \geq 0$ then

$n = 4$

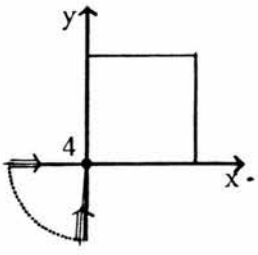

Figure III.5 Determination of the closest corner to the sun

where the integer n is used to characterize each case.

The two surfaces W_n and W_{n+1} meeting at the edge nn' are in shade as shown in figure III.6. In order to determine the shading conditions of the other two vertical surfaces and the ground surface , consider a vector parallel to the sun's rays passing the point n and intersecting one of these surfaces in point n_s. The point n_s is the shadow of the point n. Four cases of shading may emerge, depending on the location of n_s as shown in figure III.6.

(i) n_s lies on the ground surface

(ii) n_s lies on surface W_{n+2}

(iii) n_s lies on surface W_{n+3}

(iv) n_s lies on the edge n+1 - n'+1

The fourth case occurs when the sun's rays are parallel to either the x or y direction, i.e., if b = 0 or a = 0. In order to find the conditions which determine the location of n_s, consider the two points u and v which are defined in figure III.7. Here u denotes the point on the top of wall W_n through which the first sunray to touch the ground would pass were wall W_{n+2} absent. Conversely, point v is a point on W_n through which the first sunray to touch W_{n+2} would pass were the ground absent. Let $\vec{M}$ be a unit vector running from point n along the top edge of the surface W_n, then the

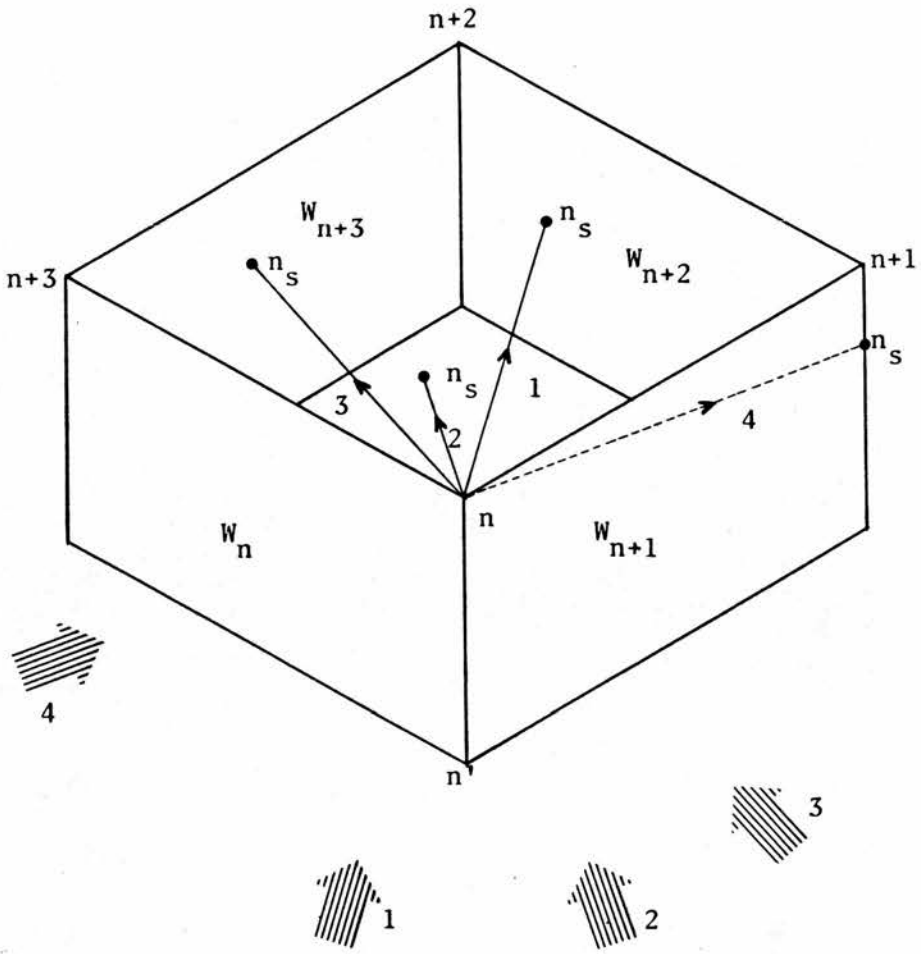

Figure III.6 The possible cases of shading determined according to the location of the point n_s

two vectors $\vec{nu}$ and $\vec{nv}$ may be defined as :

$$\vec{nu} = u_1 \cdot \vec{M}$$

$$\vec{nv} = u_2 \cdot \vec{M}$$

If both u_1 and u_2 have negative values, then n_s lies on the surface W_{n+3}; i.e., case (iii). If at least one of them has positive value, then the resulting case is that which corresponds to the greater value of them. That is, n_s lies on the ground (case (i)) if u_1 is the greater and n_s lies on W_{n+2} (case (ii)) if u_2 is the greater (figure III.7).

Values of u_1 and u_2 are obtained as follows :

The equation of the plane of rays touching the top edge of the surface W_n is :

$$(x_n, y_n, z_n) + u^* \cdot (m_1, m_2, m_3) + s \cdot (a, b, c)$$

where m_1, m_2 and m_3 are the components of the unit vector $\vec{M}$.

By solving this equation with the equation of the surface W_{n+3} we get the equation of the line of intersection. u_1 is the value of u* which satisfies the equation for the case of n_s lying on the ground surface. u_2 is the value of u* which satisfies the equation for the case of n_s lying on the surface W_{n+2}.

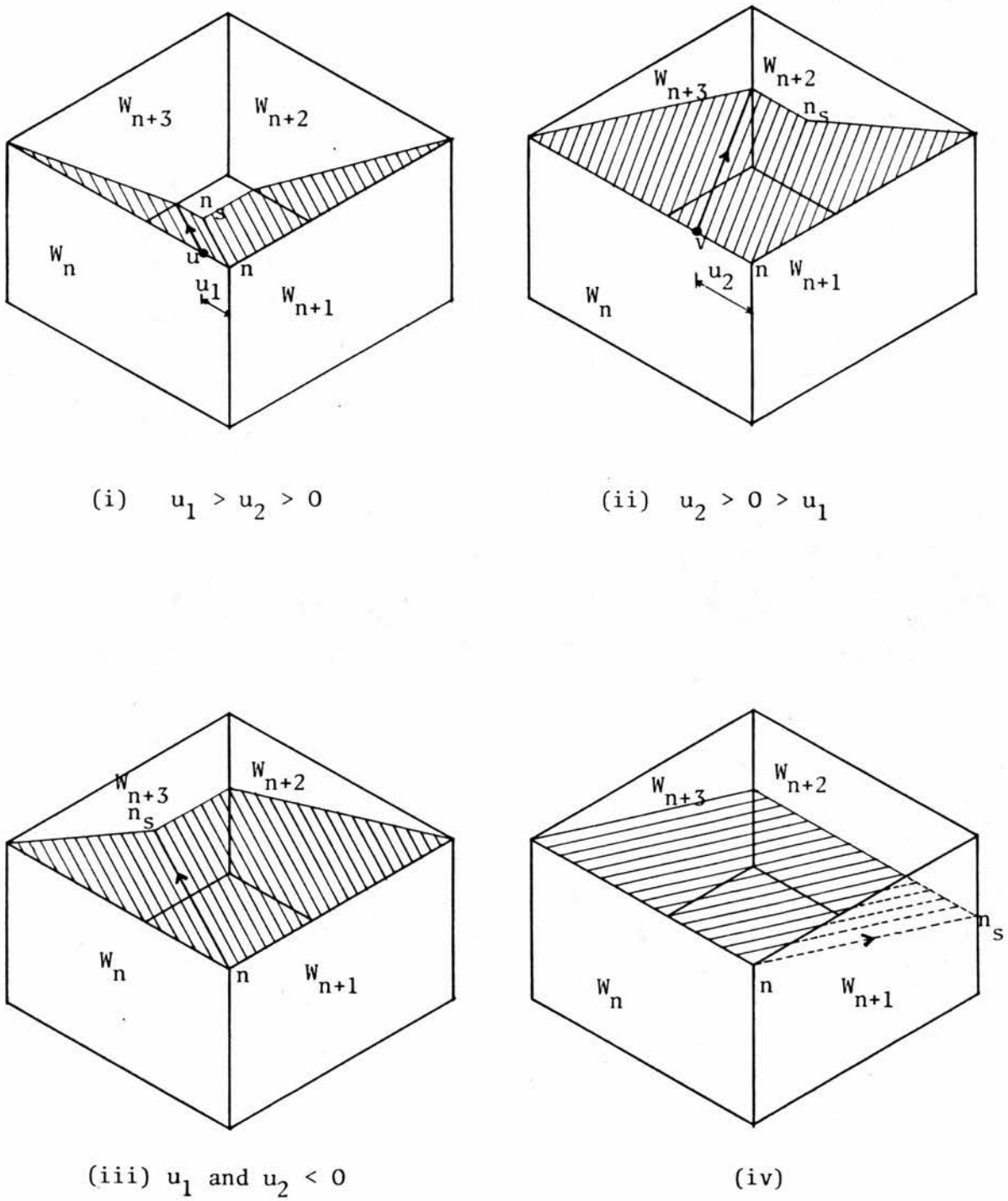

Figure III.7 The four cases of shading and the determining geometrical conditions

III.4 Courtyard's Geometry

The geometries which are included in the study are rectangular shaped forms. The geometrical parameters that affect the extent to which the surfaces of the form are exposed to the sun are the proportions, size and orientation of the form.

III.4.1 Proportions of the Courtyard

The ratios between the dimensions of the surfaces defining the courtyard form affect the ratio of the insolated to the whole area of the envelope's surfaces irrespective of the courtyard's size. The ratio, R_1, of perimeter, P, to height, H, of a courtyard indicates the deepness of the form (see figure III.8). The ratio, R_2, of width, W, to length, L, indicates the elongation of its plan. If projecting roofs over the courtyard walls are introduced, the ratio, R_3, of the area of the top opening, A_T, to the area of the ground, A_G, determines the degree of openness to the sky. The change of any of these sets of proportions produces a corresponding change in the insolation of the form.

III.4.2 Size of the Courtyard

The ratio of insolated to shaded area of the form's envelope is determined by the proportions of the form irrespective of its size. However, the effect of size on

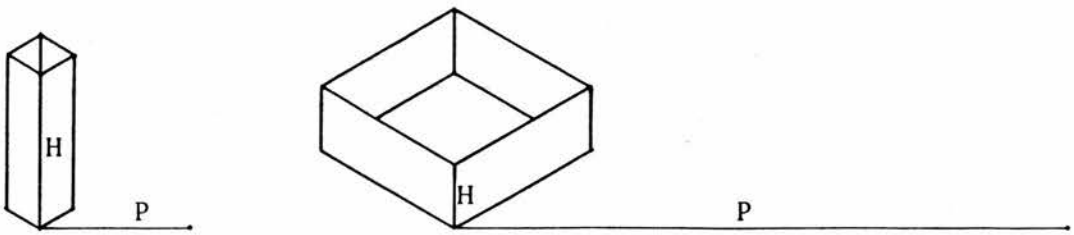

(i) Deepness of the form $R_1 = P/H$

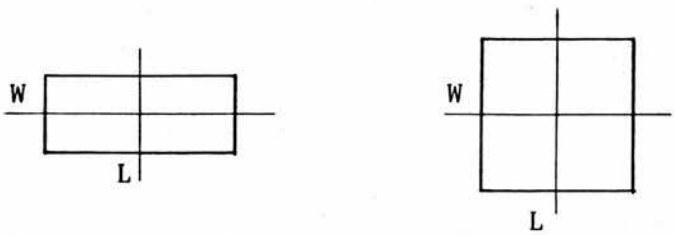

(ii) Elongation of the plan $R_2 = W/L$

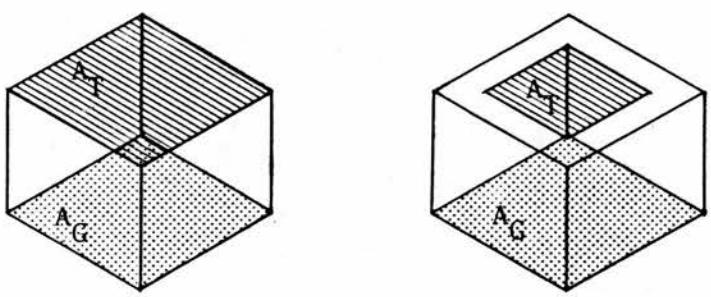

(iii) Openness to the sky $R_3 = A_T/A_G$

Figure III.8 The three sets of proportions of the courtyard form

determining the radiation impact on the form is explained as follows. Consider two forms having identical proportions. The first is one floor high and the other is two floors high. Assuming the same height of floor and the same levels of window sills and lintels, one can define, on the surface of each envelope, stripes in which windows are likely to be located.

Figure III.9a illustrates that the lower stripe in the large form is likely to receive less sun's rays than that of the smaller one. On the other hand,the upper stripe is likely to receive more sun's rays. This shows that although the two forms have the same ratio of insolated to shaded areas, the distributions of insolation over opaque and transparent parts of the envelope are different and consequently the thermal impacts on the indoor spaces are different.

Figure III.9b shows another example, two forms identical in proportions, both of them are one floor high. The envelope of the first one is extended above the level of the roof forming a parapet, hence the size of this form is larger than the other one. In spite of having identical ratios of insolated to shaded areas, solar radiation received by the effective part of the envelope - i.e., excluding the parapet part - is smaller in the case of the larger form. Furthermore, the windows of the larger form are likely to receive less radiation.

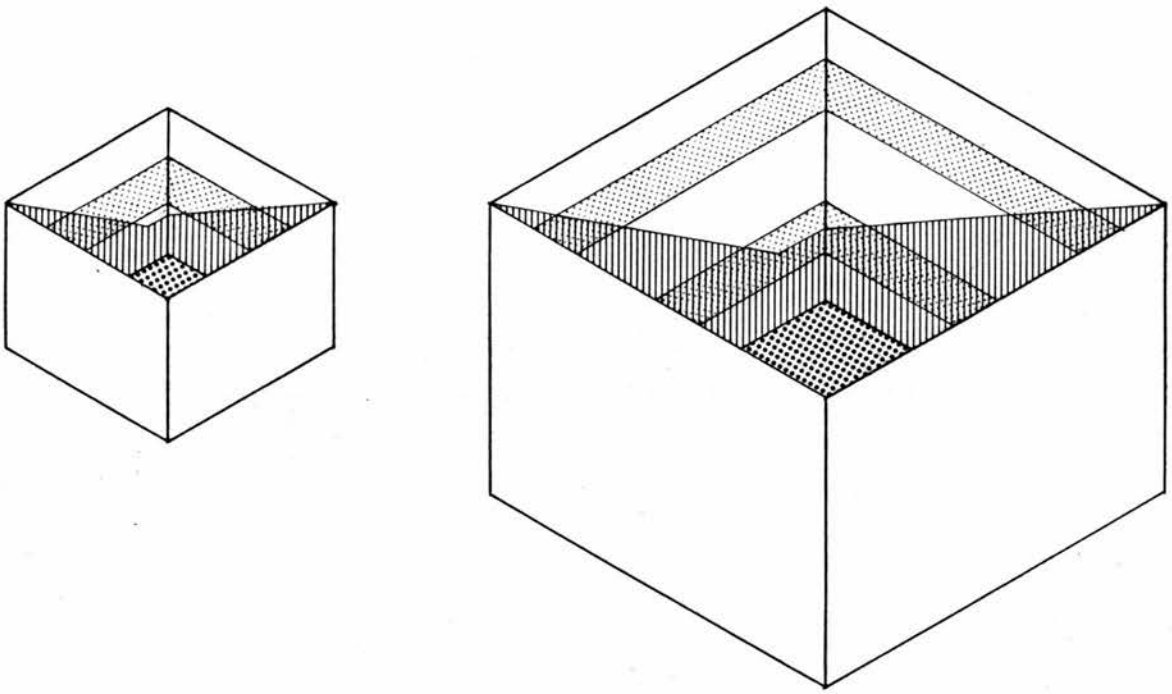

(a)

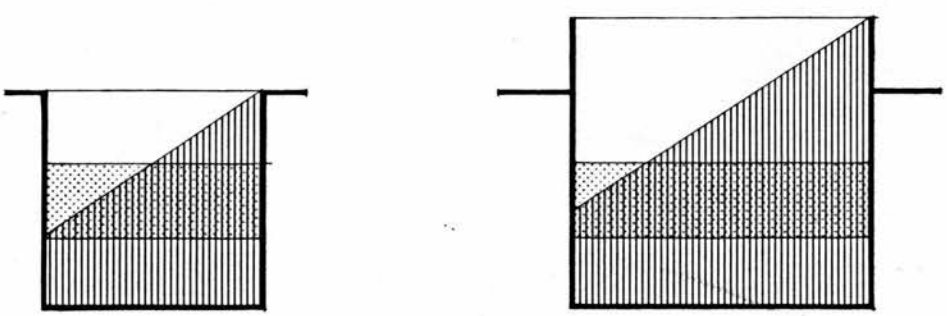

(b)

Figure III.9 Effect of size on the insolation of the form

III.4.3 Orientation of the courtyard

The orientation of a vertical surface indicates its position in relation to the four cardinal directions. Owing to the symmetry of the apparent movement of the sun on both a daily and a seasonal basis, there are two axes about which the daily amounts of solar radiation received at a surface are symmetrical. The first one which is the north-south axis concerns the symmetry of the sun's position during the day. The values of the direction cosines b and c are identical, and the values of the direction cosine a are equal and of opposite sign (see figure III.3). The second axis concerns the symmetry of the sun's position on a seasonal basis; the direction cosines a, b and c are identical around an axis representing the summer solstice. That is, the positions of the sun are identical in days at equal distances from the summer solstice (see figures III.2 and III.12).

For the latitude under consideration (30^{o} North) the change of the irradiation of differently oriented surfaces with the time of year is as follows (Olgyay, 1969) :

(a) For eastern and western surfaces, the radiation impact is at its maximum at the summer solstice, the minimum is attained at the winter solstice.

(b) For southern surfaces,the maximum impact occurs at the winter solstice, the minimum occurs at the summer solstice.

(c) For nothern surfaces, the maximum impact occurs at the summer solstice, the minimum occurs at the winter solstice.

In general, in summer the largest amount of solar radiation is attained at eastern and western surfaces, whereas the southern surface receives the smallest amount. In winter the largest amount of solar radiation is attained at the southern surface. The northern surface receives no radiation at all.

Regarding a three dimensional rectilinear form such as that of a courtyard where each two surfaces are directly opposed, the angle which the longitudinal axis of the form makes with the east direction measured anti-clockwise may be taken to denote the orientation of the form (see figure III.16). So, if the longitudinal axis is parallel to the east-west direction, the orientation is said to be zero degrees.

Since the geometries of all the forms considered in this study are symmetrical about two axes (see section III.4) it is clear that the range of the angles of orientation that might produce unique cases of insolation is limited to

the range 0^{o} to 180^{o}. However, because of the symmetry of the apparent solar movement, identical cases, as far as the daily insolation of the form is concerned, are found around a 90^{o} axis. Therefore, the range of the angles of orientation is defined, in the present study, between 0^{o} and 90^{o}.

The effects of changing a form's orientation can be studied by either modifying the foregoing procedure to account for non-zero orientations or by returning an orientated form to the cardinal directions and finding a set of modified sun positions which produce equivalent shading patterns. The latter procedure was found to be more convenient for this study and it will be discussed in the following.

Let us consider two forms identical in size and proportions but having different angles of orientation. Suppose they are exposed to the sun at quite different times. Figure III.10 illustrates that two identical cases of exposure to the sun could be obtained as long as the directions of the sun's rays in relation to their surfaces are kept identical. This suggests that the transformation to the zero orientation means producing new values of the fundamental parameters of the solar position, i.e., solar declination and hour angle. It should be mentioned that the new declinations and hour angles are

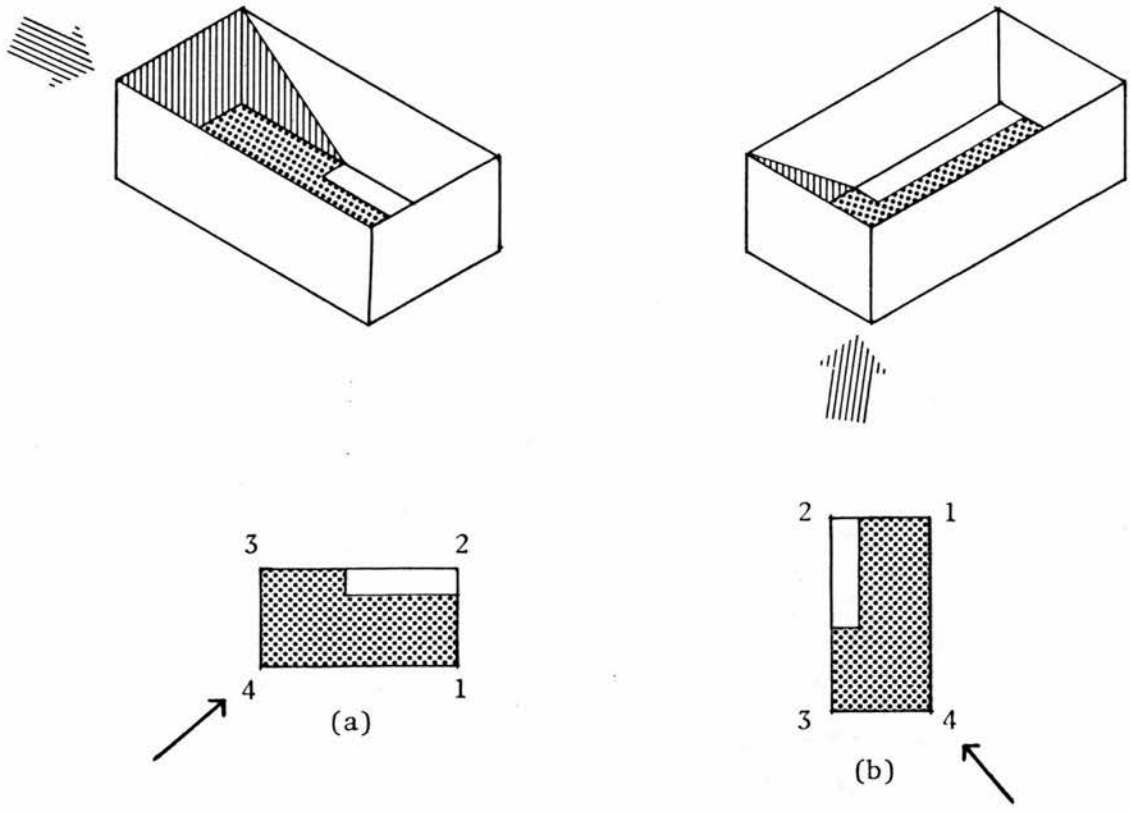

Figure III.10 Identical pattern of insolation at different times for forms identical in geometry and having different angles of orientation

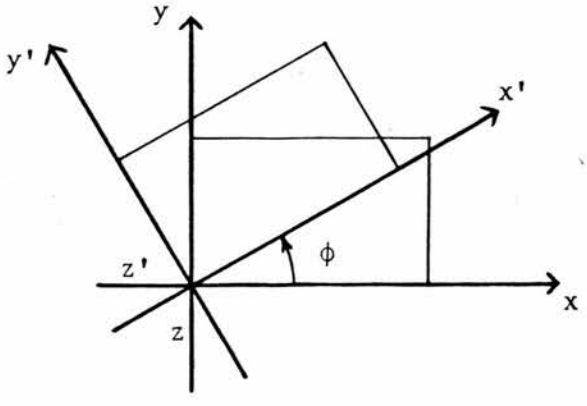

Figure III.11 Rotation of the reference frame

entirely a mathematical device, hence some values of declination are expected to lie outside the range + and -23.45^{o}. The required mathematical relations are derived as follows.

Let a courtyard form be rotated by an angle of ϕ so that its surfaces are parallel to a new co-ordinate system (x', y', z') as shown in figure III.11. For a specified time, the three components a, b and c in the (x, y, z) system could be calculated using equations III.1-3. Given the angle of rotation, the components a', b', and c' in the (x', y', z') system could be calculated using equations III.8 and III.9 (Porter, 1970).

$$a' = a \cos \phi + b \sin \phi \qquad \text{III.8}$$

$$b' = -a \sin \phi + b \cos \phi \qquad \text{III.9}$$

Since the third direction in the two systems is identical then :

$$c' = c$$

The unit vector representing the sun's rays, $\vec{s}$, equals $(a'\vec{i}, b'\vec{j}, c'\vec{k})$ where $\vec{i}$, $\vec{j}$ and $\vec{k}$ are unit vectors in the (x', y', z') system. Since the condition of identity means the equality of the direction cosines in both of the reference frames then :

$$(a'\vec{i}, b'\vec{j}, c'\vec{k}) = (a_1\vec{l}, b_1\vec{m}, c_1\vec{n})$$

where $\vec{l}$, $\vec{m}$ and $\vec{n}$ are unit vectors in the (x, y, z) system.

It is required then to find the values of hour angles and solar declination that satisfy this equality. From equations III.1 and III.2 :

$$\frac{c_1}{a_1} = \frac{\cos l \cos d \cos h + \sin l \sin d}{\cos d \sin h}$$

$$\text{let } f_1 = \frac{c_1}{a_1}$$

$$\therefore \quad f_1 = \frac{\cos l \cos h + \sin l \tan d}{\sin h} \qquad \text{III.10}$$

From equations III.2 and III.3 :

$$\frac{b_1}{a_1} = \frac{-(\sin l \cos d \cos h - \cos l \sin d)}{\cos d \sin h}$$

$$\text{let } f_2 = \frac{b_1}{a_1}$$

$$\therefore \quad f_2 = \frac{-(\sin l \cos h - \cos l \tan d)}{\sin h} \qquad \text{III.11}$$

Solving equations III.10 and III.11 :

$$\tan h = \frac{1}{f_1 \cos l - f_2 \sin l} \qquad \text{III.12}$$

$$\tan d = \sin h(f_1 \sin l + f_2 \cos l) \qquad \text{III.13}$$

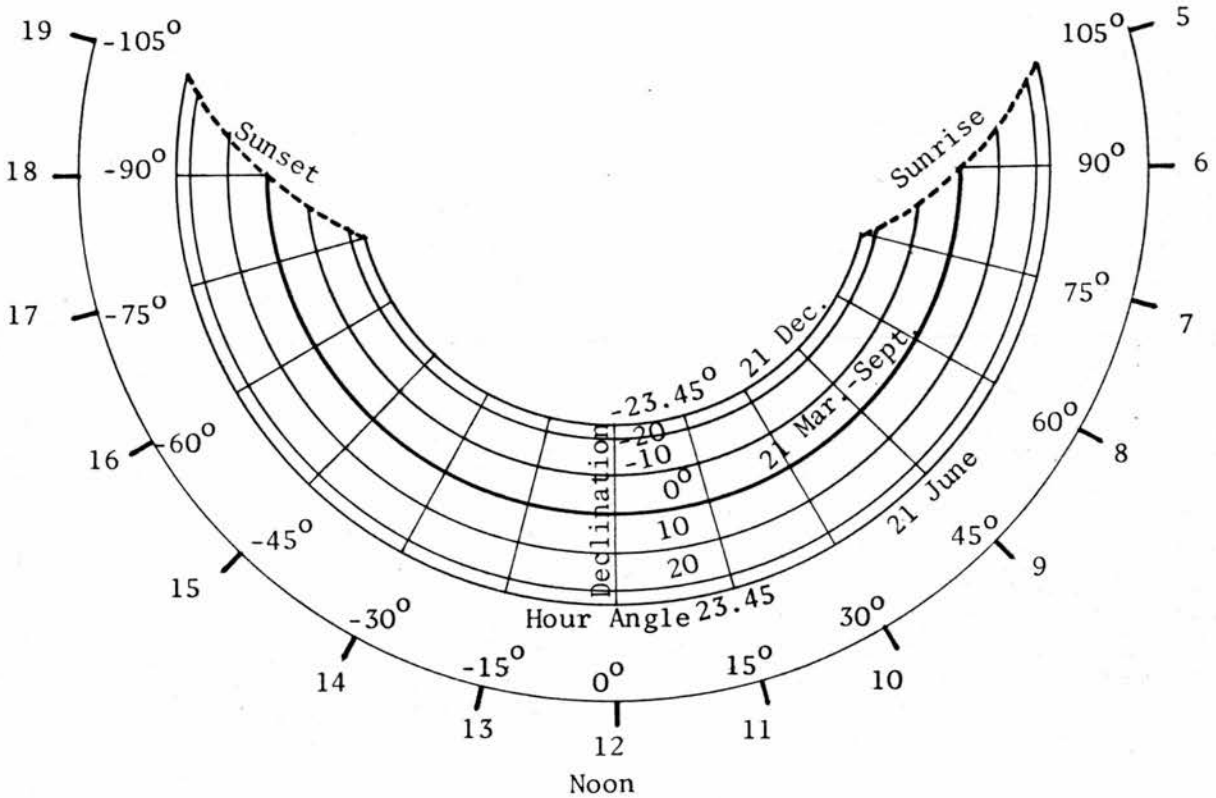

(a)

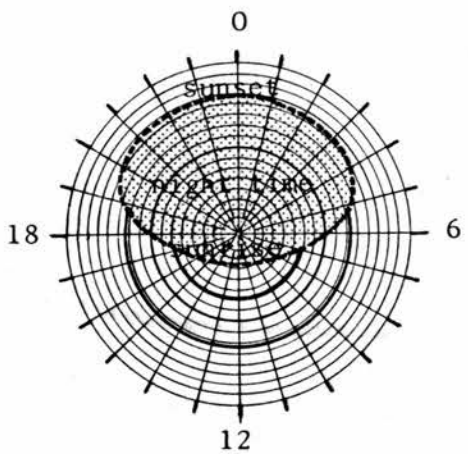

(b)

Figure III.12 Values of declination and hour angle

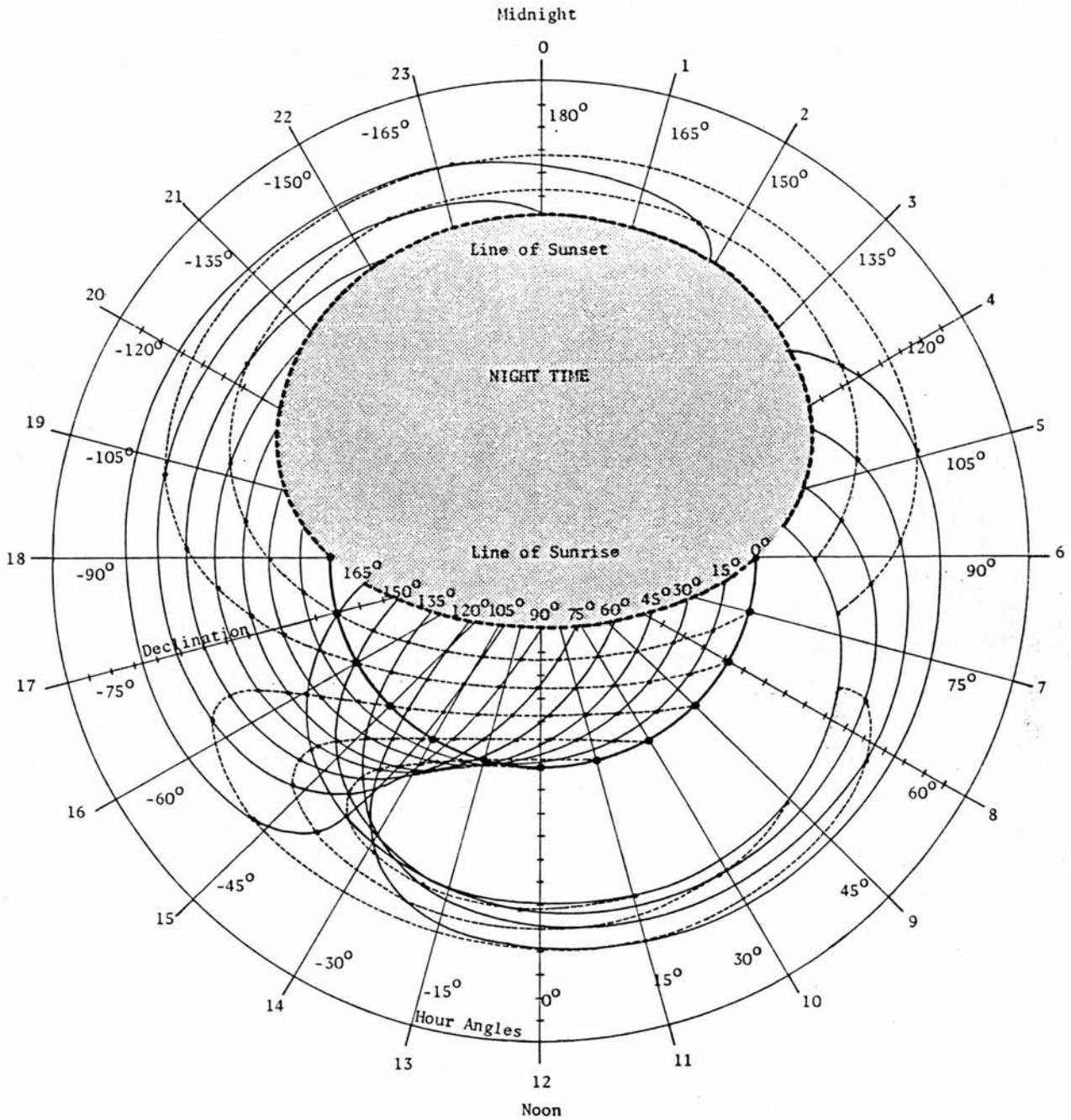

Figure III.13 Calculated values of d and h that correspond to different cases of orientation at the equinox

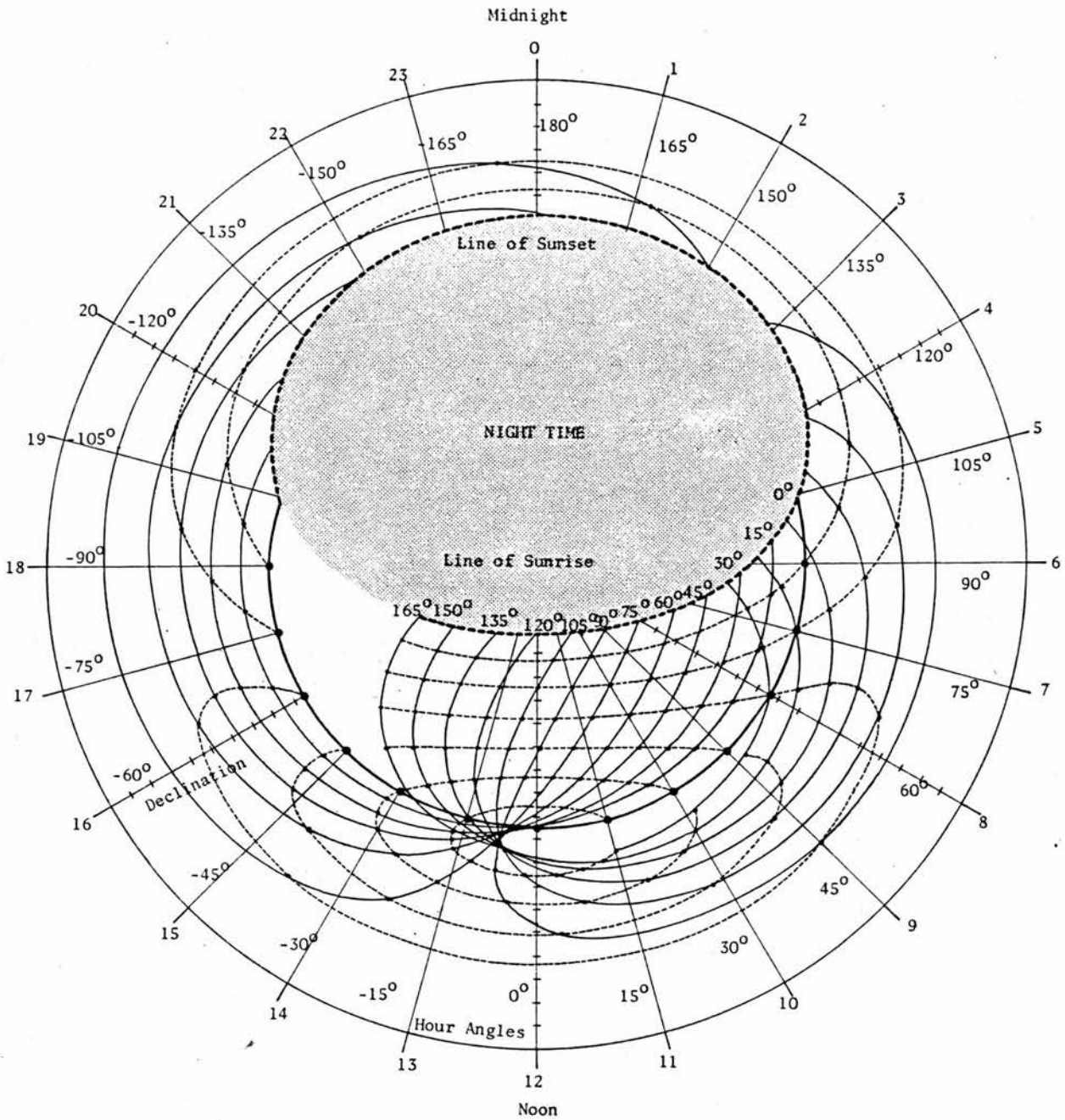

Figure III.14 Calculated values of d and h that correspond to different cases of orientation at the summer solstice

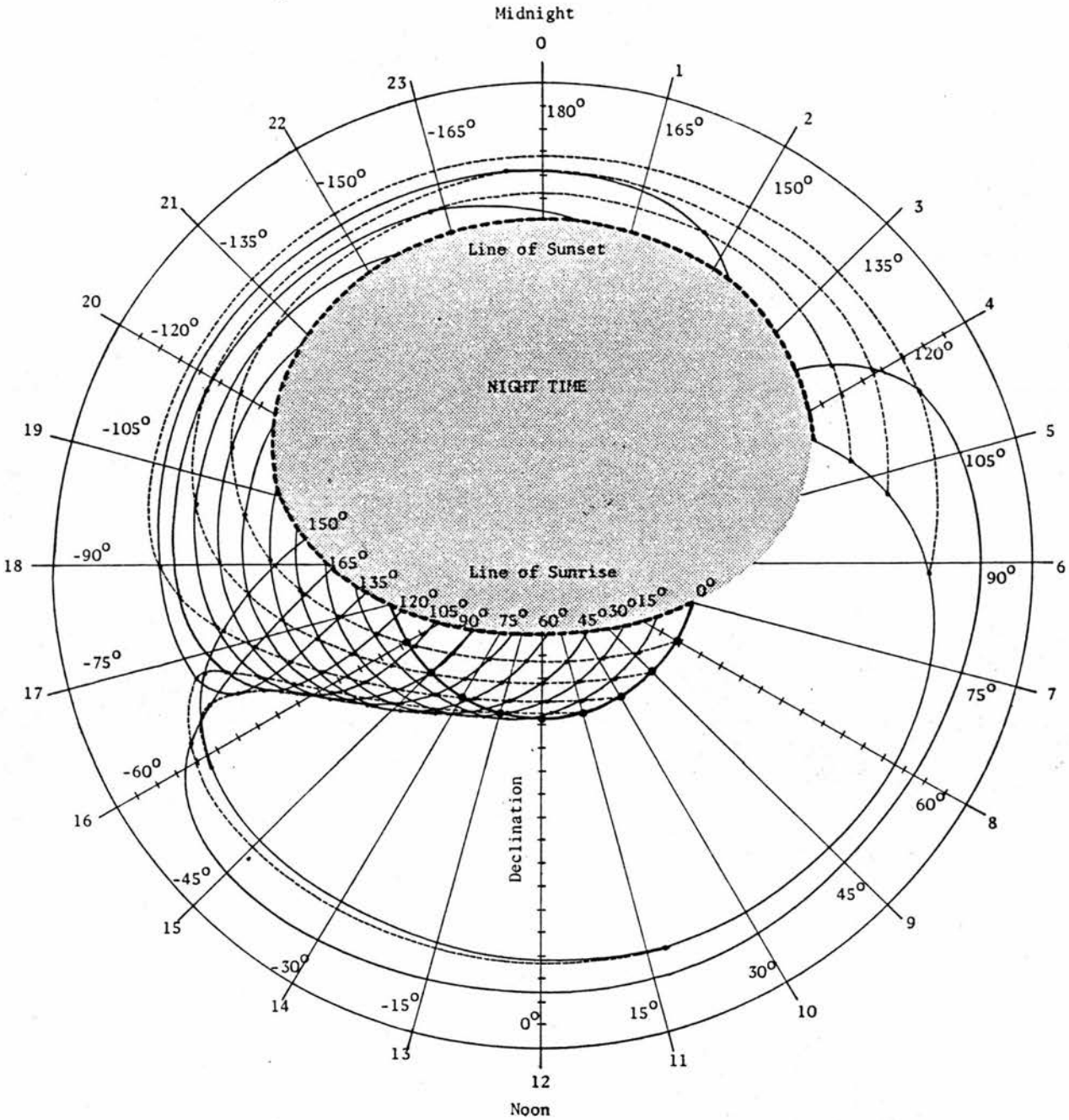

Figure III.15 Calculated values of d and h that correspond to different cases of orientation at the winter solstice

In figure III.12, the concentric circles represent the angles of solar declination (from -23.45^{o} in midwinter to $+23.45^{o}$ in midsummer), the radial lines represent the time of day; i.e., hour angles. Figure III.12b illustrates the idea of extending the ranges of values of solar declination and hour angle to wider ranges that cater for varying the angle of orientation. Figures III.13-15 show the values of d and h that correspond to all cases of orientation for some given days as produced by equations III.8 - 13. Based on these equations, a computer subroutine ROTATE was developed, a description of which is presented in Chapter V.

III.5 The Model

A representation of the model upon which the study is based, is given in figure III.16 showing the descriptors of the form and the descriptors of solar radiation. The geometrical descriptors of the form are: the proportions, size and orientation. They are measured in terms of: deepness of the form, R_1, elongation of the plan, R_2, openness to the sky, R_3, height of the form, H, and the angle ϕ which the longitudinal axis of the plan makes with the east direction measured anticlockwise. The physical descriptors of the form are the thermophysical properties of its surfaces measured in terms of the reflectivity of its walls and ground, ρ_W and ρ_G respectively.

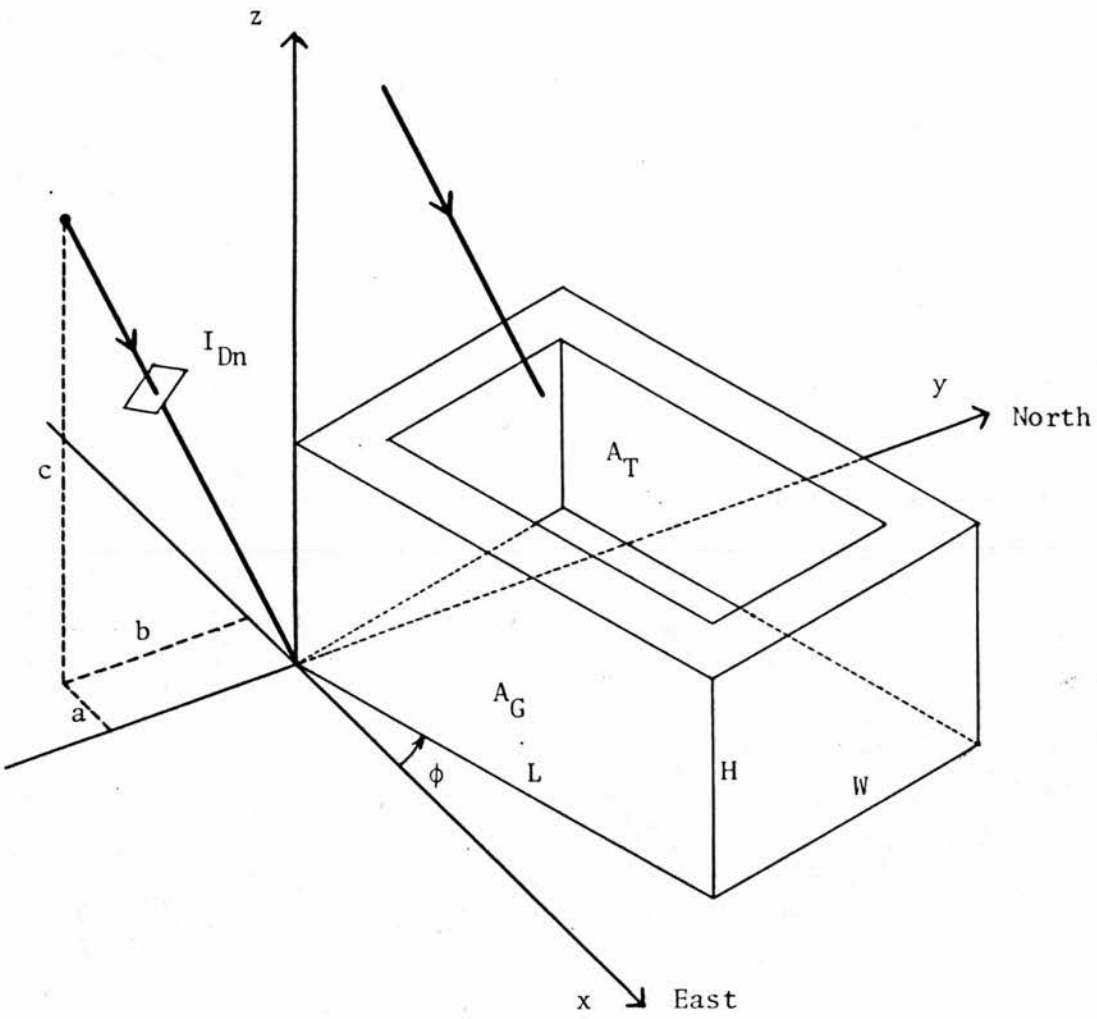

	Measures of the Descriptors of Solar Radiation	Measures of the Descriptors of the Form
Geometrical	the direction cosines : a b c	$R_1 = W/L$ $R_2 = 2(W + L)/H$ $R_3 = A_T/A_G$ H ϕ
Physical	Intensity of radiation at normal incidence I_{Dn}	Surfaces reflectivity ρ_W, ρ_G

Descriptor of the performance in the first stage of the model : Initial irradiation of the surfaces

Descriptor of the performance in the second stage of the model : Final irradiation of the surfaces

Figure III.16 The model

The geometrical descriptor of solar radiation is the position of the sun measured in terms of the direction cosines, a, b and c, of a unit vector parallel to the sun's rays. The physical descriptor of solar radiation is measured in terms of its intensity, it is discussed in detail in Chapter IV.

CHAPTER IV

STUDY OF THE SOLAR IMPACT ON A COURTYARD'S SURFACES

IV.1 Introduction

The estimation of the solar radiation reaching the surface of the earth should be based on a statistical analysis of the records of direct and diffuse radiation in the locality concerned. Such records are not available in Egypt where the measurements of solar radiation were only recently begun. In the two stations measuring the solar radiation, the values of total radiation on a horizontal surface are recorded. The monthly averages of daily radiation received on a horizontal surface, averaged over ten years of recording at Giza Station are shown in table A2.1 in Appendix 2.

The need arises for a computational technique which enables the derivation, from the available data, of the necessary information for evaluating the solar impact on differently located surfaces. Investigations done by Parmelee (1954), Threlkeld and Jordan (1958), Liu and Jordan (1960) and Sharma and Pal (1965) are reviewed in the next section.

IV.2 Attempts to Derive Intensities of Solar Radiation

Parmelee (1954) and Sharma and Pal (1965) established relationships between the intensities of direct, diffuse and

total solar radiation in localities where detailed observations have been made. The aim was to utilize such relationships for estimating the direct and diffuse components in localities where observations are only made for the intensity of total radiation on horizontal surfaces. The work of Parmelee (1954) includes observations of solar radiation intensities on horizontal and on variously oriented vertical surfaces obtained on thirty cloud-free days over five years of measurements in Cleveland, U.S.A. He produced curves which yield estimates of the diffuse solar radiation incident upon a horizontal surface and on vertical surfaces of any orientation, provided that the solar altitude and the atmospheric clearness are known. Since atmospheric clearness, as defined in his work, is the ratio of the observed intensity of direct radiation to that of the standardized atmospheric conditions as given by Moon (1940) for the same altitude, it seems that the application of Parmelee's curves would be restricted to the cases where the direct component of radiation is known and it is required to estimate the diffuse component. Another restriction of their applicability follows from the fact that his findings are based on data from only one station in the United States.

Sharma and Pal (1965) based their work on data collected in many stations in India. Hourly figures of total and

diffuse radiation on a horizontal surface were recorded, the direct radiation figures were obtained by subtraction. They derived empirical formulae which express ratios between direct, diffuse and total radiation in terms of solar altitude and atmospheric conditions. The term 'clearness number' was used to relate the prevailing atmospheric conditions to the standard tropical atmospheric conditions as defined by Rao and Seshadri (1961). The outcome of their work is rather similar to that of Parmelee (1954), with the added benefit that the mathematical formulae are more convenient for computer programming. The formulae provide estimates for direct and diffuse radiation intensities at places in India where only the hourly intensity of total radiation is measured, provided that the values of clearness number for such places are known.

The investigations made by Liu and Jordan (1960) were based on data obtained from widely spread stations over the United States (latitudes 19^{o} to 55^{o} N). They developed relationships for the determination, on a horizontal surface, of the instantaneous intensity of diffuse radiation from the knowledge of the total radiation on a horizontal surface. They presented probability distribution curves, obtained by correlating the available data, for the statistical distribution of daily total radiation over a month. Their conclusions are very useful for the present study.

IV.2.1 Derivation of the monthly average of daily direct radiation

Building on the work of Liu and Jordan (1960), a quantity referred to here as the cloudiness index $\overline{K}$ represents the overall factor by which radiation is depleted while passing through the atmosphere. It is defined as the ratio between the monthly average value of daily total radiation received on a horizontal surface and the monthly average value of the total possible radiation (i.e., outside the atmosphere) on a horizontal surface. Values of the former are recorded in the locality under consideration (see Appendix 2). Values of the latter can be calculated as follows :

The intensity of solar radiation at normal incidence outside the atmosphere is equal to the solar constant, I_{sc}, which is adjusted by a ratio r. Since the solar constant, by definition, is the rate at which energy is received by a unit surface normal to the direction of the sun's rays at the mean earth-to-sun distance (ASHRAE, 1968), the ratio r must take into account the variation of the actual distance from the mean distance. The currently adopted value for the solar constant, with a probable error of 2 percent, is 2.0 langley per minute in terms of the Smithsonian Pyrheliometric Scale of 1932 (Johnson, 1954). This is equivalent to 1395 watts per square meter. Values of the ratio r are given by

Liu and Jordan (1960) for selected days in each month. Table IV.1 presents the values of r for the 15th day of each month.

Jan.	Feb.	Mar.	Apr.	May	June
1.0315	1.0235	1.0103	0.9913	0.9757	0.9680

July	Aug.	Sept.	Oct.	Nov.	Dec.
0.9680	0.9757	0.9898	1.0087	1.0238	1.0318

Table IV.1 The monthly values of the ratio r

For a horizontal surface outside the atmosphere, the received intensity of radiation, I_{oh}, is equal to the intensity at normal incidence outside the atmosphere multiplied by the absolute value of c, the direction cosine of the sun'srays in the vertical direction.

$$I_{oh} = r\, I_{sc} \mid c \mid$$

Substituting c from equation III.1

Then $$I_{oh} = r\, I_{sc}(\cos l \cos d \cos h_a + \sin l \sin d)$$

where h_a is the absolute value of hour angle in radians.

$$I_{oh} = r\, I_{sc}(\cos l \cos d \cos(\tfrac{\pi}{12} t_a) + \sin l \sin d) \qquad \text{IV.1}$$

where t_a is the absolute value of time in hours from noon.

The daily value of total radiation, T_{oh}, can be obtained by integrating equation IV.1 over the time from sunrise to sunset or, using symmetry about solar noon, by doubling the integration from noon to sunset.

$$T_{oh} = 2 \int_{t_a = 0}^{t_a = t_{sa}} I_{oh} \, d\, t_a$$

where t_{sa} is the absolute value of sunset time measured in hours from noon.

$$T_{oh} = 2\, r\, I_{sc} \left[\cos l \cos d \sin\left(\frac{\pi}{12} t_a\right) + \sin l \sin d\, t_a\right]_{t_a=0}^{t_a=t_{sa}}$$

$$= 2\, r\, I_{sc} \left[\left\{\cos l \cos d \sin\left(\frac{\pi}{12} t_s\right)\left(\frac{12}{\pi}\right) + \sin l \sin d\, t_s\right\} - \right.$$

$$\left.\left\{\cos l \cos d \sin 0^{o} + \sin l \sin d \times 0\right\}\right]$$

$$= 2\, r\, I_{sc} \left\{\cos l \cos d \sin\left(\frac{\pi}{12} t_{sa}\right)\left(\frac{12}{\pi}\right) + \sin l \sin d\, t_{sa}\right\}$$

$$= \frac{24}{\pi}\, r\, I_{sc} \left\{\cos l \cos d \sin\left(\frac{\pi}{12} t_{sa}\right) + \frac{\pi}{12} \sin l \sin d\, t_{sa}\right\}$$

Then $T_{oh} = \frac{24}{\pi}\, r\, I_{sc} \left(\cos l \cos d \sin h_{sa} + \sin l \sin d\, h_{sa}\right)$

where h_s is the absolute value of sunset hour angle in radians.

When values of solar declination, d, and the ratio r for the middle day of each month are substituted in equation IV.2, the values which result, $\overline{T_{oh}}$, represent the monthly average amounts of daily radiation received by a horizontal surface outside the atmosphere. Monthly values of cloudiness index can then be calculated as follows.

$$\overline{K} = \frac{\overline{T_h}}{\overline{T_{oh}}} \qquad \text{IV.3}$$

where $\overline{T_h}$ is the monthly mean value of daily total radiation given in Table A2.1.

Liu and Jordan (1960) plotted the ratio, f_d, of the monthly average daily diffuse radiation to the monthly average daily total radiation as a function of the cloudiness index, $\overline{K}$. Based on the records of four stations, a good correlation between the two variables was found. The graph representing this relation is given in figure IV.1. The monthly value of direct solar radiation on a horizontal surface is then deduced as :

$$\overline{D_h} = \overline{T_h} (1 - f_d) \qquad \text{IV.4}$$

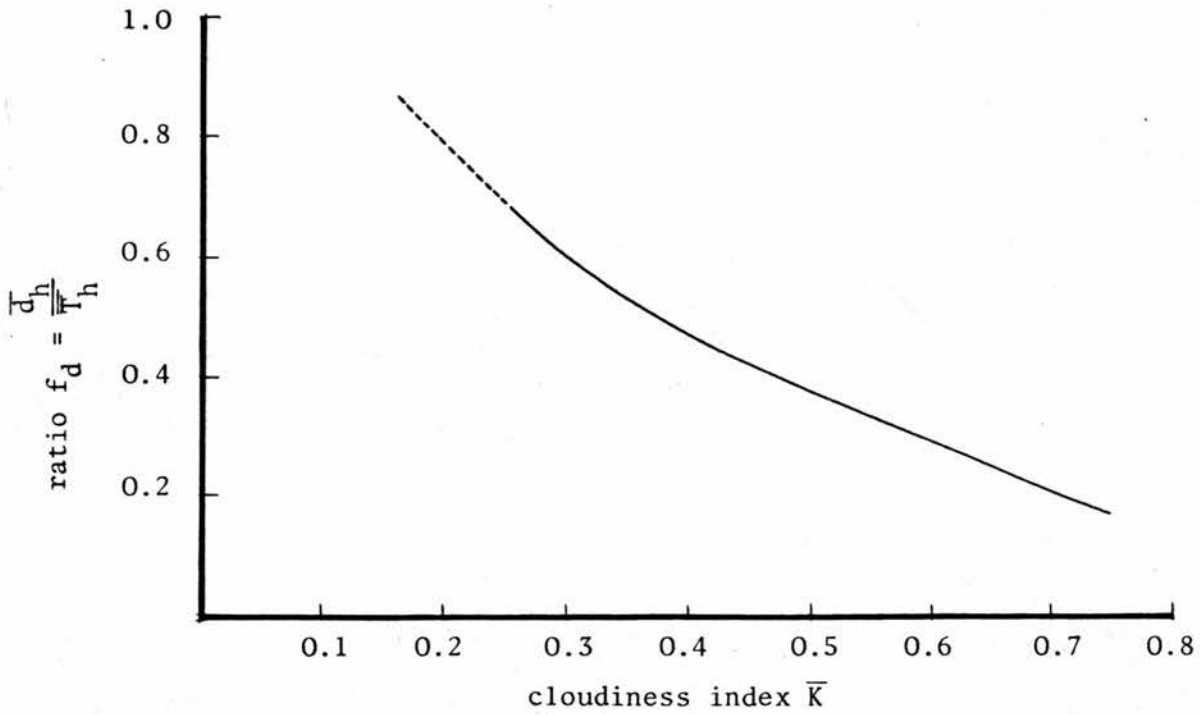

Figure IV.1 The ratio of the monthly average daily diffuse radiation to the monthly average daily total radiation as a function of the cloudiness index (After Liu and Jordan (1960))

IV.2.2 Estimating the intensities of direct radiation received by a surface at any time

The intensity of the direct component of radiation reaching a surface on the earth is the product of the direct normal irradiation, I_{Dn}, and the cosine of the angle of incidence between the sun's rays and a line perpendicular to the surface. An attempt has been made by Stephenson (1965) to establish an equation for calculating the values of I_{Dn}.

He analysed the records of direct normal radiation obtained at the Scarborough station in Canada over a period of three years. Only the data for the clearest days in all seasons were chosen for analysis. Values of I_{Dn} were plotted on a logarithmic scale against values of air mass, m, a term used to represent the length of the path crossed by the sun's rays as a ratio to the depth of atmosphere. It is equivalent to the cosecant of the solar altitude θ. The relationship was found to be closely represented by a straight line which, when extended, intersects the axis of m = 0 at the logarithm of what is defined as the apparent solar constant, I_{as}. It was found that I_{as} has a value of about 85 percent of the true solar constant (Degelman, 1966).

The equation for I_{Dn} can be written as follows :

$$I_{Dn} = I_{as}\, e^{(-Am)}$$

$$\therefore \quad I_{Dn} = 0.85\, r I_{sc}\, e^{(-A/\sin\theta)} \qquad \text{IV.5}$$

The term A represents the atmospheric extinction coefficient. Stephenson (1965) has found that value of A varies during the year and that its summer value is double its winter value. Since the extinction coefficient indicates the degree of haziness or cloudiness of the locality where observations are made, its values are strictly valid for use

only in such a locality. In order to find the values that would be suitable for the locality concerned in the present study, let I_{Dh} be the intensity of direct radiation on a horizontal surface. As mentioned above it is equal to the intensity of direct radiation at normal incidence, I_{Dn}, reduced by the cosine of the angle of incidence which, in the case of a horizontal surface, is equal to the sine of solar altitude.

Then

$$I_{Dh} = I_{Dn} \sin \theta \qquad \text{IV.6}$$

From equation IV.5 then :

$$I_{Dh} = \frac{0.85\ r\ I_{sc} \sin \theta}{e^{(A/\sin \theta)}} \qquad \text{IV.7}$$

Since the daily direct radiation on a horizontal surface equals the integration of the values of radiation intensity over the time from sunrise to sunset, the daily direct radiation is given by :

$$D_h = \int_{t=t_R}^{t=t_S} I_{Dh}\, dt \qquad \text{IV.8}$$

The monthly average of daily direct radiation, $\overline{D_h}$, is expressed as follows :

$$\overline{D_h} = \left(\sum_{N=N_f}^{N_L} D_h \right) / (N_L - N_f + 1)$$

where N_f is the first day of the month and N_L is the last day.

Since the values of solar altitude are symmetrical about solar noon, the integration in equation IV.8 needs to be evaluated only over the time from sunrise to noon and then doubled. The daily direct radiation received on a horizontal surface is

$$D_h = 2 \int_{t=t_R}^{t=12} 0.85 \; r \; I_{sc} \; e^{(-A/\sin \theta)} \sin \theta \; dt \qquad \text{IV.9}$$

For approximate evaluation of the integration in equation IV.9, let the time span be divided into ν intervals, then the interval, ω, equals $\dfrac{12 - t_R}{\nu}$

$$D_h = 0.85 \; r \; I_{sc} \; \omega (e^{-A/\sin 0^o} \sin 0^o + 2 \, e^{-A/\sin \theta_1} \sin \theta_1 \; \ldots\ldots$$

$$\ldots\ldots + 2 \, e^{-A/\sin \theta_{\nu-1}} \sin \theta_{\nu-1} + e^{-A/\sin \theta_\nu} \sin \theta_\nu)$$

where θ_ν is the maximum solar altitude; i.e., at noon. It is found by substituting the hour angle by zero in the expression : $\sin \theta = \cos l \cos d \cos h + \sin l \sin d$

$$D_h = 0.85\ r\ I_{sc}\ \omega \left\{ \sum_{i=1}^{i=\nu-1} \left(e^{-A/\sin \theta_i} \sin \theta_i \right) + e^{-A/\sin \theta_\nu} \sin \theta_\nu \right\}$$

IV.10

From equation IV.10, D_h could be expressed in terms of A by choosing a small value for A, evaluating D_h and repeating for all days of the month. The monthly average is obtained and then compared with the corresponding value of $\overline{D_h}$ obtained from equation IV.4. This procedure may be repeated, making small changes to the value of A, until the difference between the two computed values is negligible and thence the appropriate value of A is reached.

Knowing the monthly values of A, equation IV.5 is then used to calculate the instantaneous values of I_{Dn} for the middle day of each month.

The equations IV.2 to IV.10 were incorporated in a computer subroutine SOLRAD. The input data include values of the solar constant, the latitude of the locality and solar declination. They also include values of the monthly average of daily total radiation given in Table A2.1, values of f_d extracted from figure IV.1 and values of the ratio r given in table IV.1. Figures IV.2 and IV.3 show the variations of the computed values of I_{Dn} with the time of day for the middle day of both the summer months and the winter months.

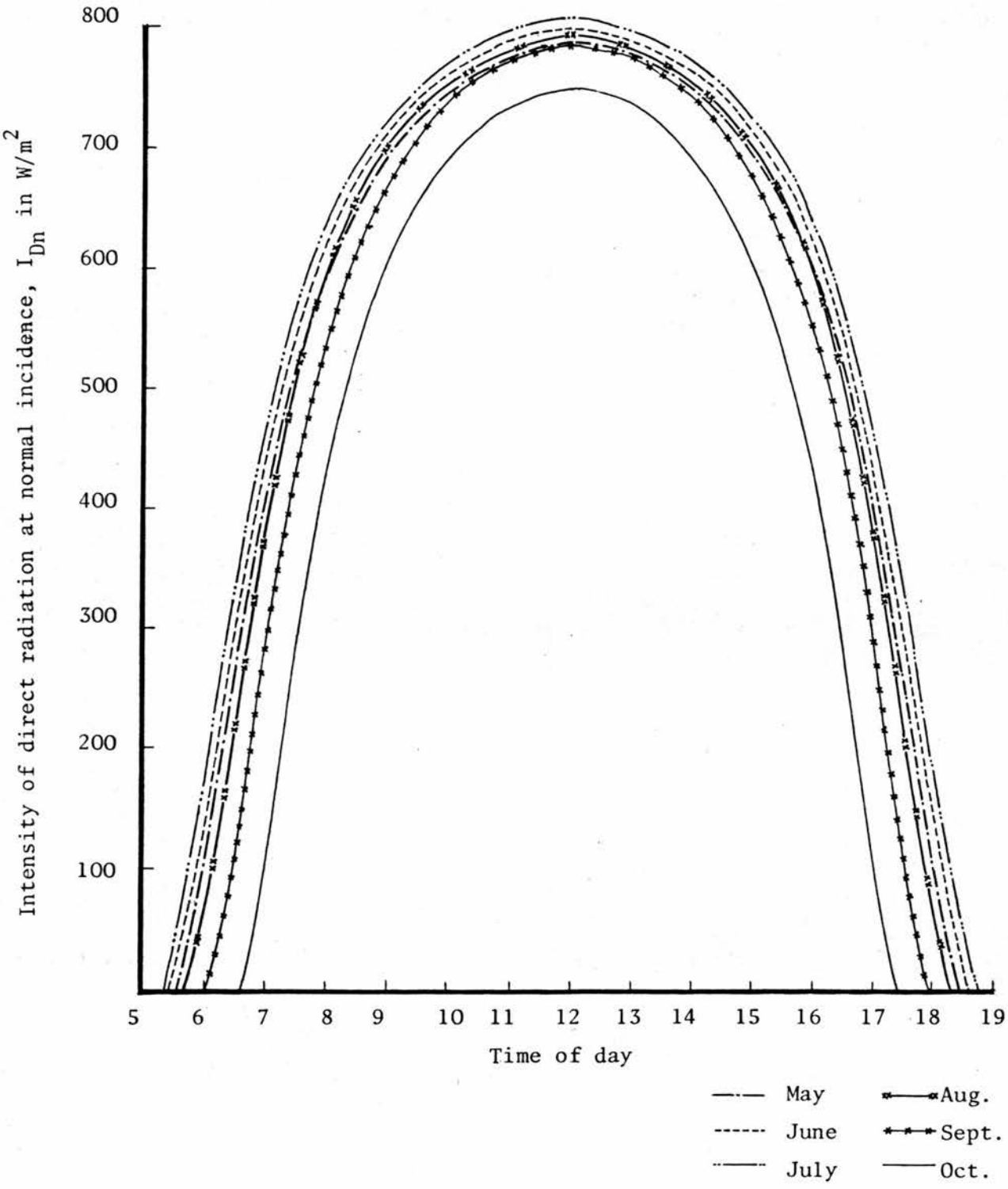

Figure IV.1 Variation of the values of I_{Dn} with the time of day for the middle day of summer months

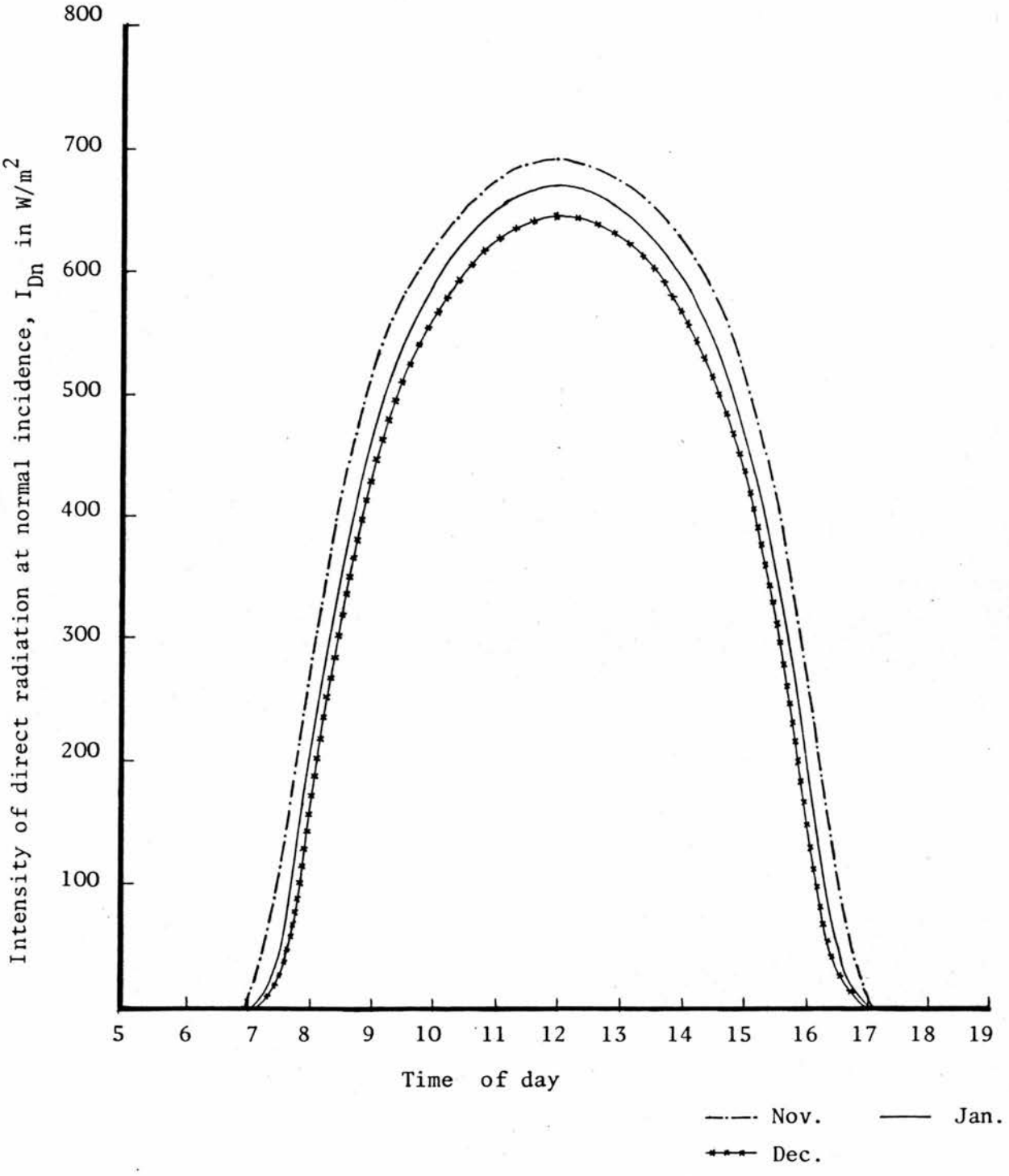

Figure IV.2 Variation of the values of I_{Dn} with the time of day for the middle day of winter months

IV.2.3 Diffuse radiation from the sky

Studies directed towards establishing techniques for estimating the diffuse short-wave radiation coming from the sky (Liu and Jordan, 1960, Threlkeld, 1963, Stephenson, 1965 and Degelman, 1966) have presented two sets of relationships. The first one concerns the relationship between the diffuse sky radiation incident on a horizontal surface and the intensity of direct normal radiation. Stephenson (1965) has concluded that, on clear days, the first quantity is directly proportional to the second one :

$$I_{dh} = B\, I_{Dn} \qquad \text{IV.12}$$

The value of B can be assessed in the light of the investigations conducted by Liu and Jordan (1960) who have introduced two dimensionless coefficients : τ_D, the transmission coefficient for direct solar radiation and τ_d, the transmission coefficient for diffuse radiation on a horizontal surface. By definition :

$$\tau_D = \frac{I_{Dh}}{I_{oh}} \quad \text{and} \quad \tau_d = \frac{I_{dh}}{I_{oh}}$$

The two coefficients are functions of the solar altitude, water vapour content and the other depleting contents in the atmosphere. The functional relationship between τ_D and τ_d

has been presented in the following form (Liu and Jordan, 1960) :

$$\tau_d = 0.2710 - 0.2939\ \tau_D$$

Hence $$\frac{I_{dh}}{I_{Dh}} = \frac{0.2710}{\tau_D} - 0.2939$$

and since $I_{Dh} = I_{Dn} \sin \theta$

where θ is the solar altitude

Then $$\frac{I_{dh}}{I_{Dn} \sin \theta} = \left(\frac{0.2710}{\tau_D} - 0.2939 \right)$$

$$\frac{B}{\sin \theta} = \left(\frac{0.2710}{\tau_D} - 0.2939 \right)$$

But $$\tau_D = \frac{I_{Dn}}{I_{on}} = \frac{I_{Dn}}{rI_{sc}} = \frac{0.85\ rI_{sc}\ e^{-A/\sin \theta}}{rI_{sc}}$$

Then $$\frac{B}{\sin \theta} = \left(\frac{0.2710}{0.85\ e^{-A/\sin \theta}} \right) - 0.2939$$

IV.13

The expression given in equation IV.13 shows that the value of B depends on the atmospheric extinction coefficient, A, and the solar altitude, θ. For a given value of A (e.g., the monthly average value), values of $\frac{B}{\sin \theta}$ that

correspond to different values of θ were calculated and plotted in figure IV.4. The figure shows that for all values of θ greater than 25°, $\frac{B}{\sin \theta}$ has values between 0.10 and 0.20. As the value of θ approaches zero, the value of $\frac{B}{\sin \theta}$ increases progressively.

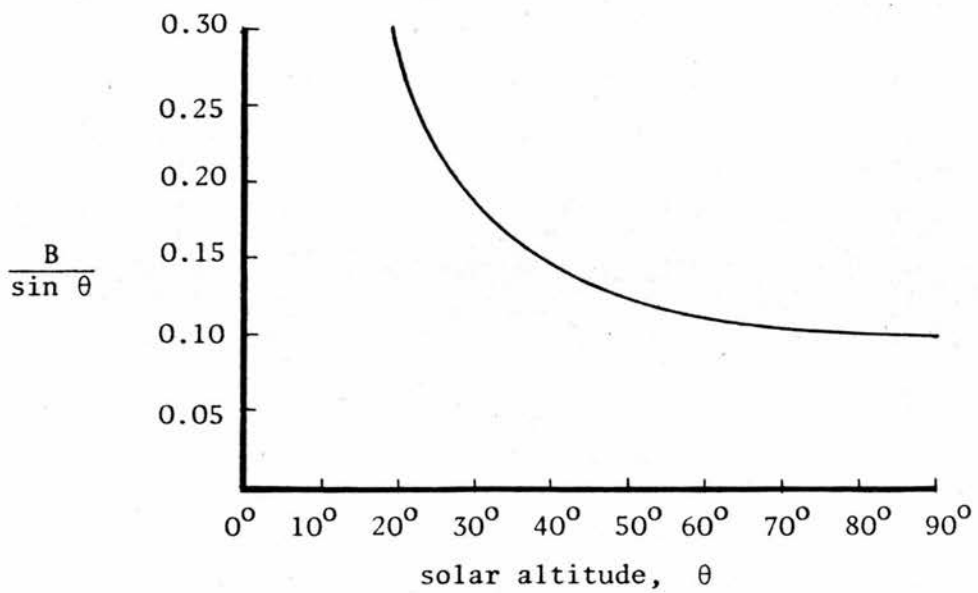

Figure IV.4 Variation of values of $\frac{B}{\sin \theta}$ against variation of solar altitude (for a given value of A, A = 0.207)

The second set of relationships concerns the dependence of the diffuse sky radiation incident on vertical surfaces on the diffuse irradiation of a horizontal surface. Observations have shown that, on clear days, the sky is non-uniform radiator of diffuse radiation and that the angle of incidence of the

sun's direct rays has a strong influence upon the incidence of diffuse sky radiation upon a vertical surface (Threlkeld, 1963). It has been shown by Threlkeld (1963) that the diffuse short-wave radiation incident on a vertical surface could be related to the diffuse irradiation of a horizontal surface and the cosine of the sun's incidence angle to the vertical surface. This relationship has been represented by the following expressions (Stephenson, 1965) :

$$I_{dv} = I_{dh} F \qquad \text{IV.14}$$

where $F = 0.55 + 0.437 \cos \gamma + 0.313 \cos^2 \gamma$

when $\cos \gamma > -0.2$

and $F = 0.45$

when $\cos \gamma < -0.2$

γ is the sun's incidence angle to the vertical surface.

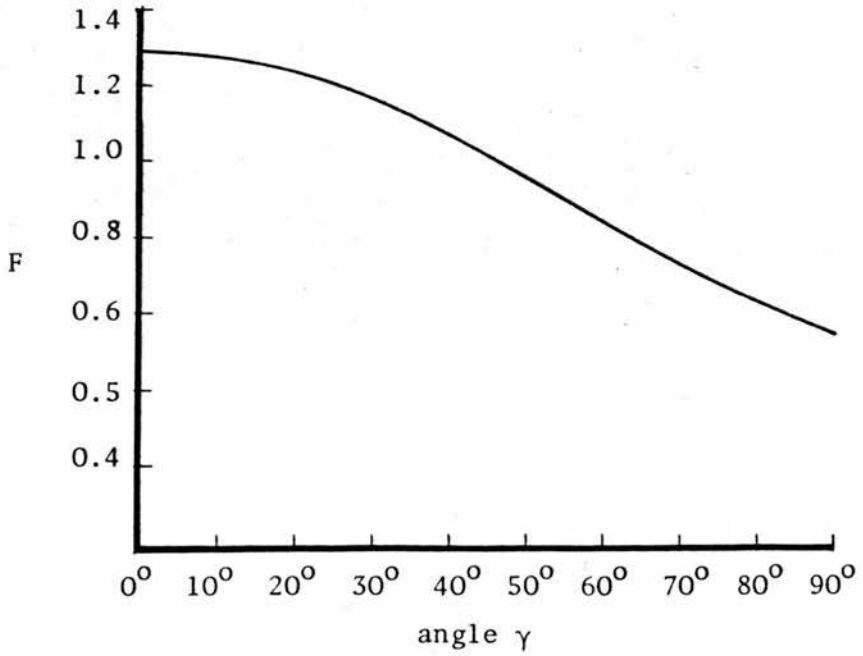

Figure IV.5 Variation of values of F against variation of the angle γ

From equations IV.12 and IV.14

$$I_{dv} = I_{Dn} \; B \; F$$

But $$I_{Dv} = I_{Dn} \sin \theta$$

$$\therefore \quad \frac{I_{dv}}{I_{Dv}} = \frac{B}{\sin \theta} \; F \qquad \text{IV.15}$$

Inspection of the values of $\frac{B}{\sin \theta}$ and F produced in figures IV.4 and IV.5 shows that, excluding the small values of the angles θ and γ, the value of $\frac{B}{\sin \theta}$ ranges from 0.1 to 0.2 according to the value of θ, and that the value of F ranges from 0.6 to 1.2 according to the value of γ. This suggests that the ratio $\frac{I_{dv}}{I_{Dv}}$ ranges from 0.06 to 0.24 for all cases of the sun's incidence angle to the surface.

The foregoing discussion reveals the following :

(i) In the clear sky conditions which are presumed to prevail in the locality under consideration, the diffuse sky radiation is not uniformly distributed over the sky dome.

(ii) The diffused radiation received by a vertical surface is directly proportional to the direct irradiation of the surface.

(iii) For high altitudes the ratio of $\frac{I_{dv}}{I_{Dv}}$ is very small, it increases with the decrease of solar altitude.

(iv) An attempt to include the diffuse sky radiation in the calculation of the solar radiation impact on the form's surfaces would only result in increasing the magnitude of the irradiation by a small percentage, but it would not affect the outcome of a comparative study based on considering the direct radiation component alone and excluding the diffuse component.

IV.3 Remarks on Evaluating the Solar Radiation Impact on a Courtyard's Surfaces

(a) The main objective of constructing the model described in this part was to generate the detailed irradiation data for a wide range and combinations of form parameters. The investigation was carried out in two stages: the first one, which has been discussed so far, dealt with the initial irradiation input, whereas the second stage, which will be described in Chapter VII deals with the final thermal load absorbed at the surfaces of the form.

(b) Regarding the initial irradiation input, the direct component of the solar radiation is the dominant source of the thermal excitation to which the form is exposed. It was decided to consider the value of the direct irradiation of the form using a comparative index of the initial irradiation load received at the surfaces of the form.

(c) Equations for calculating the exposed areas of a form's surfaces at any time were presented in Chapter III. When such equations are coupled with the equations presented in the present chapter, the instantaneous initial irradiation of the different surfaces can be calculated.

(d) The climate considered in the study is characterised by hot summers and cold winters, therefore it is desirable to minimize the irradiation input during the summer time and to maximize it during the winter. Accordingly, it was decided to conduct the investigations for two distinctive seasons, each one being represented by the middle days of its months as described in section I.3. The irradiation input is calculated for any specified day from the values calculated at small intervals during day time (see section III.2). The seasonal figure of daily irradiation

is then calculated by averaging the daily figures of the representative days of the season. Accordingly, there are two measures of the initial irradiation input of the form's surfaces : the summer average daily irradiation and the winter average daily irradiation.

CHAPTER V

THE COMPUTER PROGRAM

V.1 Description of the Program

A computer program was developed for assessing the direct solar irradiation on the surfaces of courtyard form. This was written in FORTRAN IV for the university's IBM 370 computer. The program was made sufficiently general to allow the assessment of the irradiation of courtyards of any proportion, size or orientation, located at any point on the earth and integrated over any time span. A descriptive outline of the program is presented below.

The task of the program is divided into the following interlinked steps :

Step 1 : is to read and organize the data of the geometry of the form. It is instructed in subroutine CYDATA. The data include values of the angle of orientation, ranging from 0^{o} to 90^{o} in steps of 15^{o}, and values of the three sets of ratios, R_1, R_2 and R_3. The ratio, R_1, of perimeter, P, to height, H, is chosen to range from 1 to 10 in unit steps. The ratio, R_2, of width, W, to length, L, is given the values from 0.1 to 1. Assuming a unit area of walls' surfaces, a set of proportions of W:L:H is generated. A variation on this main set is produced by varying the ratio, R_3, of the top

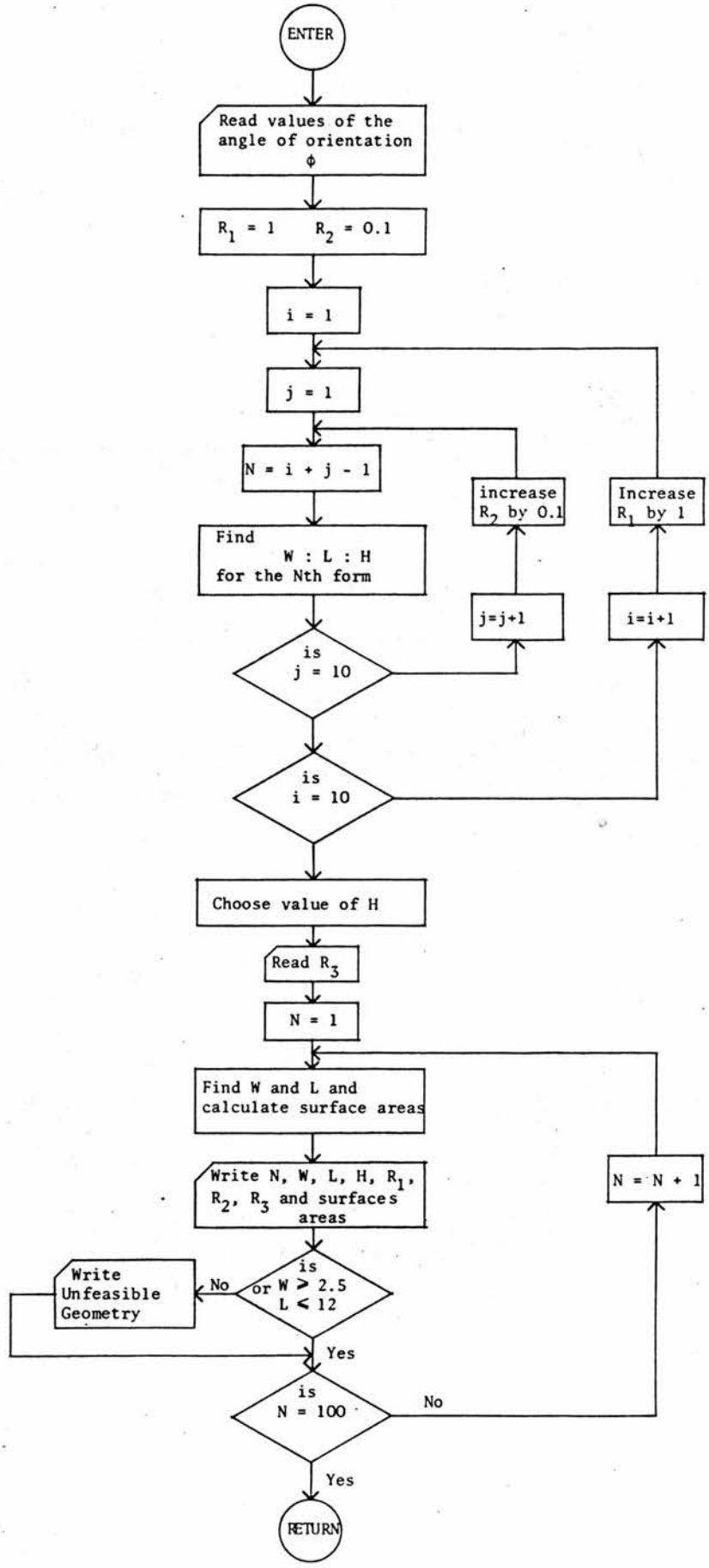

Figure V.1 Flow chart for subroutine CYDATA

opening of the form, A_T, to its ground area, A_G. The height, H, is given some actual dimensions, then the corresponding values of width and length are produced and arranged in a two-dimensional array. The subroutine includes a check on the dimensions of the plan. A minimum width of 2.5 m and a maximum length of 12 m are considered the limits for an architecturally acceptable domestic courtyard.

Step 2 : is to establish a table of insolation factors for each selected case of geometry. Subroutine INSOL is constructed for this purpose; it considers a wide range of values of declination and hour angle (see section III.4.3). For each combination it calculates the values of the direction cosines, a, b and c. It examines these values to find which of the form's top corners is closer to the sun; that is,to determine the location of the point n. Then it checks the location of the point n_s (shadow of n) in order to determine the case of shading. Four cases are distinguished as explained in section III.3. In order to calculate the areas of the insolated surfaces of a courtyard's envelope, four subroutines (SHADE 1, SHADE 2, SHADE 3 and SHADE 4) are prepared, one for each case of shading. When the area of an insolated surface is multiplied by the relevant component, a, b or c that lies perpendicular to the surface under consideration, the product is called the

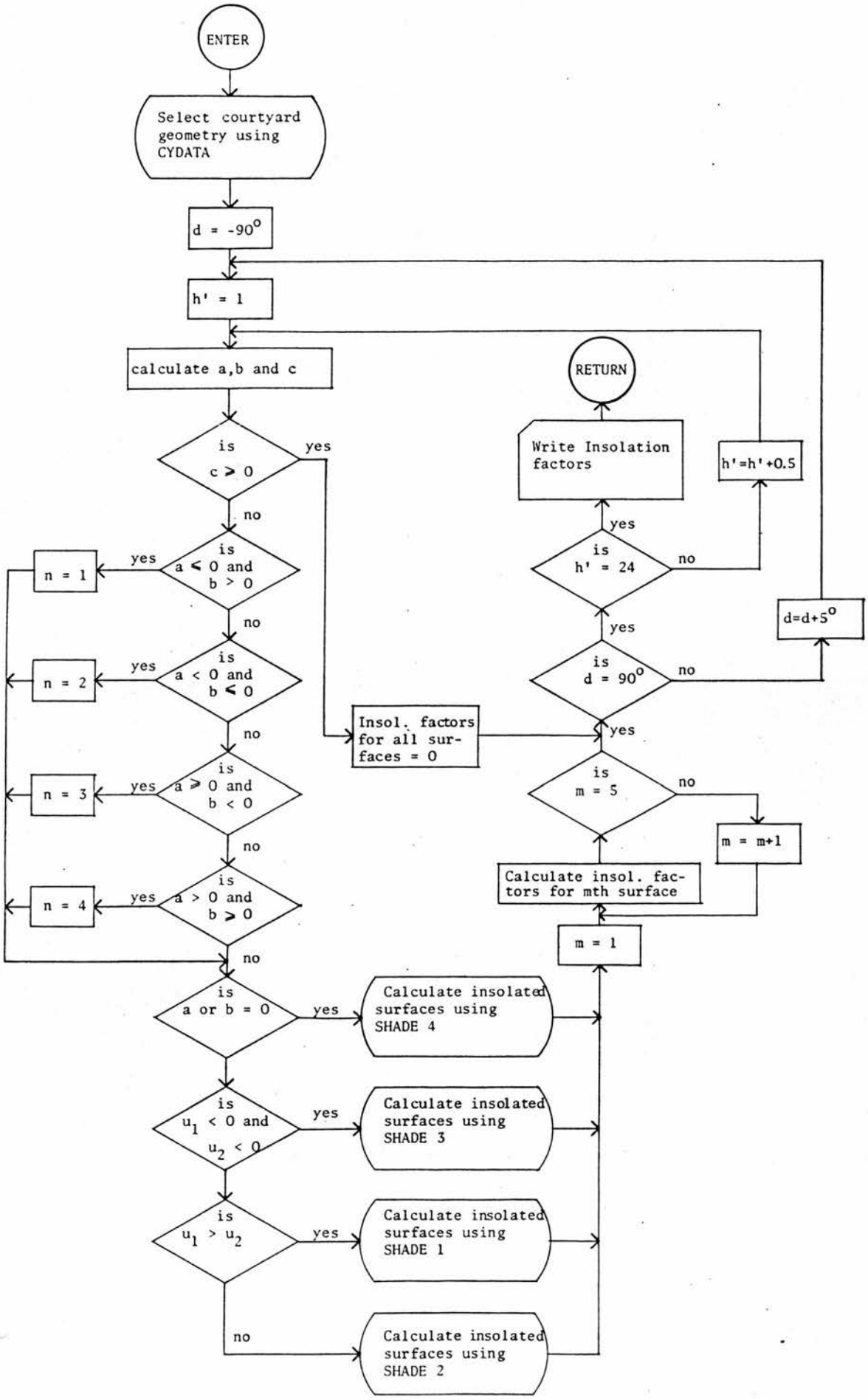

Figure V.2 Flow chart for subroutine INSOL

insolation factor of the surface. Values of the insolation factors are arranged in a three-dimensional array according to the surface's number, the solar declination and the hour angle. A flow chart of the subroutine INSOL is shown in figure V.2.

Step 3 : is to prepare the necessary data concerning the solar geometry. Subroutine SOLGEO (see figure V.3) is constructed to calculate, for any day, the sunrise and sunset times, length of day time and values of the hour angle at any time during the day. Days are numbered in annual sequence taking the first of January as day number 1. Starting from day number 15 with an interval of 30, 12 days are considered to represent the twelve months. The subroutine is instructed to select the days that represent the season under consideration and to calculate the values of the hour angle at small invervals (from 20 to 30 minutes) during the day. A table containing values of solar declination and hour angle is produced. It describes the sun's position at some instances that are taken to represent a whole season.

Step 4 : is to check the angle of orientation, ϕ. If it is equal to zero,then this step will be ignored, otherwise the subroutine ROTATE, referred to in section III.4.3, is used for transforming the values of the hour angle and the solar declination, which are produced in the previous steps, to new combinations of values that retain the same geometrical relationships between the sun and the surfaces of the form.

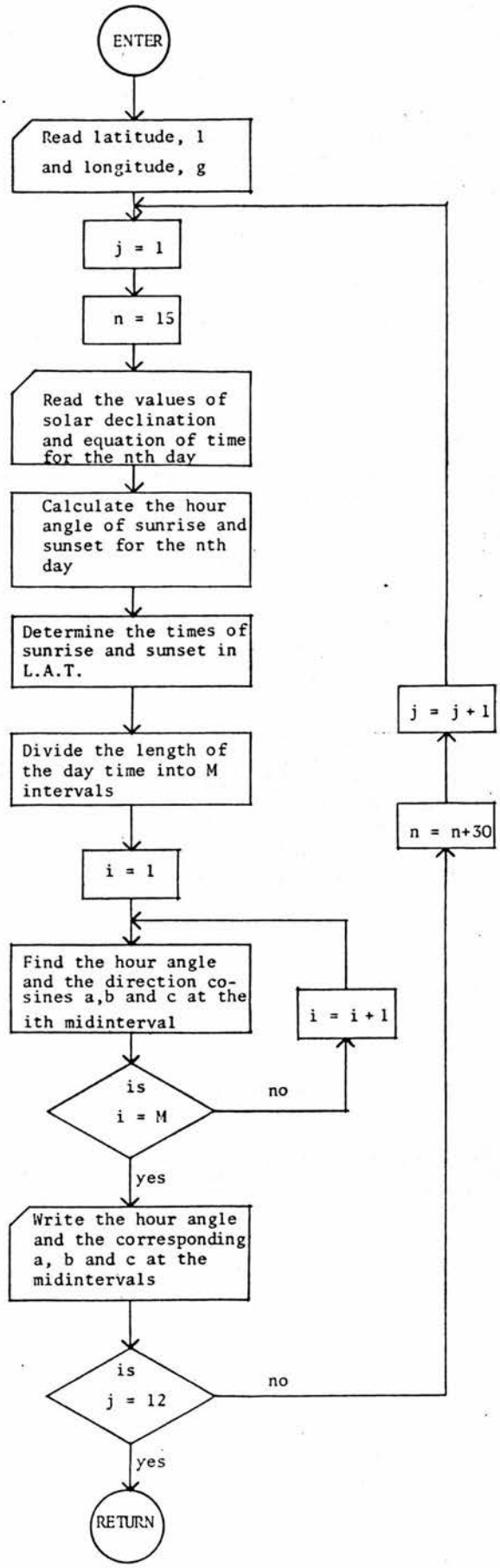

Figure V.3 Flow chart for subroutine SOLGEO

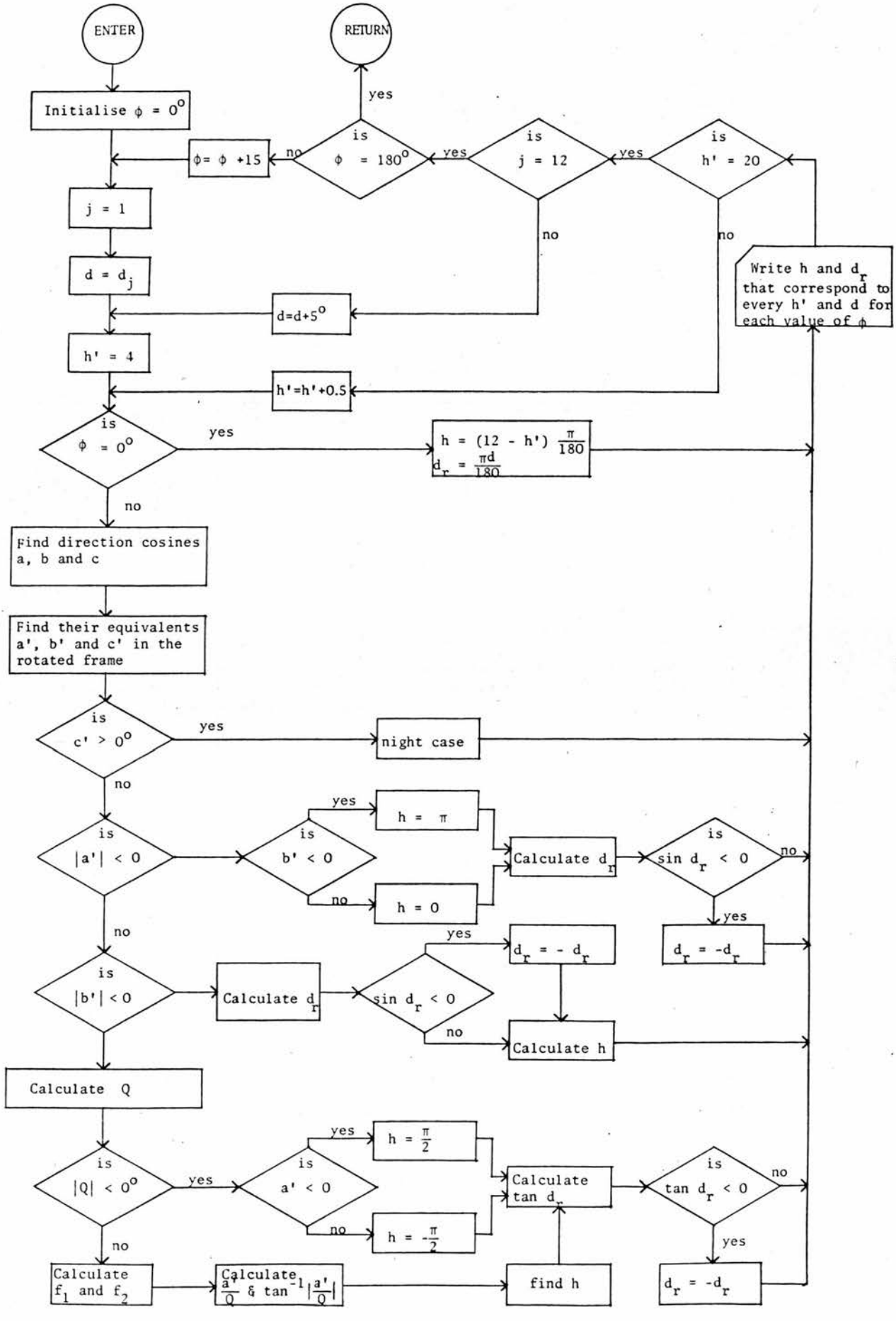

Figure V.4 Flow chart for subroutine ROTATE

The set of values of the hour angle is arranged in a three-dimensional array according to the angle of orientation, the day's number and the chosen times during the day. Another array is prepared for the values of the solar declination (see figure V.4).

Step 5 : is to check the computed values of hour angle and declination against those listed in the tables of insolation factors in order to find, by interpolation, the corresponding insolation factors. Subroutine SOLRAD is then called to produce the necessary data concerning the solar radiation. The subroutine is constructed to read a table of monthly average values of daily total radiation in the locality under consideration. By applying the mathematical procedure described in IV.2.2, it calculates the direct solar irradiation on a surface normal to the sun's rays, I_{Dn}, at any specified time. The values of the insolation factors are then multiplied by the corresponding values of I_{Dn} to get the direct irradiation on each surface at the chosen intervals during the representative days. A flow chart of the subroutine SOLRAD is shown in figure V.5.

Step 6 : is to compute the daily direct irradiation of each surface, and to find the total for all the surfaces. The seasonal average is then computed. The results are arranged in tables showing the angle of orientation, the case of geometry and the irradiation of each surface.

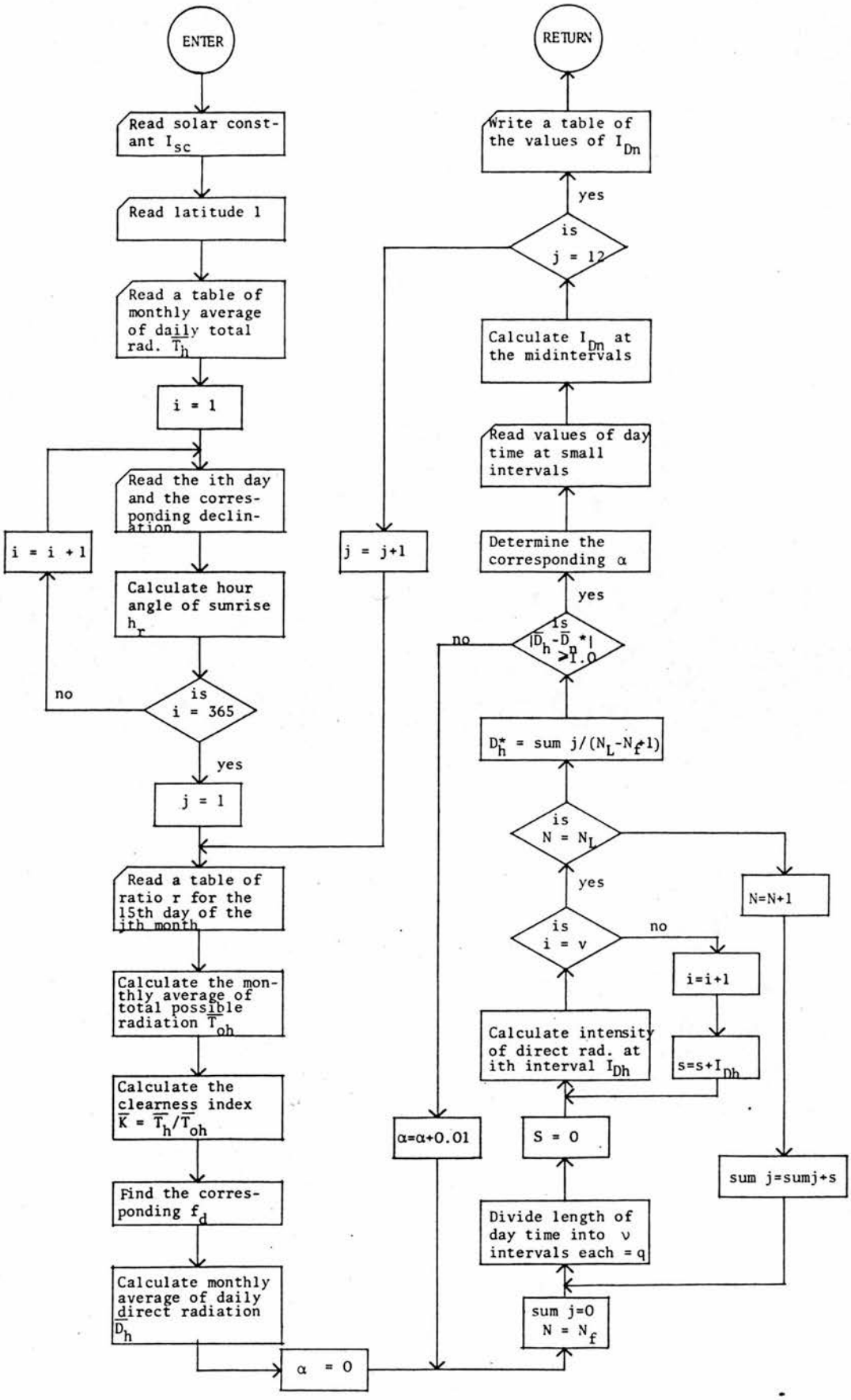

Figure V.5 Flow chart for subroutine SOLRAD

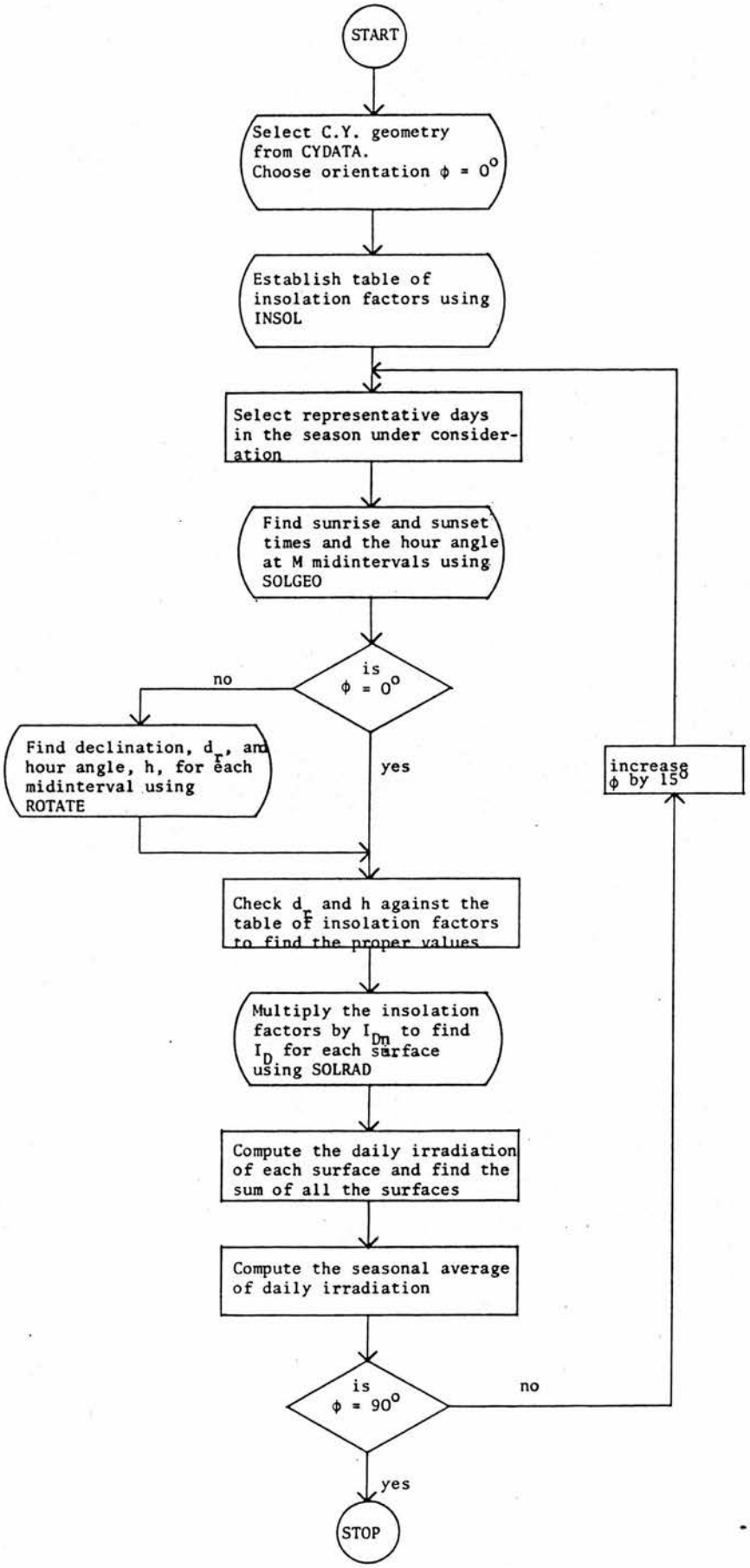

Figure V.6 Flow chart for the main program

The structure of the whole program is shown in figure V.6.

V.2 Remarks on Applying the Program

The program was applied for Cairo (Latitude 30^{o}N, Longitude 31^{o}E) as an example of a typical hot dry climate. The geographical parameters were specified to the program. The range of geometries described in Section V.1 was also specified. Firstly, forms were assumed to have a unit area of wall surface, the effect of changing the proportions was considered by changing each set of the ratios R_1, R_2 and R_3 in turn, while assuming a constant value of orientation of zero degrees. Different values of the angle of orientation were then considered. For each case of geometry, the seasonal averages of the daily direct irradiation of the surfaces of the four walls as well as that of the ground surface were calculated. Two sets of values were produced; one for summer and the other for winter.

To illustrate the effect of size, two cases of height were considered, 3 metres and 6 metres, that correspond to forms of one storey and two storey height respectively.

PART THREE : THE INVESTIGATION

CHAPTER VI

DISCUSSION OF THE RESULTS

VI.1 Objectives and Guidelines

The main objective of constructing the model presented in Chapters III and IV was to carry out detailed investigation into the thermal performance of courtyard forms. The following aims are adhered to during the analysis of the results :

(a) to develop measures and indices of solar irradiation for evaluating the thermal performance of the courtyard form.

(b) to represent the variation of the irradiation of the form in relation to the variation of the parameters of the form.

(c) to identify the ranges within which the parameters of the form significantly affect the thermal performance.

The investigation was carried out in two stages : the first dealt with generating the data of the initial irradiation load on the form's surfaces for a wide range of combinations of the geometrical parameters of the form. Discussion of the results of this stage of investigation is presented in this chapter. Chapter VII is concerned with the second stage of

investigation which dealt with the final irradiation load on the form's surfaces. In each stage, the irradiation data were generated in terms of the seasonal average load. The reason for this was the thermal design criterion of minimizing the thermal load in summer and maximizing it in winter. The seasonal figures were obtained by averaging the data of the daily irradiation load for representative days of the season as described in section I.3.

VI.1.1 Irradiation numbers

Prior to deciding on the means of measuring the thermal performance of the courtyard form with respect to solar radiation, it is interesting to examine the dependence of the total initial irradiation of the form's surfaces on the geometrical parameters of the form. By the 'total initial irradiation' is meant the initial irradiation of the surfaces of the four walls plus that of the ground surface.

Consider a form having a unit floor area and fully open to the sky, i.e., with no projecting roof over its walls. Since the surfaces of the form receive that beam of the sun's rays which is bounded by the edges of its top opening, the total initial irradiation of the form's surfaces is equal to the irradiation of a horizontal unit surface, I_h. This quantity can be obtained by multiplying the value of I_{Dn}, as produced by

the subroutine SOLRAD, by the corresponding component, c, as produced by the subroutine SOLGEO.

$$I_h = c\, I_{Dn}$$

The integration of the previous expression over the period from sunrise to sunset yields the daily value of direct irradiation over a unit area of a horizontal surface.

$$D_h = 2 \int_{|c|=0}^{|c|=max} c\, I_{Dn}\, d\, c$$

Values of D_h were computed for the representative days of both summer and winter, and the seasonal averages were calculated. These averages are referred to as the summer irradiation number, N_s, and the winter irradiation number, N_W. For the locality under consideration (30^oN latitude), the numbers are found to be : $N_S = 0.49$ Kw/m^2 and $N_W = 0.39$ Kw/m^2. The total initial irradiation of the form's surfaces is then given by :

$$T_S = N_S\, A_T \qquad \text{Kw}$$

$$T_W = N_W\, A_T \qquad \text{Kw}$$

where T_S and T_W are the total irradiation of the form's surfaces in summer and winter respectively. A_T is the area of the top

opening of the form and it is the governing parameter as far as the total initial irradiation load on the form's surfaces is concerned. It is equal to the ground area A_G multiplied by the ratio R_3 (see section III .4.1). However, the distribution of this irradiation load over the ground and the walls surfaces depends mainly on the values of the ratios R_1 and R_2.

It is evident that the contribution of the walls' surfaces to the thermal load imposed on the indoor space - which is the ultimate concern in thermal design problems - is more significant than that of the ground surface. Therefore, it was decided to consider the area of walls surfaces as a basis for comparison between the thermal performance of different forms. On this basis, the forms considered in the study have been defined so that they have a unit area of wall surface. Two sets of values for the ratios R_1 and R_2 were chosen as described in section V.1.

A preliminary investigation was conducted concerning the distribution of the initial irradiation over the walls and the ground. The dependence of this distribution on the individual values of R_1 and R_2 may be described as follows. As R_1 becomes greater (i.e., the form gets shallower), the percentage of the radiation which is received by the ground surface, C_G, increases. Ultimately, it reaches 100% of the total irradiation of the form (when the height is equal to zero).

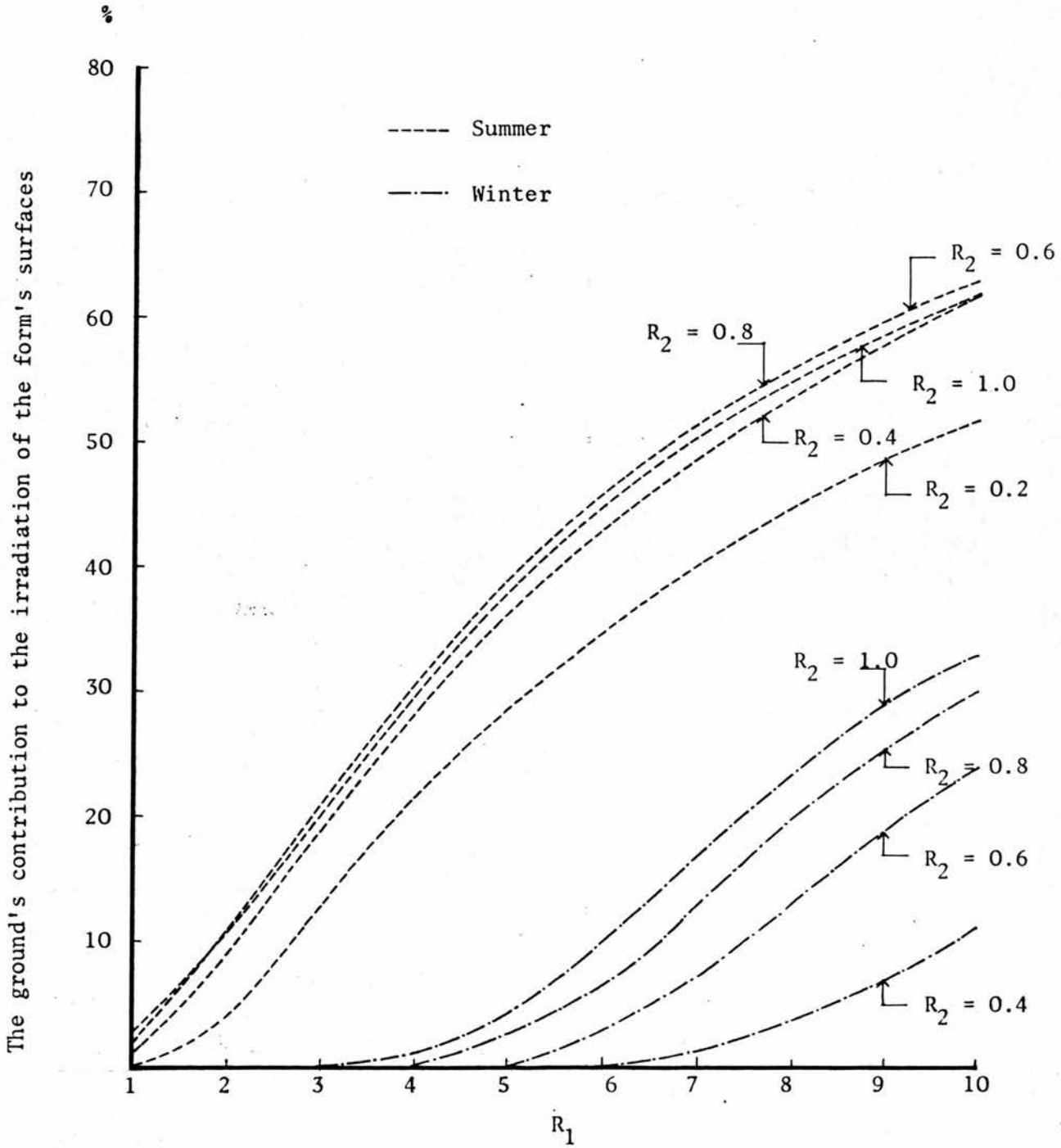

Figure VI.1 Contribution of the ground surface to the irradiation of the form's surfaces

The rate of this increase becomes greater as the ratio R_2 approaches unity (see figure VI.1).

In summer, the increase in the value of R_2 results in a corresponding increase in the percentage of the irradiation of the ground surface. As the value of R_2 approaches 0.5, any further increase has almost no effect on such a percentage (see figure VI.2). In winter, the contribution of the ground surface is considerably smaller as shown in figure VI.3. It approaches zero, for all values of R_2, as the ratio R_1 becomes smaller than 5. This explains how, for shallow forms, the irradiation values of the walls surfaces in winter might exceed the corresponding summer values.

VI.1.2 Measures of thermal performance

A preliminary investigation was carried out to develop an index for evaluating the effect of the mutual shading among the surfaces of the form on reducing the initial irradiation load. A set of elemental forms was generated by assuming a unit area of walls surface and varying the plan ratio from 0.1 to 1.0. Suppose that the surfaces of these forms are totally exposed to solar radiation (i.e., no shade cast by any wall over the others), the seasonal initial irradiation loads on the surfaces of the walls were calculated. The calculated values represent the potentials of the forms, with respect to plan ratio, to receive direct solar radiation. The effect of

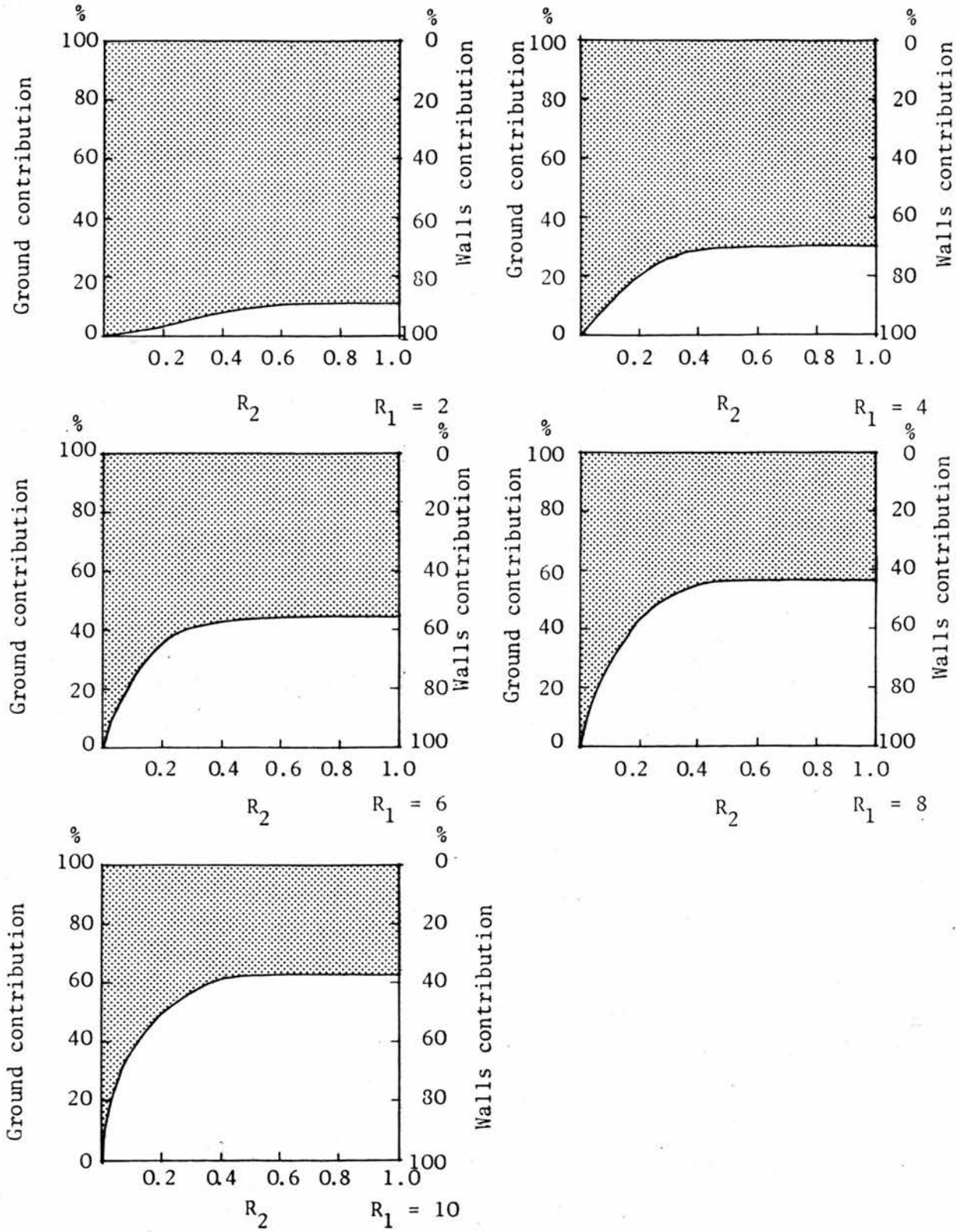

Figure VI.2 Distribution of the irradiation of the courtyard form between the ground and the four walls in summer

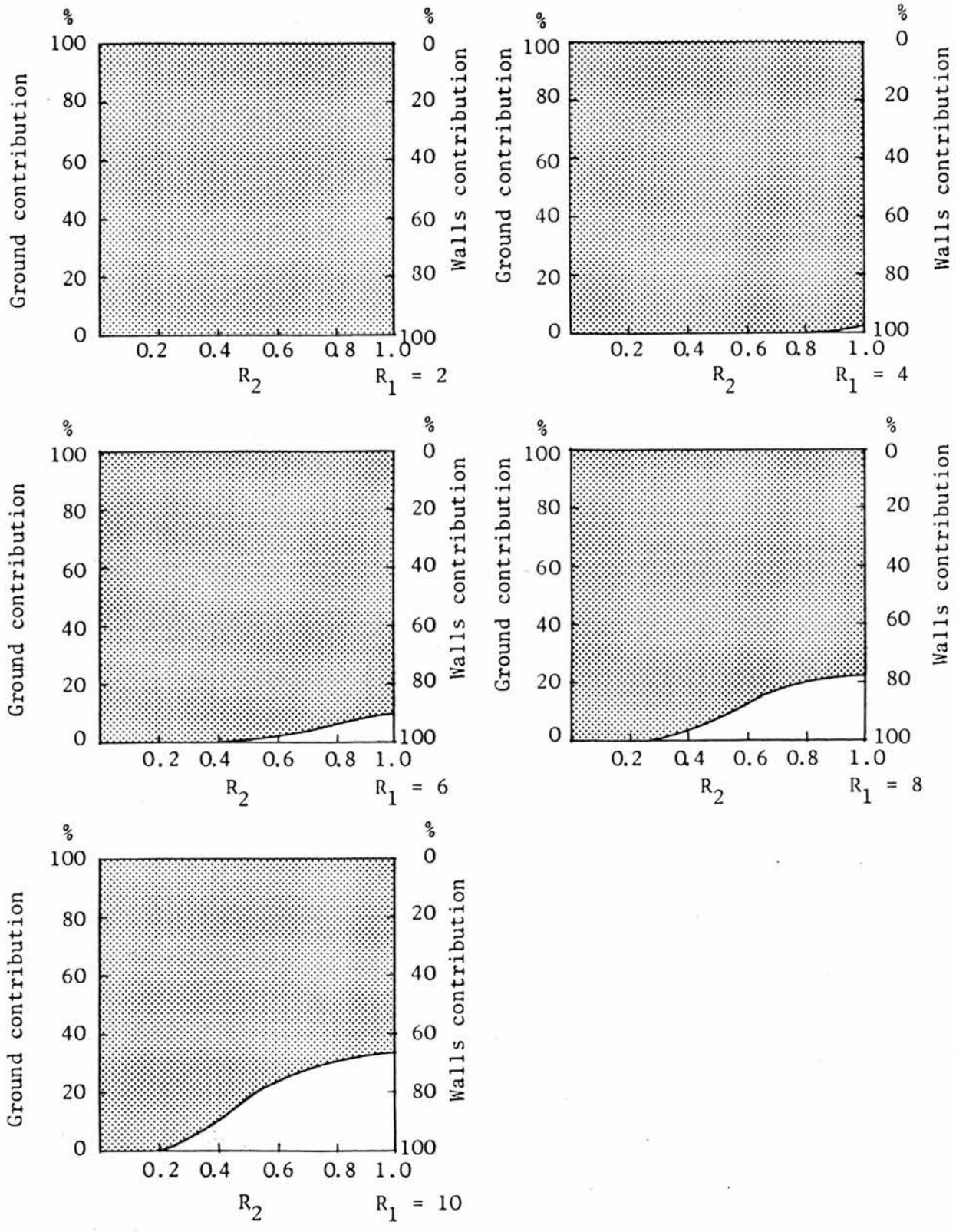

Figure VI.3 Distribution of the irradiation of the courtyard-form between the ground and the form walls in winter

mutual shading was then considered by calculating the irradiation load on the surfaces of courtyard forms having dimensions identical to these of the elemental forms. The term 'irradiation index' is introduced to indicate the performance of a courtyard form against the corresponding elemental form. It is equal to the ratio of the initial irradiation of the courtyard form to the potential irradiation of the elementary form.

Figures VI.4 and VI.5 show the irradiation index for the range of the forms considered in the study in both summer and winter. It is evident that the irradiation index is directly proportional to the ratio R_1, but the effect of changing the value of R_2 is not clearly expressed in the index. Such an effect can be studied among forms having the same value of R_1 by comparing the initial irradiation load on the surfaces of each form with the initial irradiation of a reference form. In summer, the reference form is defined as that one which receives the minimum initial irradiation load, within the chosen set of forms which have identical values of R_1. The deviation of the irradiation load of the other forms from the minimum is taken to represent the effect of changing the value of R_2. In winter, the deviation from the maximum attainable load is taken to represent the effect of changing the value of R_2. Figure VI.6 shows the percentage deviation of the irradiation load from the minimum and maximum irradiation loads in summer and winter respectively.

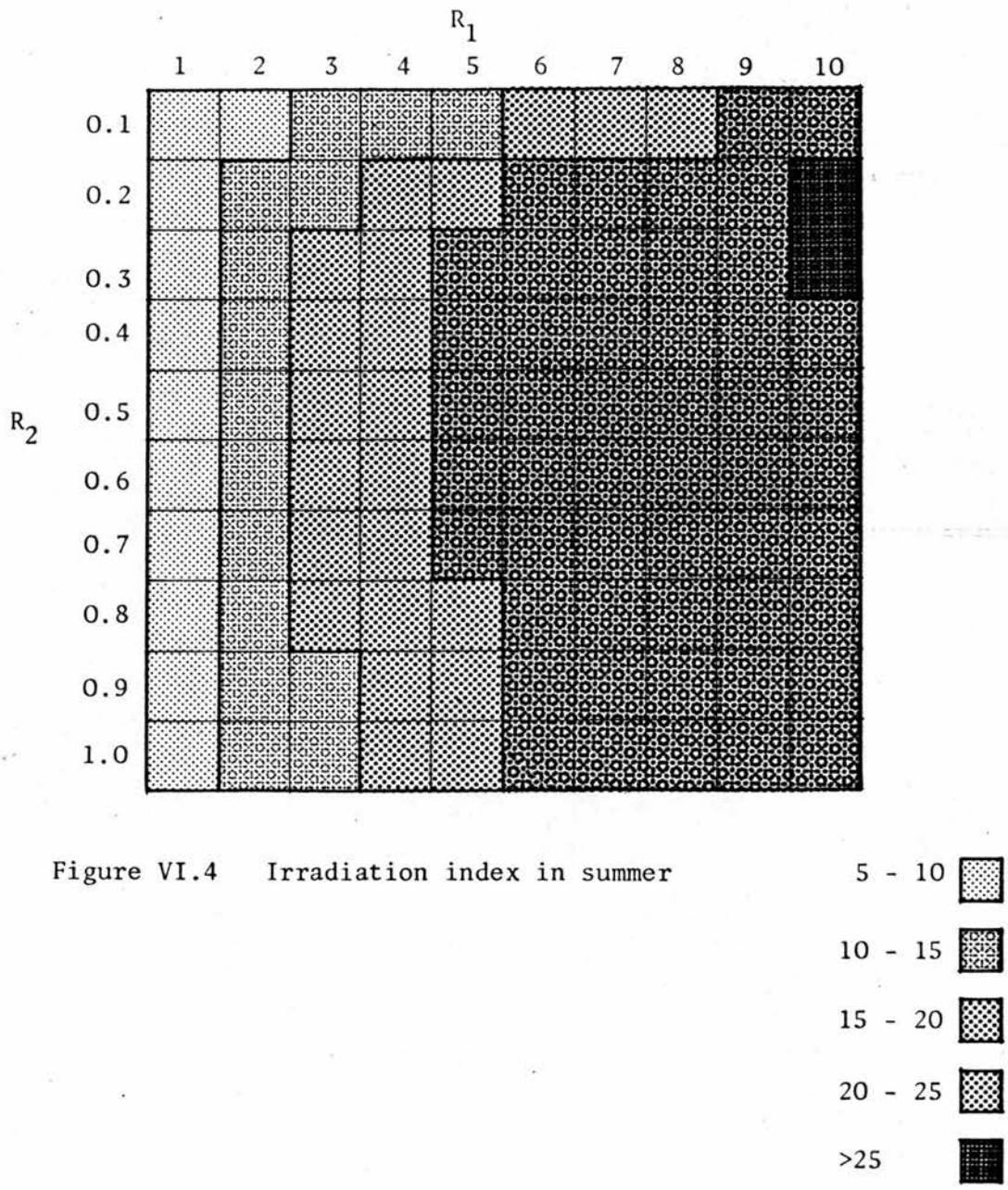

Figure VI.4 Irradiation index in summer

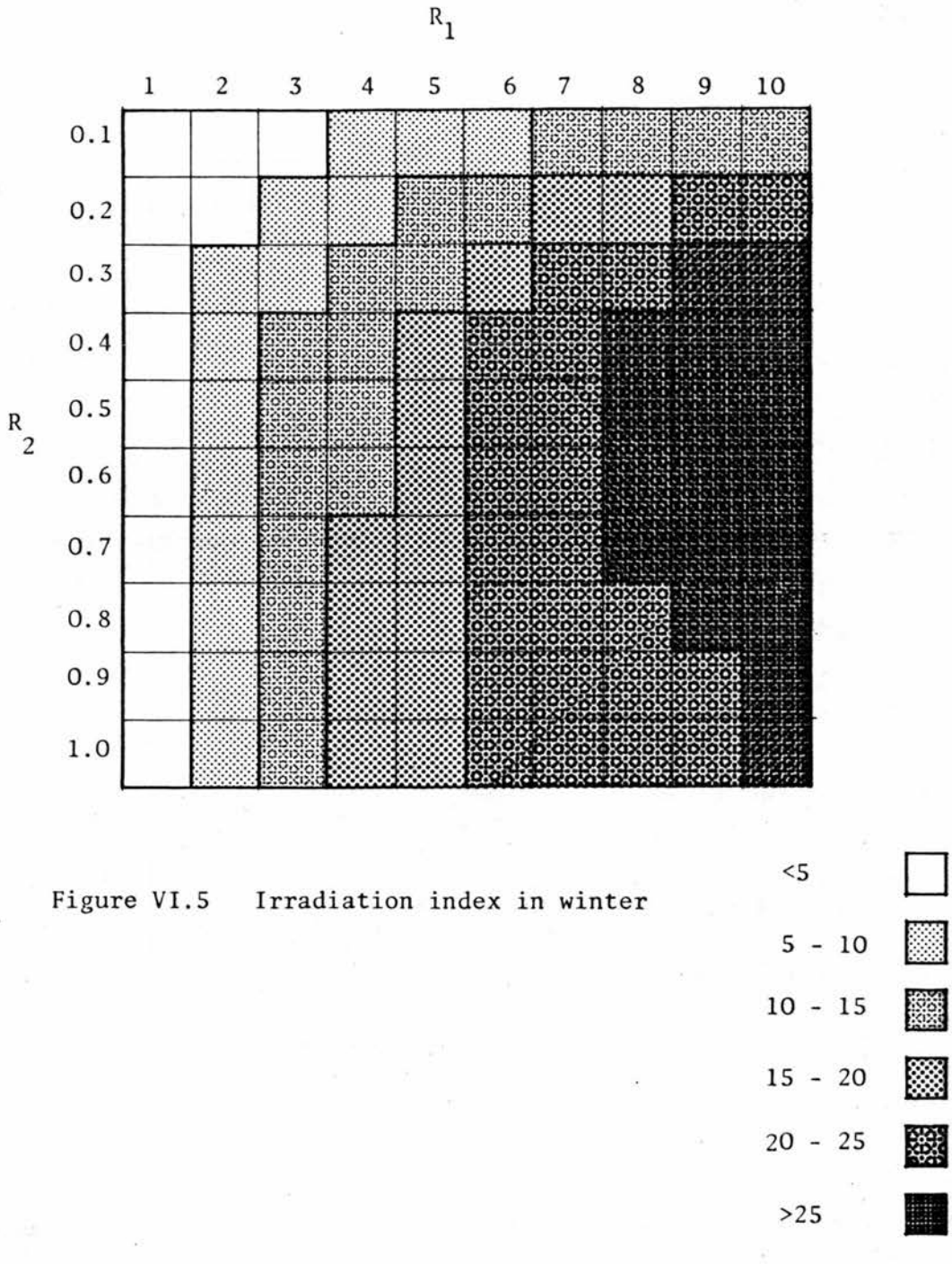

Figure VI.5 Irradiation index in winter

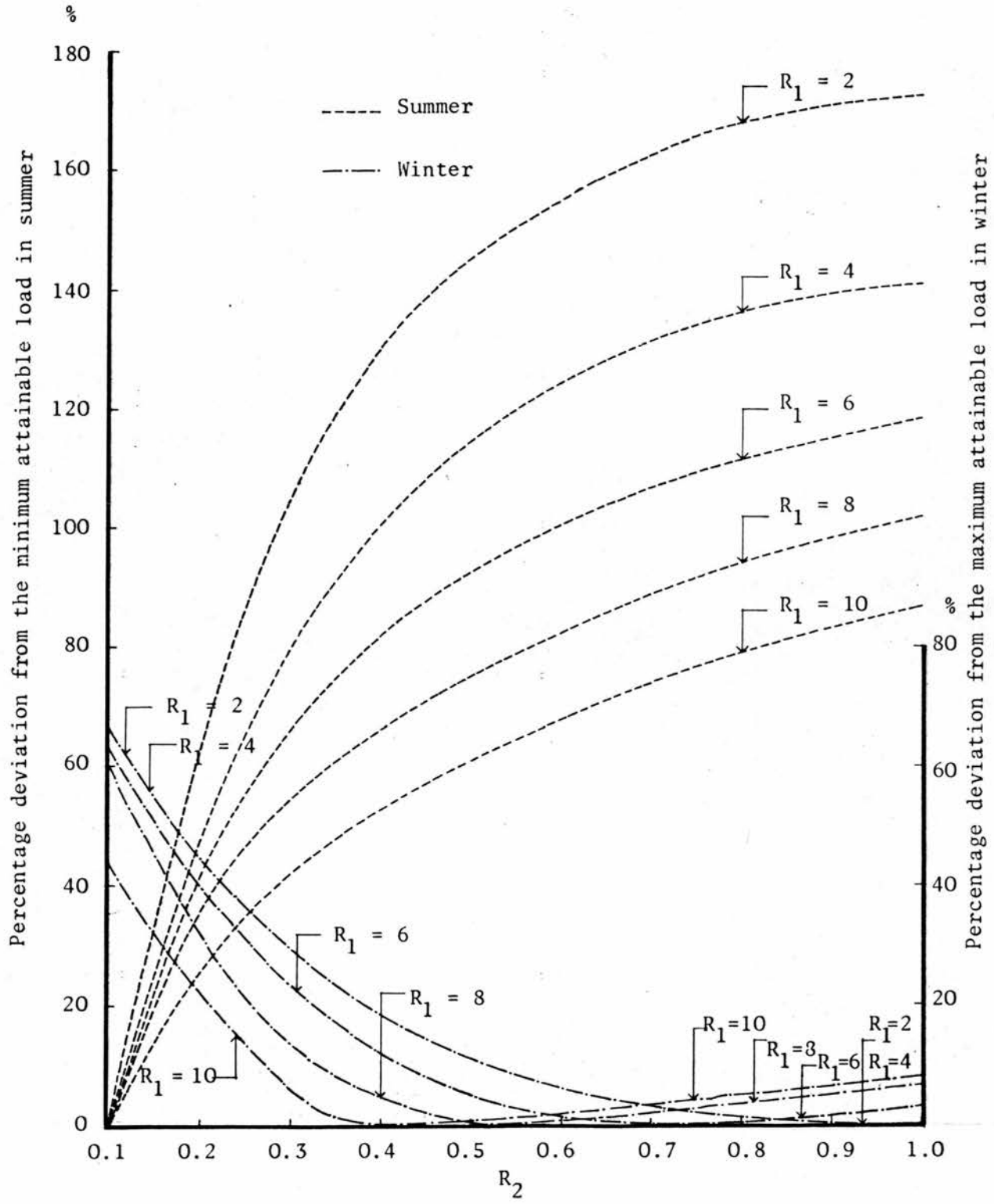

Figure VI.6 Variation of the initial irradiation load with the elongation of the plan, R_2. The irradiation load is represented in percentage deviation from the minimum attainable and the maximum attainable load in summer and winter respectively

Since it is required to develop a measure for studying the thermal performance of the courtyard form that takes into account the effect of changing the different sets of proportions and orientation, it was decided to define the measure for this stage of investigation in terms of the initial irradiation load received by the unit area of the walls surface.

VI.2 Effect of Changing the Ratios R_1 and R_2

Regarding the plan ratio R_2, it was decided to consider the range from 0.1 to 1.0; this means forms ranging from those having a rectangular plan with the two sides facing east and west equal to 0.1 of the two sides facing north and south, to forms having square plan. Forms having R_2 greater than one (i.e., the east and west sides are greater than the north and south sides) are included when discussing the cases of orientation. For example, a form having the east and west sides twice as much the north and south sides is defined as a form having $R_2 = 0.5$ with an angle of orientation equal to 90^{o}.

Figures VI.7 and VI.8 illustrate the effect of changing the ratios R_1 and R_2 on the initial irradiation of the wall's surfaces. It is clear that, for all values of R_2, the greater the ratio R_1 (the shallower the form), the greater the received irradiation load. However, in summer, the increase in the irradiation that takes place as R_1 is given larger

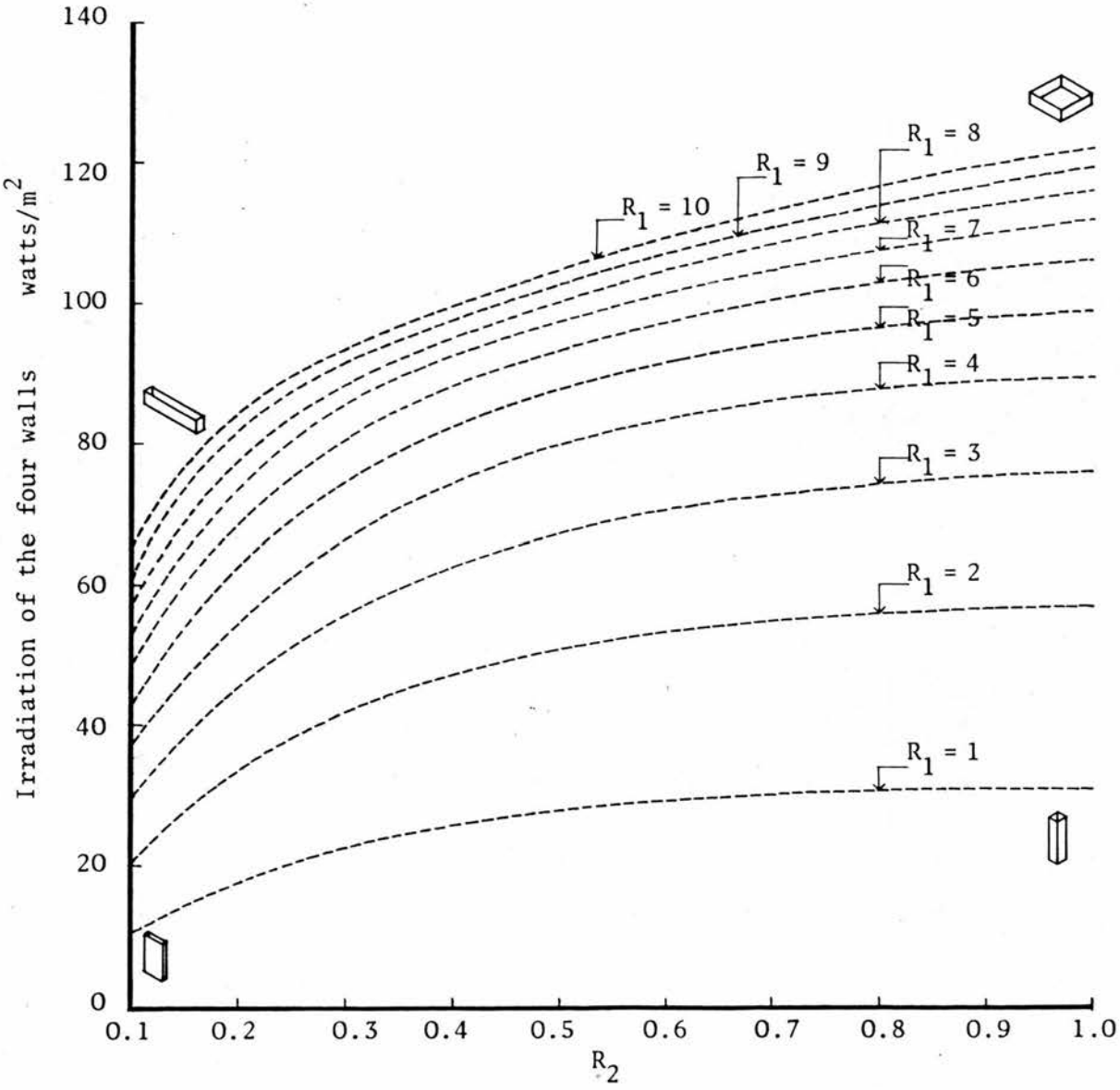

Figure VI.7 The effect of changing the ratios R_1 and R_2 on the irradiation of the courtyard envelope in summer

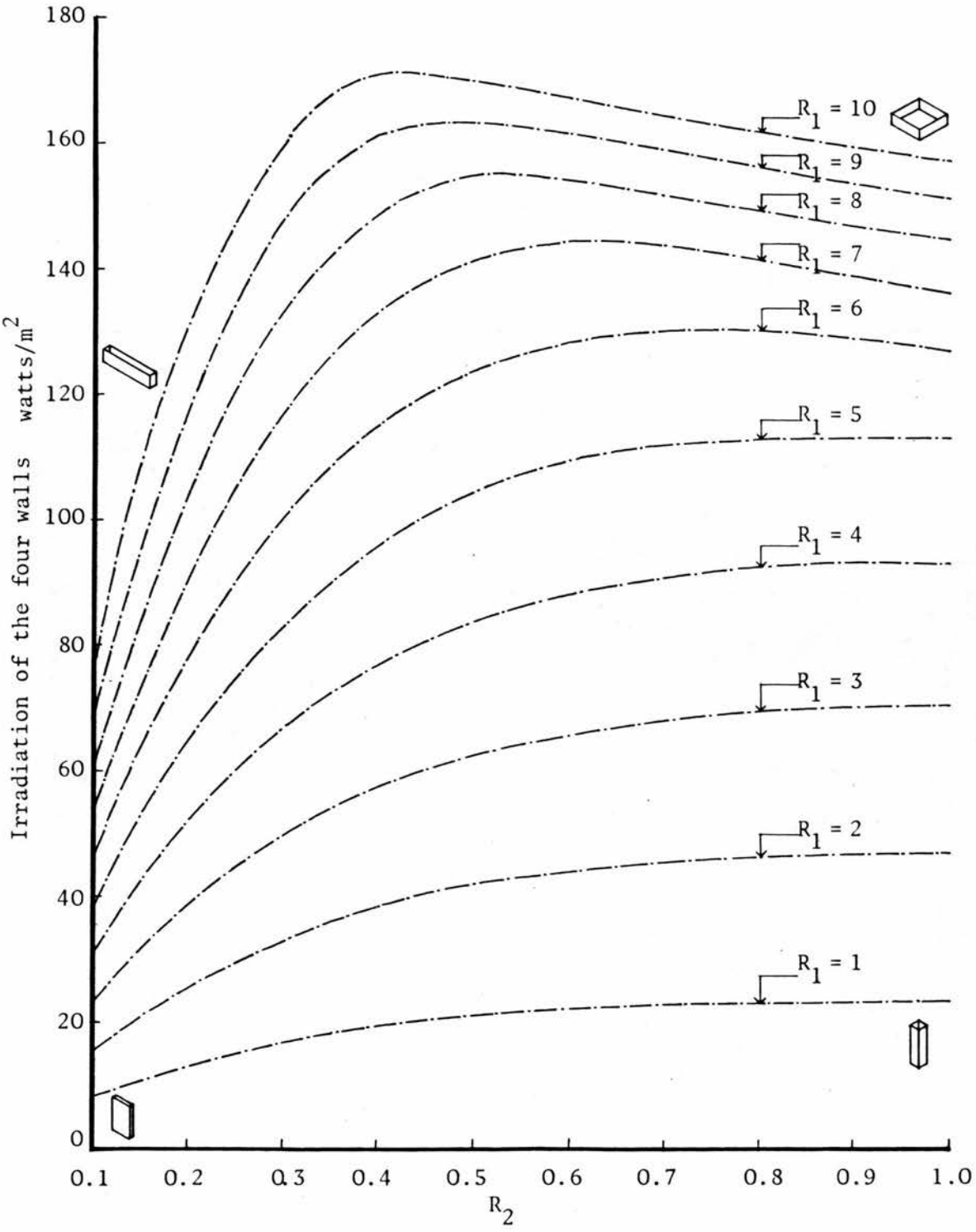

Figure VI.8 The effect of changing the ratios R_1 and R_2 on the irradiation of the courtyard envelope in winter

values is more significant in the case of a square plan than in the cases of elongated plans. For all values of R_1, the summer irradiation increases with the increase of the ratio R_2; i.e., as the plan tends to be square. The rate of this increase gets smaller as the ratio R_2 approaches unity (figure VI.7).

The changes in the irradiation load that correspond to the changes in the ratios R_1 and R_2 are more pronounced in winter than in summer. Figure VI.8 shows that as the value of R_2 is increased, the winter irradiation value increases; the effect is more remarkable at the small values of R_2. As the value of R_1 approaches 10, the rate of increase of irradiation with the increase of the value of R_2 becomes greater. As the value of R_2 approaches unity, the rate of increase becomes less noticeable. For very shallow forms, a decrease of irradiation takes place instead.

In order to find the location of the maximum and minimum irradiation loads among the different cases of the form's proportions, the extended range of R_2 (i.e., with values greater than unity), is considered and the corresponding values of the initial irradiation load are plotted in figure VI.9. By drawing the lines of maxima and minima irradiation in both summer and winter, it becomes evident that in summer the minimum irradiation favours forms having the smallest values of R_2, whereas the maximum irradiation load takes place when

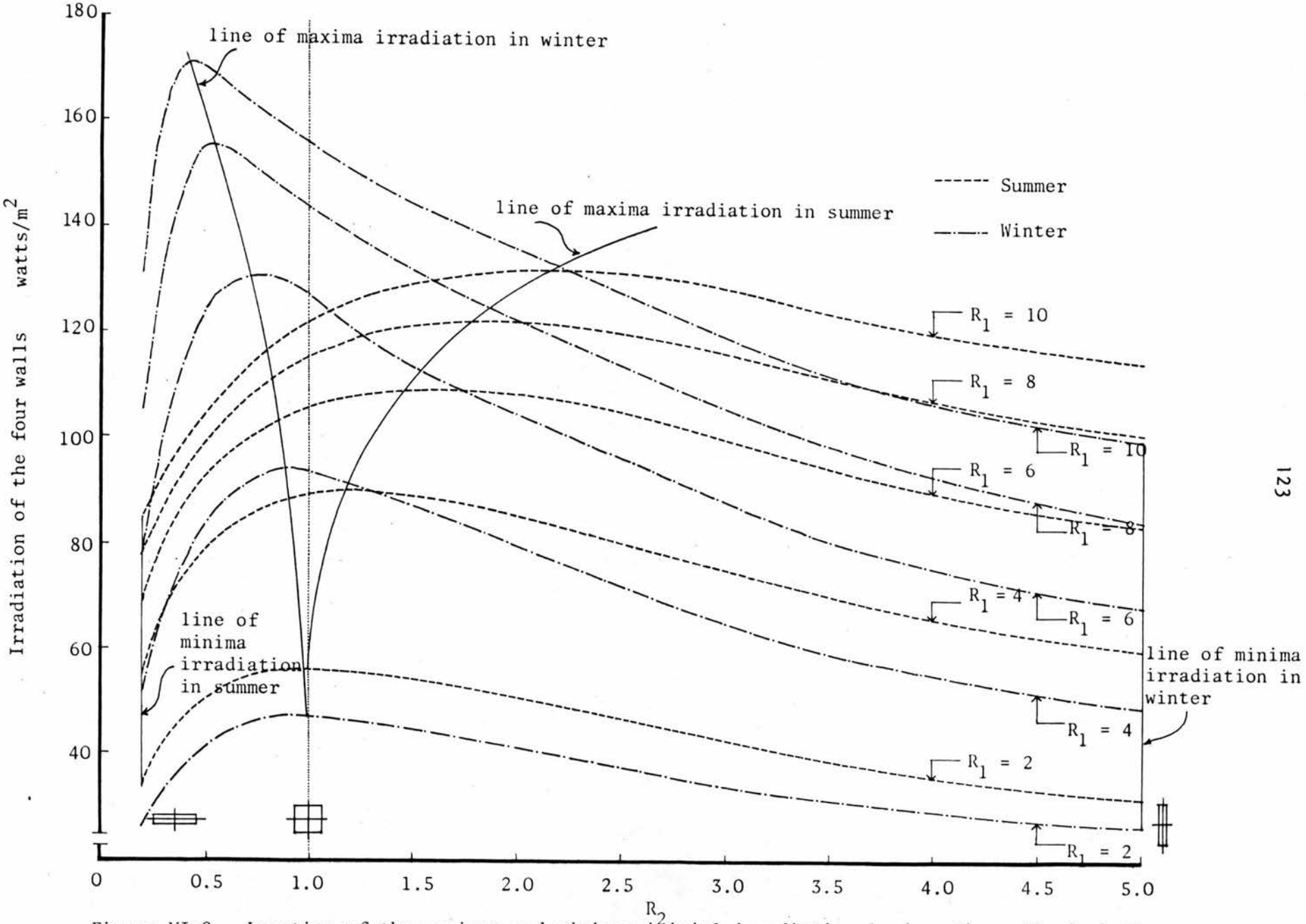

Figure VI.9 Location of the maximum and minimum initial irradiation load on the walls in both summer and winter

R_2 equals unity, provided that R_1 has a small value. As the value of R_1 is increased, the location of the maximum is progressively shifted from the square forms to the more elongated forms with the longitudinal axis parallel to the north-south axis.

On the other hand, in winter the maximum irradiation load takes place as the ratio $R_2$is increased (i.e., the plan has its longitudinal axis parallel to the north-south axis). The maximum takes place when the plan is square provided that R_1 has a small value. As the value of R_1 is increased, the location of the maximum is shifted towards the more elongated forms with the longitudinal axis parallel to the east-west axis.

VI.2.1 Distribution of the irradiation over the four walls

Figures VI.10 and VI.11 show the initial irradiation load on each wall expressed as a percentage of the initial irradiation load on the four walls for the different cases of R_2. The change of the ratio R_1 produces very slight deviations, hence the plotted values in the two graphs are the averages of the values of irradiation that correspond to different values of R_1. In summer, the contribution of the south wall is very considerable provided R_2 has small values. It decreases as R_2 approaches unity, whereupon the irradiation

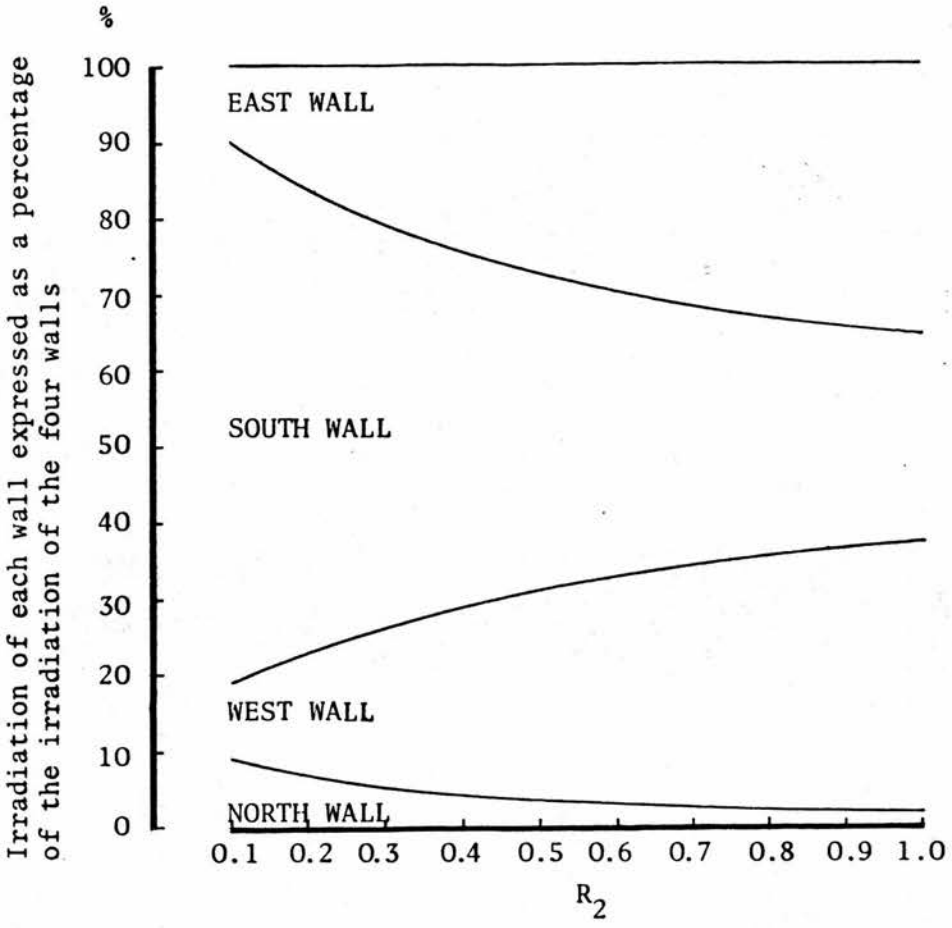

Figure VI.10 Distribution of the Irradiation of the four walls of a courtyard (summer)

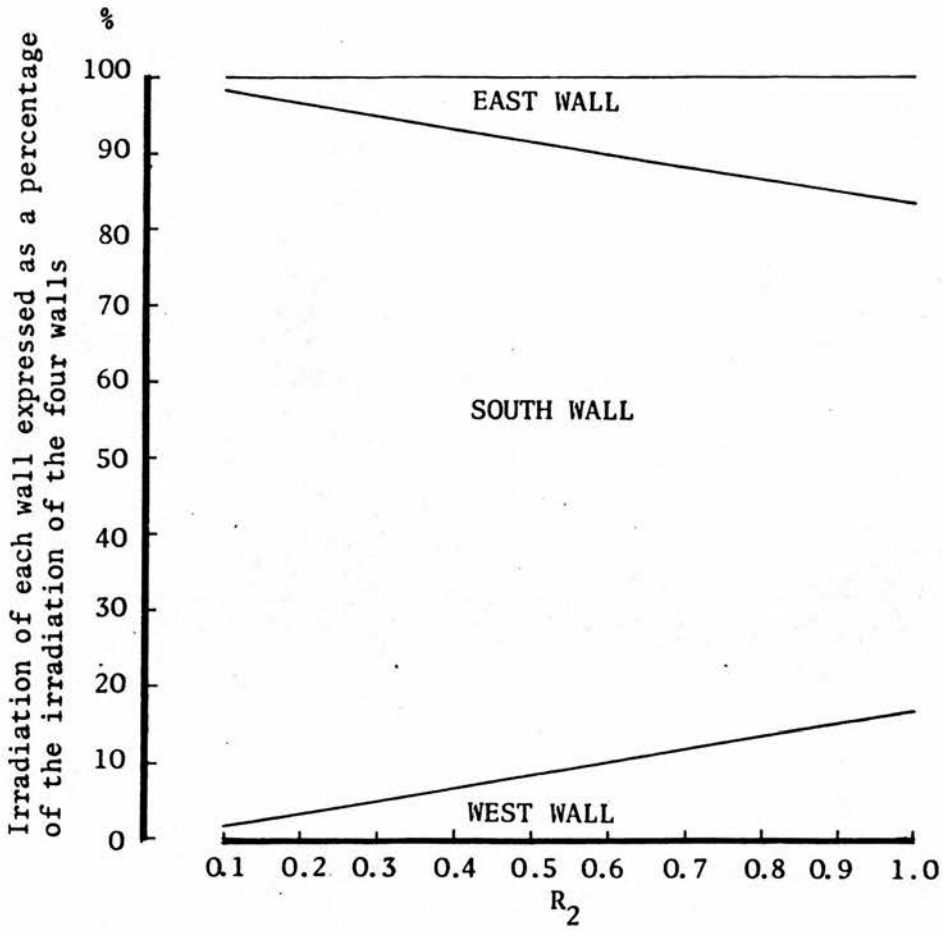

Figure VI.11 Distribution of the irradiation of the four walls of a courtyard (winter)

of each of the east and west walls is greater than that of the south wall. The north wall gets the least irradiation especially for forms having large values of R_2. In winter, the north wall receives no direct radiation at all. The east and west walls receive a considerably smaller percentage, but it increases with the increase of R_2. The contribution of the south wall is very significant.

VI.3 Effect of the Projection of the Roof over the Courtyard's Walls

In order to study the effect of a roof projecting over the walls, the irradiation of the walls was calculated for different values of s_1, s_2, s_3 and s_4 (ratios of the projected part of the roof to the plan's dimension perpendicular to the walls W_1, W_2, W_3 and W_4 respectively). A comparison between the results showed that, in both summer and winter, the total initial irradiation of the form's surfaces (walls and ground) are reduced by a ratio R_3, defined as the ratio between the area of the top opening of the form and its ground area, irrespective of the location of the projecting part.

Considering the irradiation of the walls only, the same relation holds true in winter where the walls receive most of the incoming radiation. In summer, the reduction is considerably greater, especially for forms having large values of R_1. For example, a decrease of 30% in the ratio R_3

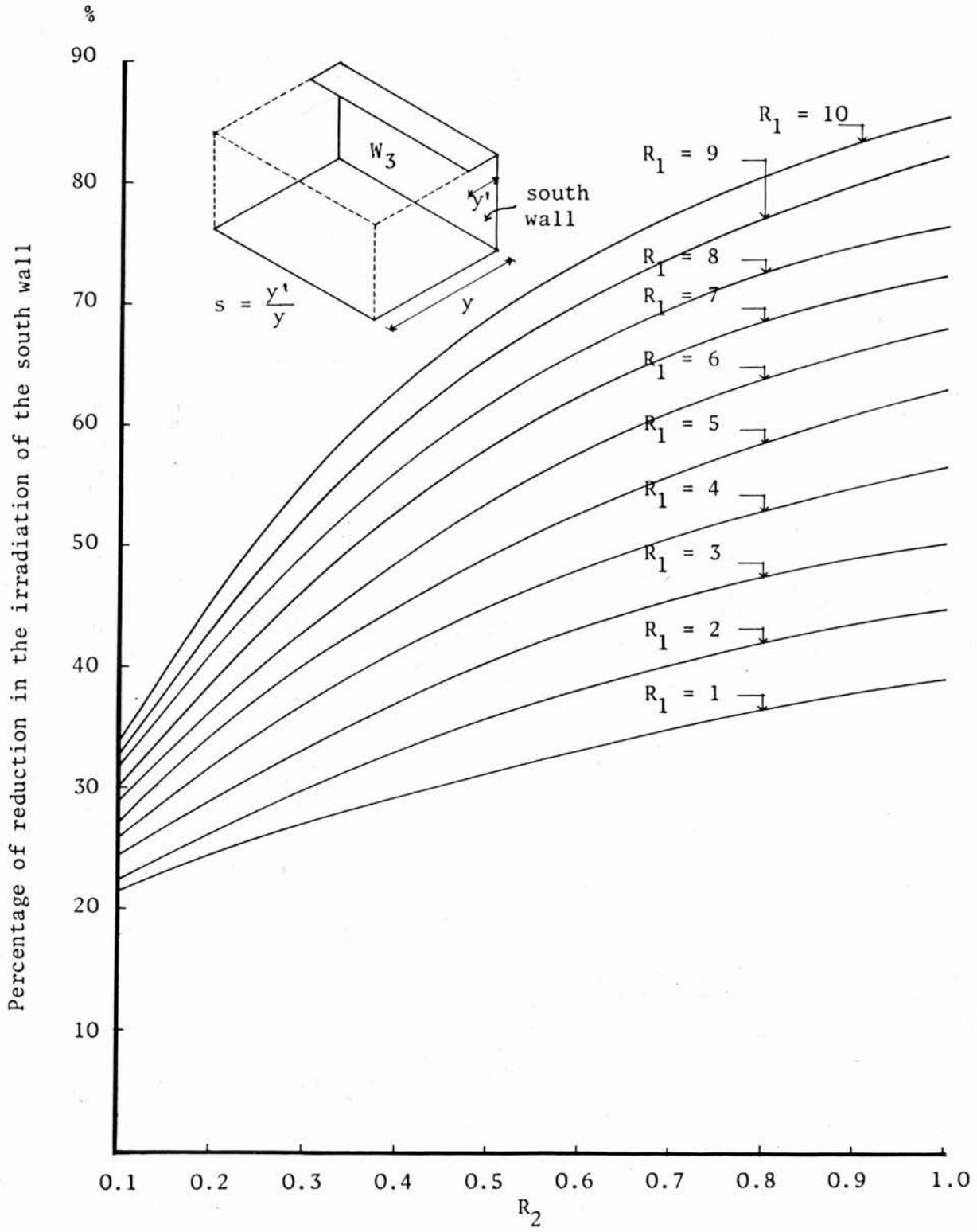

Figure VI.12 The effect of projecting over the south wall on the irradiation of the south wall in summer (s = 0.2)

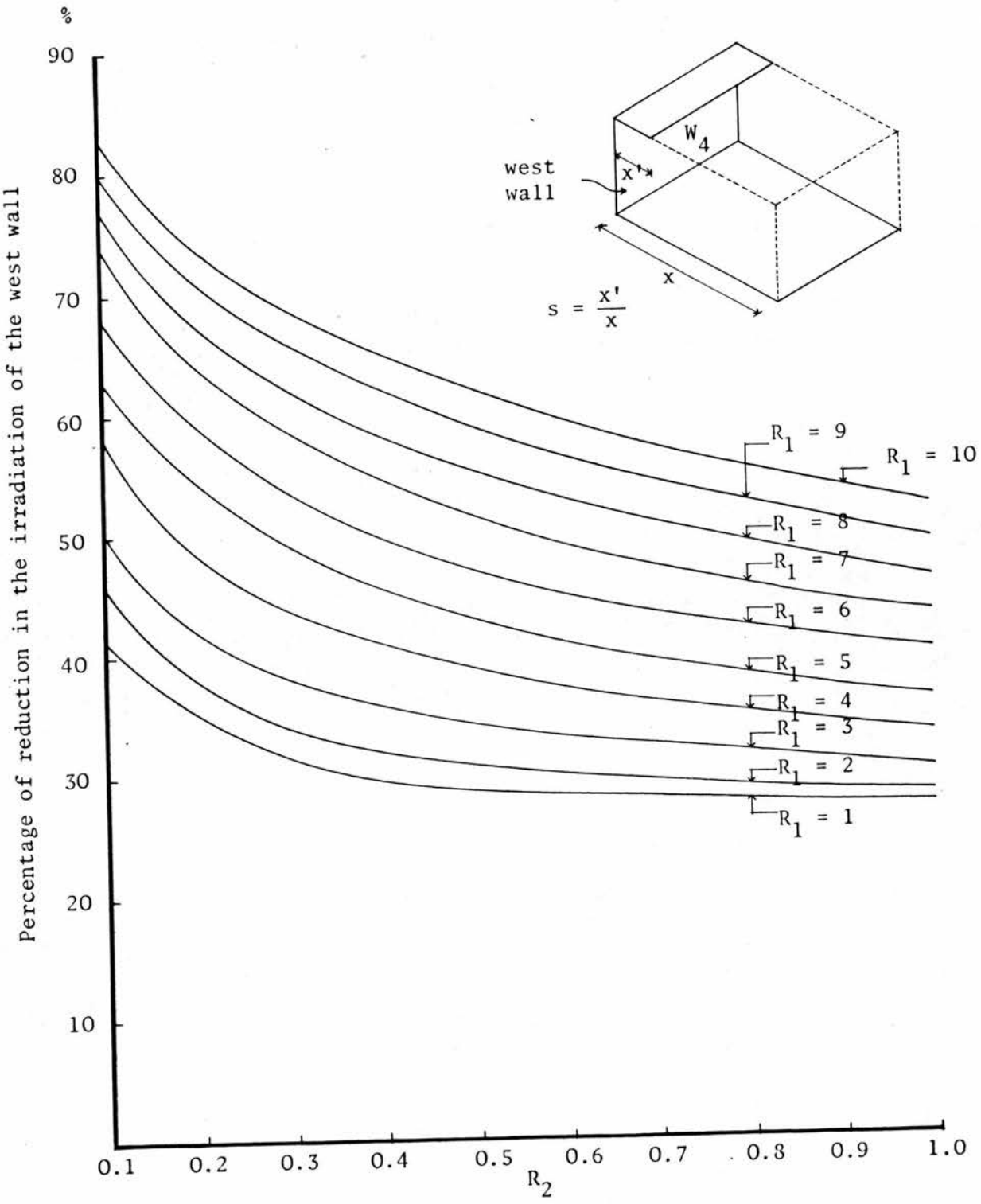

Figure VI.13 The effect of projecting over the west wall on the irradiation of the west wall in summer (s = 0.2)

would produce a reduction of about 50% of the irradiation of the walls of a square form having $R_1 = 10$.

The reduction of the irradiation of a south wall that results from projections over it becomes more significant as the form under consideration becomes more square in plan (figure VI.12). A projection over a west wall produces smaller reduction as the plan tends to the square. More noticeable reduction is obtained as R_2 gets smaller (figure VI.13).

The effect of changing the size and the location of the projected part of the roof on the resulting irradiation of the four walls is shown in figures VI.14, VI.15 and VI.16. The reduction of the irradiation of the four walls caused by increasing the projection over a south wall is greater than that caused by increasing the projection over all the other walls. In the three graphs, the area enclosed between the maximum and the minimum percentages of the reduction represents a range that corresponds to varying the values of R_1 and R_2. This range is wide in the case of projecting over the south wall. In the case of western (or eastern) projection, it is very narrow. The range that corresponds to the northern projection lies between the previous two cases.

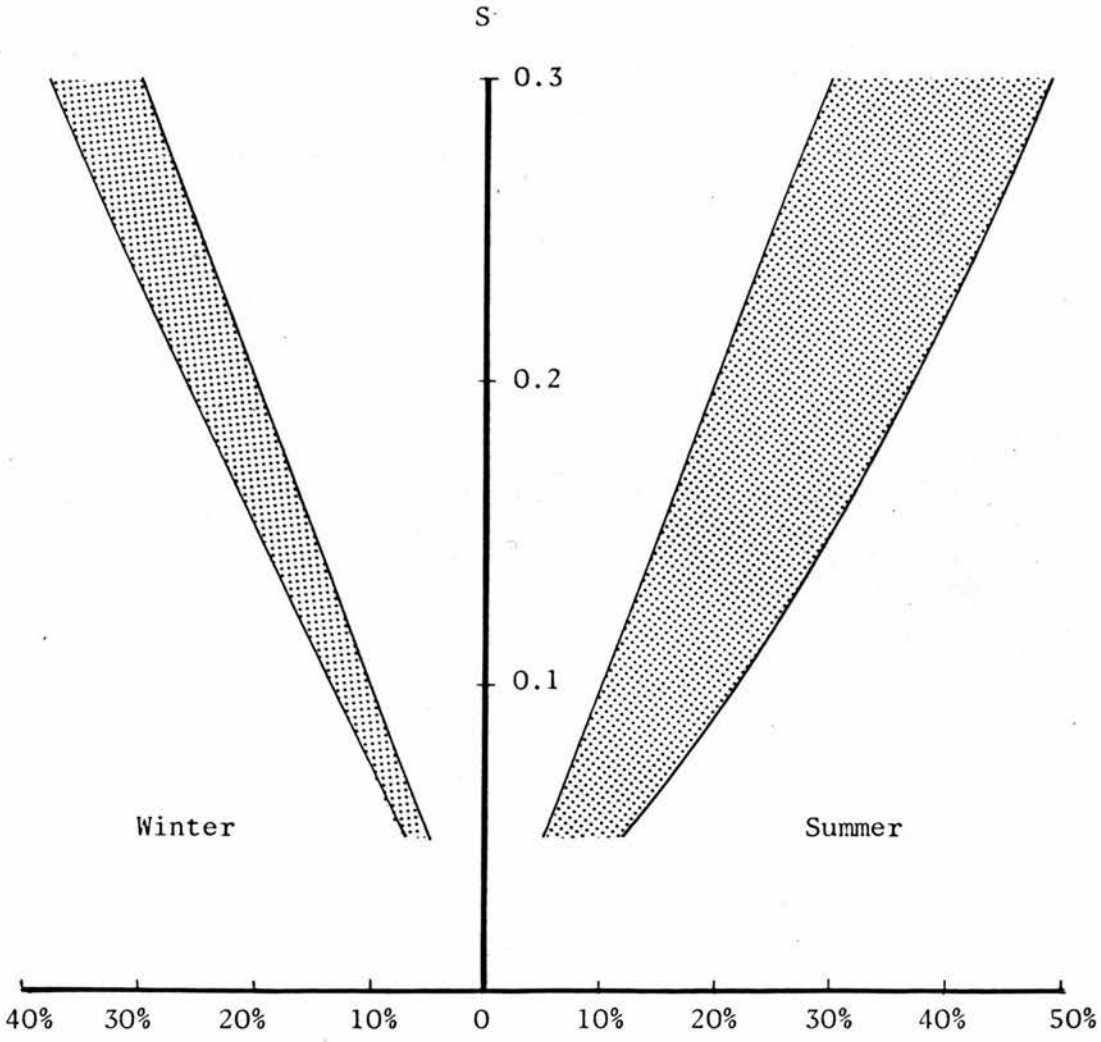

Figure VI.14 Change in the irradiation of the four walls caused by changing the projection over the south wall

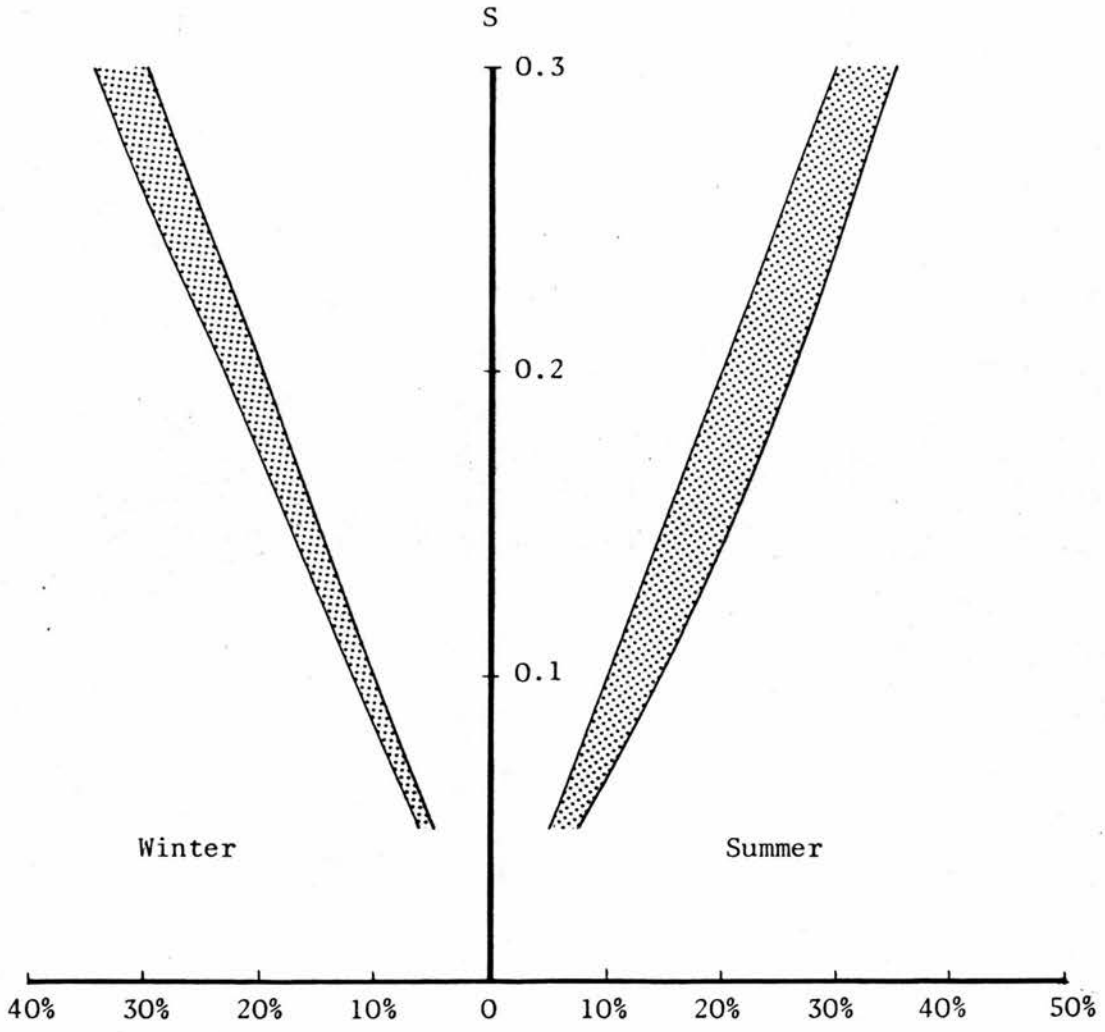

Figure VI.15 Change in the irradiation of the four walls caused by changing the projection over the west wall

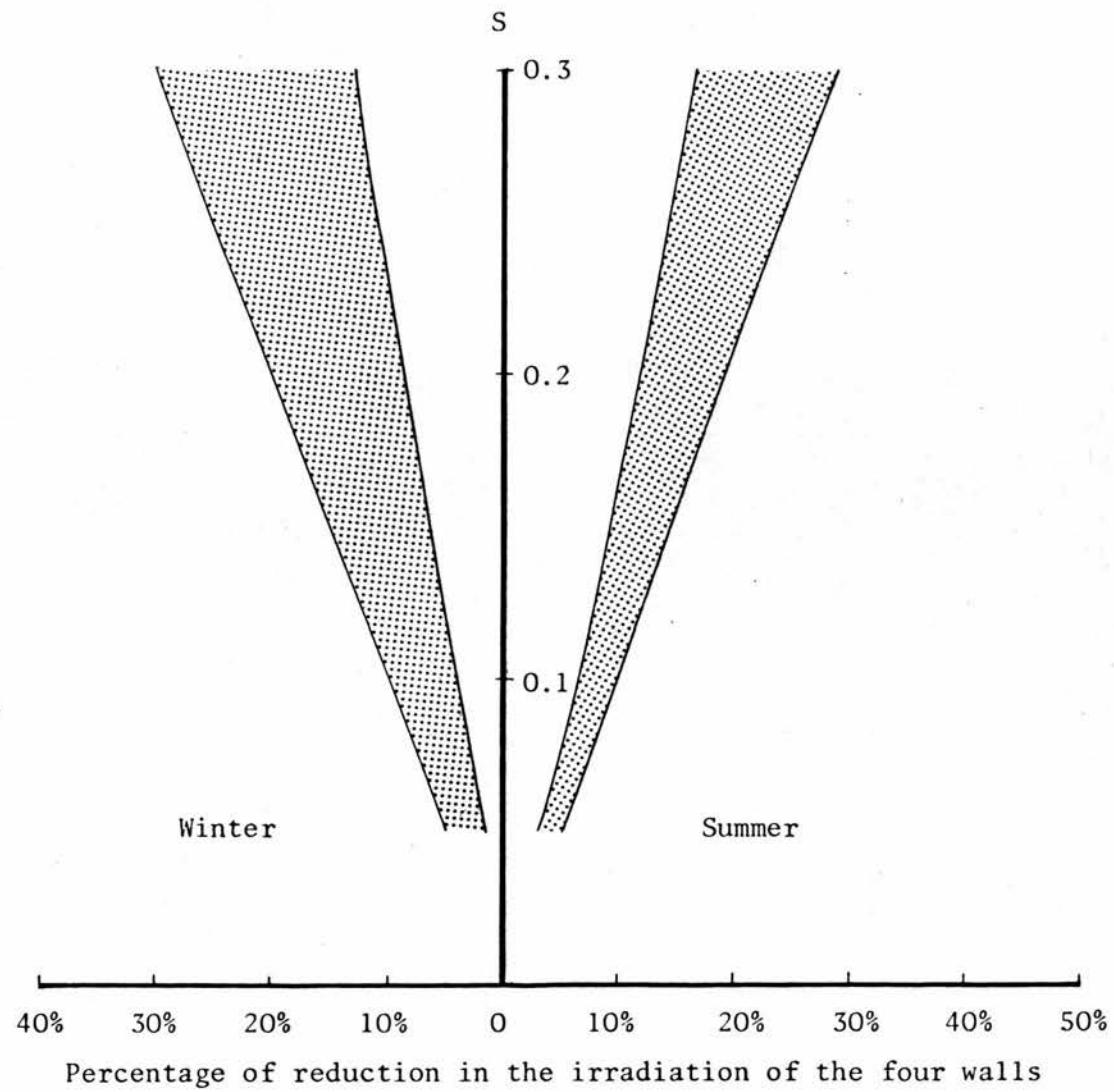

Figure VI.16 Change in the irradiation of the four walls caused by changing the projection over the north wall

VI.4 Effect of the Introduction of a Parapet on the Top of the Walls

A parapet added to the top of the courtyard walls increases the deepness of the form so that, as the parapet gets higher, the irradiation is progressively reduced. The effect varies for forms having different values of the ratio R_1; the smaller R_1, the greater the effect of introducing a parapet. As shown in figures VI.17 and VI.18, in summer, the relationship between p' (parapet's height to the form's height) and the irradiation of the form is not affected by changing the ratio R_2. The reduction of irradiation is more considerable in winter especially as R_2 gets smaller.

VI.5 Effect of Changing the Size on the Irradiation of the Form

In order to study the effect of size on determining the irradiation load on the surfaces of the form, two cases of height were considered: three and six metres. When interpreting the chosen set of proportions (see section V.1) into actual dimensions for the two cases of heights, a constraint to maintain the width greater than or equal to 2.5 metres and the length smaller than or equal to 12 metres is applied. These values are considered the lower and upper limits for the plan's dimensions of a domestically acceptable form (see section V.1). The ranges of geometries that satisfy

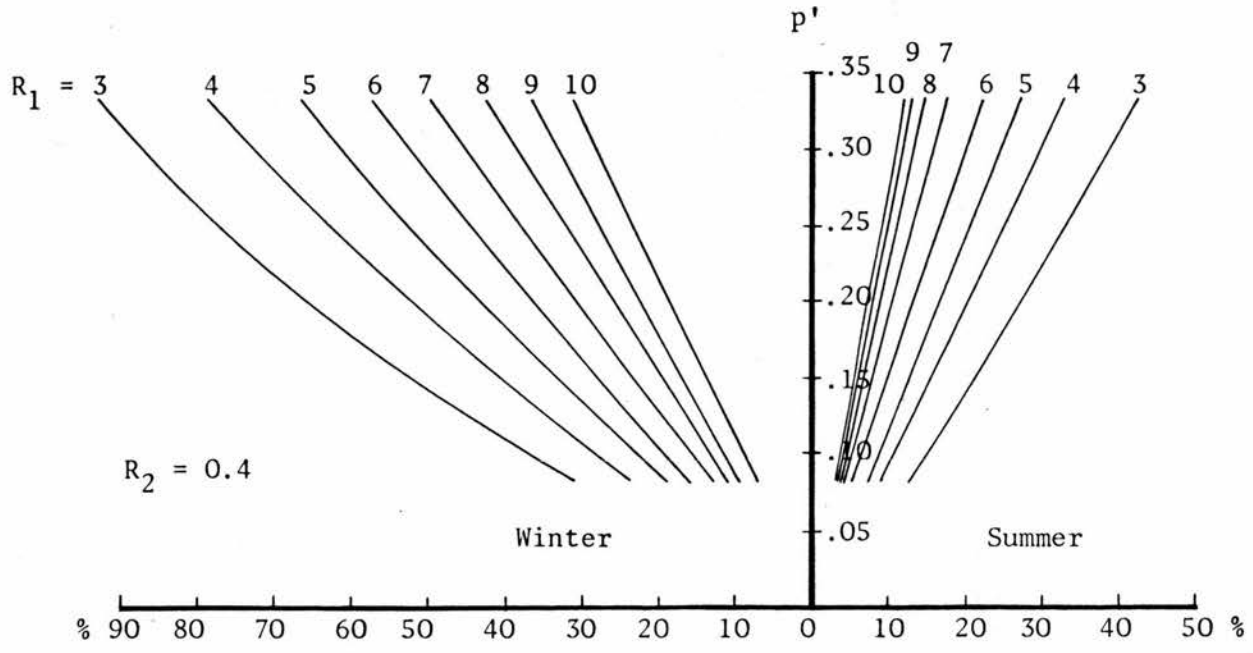

(a)

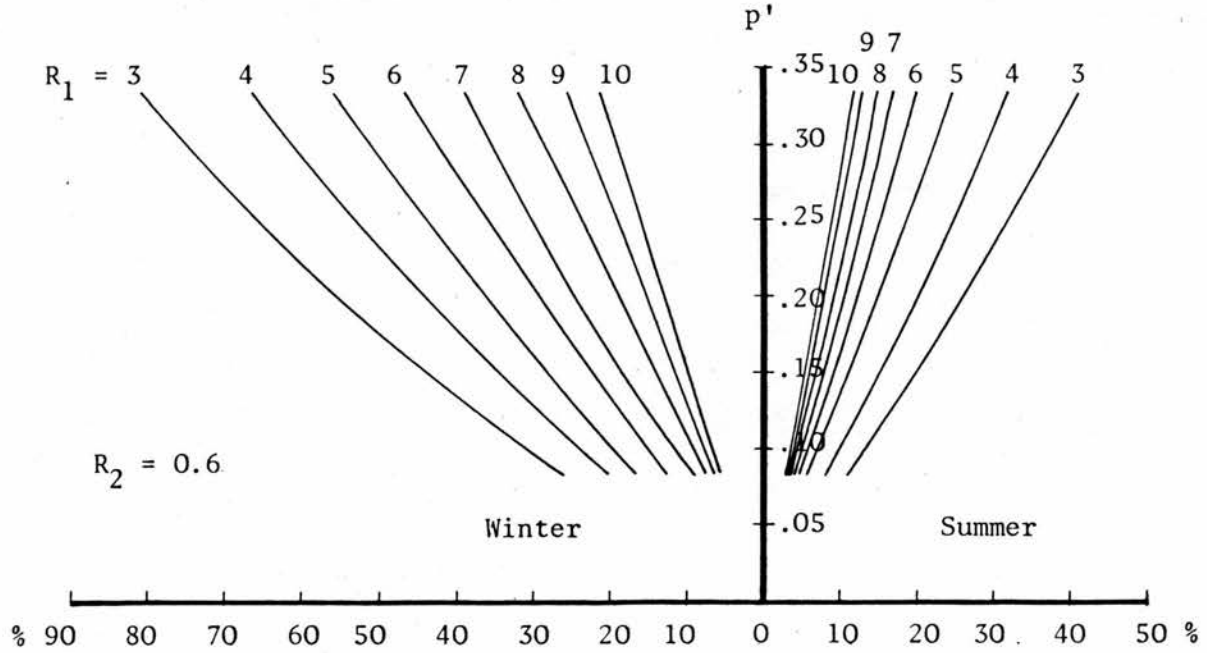

(b)

Figure VI.17 Change in the irradiation of the four walls caused by changing the values of p'

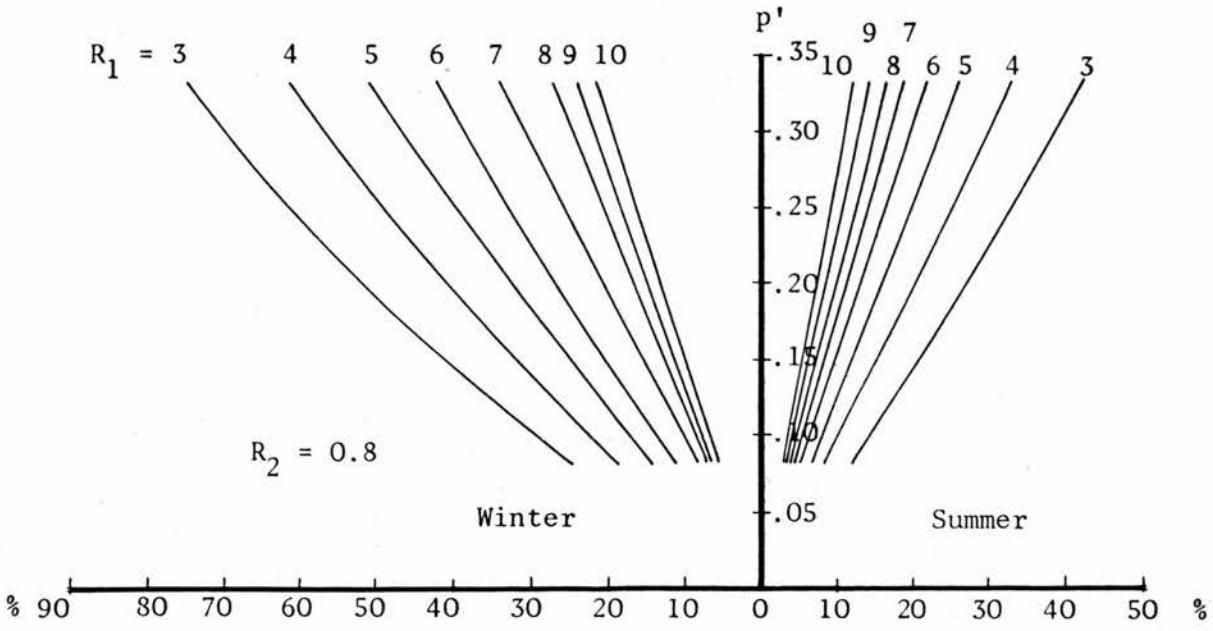

Percentage of reduction in the irradiation of the four walls

(a)

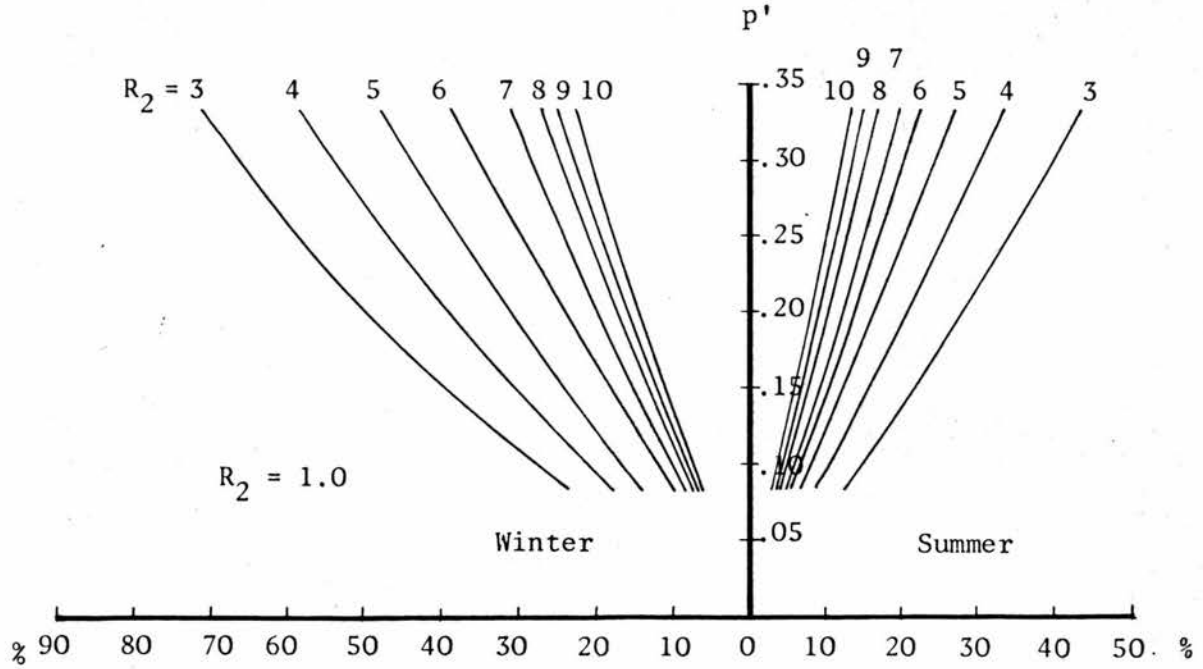

Percentage of reduction in the irradiation of the four walls

(b)

Figure VI.18 Change in the irradiation of the four walls caused by changing the values of p'

this constraint are shown in figure VI.19 for both the one storey and the two storey forms.

The values of the irradiation of the forms were calculated per unit area of the walls surface. It is evident that for the two storey forms, the walls of the upper storey receive radiation in excess to that received by the lower storey. The difference between the two values becomes more marked as R_1 takes smaller values as shown in figure VI.20. The value of the irradiation that corresponds to a single storey form lies between the two values that correspond to a two storey form having the same proportions.

The discussion in section VI.2 revealed that in summer the irradiation load is least when the form has the smallest value of R_1 and its plan is square. In winter the maximum irradiation load takes place when R_1 has the greatest value and when R_2 is in the vicinity of 0.4 - 0.6. Figure VI.21 shows that among the feasible one storey forms, the minimum load takes place when $R_1 = 3.33$ and $R_2 = 1.0$ (i.e., a form 3 metres high and having a square plan 2.5 m x 2.5 m). The maximum winter irradiation load is obtained when R_2 is equal to 0.4 and R_1 has the greatest value. This is represented by a form 3 metres high, having the plan's dimensions equal to 4.3 metres and 10.7 metres.

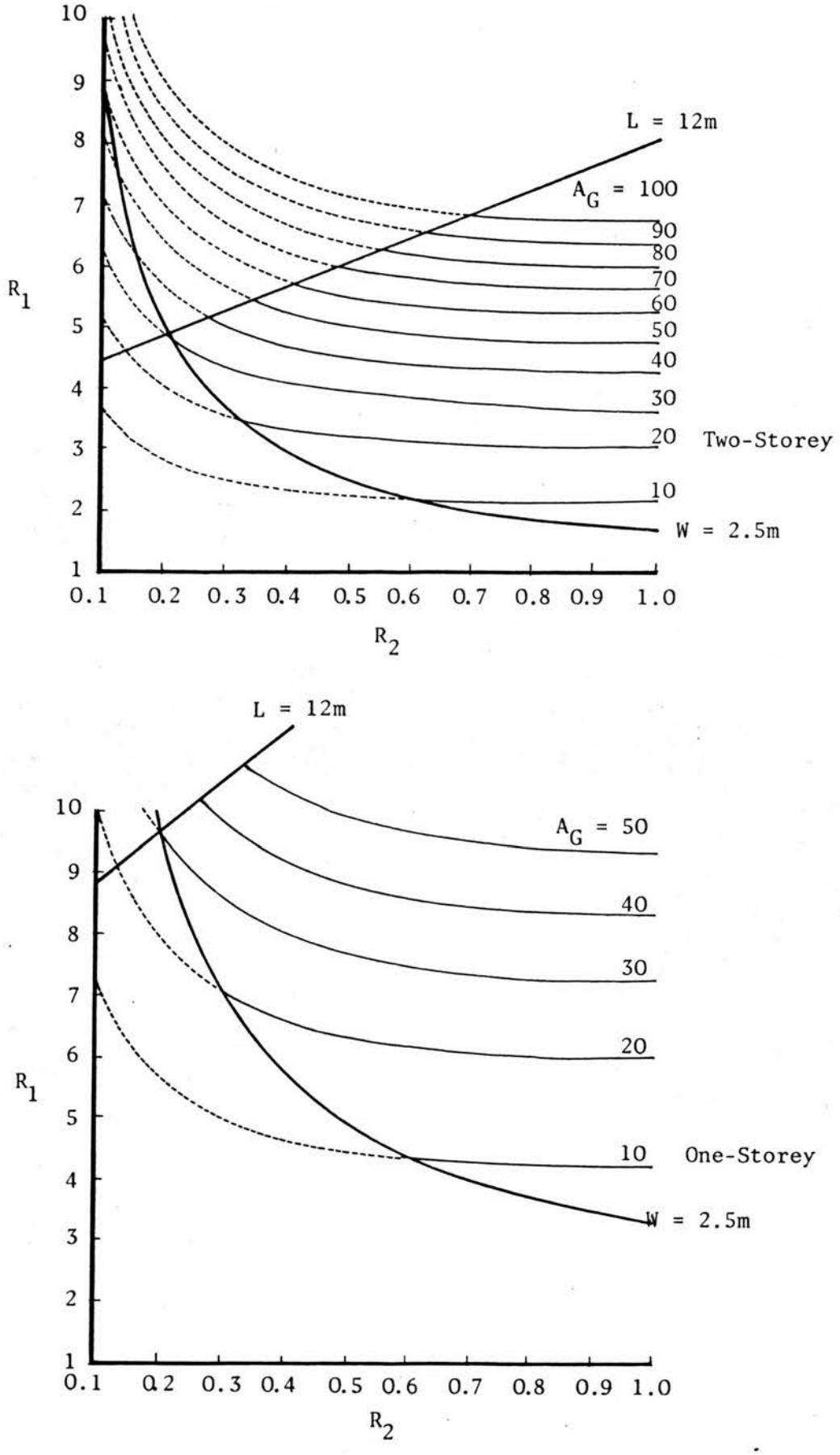

Figure VI.19 The range of geometries that satisfy the constraints of the plan dimensions

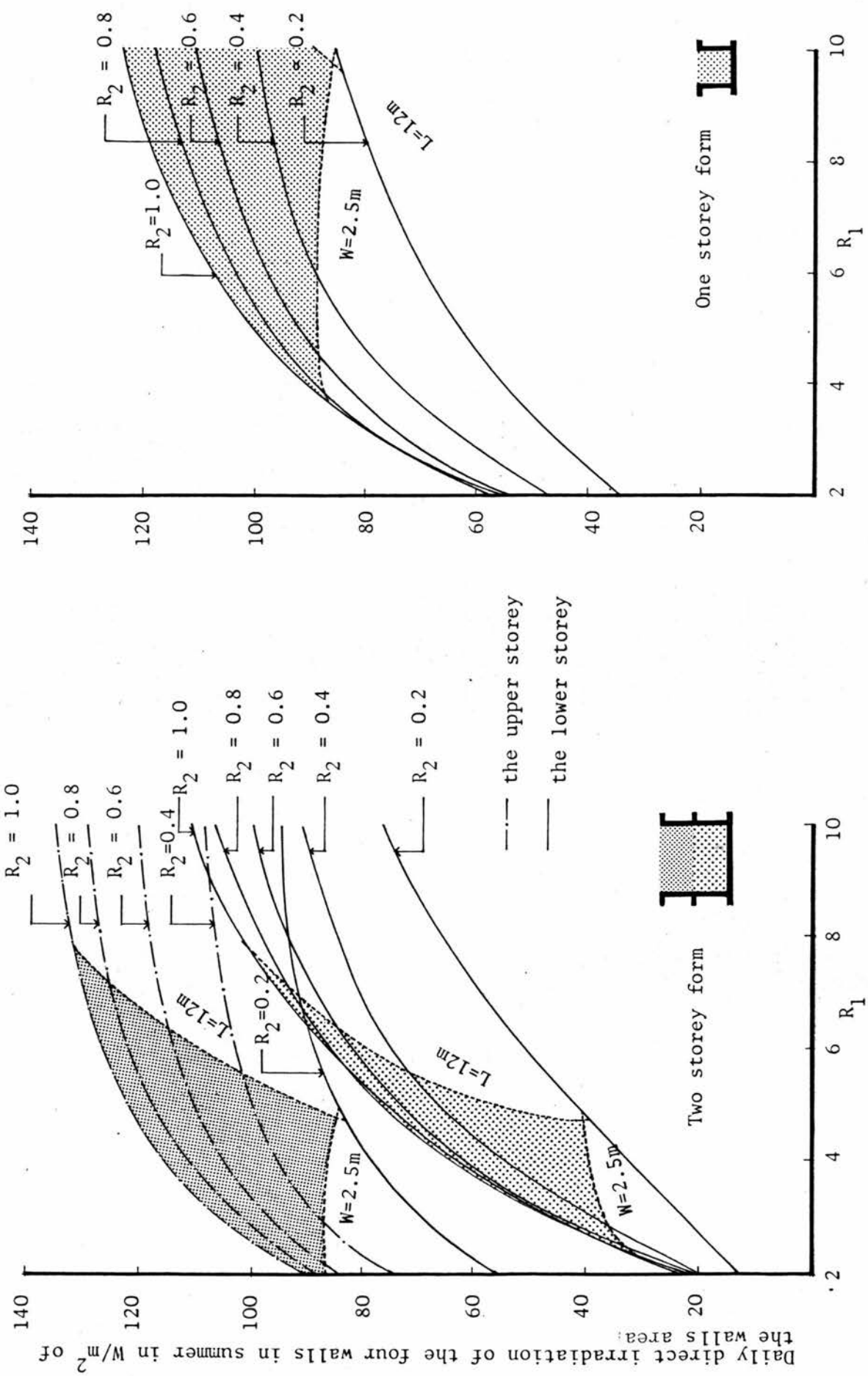

Figure VI.20 Comparison between courtyards having the same proportions but varying in size

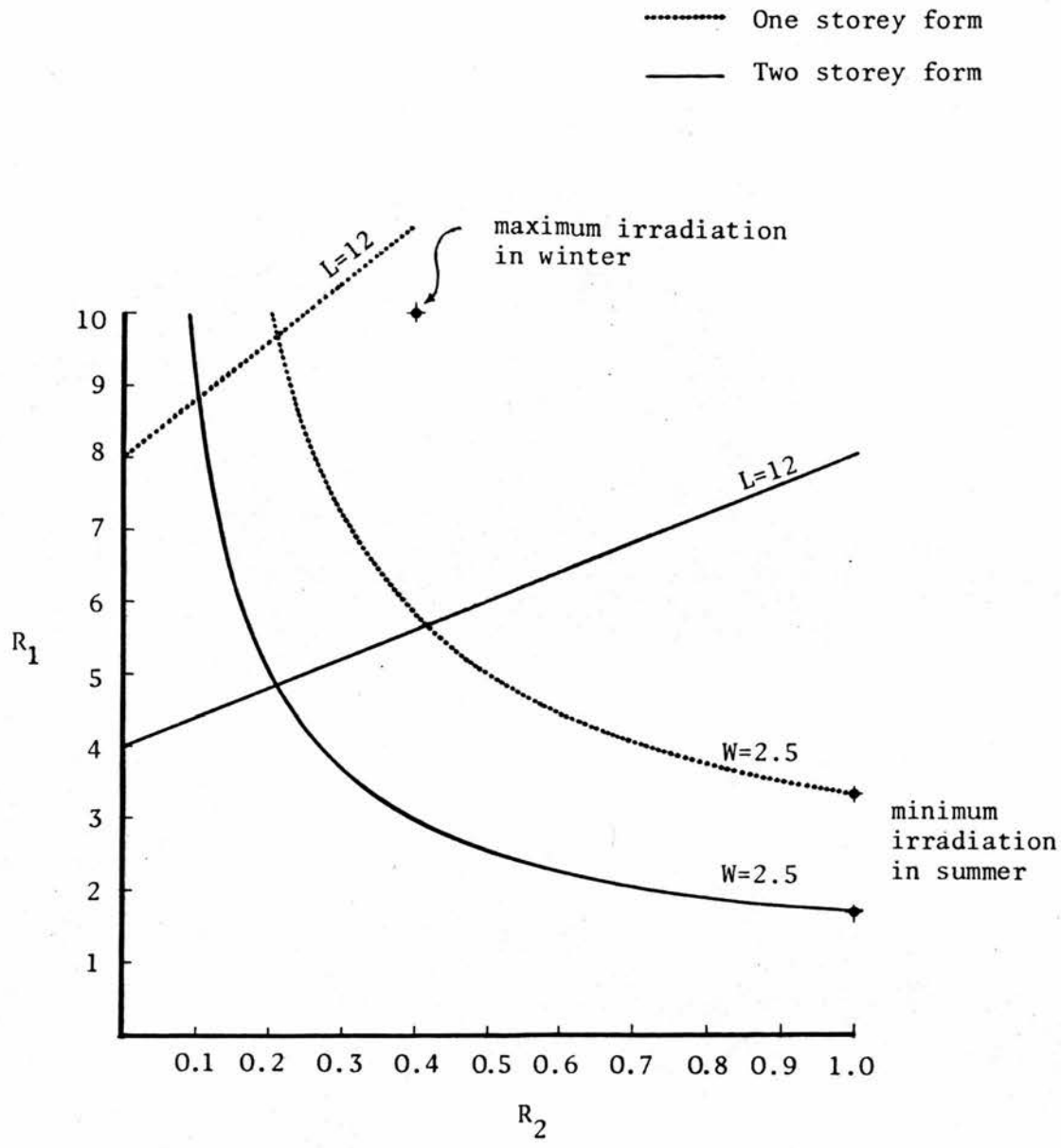

Figure VI.21 Optimum forms in summer and winter within the range of geometries that satisfy the constraints of the plan dimensions

It is not the aim of this study to restrict attention to finding the case of geometry which satisfies the optimum thermal design criterion in either summer or winter, but rather, in the interest of designers, it is intended to identify the range of geometries whose thermal performance lies within specified ranges of the optimum both in summer and winter. On this basis, both the optimum form in summer and the optimum form in winter are plotted in figure VI.22, the lines representing deviations of 5, 10, 20 and 30 percent of the optimum are drawn for the two seasons. Ranges within which the irradiation load on the form is far from the optimum by not more than 5, 10, 20 and 30 percent are identified for each season. Areas of intersection in the graph represent the ranges within which the thermal performance of a form deviates by specified percentages from the corresponding optimums.

VI.6 Effect of Changing the Orientation on the Irradiation of the Form

In order to assess the effect of changing the orientation of the form on the irradiation of its surfaces, it was decided to find for each case of orientation its deviation from the maximum and the minimum obtainable irradiation in winter and summer respectively. When R_1 is small (1 or 2), there is almost no effect caused by changing the orientation.

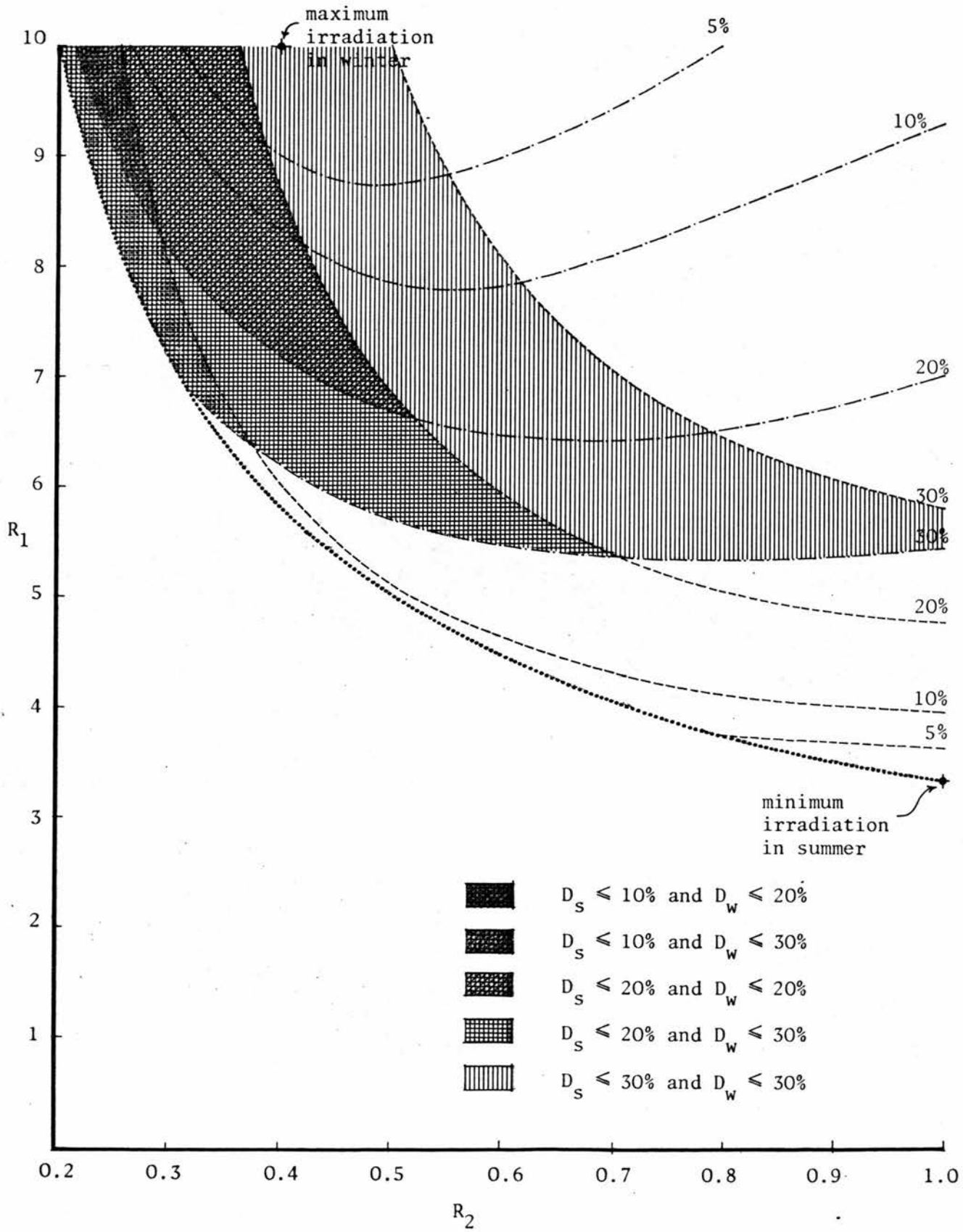

Figure VI.22 Deviations from the optimum in summer and the optimum in winter for a single storey courtyard

For larger values of R_1 (3 and more), it is noticed that in winter a maximum is obtained at an orientation of 0^o and a minimum is obtained at an orientation of 90^o, while in summer a maximum occurs at an orientation of 90^o and a minimum at an orientation of 0^o. Values of the irradiation obtained for the other cases of orientation lie between the two extremes.

The greater the value of R_1, the greater the deviation that is produced by changing the orientation. It is noticed that for each case of R_1, the deviation varies with the variation of R_2; it is very small when $R_2 = 1$ (square form) and it reaches a maximum when $R_2 = 0.3$ in both summer and winter.

It could be concluded that square forms, whatever their degree of deepness, yield the least change in irradiation caused by changing the orientation. Forms which have small values of R_2 are most affected. In general, the effect of changing the orientation is greater in summer than in winter.

To illustrate the effect of changing the orientation, consider a form having $R_2 = 0.4$, a change from 0^o to 90^o would result in increasing the irradiation in summer by 33% if $R_1 = 10$, and by just 5% if $R_1 = 3$. On the other hand, the irradiation in winter would be reduced by 24% and 1% respectively.

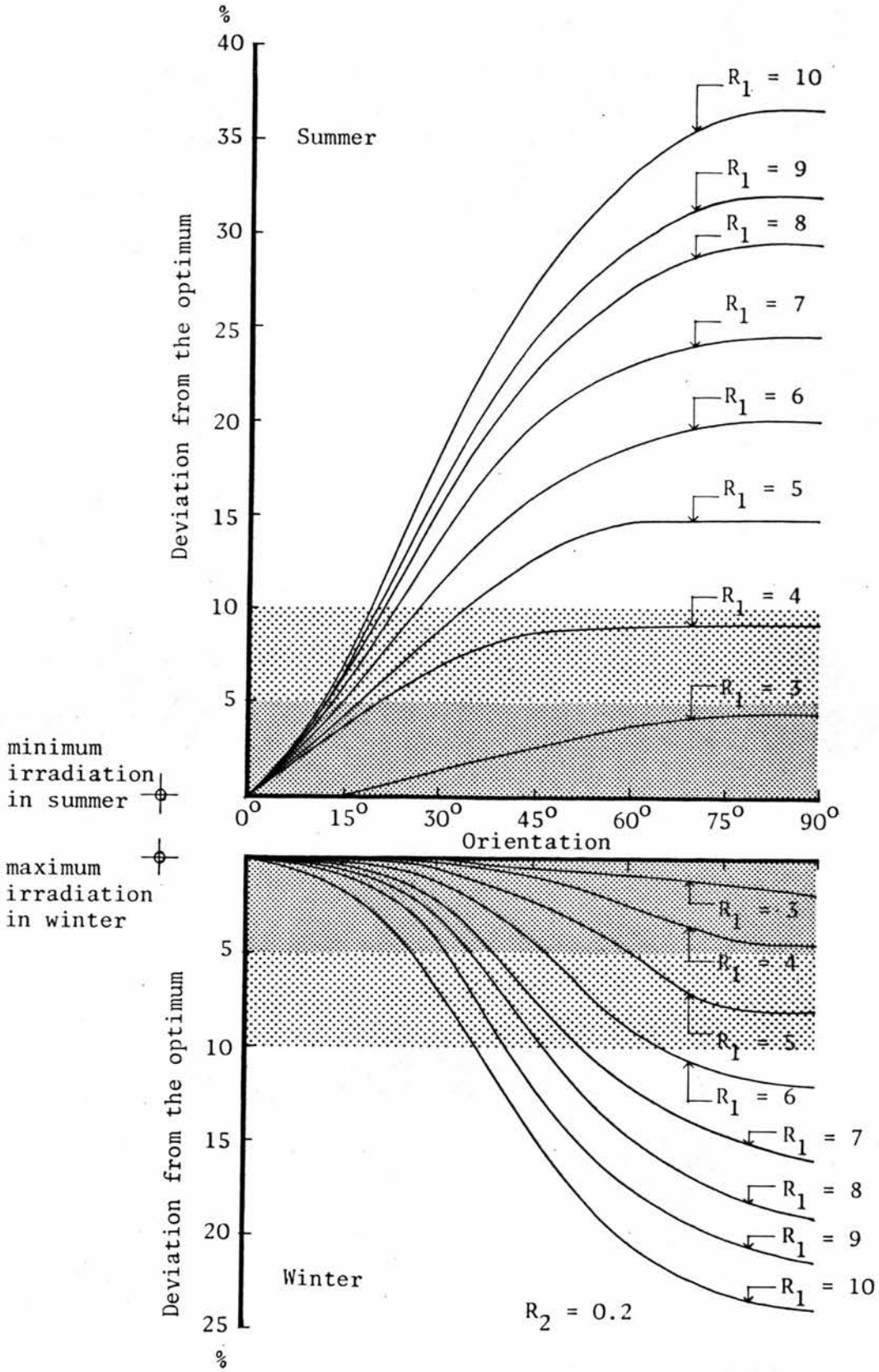

Figure VI.23 Effect of changing the orientation on the irradiation of the four walls

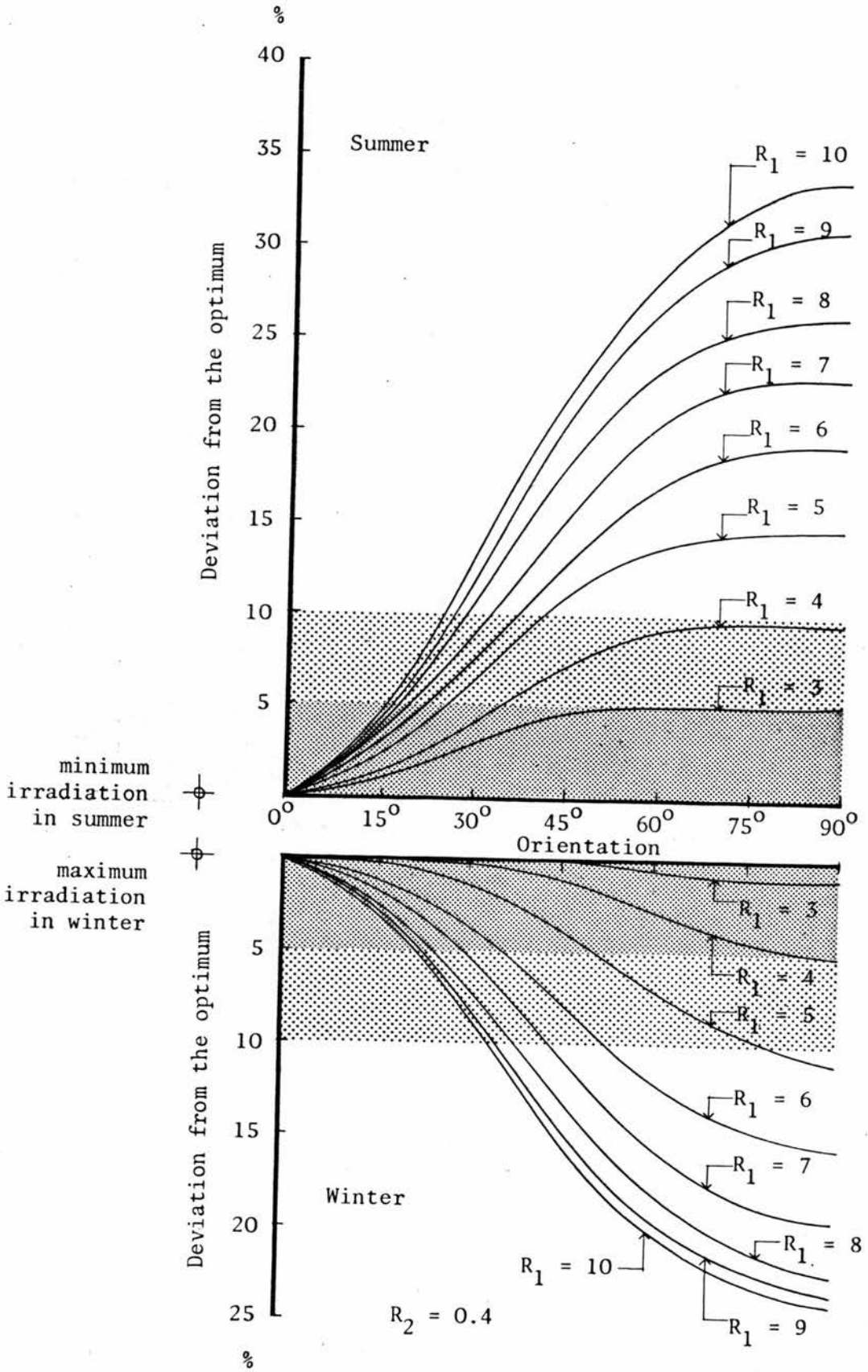

Figure VI.24 Effect of changing the orientation on the irradiation of the four walls

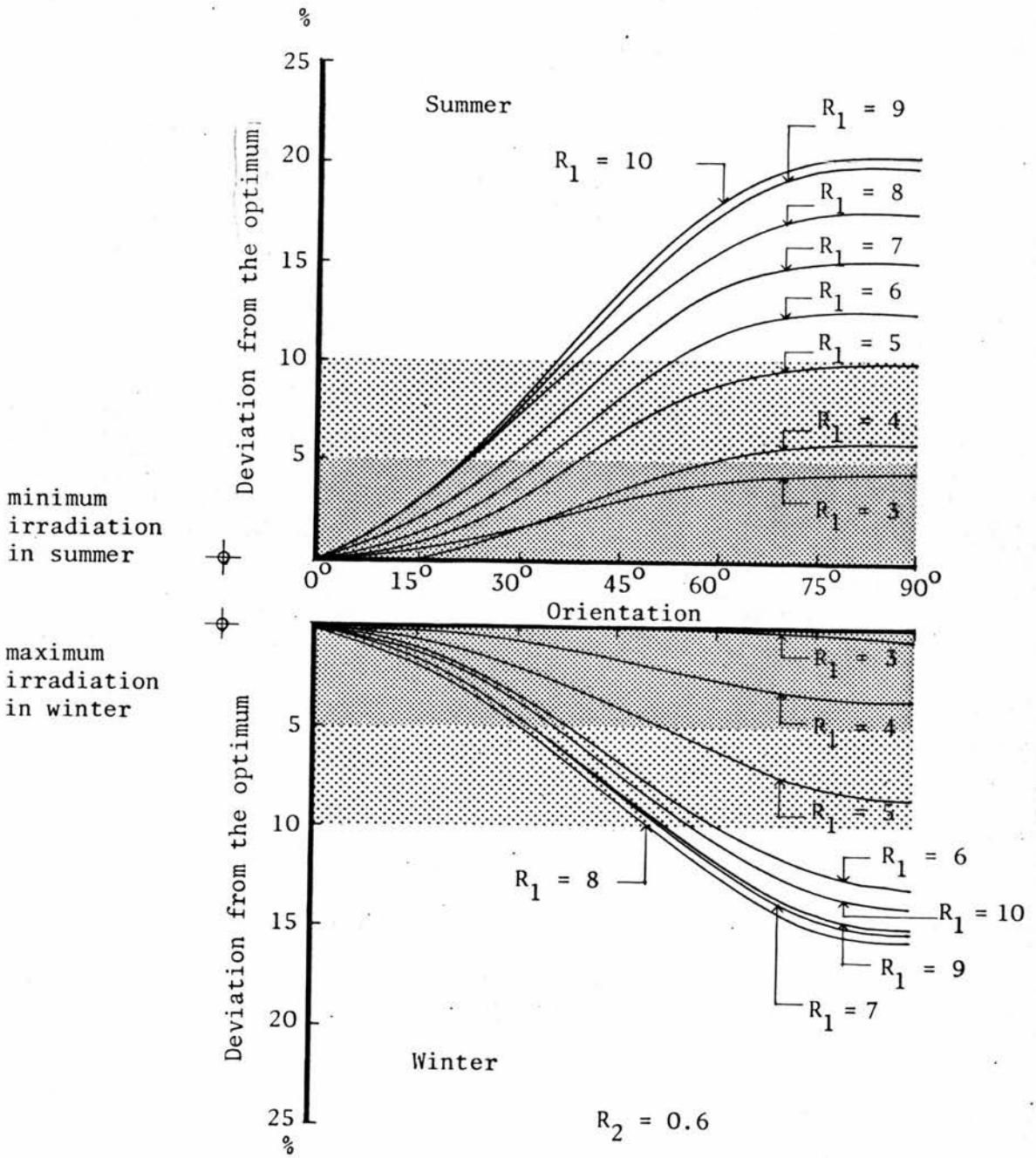

Figure VI.25 Effect of changing the orientation on the irradiation of the four walls

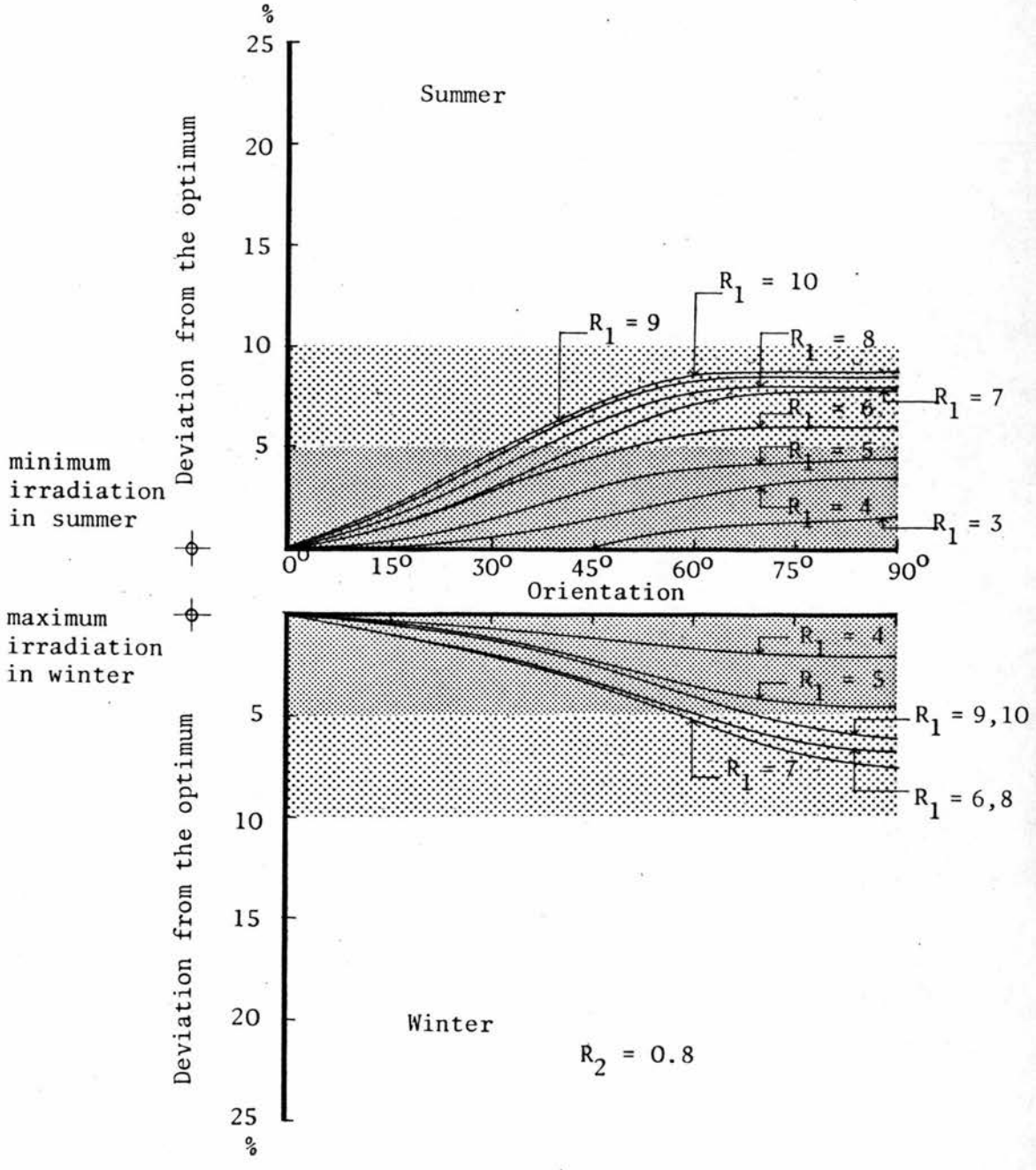

Figure VI.26 Effect of changing the orientation on the irradiation of the four walls

The study revealed that the optimum irradiation of a courtyard form is obtained by placing its longitudinal axis parallel to the east-west direction (orientation 0^{o}). However, a form might be oriented as much as 15^{o} off that optimum direction without increasing the radiation load on the surfaces in summer by more than 5% (for all cases where R_2 is greater than 0.2), or decreasing the winter irradiation by more than 2%. Even a 30^{o} deviation from the optimum does not produce more than an 8% increase in summer and 5% decrease in winter in the case of forms having R_2 = 0.6 or more. For forms having R_2 = 0.8, all cases of orientation lie within +8% of the summer optimum and within -8% of the winter optimum. Figures VI.23, VI.24, VI.25 and VI.26 show the percentage deviation from the optimum irradiation in both summer and winter that is caused by orienting the form 90^{o} away from the optimum orientation for different cases of geometries.

VI.6.1 Effect of changing the orientation on the distribution of the irradiation over the four walls

Figures VI.27 and VI.28 illustrate the change of the distribution of the irradiation over the four walls caused by changing the orientation of the form. The irradiation of each wall is expressed as a percentage of the irradiation of the four walls. The values plotted in the figures were

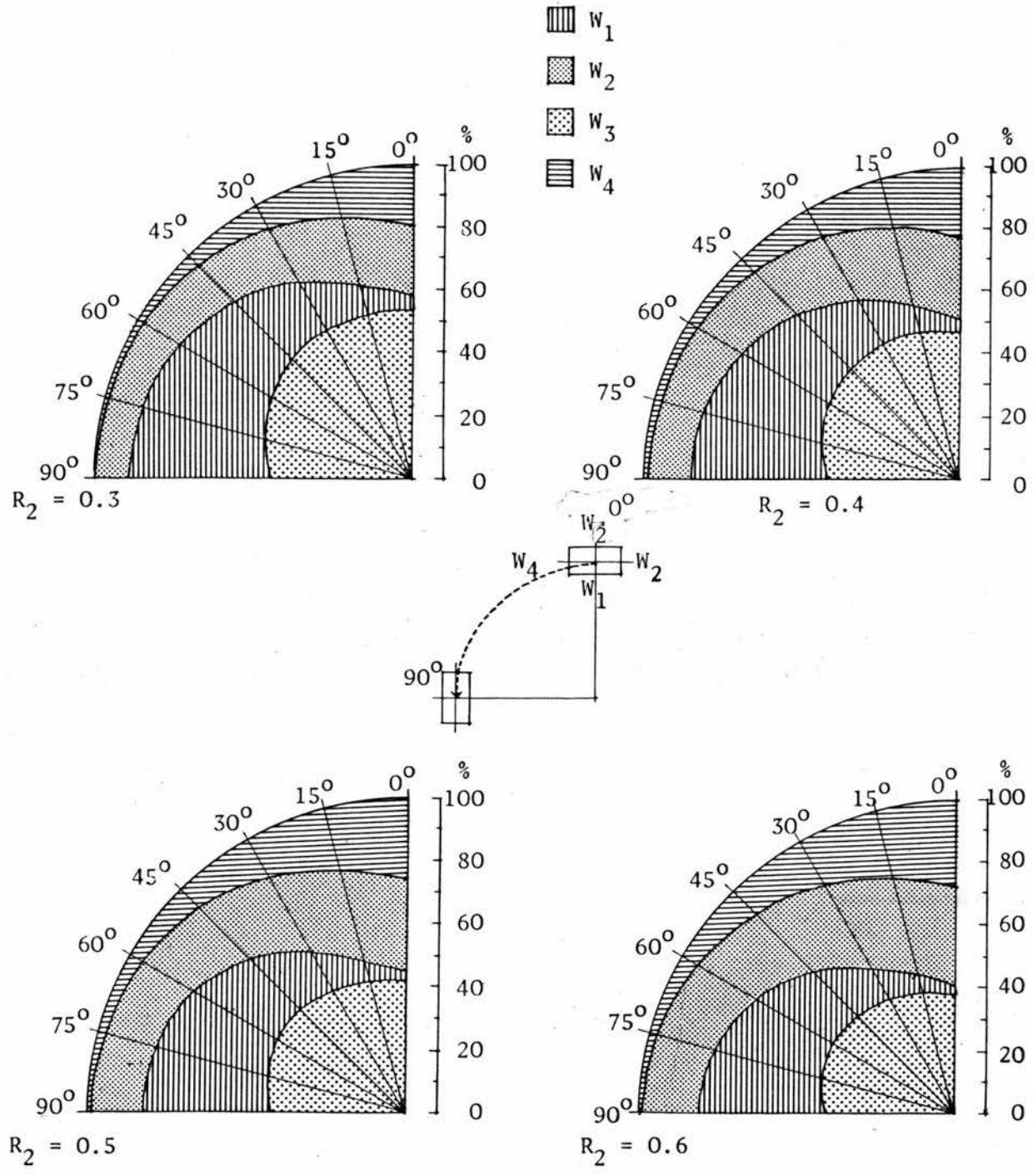

Figure VI.27 The change of the distribution of the irradiation over the four walls due to the change of orientation

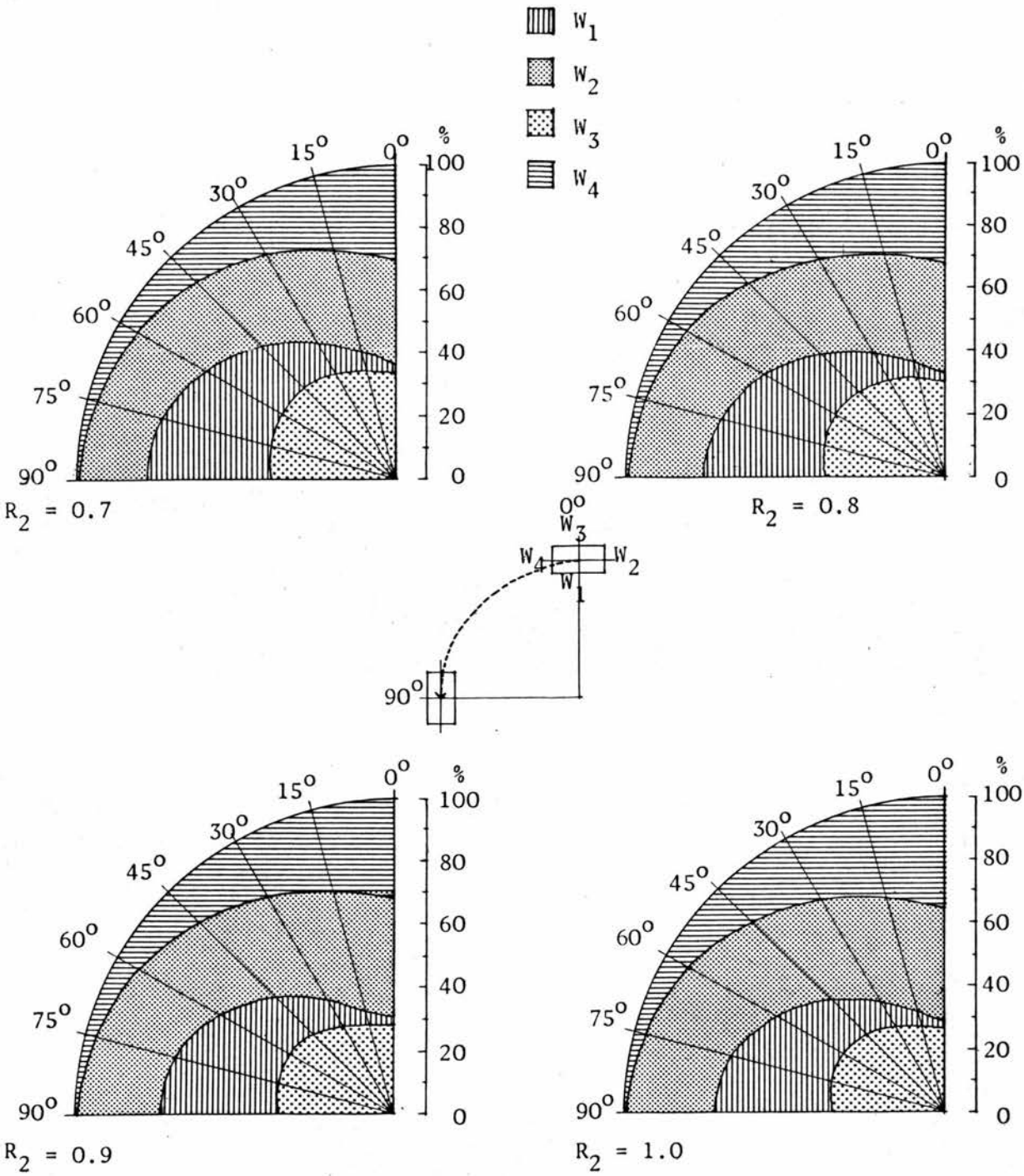

Figure VI.28 The change of the distribution of the irradiation over the four walls due to the change of orientation

produced by averaging the values that correspond to the range of the ratio R_1 considered in the study, since changing the ratio R_1 does not influence the relation between the ratio R_2 and the distribution of the irradiation (see section VI.2.1).

The contribution of the two walls W_1 and W_3 together is significant for forms having small values of R_2. It gradually increases as the orientation approaches 90^o(i.e., the long axis becomes parallel to the north-south axis). W_1 contributes the major part of such an increase: at orientation 0^o it receives very small amounts of radiation, and at orientation 90^o it receives as much as W_3.

Walls W_2 and W_4 receive equal amounts of radiation when the form is oriented at 0^o. The deviation from that direction causes a substantial decrease in the irradiation of W_4. It receives almost no radiation when the form is oriented at 90^o for all cases of R_2. The decrease in the irradiation of W_2 is less significant. Figure VI.29 summarizes the effect of changing the orientation on the contribution of each wall to the irradiation load on the four walls.

VI.7 Concluding Remarks

This stage of investigation concerns the initial irradiation of the form's surfaces. The initial irradiation load on the walls surfaces was evaluated for different combinations

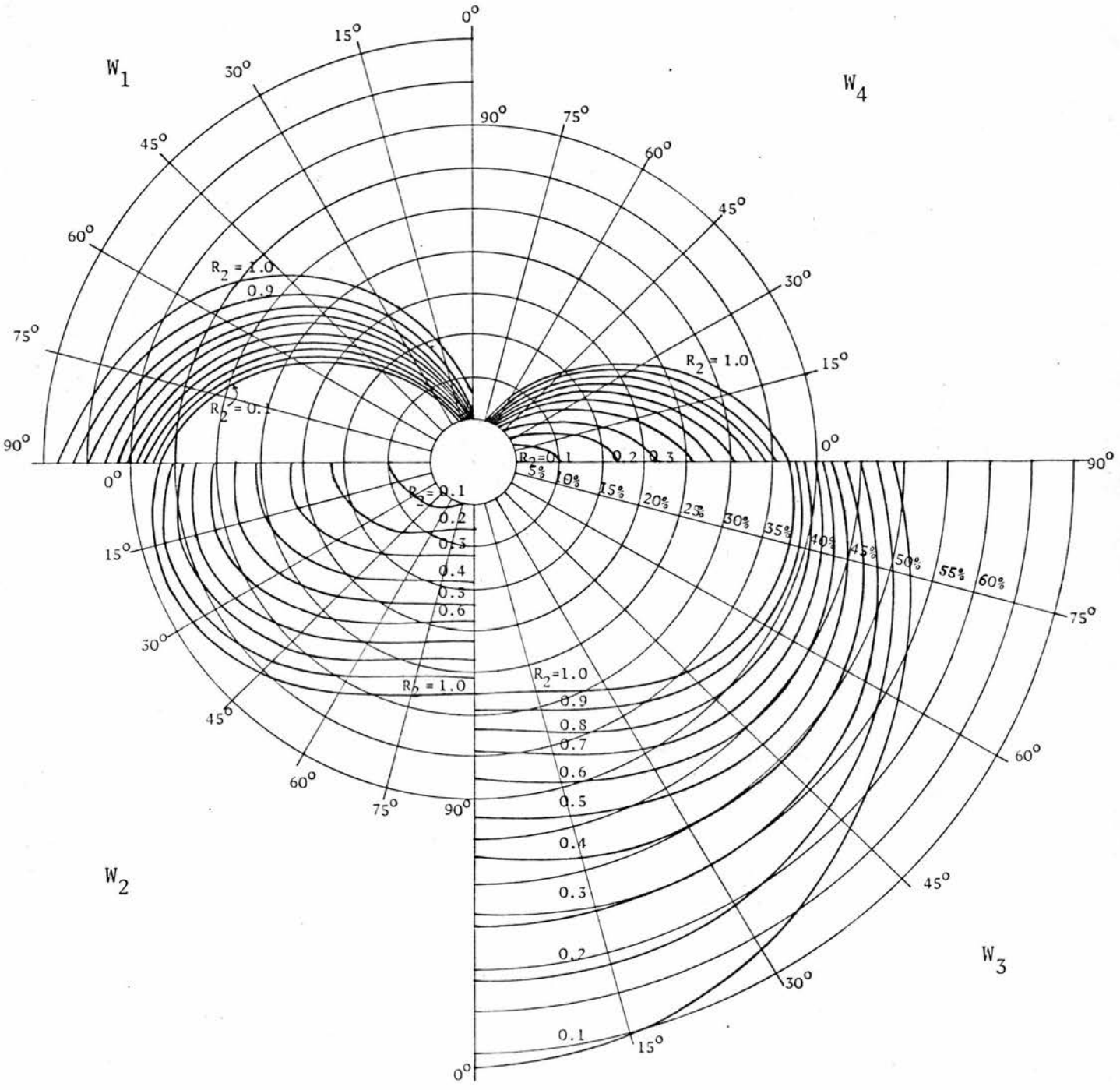

Figure VI.29 The distribution of the initial irradiation load over the four walls for different cases of orientation

of the form's parameters. The measure for evaluating the initial irradiation load on the surfaces of the form was established; it was suggested that the seasonal daily average irradiation of the surfaces of the walls is a suitable measure that allows the effect of changing the geometrical parameters of the form (proportions, size and orientation) to be studied.

The analysis of the results was guided by the criterion of thermal design in the hot-dry climate, that is to minimize the thermal load in summer and to maximize it in winter. On the basis of the analysis of the variation of the irradiation load with the variation of the geometrical parameters of the form, the following remarks are concluded :

1. The three sets of proportions which affect the irradiation load on the form's surfaces are defined as : R_1 indicating the deepness of the form, R_2 indicating the elongation of its plan and R_3 indicating its openness to the sky. The first set relates the perimeter of the form to its height, the second set relates the width to the length of the form, and the third one relates the area of the top opening to the ground area of the form.

2. The change in the value of R_1 significantly affects the irradiation load especially in winter. Changing the value of R_1 from 10 to 1 is accompanied by a decrease of about 75% of the summer irradiation load and a decrease of about 85% of the winter

irradiation load in the case of square forms. The rate of such decrease becomes less marked as the plan becomes more elongated (R_2 having smaller values).

3. As the deepness of the form is increased by adding a parapet to the top of the form's walls, the irradiation load is progressively decreasing with the increase in the parapet's height. The effect is greater in the case of small values of R_1. The following table shows the reductions in the irradiation load on the walls of square forms in summer that results from introducing different heights of parapet, p' (expressed as a ratio of the form's height).

p' \ R_1	2	4	6	8	10
0.10	21%	10%	7%	5%	4%
0.20	39%	20%	13%	10%	7%
0.30	53%	30%	20%	15%	12%

In winter the relationship between the parapet's height and the reduction in the irradiation load on the walls of square forms is shown in the following table.

p' \ R_1	2	4	6	8	10
0.10	40%	21%	12%	9%	7%
0.20	67%	40%	25%	18%	15%
0.30	86%	55%	35%	25%	21%

4. The effect of changing the plan ratio is more pronounced in winter. It is evident that the maximum irradiation load in winter favours forms having plan ratio $R_2 \leqslant 1$. The location of the maximum is partially affected by the ratio R_1: as the form becomes deeper, the maximum irradiation takes place in the vicinity of $R_2 = 1$. The following table shows the values of R_2 at which the maximum irradiation load is attained for different values of R_1.

R_1	2	4	6	8	10
R_2	1.0	0.9	0.7	0.5	0.4

The rate of decrease of the irradiation load which accompanies the change in the plan ratio R_2 is more pronounced for values of R_2 smaller than unity, however, a minimum load is attained as the ratio R_2 approaches its highest value within the chosen range.

5. The change of the irradiation load in summer which results from a change in the plan ratio is explained as follows : forms having the smallest plan ratio in the chosen range of geometries receive the minimum irradiation load. As the plan ratio is increased, the irradiation load is increased accordingly: it reaches a maximum as the ratio R_2 approaches unity in the case of deep forms. As the forms become shallower, the location of the maximum is shifted towards the cases of more elongated plans with the longitudinal axis parallel to the north-south axis.

6. The irradiation load on the form's surfaces is significantly reduced by introducing a roof projecting over the south wall. The reduction of the irradiation load caused by projecting over the south wall is greater than that caused by projecting over any of the other three walls. The following table shows the reductions of the irradiation load in summer that correspond to different values of roof projection over the south wall for square forms.

S \ R_1	2	4	6	8	10
0.1	13%	15%	17%	19%	20%
0.2	24%	27%	30%	32%	34%
0.3	35%	38%	41%	43%	44%

In winter, the reduction is slightly lower: it is less than the corresponding summer value by 2% for the deep forms and by 5% for the shallow forms. Regarding the roof projection over the west walls, the following table shows the reduction of the irradiation load in summer.

S \ R_1	2	4	6	8	10
0.1	10%	10%	11%	12%	14%
0.2	20%	21%	22%	23%	25%
0.3	30%	30%	31%	33%	34%

The corresponding winter values are less by 2% in the case of deep forms and greater by 2% in the case of shallow forms.

7. It is evident that for the very deep forms (those having R_1 less than 3), the effect of changing the orientation on the irradiation of the walls surfaces is negligible. For shallower forms, the effect is explained as follows : when the longitudinal axis is parallel to the east-west axis (orientation angle equals to zero degrees), the initial irradiation load is at its minimum in summer and at its maximum in winter. Any deviation from the zero orientation produces a corresponding increase in the irradiation load in summer and a decrease in winter. When the orientation angle becomes 90^{o}, a maximum load is received in summer and a minimum is received in winter. Hence, the optimum

orientation for summer coincides with the optimum orientation for winter. However, the change of irradiation that is caused by a change in orientation depends on the plan ratio : for square forms, the change of orientation has almost no effect on the irradiation load. As the plan gets more elongated, the effect becomes more significant. The following tables show the combined effect of the two ratios R_1 and R_2 on the significance of changing the orientation. The figures shown in the tables are the orientation angles that produce a deviation within 5% and 10% from the optimum orientation in both summer and winter.

R_1 \ R_2	0.2	0.4	0.6	0.8	1.0
4	20^o	35^o	60^o	90^o	90^o
7	15^o	20^o	30^o	45^o	90^o
10	10^o	15^o	20^o	30^o	90^o

The first table shows the orientation angles that produce deviations not more than 5% of the optimum in summer.

R_1 \ R_2	0.2	0.4	0.6	0.8	1.0
4	90^o	90^o	90^o	90^o	90^o
7	22^o	30^o	45^o	90^o	90^o
10	20^o	25^o	35^o	90^o	90^o

The second table shows the orientation angles that produce deviations not more than 10% of the optimum in summer. The following two tables show the orientation angles that produce 5% and 10% deviation from the optimum in winter.

R_1 \ R_2	0.2	0.4	0.6	0.8	1.0
4	90°	90°	90°	90°	90°
7	40°	30°	30°	60°	90°
10	25°	22°	30°	60°	90°

R_1 \ R_2	0.2	0.4	0.6	0.8	1.0
4	90°	90°	90°	90°	90°
7	52°	45°	52°	90°	90°
10	35°	35°	52°	90°	90°

8. Regarding the distribution of the initial irradiation load on the surfaces of the form, the change of the ratio R_1, has negligible effect. The effect of changing the ratio R_2 and the angle of orientation is explained as follows : for forms having zero degree orientation, the contribution of the wall W_1 (north wall) is very small, it does not exceed 10% even for the most elongated forms. The two walls W_2 and W_4 (east and west walls) together contribute

about 25% in the case of forms having small ratio R_2. However, this contribution increases to 70% as the ratio R_2 approaches unity. The contribution of W_3 (south wall) varies from about 60% in the case of very elongated forms to about 25% in the case of square forms.

The change of orientation produces a corresponding change in the distribution of the initial irradiation load on the surfaces of the four walls. By orienting a square form at 45^{o}, each of W_2 and W_3 contributes about 33% of the whole load. The remaining third is distributed equally between the other two walls. For forms having small ratio R_2, the contribution of the two long walls W_1 and W_3 increases significantly as the orientation angle is increased : at orientation 90^{o}, W_1 receives radiation as much as W_3. On the other hand, the contribution of W_4 is substantially decreased.

9. When considering the actual dimensions of the form, it is evident that in a two storey courtyard the walls of the upper storey receive more irradiation load than that received by the walls of a single storey courtyard having the same proportions. On the other hand, the irradiation load on the surfaces of the lower storey is far less than that on the surfaces of the single storey courtyard.

10. The example given in figure VI.22 shows that for a single storey courtyard, the case of geometry which satisfies the minimum irradiation load in summer differs from the case of geometry which satisfies the maximum irradiation load in winter. However, the ranges of geometries whose irradiation loads lie within specified ranges from the optimum both in summer and winter were identified. It is evident that there are ranges of geometries which are sufficiently close to the optimum in summer as well as the optimum in winter. In figures VI.30 and VI.31 the idea of identifying such ranges of geometries is extended to include another variable; that is the angle of orientation. The three-dimensional ranges illustrated in the figures resulted from changing the values of the ratios R_1, R_2 and the orientation angle θ.

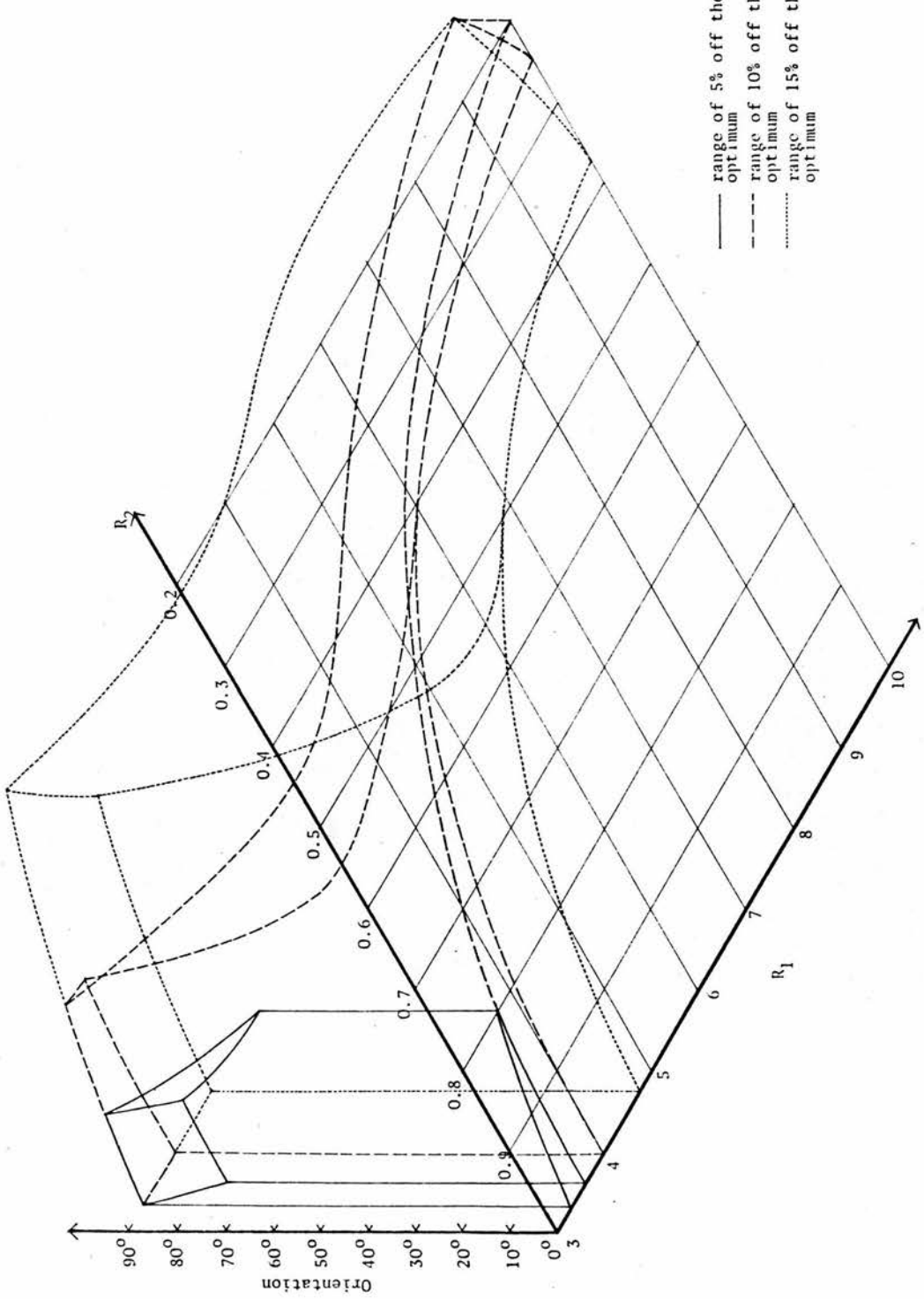

Figure VI.30 Ranges of geometries whose performance is within specified ranges of the optimum in summer (single storey forms)

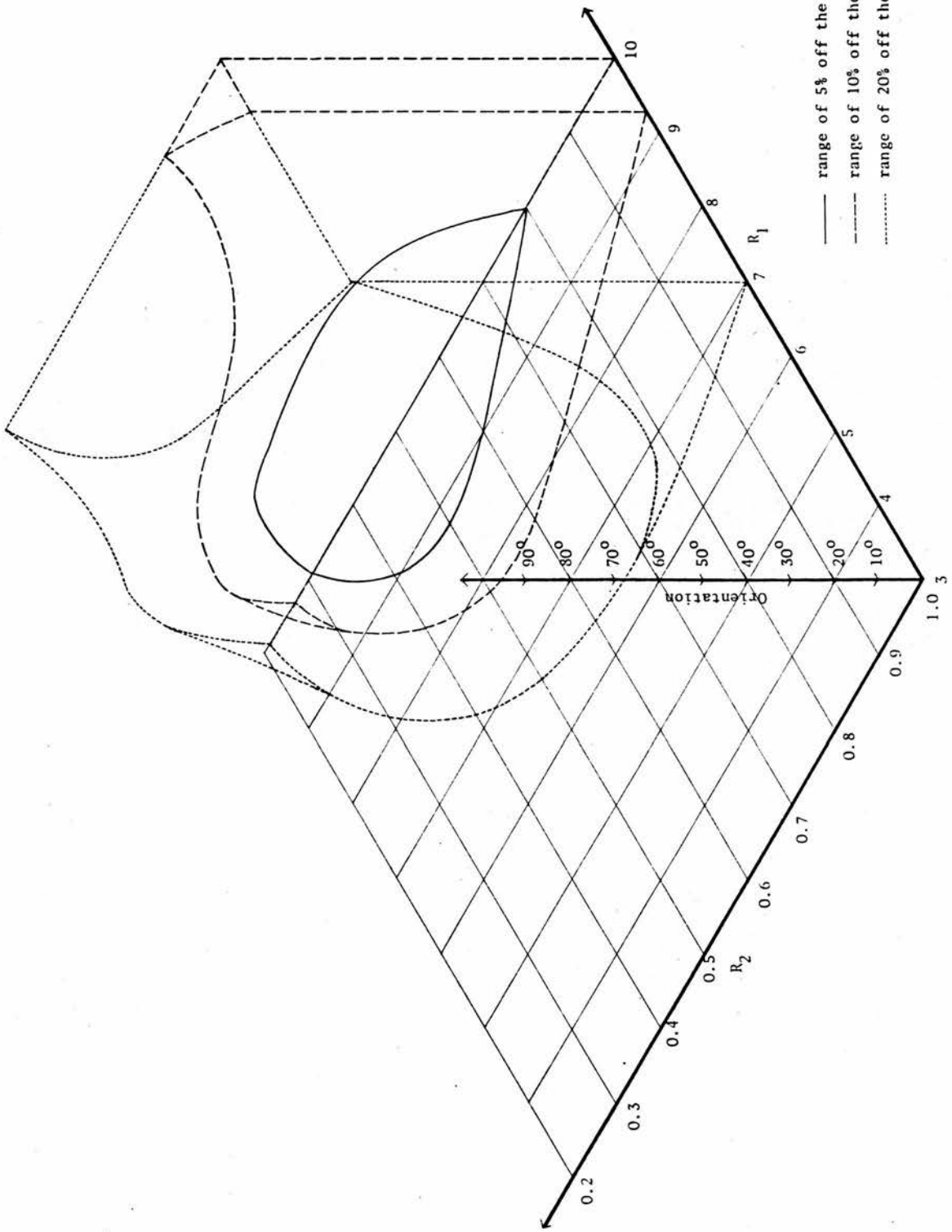

Figure VI.31 Ranges of geometries whose performance is within specified ranges of the optimum in winter (single storey forms)

CHAPTER VII

FURTHER ASPECTS IN THE FORM - PERFORMANCE RELATIONSHIP

VII.1 Radiant Exchange among the Surfaces of a Courtyard's Envelope

As outlined in Chapter II, the surfaces of a courtyard's envelope are subjected to radiant excitation caused by : (a) incident direct solar radiation and (b) diffuse radiation coming from the sky. Discussions of the interaction between these sources of energy and the geometry of the form have shown that, for the present study, the incident direct radiation is justifiably considered the initial load acting upon the surfaces of the form (see section IV.3).

In the present chapter attention is directed to the thermal exchanges taking place at the surfaces of the envelope. As mentioned in section II.2.1, part of the direct radiation incident upon an opaque surface is absorbed and the rest is reflected according to the reflectivity of the material of the surface. Concerning a courtyard form enclosed with vertical opaque surfaces, part of the radiation reflected by one surface will be received by the others according to the geometrical configuration of the form. The absorbed radiation elevates the temperature of the surface which will be exchanging heat, in one direction, by conduction through the fabric of the structure and in the other direction by convection and by

emitting long-wave radiation to the sky and surrounding surfaces.

The result of the interreflection of the radiation among the surfaces of the form, and the consequent absorption and emission of heat is the concern of this chapter. It is referred to as the final irradiation load that acts upon the fabric of the structure. To investigate the interreflection processes in relation to the physical and geometrical parameters of the form, without becoming involved with excessively complicated techniques, it is necessary to make some assumptions. First, to assume that the direct component of solar radiation is the only source of external energy. Second, to consider all the surfaces to be perfectly diffuse emitters and reflectors which means that the angle of incidence at which the sun's rays impinge on the surface is not significant. The third assumption is that the energy incident upon a surface is uniform over all the parts of that surface. This means simplifying the real situation, where a surface is partially insolated and consequently the energy is transferring between its different parts to a situation where the surface is uniformly irradiated.

In a study carried out by Sparrow and others in 1961, comparisons between the simpified approach of uniform irradiation and a more detailed approach have shown that, in

spite of the variations in the local heat transfer, the assumption of uniformity leads to good overall heat transfer prediction (Sparrow et al, 1961).

VII.1.1 Configuration factors

Based on these assumptions, the present chapter examines the radiant heat exchanges taking place at the surfaces of the courtyard envelope. The fraction of the energy leaving one surface and directly incident upon another surface is known as the configuration factor (Wiebelt, 1965). In an enclosure composed of black surfaces, the energy emitted by one surface is received by the others, each according to the configuration factor from the emitting surface to the receiving one. The sum of the fractions of the incident energy must add to the total energy leaving the emitting surface. This is expressed as follows :

$$\sum_{j=1}^{n} F_{ij} = 1 \qquad \text{VII.1}$$

where F_{ij} is the configuration factor from the surface i to the surface j.

The second basic relation that simplifies the evaluation of the configuration factors in an enclosure of finite surfaces is the reciprocity that exists between the configuration factors. This is expressed as follows :

$$F_{ij} A_i = F_{ji} A_j \qquad \text{VII.2}$$

where A_i and A_j are the areas of the surfaces i and j respectively.

Wiebelt (1955) presented expressions for determining the configuration factors for various geometrical relations between surfaces. The two configurations which are of interest in the present study are :

(a) Two identical parallel directly opposed rectangles and

(b) Two rectangles with one common edge.

The expressions for evaluating the configuration factors in these two cases are given in Appendix 1.

VII.1.2 Absorption factors

In an enclosure composed of non-black surfaces, only a part of the radiation impinging on a surface is absorbed according to the absorptivity of its material to short-wave radiation. The rest of the radiation is diffusely reflected. The contribution of the reflected radiation to each of the other surfaces is governed by the configuration factors from the reflecting surface to each one of them. Part of this radiation is absorbed and the rest is reflected and so on. The heated surfaces emit some of the gained energy according to their emissivities to long-wave radiation. The emitted radiation will be interreflected among the surfaces in a similar way

to that followed by the incident direct solar radiation.

The net rate of radiant exchange for a surface is equal to the rate of radiant energy emitted by the surface minus its total rate of absorption which includes both the direct and the reflected components. In assessing such a rate, all the paths by which the radiant energy travels must be taken into consideration.

Gebhart (1959) introduced a method for calculating the radiant exchanges in an enclosure made up of n non-black surfaces. For each surface, the rate of loss was found by subtracting from the emission rate of the surface the sum of the rates of absorption at the other surfaces. A quantity called the absorption factor was defined as the fraction of the radiant energy leaving one surface which is absorbed by another including all paths by which the energy travels. According to Gebhart's definition, the absorption factors are the generalized form of the configuration factors when the enclosure is composed of non-black surfaces (Gebhart, 1959).

Hence, the relations between the absorption factors in an enclosure are similar to those presented in equations VII.1 and VII.2.

$$\sum_{j=1}^{n} B_{ij} = 1 \qquad \text{VII.3}$$

$$B_{ij}\,\alpha_i\,A_i = B_{ji}\,\alpha_j\,A_j \qquad \text{VII.4}$$

where α_j is the absorptivity of the material of the surface j.

The absorption factor at a surface j is found by summing up the absorption rates at j due to the combined flux of the emitted and reflected radiation at the other surfaces as expressed in equation VII.5.

$$B_{1j} = F_{1j}\,\alpha_j + F_{11}\,\rho_1\,B_{1j} + F_{12}\,\rho_2\,B_{2j} + \ldots + F_{1n}\,\rho_n\,B_{nj} \qquad \text{VII.5}$$

For each surface, a similar equation can be written, the set of equations can be solved for the n unknowns of absorption factors.

In an n-surfaces enclosure, the rate of radiant heat gain of any surface j, is equal to the absorption rates at A_j of both the incident direct radiation and the portion of the combined radiant flux leaving each of the n surfaces, minus the emission rate of the surface. Determination of the emission rate of a surface involves some difficulties since it is dependent on the temperature of the surface. Besides, the contribution of the emission rate to the rate of net radiant exchange is very small when compared with the contribution of the direct solar radiation and the inter-reflected radiation. Therefore,it was decided to neglect

the emission rate. The rate of radiant heat gain of a surface, q_j, is then written as follows :

$$q_j = \alpha_j D_j A_j + B_{1j} \rho_1 D_1 A_1 + B_{2j} \rho_2 D_2 A_2 + \ldots + B_{nj} \rho_n D_n A_n$$

$$q_j = \alpha_j D_j A_j + \sum_{i=1}^{n} B_{ij} \rho_i D_i A_i \qquad \text{VII.6}$$

where D_i and D_j are the initial irradiation of the surfaces i and j per unit area.

VII.2 Evaluating the Configuration Factors and the Absorption Factors for a Courtyard Form

In an enclosure like a courtyard form there are six surfaces, four walls, a ground and a hypothetical roof with the peculiar characteristic of transmitting all the radiant energy reaching it and emitting or reflecting none. The number of the unknown configuration factors can be reduced to six by considering the symmetry of the form and by using equations VII.1 and VII.2.

To simplify the calculations, the four walls are taken together. The configuration factor from the ground surface to the hypothetical roof, F_{GR}, is calculated by using equation A1.1 which is presented by Wieblet (1965) for calculating the configuration factor between two identical

parallel directly opposed rectangles (see Appendix 1). The configuration factor from the ground surface to the walls, F_{GW}, is then found :

$$F_{GW} = 1 - F_{GR} \qquad \text{VII.7}$$

$$F_{WG} = F_{GW} \times A_G/A_W \qquad \text{VII.8}$$

$$F_{WW} = 1 - 2\,F_{WG} \qquad \text{VII.9}$$

where A_W and A_G are the areas of the walls and the ground respectively. F_{WW} is the configuration factor between the walls.

Values of the configuration factors for the cases of proportions included in the study were calculated using equations A1.1 and VII.7-9. Figure VII.1 illustrates the variation of the values of the configuration factors with the variation of the values of the two ratios R_1 and R_2. It is evident that as R_1 approaches zero the values of F_{GW} and F_{WW} approach unity. With the increase of the values of R_1, the corresponding decrease in the value of F_{WW} is more pronounced than that of F_{GW}. The effect of changing the value of R_2 is significant for small values of R_2, however, as R_2 approaches unity the effect is less pronounced.

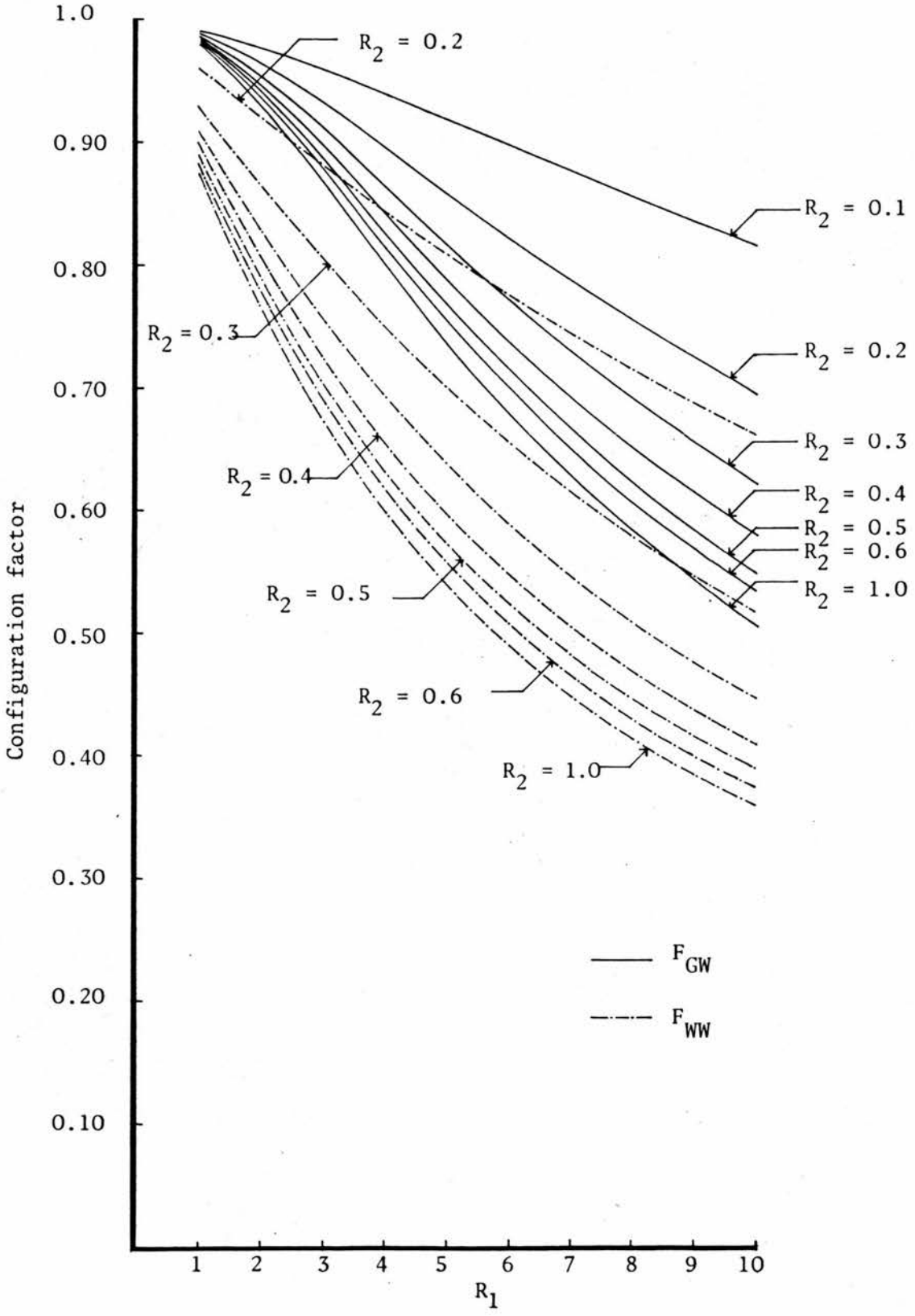

Figure VII.1 Variation of the configuration factors F_{GW} and F_{WW} with the variation of the ratios R_1 and R_2

Regarding the absorption factors, there are two unknowns : the absorption factor B_{GW} which represents the fraction of the radiation leaving the ground surface and is eventually absorbed by the walls after being multireflected. The second unknown is B_{WW} which represents the fraction of the radiation which leaves the surfaces of the walls and is eventually absorbed by the walls after being multireflected.

$$B_{WW} = F_{WW}\,\alpha_W + F_{WW}\,\rho_W\,B_{WW} + F_{WR}\,\rho_R\,B_{RW} + F_{WG}\,\rho_G\,B_{GW} \qquad \text{VII.10}$$

$$B_{GW} = F_{GW}\,\alpha_W + F_{GG}\,\rho_G\,B_{GW} + F_{GW}\,\rho_W\,B_{WW} + F_{GR}\,\rho_R\,B_{RW} \qquad \text{VII.11}$$

where α and ρ are the absorptivity and reflectivity of a surface respectively. The subscripts W, G and R designate walls, ground and roof respectively.

Since $\rho_R = 0$

Then $$(F_{WW}\,\rho_W - 1)B_{WW} + F_{WG}\,\rho_G\,B_{GW} + F_{WW}\,\alpha_W = 0 \qquad \text{VII.12}$$

$$F_{GW}\,\rho_W\,B_{WW} + (F_{GG}\,\rho_G - 1)B_{GW} + F_{GW}\,\alpha_W = 0 \qquad \text{VII.13}$$

By solving equations VII.12 and VII.13 then

$$B_{WW} = \frac{F_{GW}\,\alpha_W\,F_{WG}\,\rho_G + F_{WW}\,\alpha_W}{-F_{WW}\,\rho_W + 1 - F_{WG}\,\rho_G\,F_{GW}\,\rho_W} \qquad \text{VII.14}$$

$$B_{GW} = F_{GW}\,\rho_W\,B_{WW} + F_{GW}\,\alpha_W \qquad \text{VII.15}$$

Equations VII.14 and VII.15 were used for generating the values of B_{GW} and B_{WW} that correspond to different values of the walls absorbtivity, α_W, and different values of the ground reflectivity, ρ_G. Figures VII.2 and VII.3 illustrate the dependence of the absorption factors B_{WW} and B_{GW} on the geometrical configuration of the form as well as on the reflectivity of its surfaces. Regarding the geometrical configuration, the value of B_{WW} decreases as the plan ratio R_2 approaches unity. However, the effect of changing the plan ratio is rather small compared with the effect of changing the deepness ratio, R_1. The value of B_{WW} decreases progressively as the value of R_1 is increased, the rate of decrease is greater for the smaller values of R_1.

Regarding the reflectivity of the form's surfaces, the absorption factor B_{WW} decreases as the reflectivity of walls surfaces, ρ_W, is increased, the rate of decrease becomes greater for higher values of ρ_W. But it decreases as the reflectivity of the ground surface is decreased. The absorption factor, B_{GW} follows the same pattern of changes that correspond to the changes taking place in the values of R_1, R_2, ρ_W and ρ_G, however, the effect is more pronounced.

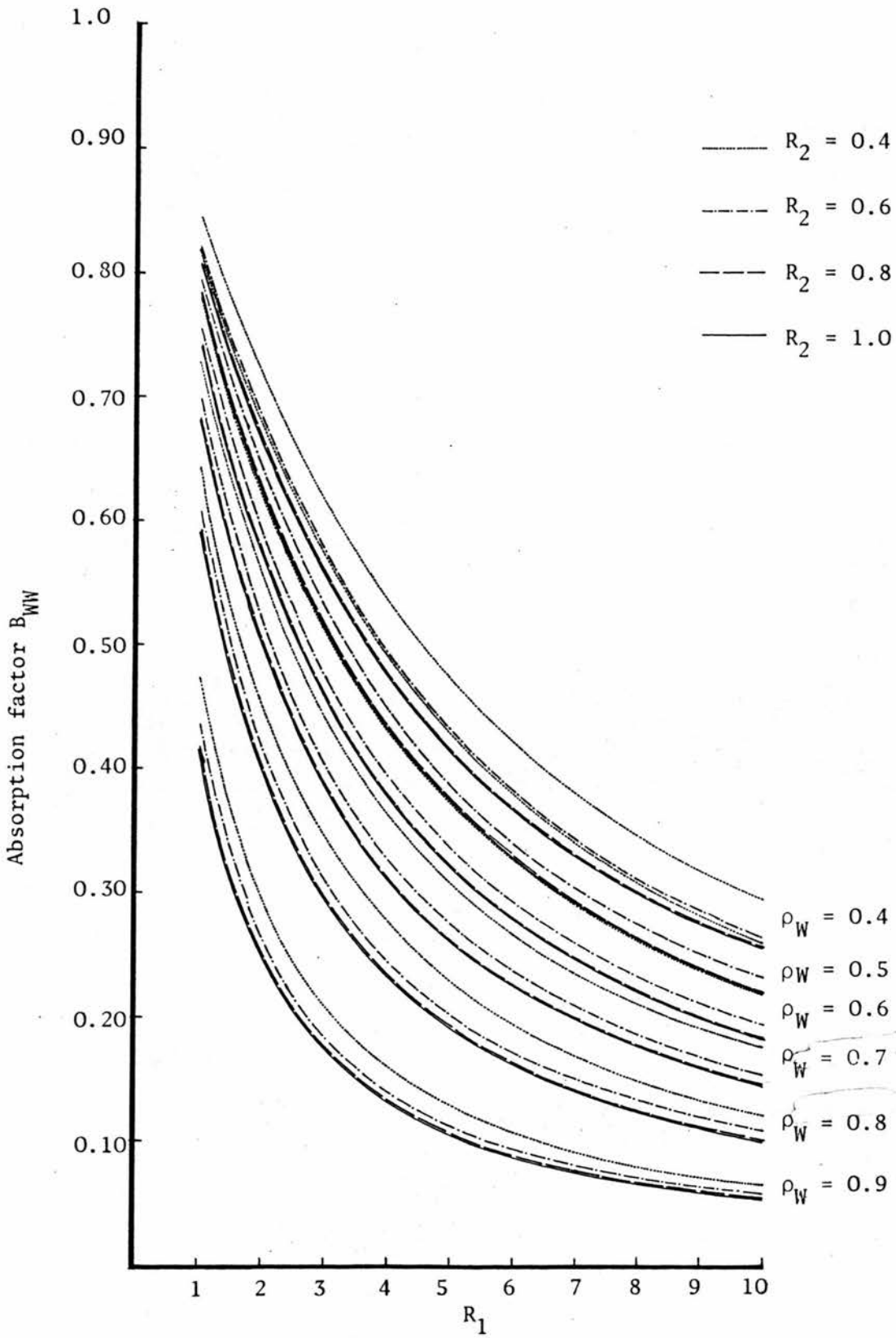

Figure VII.2 Variation of the absorption factor B_{WW} with the variation of R_1, R_2 and ρ_W for forms having ρ_G = 0.0

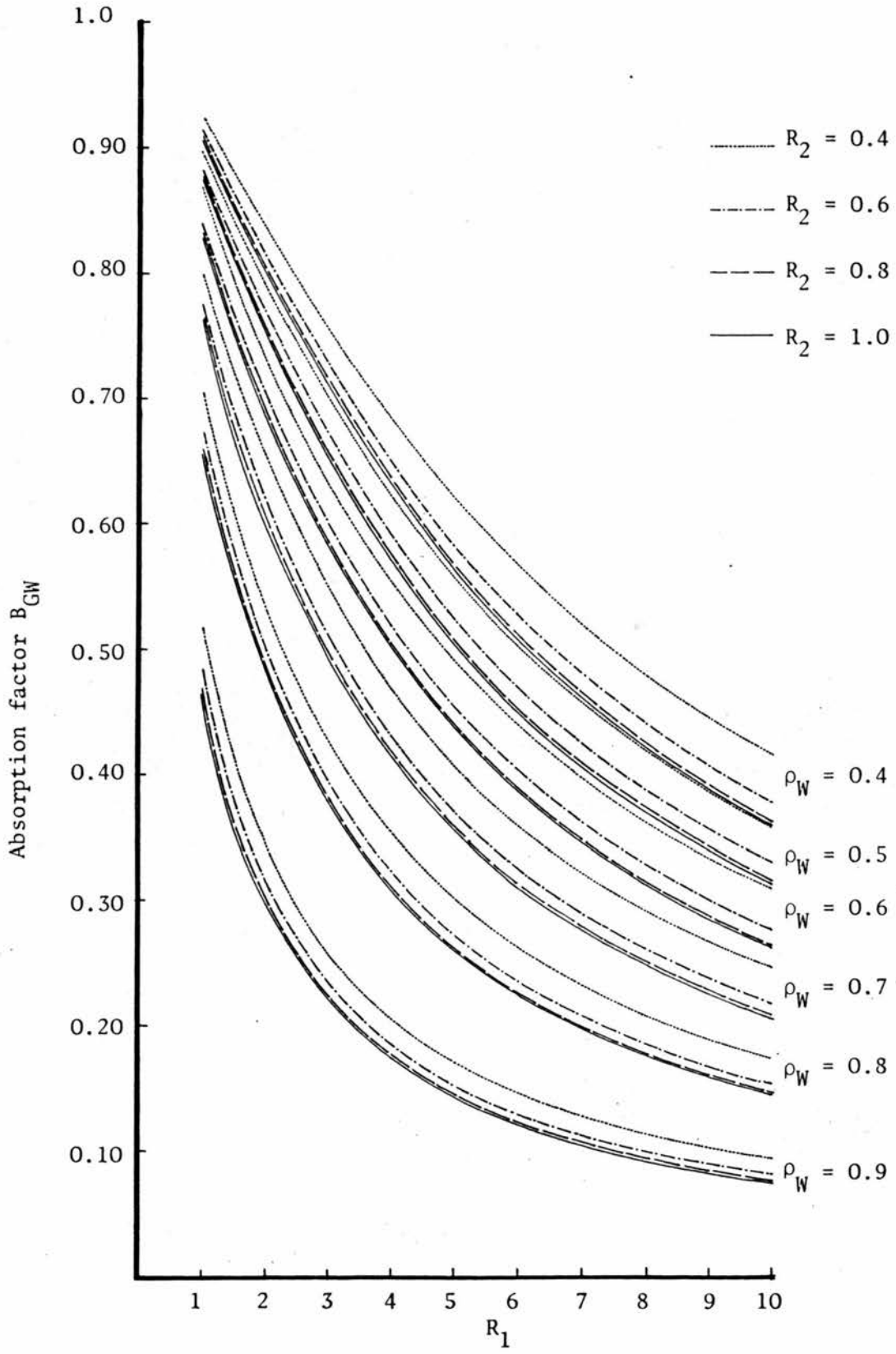

Figure VII.3 Variation of the absorption factor B_{GW} with the variation of R_1, R_2 and ρ_W for forms having ρ_G = 0.0

VII.3 Final Irradiation Load

In order to determine the final irradiation load acting on the walls of the form, substitute in equation VII.6.

$$q_W = \alpha_W D_W + B_{GW} \rho_G D_G + B_{WW} \rho_W D_W$$

$$= (\alpha_W + B_{WW} \rho_W) D_W + B_{GW} \rho_G D_G$$

Let $K_1 = \alpha_W + B_{WW} \rho_W$ and $K_2 = B_{GW} \rho_G$

Then

$$q_W = K_1 D_W + K_2 D_G \qquad \text{VII.16}$$

The two quantities D_W and D_G represent the initial irradiation load received by the surfaces of the walls and the ground respectively. It has been indicated in section VI.1.1 that the contribution of the ground surface to the total initial irradiation of the form is represented by C_G, where $C_G = \frac{D_G}{T}$. Similarly, the contribution of the walls surface to the total initial irradiation of the form is represented by C_W, where $C_W = \frac{D_W}{T}$.

Then the ratio of the final irradiation load on the walls to the initial irradiation load of the form is represented as follows :

$$\frac{q_W}{T} = K_1 C_W + K_2 C_G \qquad \text{VII.17}$$

In order to study the effect of changing the geometrical and physical parameters of the form on the ratio $\frac{q_W}{T}$, let us examine the righthand side of equation VII.17. The values of C_W and C_G are functions of the geometrical parameters of the form as illustrated in figure VI.2. It has been seen that the value of C_W decreases progressively with the increase in the value of R_1. Its value does not change with the changes in the value of R_2 in the vicinity of $R_2 = 1$, but as R_2 approaches zero, C_W and C_G approach 100% and 0% respectively.

The two ratios K_1 and K_2 are determined by the geometrical configuration of the form and the reflectivity of the materials of its surfaces (see figure VII.4). The ratio K_2 indicates the contribution of the initial irradiation load on the ground surface to the final load acting on the walls. Its value is in direct proportion to the reflectivity of the ground surface, ρ_G: it approaches zero as the value of ρ_G is decreased. The effect of the reflectivity of the walls surface is the opposite.

The ratio K_1 indicates the contribution of the initial irradiation load on the walls surface to the final load acting on the walls. The value of K_1 decreases as the value of ρ_W is increased. It also decreases as the value of ρ_G decreases. However, the effect of changing the value of ρ_G on the value of K_1 is very small: it does not exceed 2% for any case of geometry. The effect of changing the values of

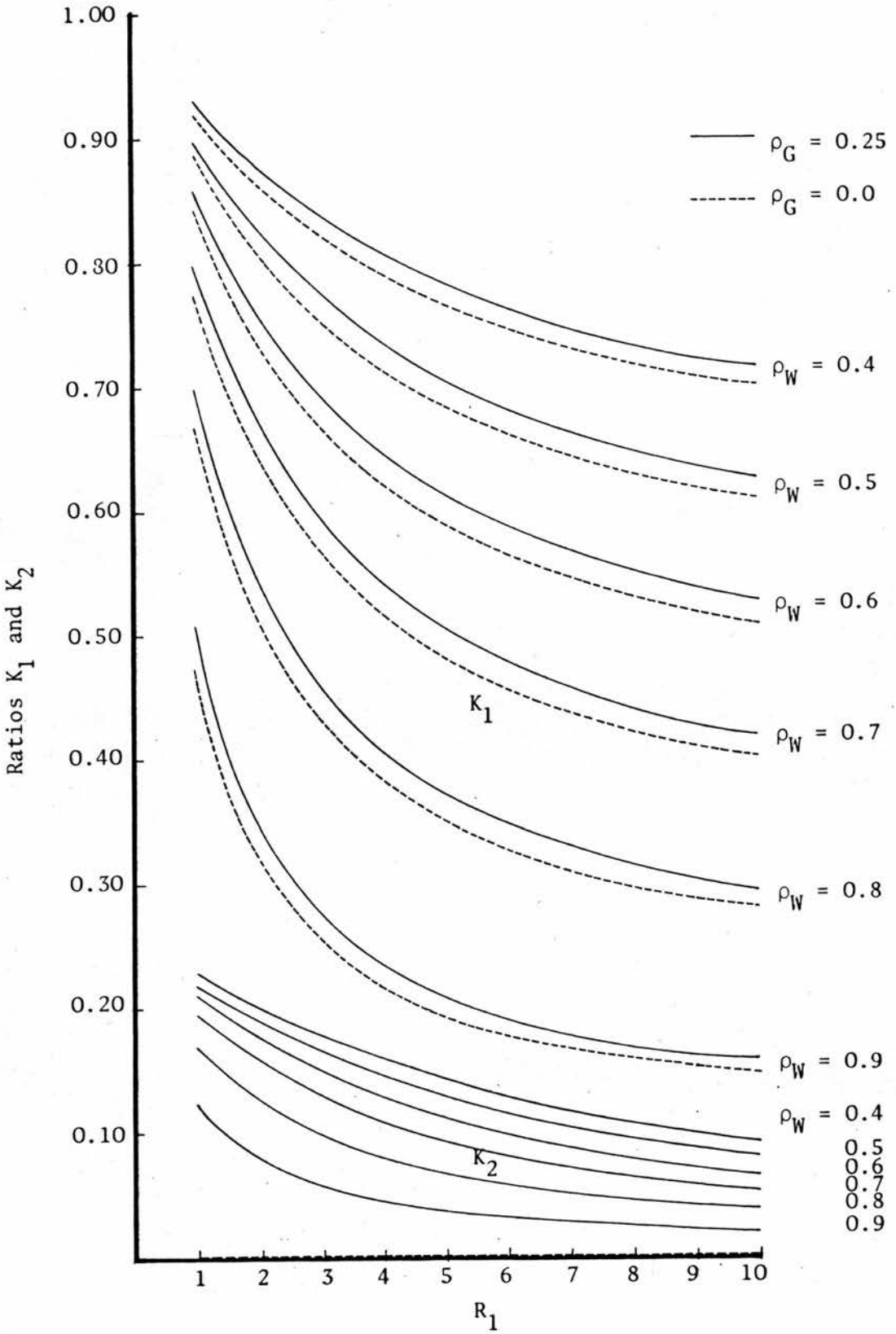

Figure VII.4 Variation of the ratios K_1 and K_2 with the variation of R_1, ρ_W and ρ_G for forms having R_2 = 1.0

ρ_W becomes very significant as the value of R_1 gets greater. It is more remarkable at the higher values of ρ_W.

It is evident that the ground component constitutes a small part of the final irradiation load on the walls. It reaches a maximum when both the value of the ratio R_1 and the value of ground reflectivity are at their maximum. The wall component increases as the value of R_1 gets smaller values, since the value of C_W increases and the value of K_1 increases. This increase can be slowed down by choosing greater values of walls reflectivity.

Figures VII.5,6,7,8 and 9 show the combined effect of the geometrical configuration and the surface reflectivity of the walls and ground on the ratio, f, of the final irradiation load to the total initial irradiation load. The effect of changing the surface reflectivity of the walls depends on the geometry of the form : for forms having small values of R_1 (deep forms) the increase in the value of ρ_W from 0.4 to 0.8 produces a drop in the ratio f from 80% to 50%. A further increase of 0.1 in the walls reflectivity brings the ratio down to 35%.

Improvements can be obtained by increasing the ground reflectivity, the effect is pronounced in the cases of low walls reflectivity : by increasing ρ_G from 0.00 to 0.25, the ratio f is reduced by 15%. In the case of higher values of ρ_W, such an effect is minimized to only 5%.

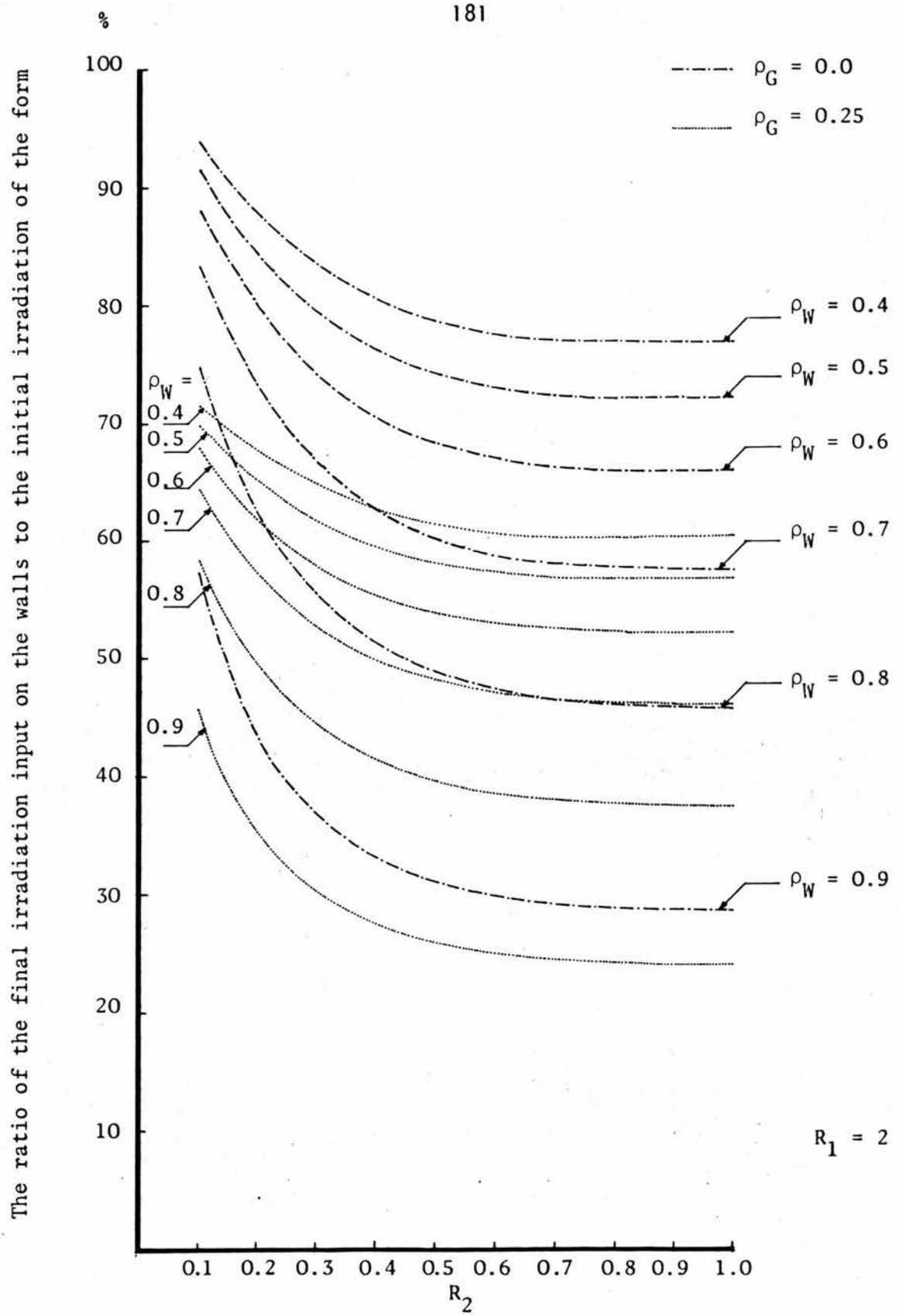

Figure VII.5 Variation of the ratio between the final irradiation input on the walls and the initial irradiation of the form with the variation of R_2, ρ_W and ρ_G

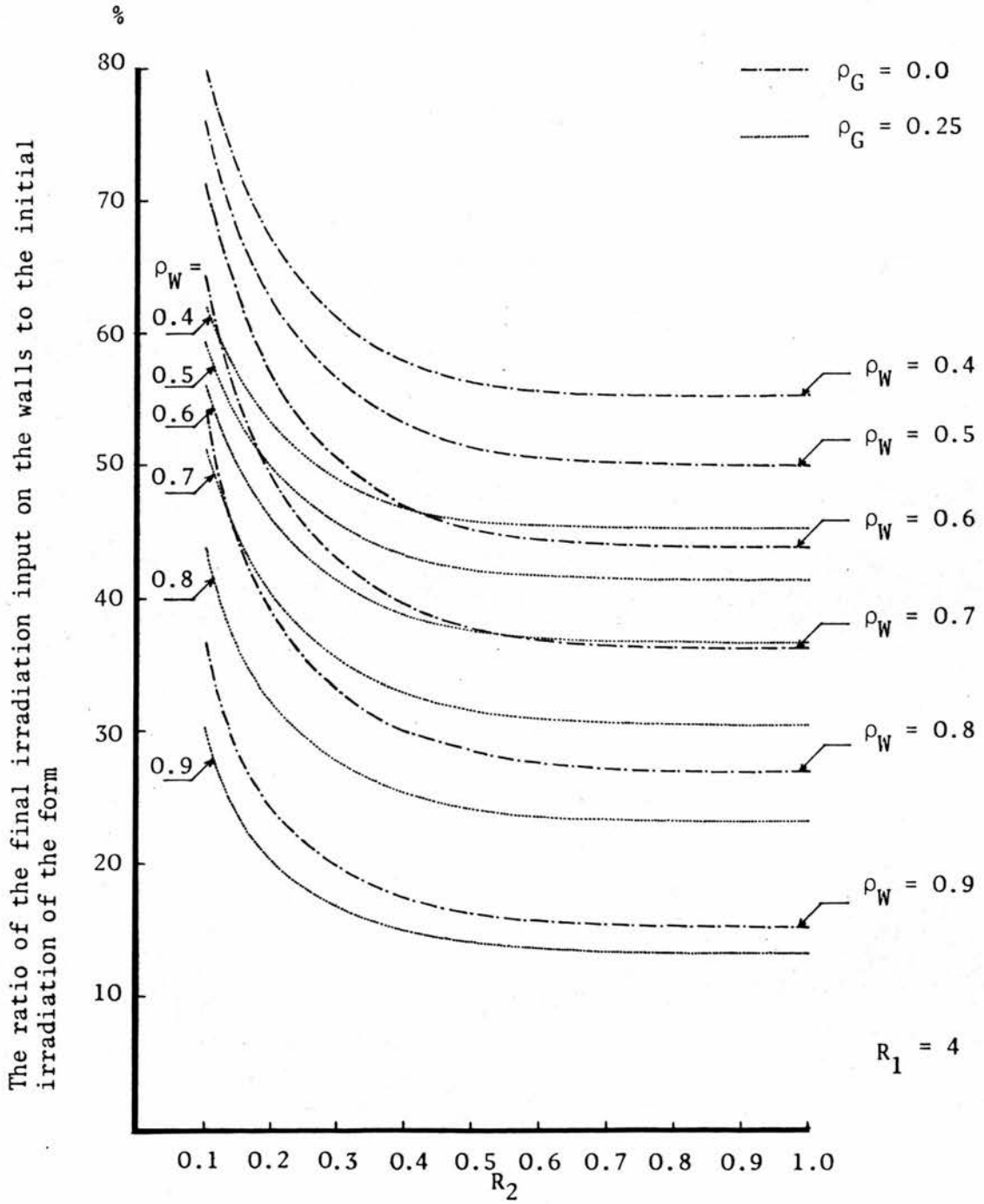

Figure VII.6 Variation of the ratio between the final irradiation input on the walls and the initial irradiation of the form with the variation of R_2, ρ_W and ρ_G

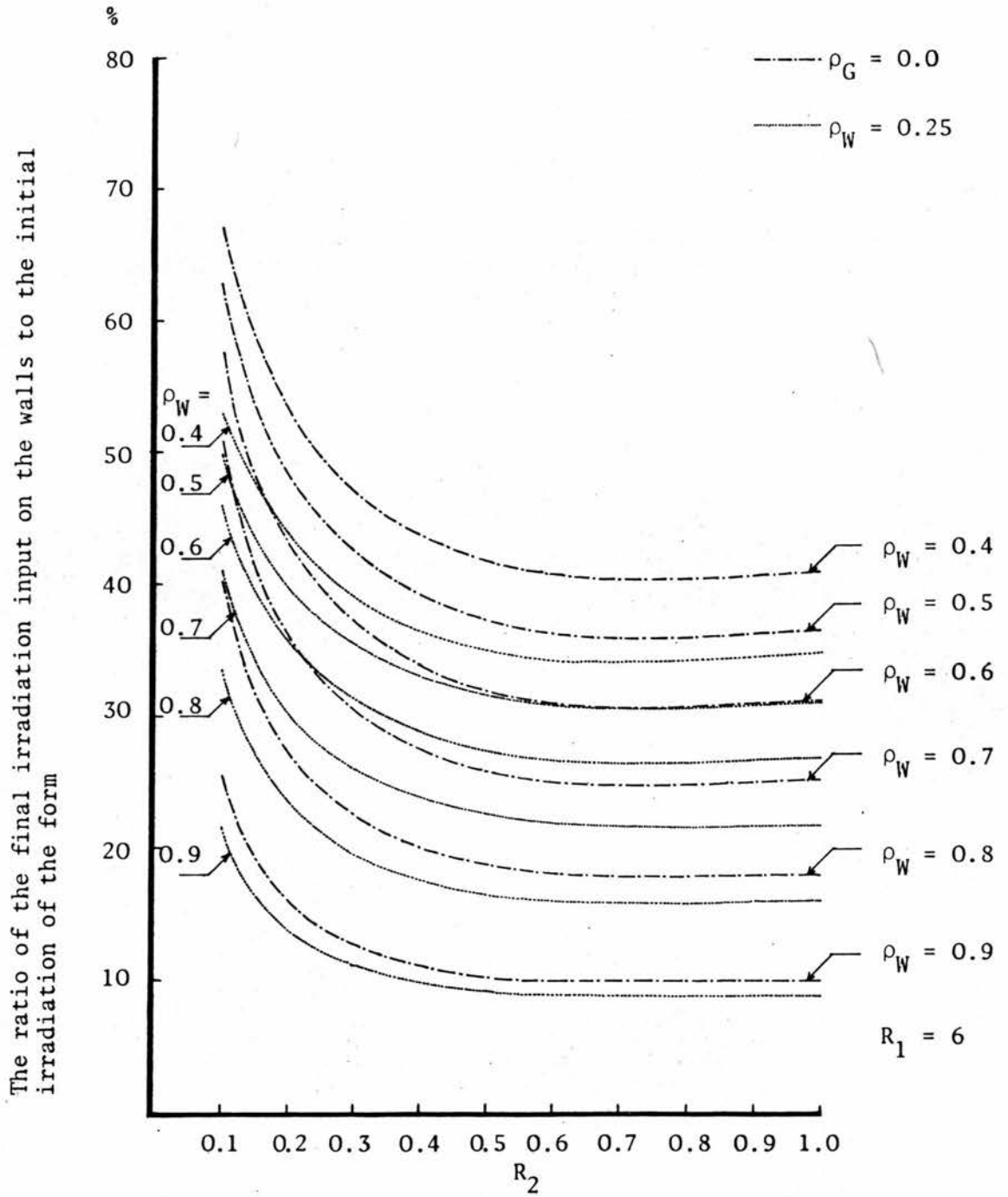

Figure VII.7 Variation of the ratio between the final irradiation input on the walls and the initial irradiation of the form with the variation of R_2, ρ_W and ρ_G .

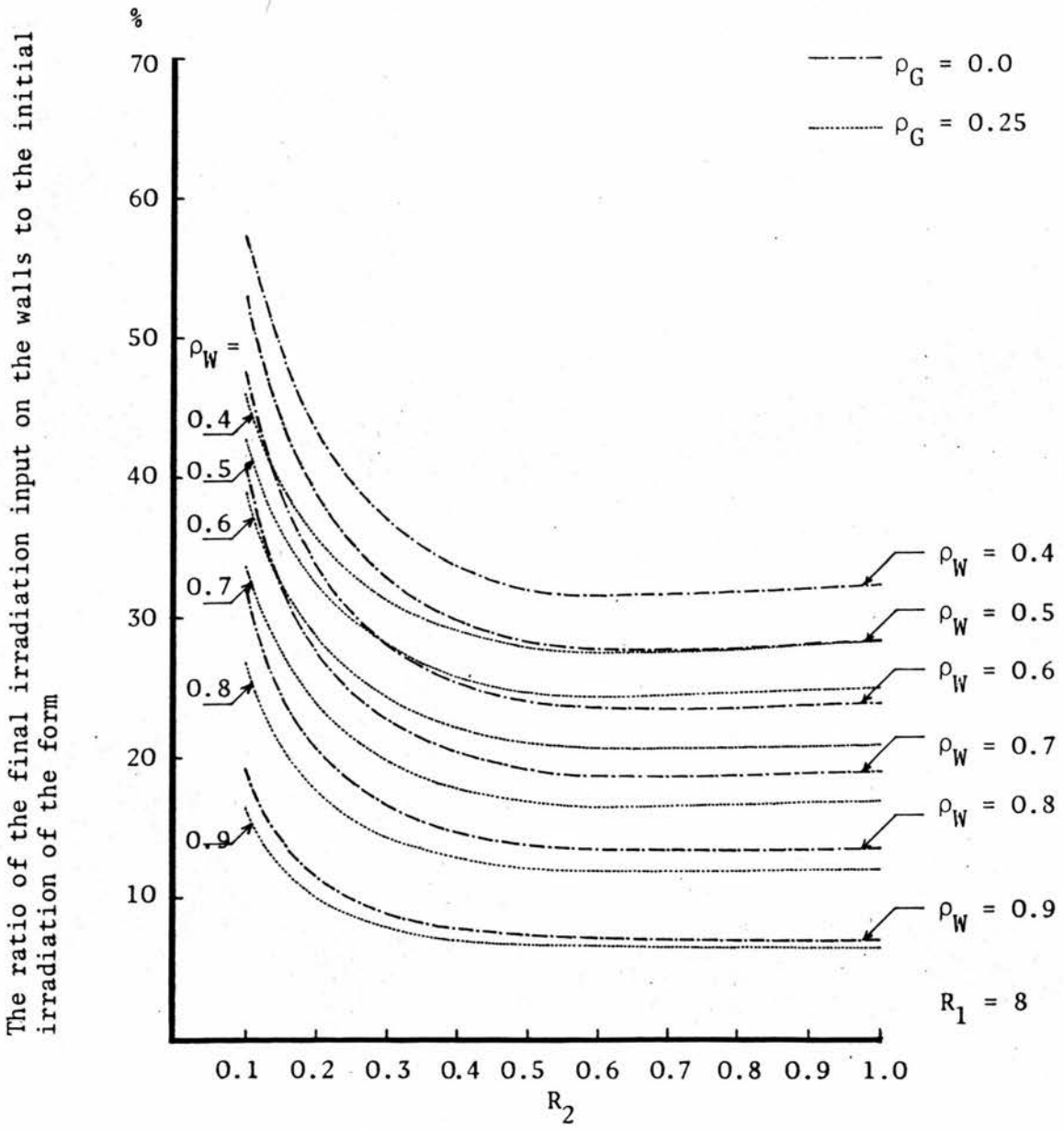

Figure VII.8 Variation of the ratio between the final irradiation input on the walls and the initial irradiation of the form with the variation of R_2, ρ_W and ρ_G

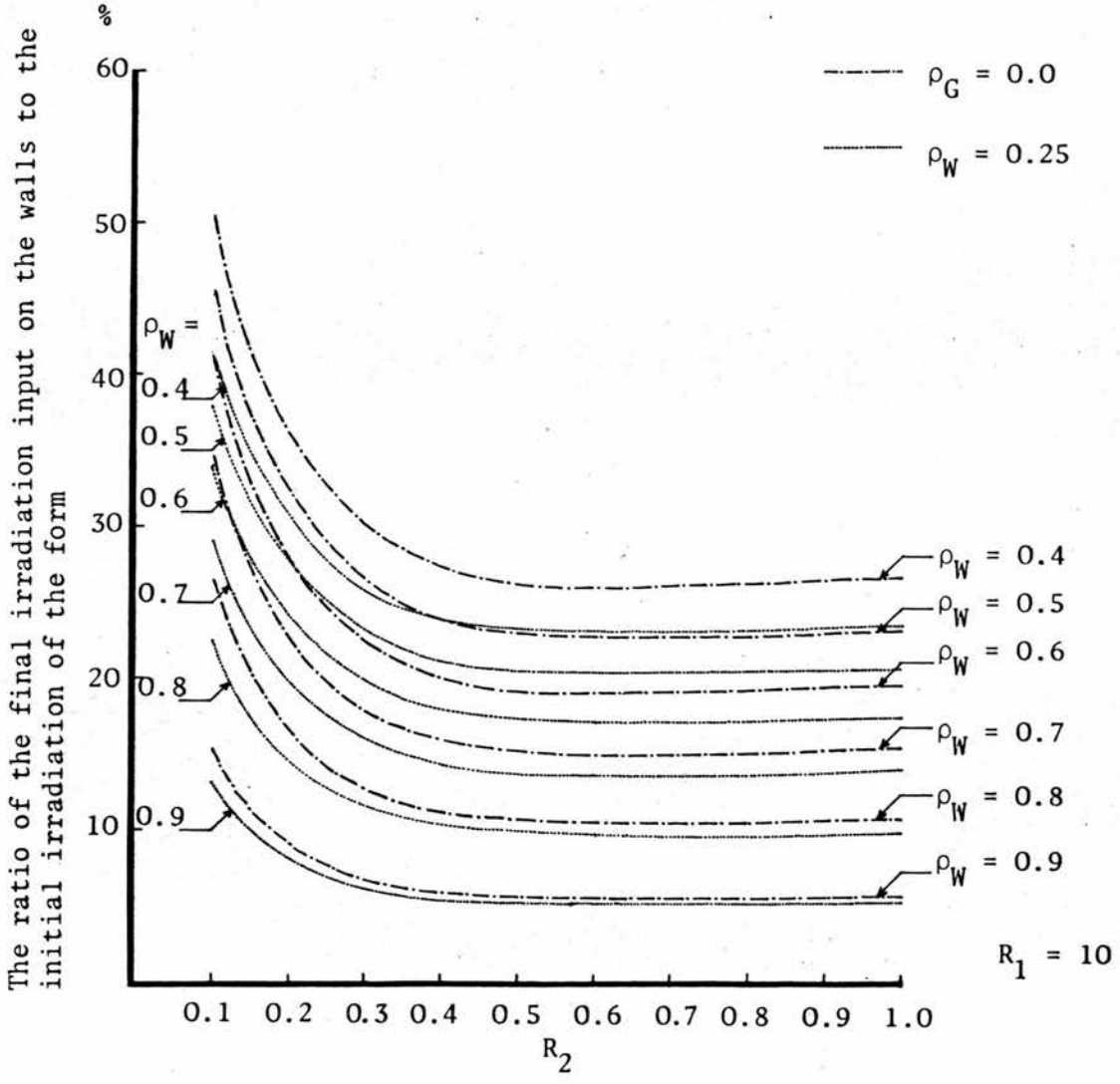

Figure VII.9 Variation of the ratio between the final irradiation input on the walls and the initial irradiation of the form with the variation of R_2, ρ_W and ρ_G

Regarding the effect of the plan ratio R_2, it is evident that the change in the walls reflectivity produces more considerable changes in the ratio f when R_2 approaches unity.

In general, the ratio f decreases progressively with the increase in the value of R_1. A steady decrease is noticed to take place as the value of R_2 at the lower end of its range is increased. By increasing the value of R_2, the rate of the decrease ceased to exist and a constant value of f is reached for all values of R_2 greater than 0.4.

In figures VII.10 and VII.11, values of the final irradiation load on the walls are plotted against the corresponding values of the initial irradiation load on the walls, both in summer and winter, for the range of geometries considered in the study. The value of the walls reflectivity ranges from 0.4 to 0.9. It is evident that the final irradiation load is in direct proportionality to the initial irradiation load on the walls and that the rate of its change with the change in the initial load depends on the surface reflectivity of walls.

VII.4 Concluding Remarks

In this chapter, the final irradiation load on the walls of a courtyard form was defined as the energy absorbed at the walls surface taking into consideration the inter-

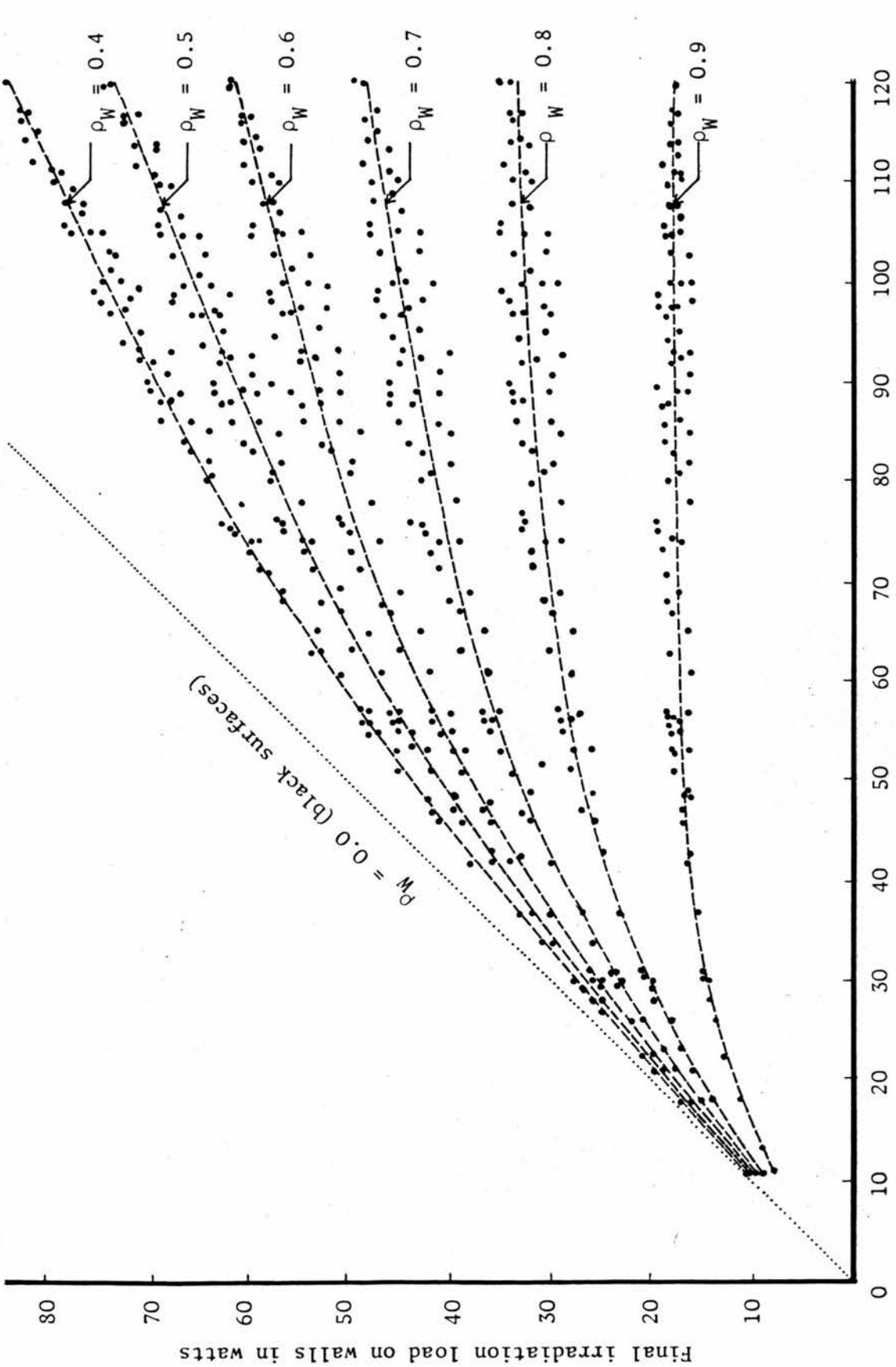

Figure VII.10 Relationship between the final irradiation load on walls and the initial irradiation load in summer

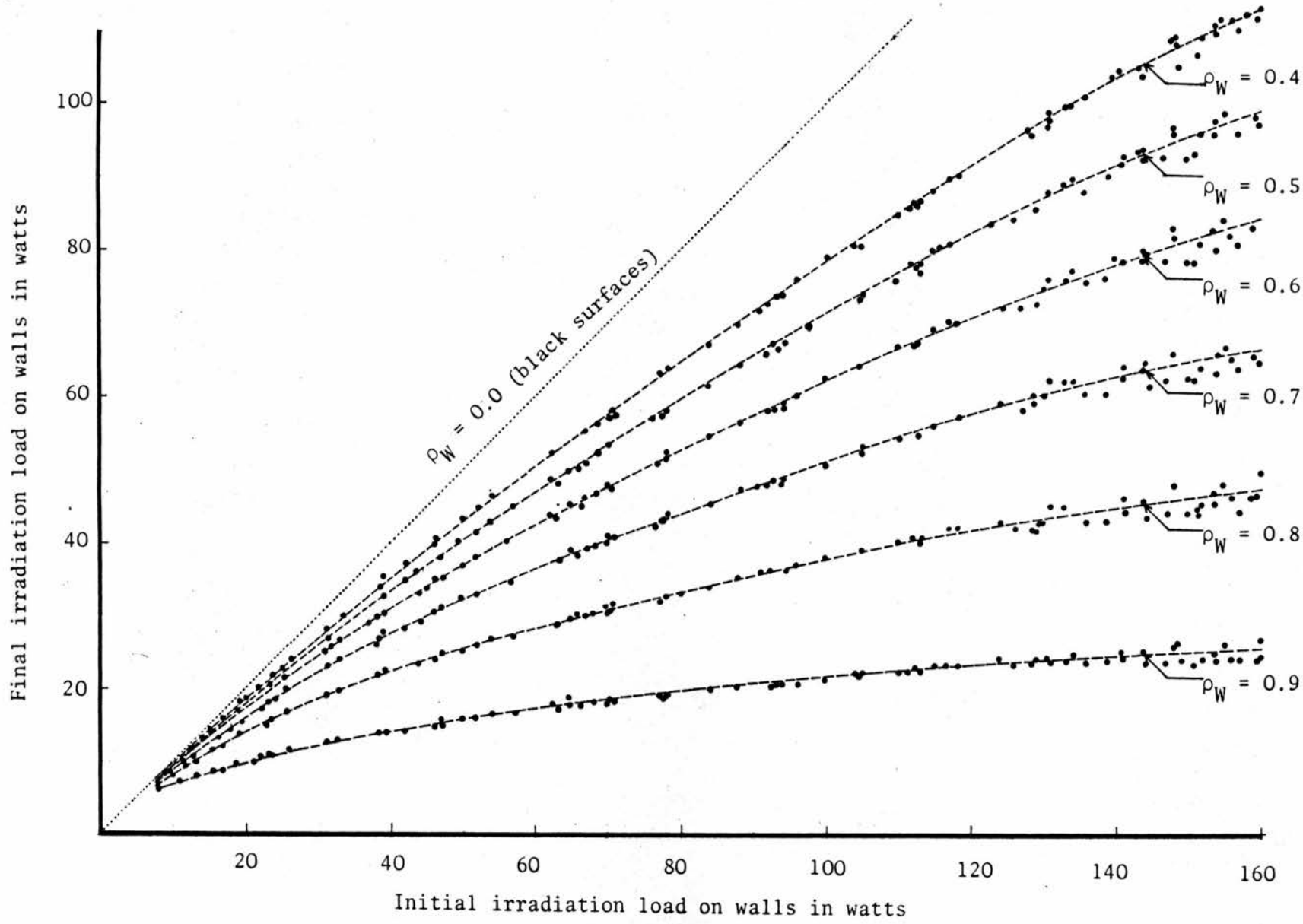

Figure VII.11 Relationship between the final irradiation load on walls and the initial irradiation load in winter

reflected components which are initiated by both the walls and ground surfaces. The effect of the geometrical and physical parameters of the form on the interreflected irradiation component, and consequently on the final irradiation load on the walls, was analysed. The analysis revealed the following points :

1. It is evident that the irradiation component initiated by the walls surface contributes more significantly to the final irradiation load acting on the walls than the component initiated by the ground surface does.

2. The interreflected components depend on the reflectivity of the form's surfaces, however, the geometrical configuration of the form determines the significance of changing the surface reflectivity on the final irradiation load.

3. The contribution of the ground surface to the final irradiation load on the walls depends on the ground surface reflectivity and the geometrical parameters of the form as well as the initial irradiation load on the ground surface which is also determined by the geometrical configuration of the form. The initial irradiation load on the ground surface increases with the increase of the ratio R_1. On the other hand, the fraction, K_2,

of this initial load adding to the final load on the walls decreases slightly with the increase of the ratio R_1. However, the contribution of the ground surface to the final irradiation load on the walls increases with the increase of the ratio R_1.

4. The final irradiation load on the walls varies proportionally with the variation of the initial irradiation load of the walls : for small values of the surface reflectivity, the increase in the initial irradiation results in a corresponding increase in the final irradiation load. As the value of the surface reflectivity increases, the change in the initial irradiation produces a slight change in the final load.

5. The added contribution of the interreflected irradiation simply results in increasing the magnitude of the irradiation received by the walls in proportion to their initial load and their surface reflectivity. By choosing surfaces of high reflectivity a significant reduction in the final load can be achieved.

PART FOUR : DISCUSSION AND CONCLUSIONS

The present study is directed towards developing insight into the thermal performance of the courtyard house form. The historical evidence of the suitability of this form for the climate of hot dry regions coupled, however, with the diminishing application of the form in urban areas at present, suggests the desirability of understanding the climatic implications for design as a prerequisite for systematizing the process of designing courtyard houses.

Appendix 3 illustrates traditional examples of courtyard houses, it shows how house design had met the climatic as well as the socio-religious needs of the time. However, a modern version of courtyard house differs from the traditional one : it is designed for a smaller family with a different way of life. Economic limitations and scarcity of land influence the size of house. The functions which had been performed in a variety of spaces are squeezed into fewer number of spaces and the design becomes more simple. The main element of the house design is that which is studied here, namely the courtyard space.

It is argued in this study that the control of the thermal performance of the indoor spaces in relation to solar radiation could be achieved by natural means through the control of the irradiation load on the external surfaces of the form. This latter control is achieved through the

manipulation of the geometrical and physical parameters of the form. It is this part of the physical system to which the scope of the investigation in the present study is confined.

The goals of the study are twofold : first, to examine how the geometrical configuration of the form and the properties of its surfaces affect its response to specific thermal conditions. Second, to express the established relationships between the parameters of the form and its thermal performance in such a way that allows the determination, in advance, of the consequences of changing the values of the parameters, thus helping the designer to reach a balance among the diversity of requirements he is facing.

The discussions presented in chapter II revealed that direct solar radiation is the main source of external thermal excitation to which the form is exposed. The contribution of the scattered radiation from the sky is of less importance. The physical system which describes the thermal performance of the courtyard form has the incoming direct solar radiation as its input and the outgoing radiation from the heated surfaces as its output. The contribution of the outgoing radiation from the ground surface to the outer space is significant and should be included if a comprehensive model

is to be developed to study the dynamic balance of heat in the courtyard form.

The model developed in this study is seen as a part of such a comprehensive model, it concentrates on the control of the input to the system. The parameters of the form that influence the thermal balance of its surfaces as affected by the incoming radiation are geometrical (proportions, size and orientation), and physical (reflectivity of the form's surfaces). The first category affects the initial irradiation load received on the surfaces of the form. The second one has bearing on the final irradiation load.

On this basis, a mathematical model was developed for the systematic evaluation of the initial and final irradiation load on the external surfaces of the form. The model allowed a detailed investigation into the effects of changing the parameters of the form on the irradiation load on the form's surfaces to be carried out. Using Cairo as an example of a typical hot dry region, and by applying computer techniques, a wide range of combinations of form parameters was studied. The detailed discussions presented in the two previous chapters give a clear understanding of the relationships between the parameters of the form and the resulting irradiation load. In the following, the main features of these relationships are presented and some general conclusions are drawn.

1. The final irradiation load is basically influenced by the initial irradiation load which is a function of the geometrical parameters of the form. However, the absorbed component of the irradiation load can be significantly cut down by reducing the absorptivity of the walls surface. This stresses the beneficial use of surfaces having a high reflectivity for short-wave radiation, i.e., light coloured surfaces. The increase of surface reflectivity from the lowest chosen value in the model (0.4) by 0.1, produces a 10% reduction in the final irradiation load. But as the reflectivity continues to increase, the reduction rate escalates : a 40% reduction in final irradiation results from increasing the surface reflectivity from 0.8 to 0.9.

2. The reflectivity of the ground surface is less critical than that of the walls in determining the final irradiation load. An increase of the ground surface reflectivity by 10% results in a reduction of the final load by about 5%.

3. Because of the direct proportionality between the final and the initial irradiation loads, the relationships established in Chapter VI between the initial irradiation load and the parameters of the form can be applied when considering the final irradiation load.

4. It is evident that the deepness of the form significantly affects the irradiation load : as the form gets shallower, the rate of increase in irradiation which accompanies decreasing the deepness, becomes less. For a given height the deepness of the form is increased by decreasing the perimeter and by increasing the parapet height.

5. For a given perimeter, the irradiation load is affected by changing the plan ratio especially in winter. In summer, the further the plan shape from square, the less the irradiation load. In winter, the maximum irradiation is received when the plan is square in the case of deep forms, and when the plan is more elongated in the east-west direction in the case of shallow forms.

6. Improvements to the thermal performance can be achieved by projecting a part of the roof over the walls especially in the south direction.

7. The orientation of the form along the east-west axis is favourable in both summer and winter. The range of orientation angles within which the irradiation load is changed by specified percentages depends on the deepness of the form and the plan ratio. In the case of forms having square plans, the change of orientation has almost no effect on the irradiation load.

The relationships, developed in this thesis, between the parameters of the form and its thermal performance are intended for use by designers in assessing the consequences of design decisions - which might be imposed by other criteria - on the thermal performance. The charts presented in figure 4.1 summarize the relationships illustrated in figures VI.2, VI.3 and VI.19. The method of using the charts for assessing the initial irradiation load on the walls surfaces of a courtyard form is as follows :

(a) Choose the floor area of the form.

(b) Find the corresponding irradiation of the whole form in both summer and winter.

(c) Select a value of R_2 within the range of geometries of either the two storey or the one storey forms.

(d) Find the value of R_1 and draw a horizontal line to intersect the two corresponding curves of R_2 for summer and winter. From each point of intersection draw a vertical line.

(e) Find the percentage of the irradiation that is received by the walls. Extend the two vertical lines to intersect the two lines drawn to joint the point 0 and the two points defined in step (b) on the irradiation scale. The two points of intersection represent the initial irradiation of the walls in summer and winter.

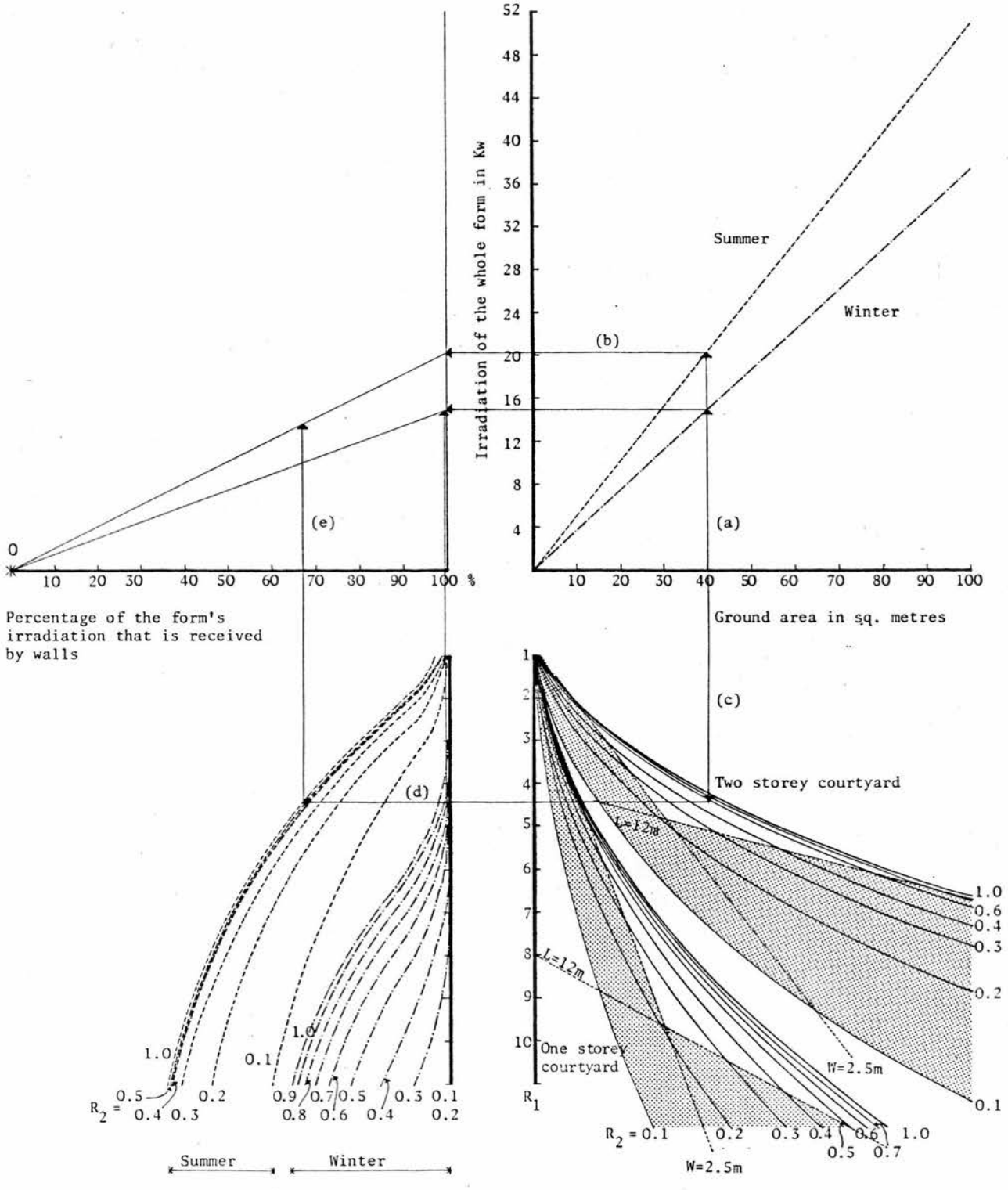

Figure 4.1 Determination of the initial irradiation load on walls' surface of the courtyard form

The charts are drawn for the case of forms having their longitudinal axis parallel to the east-west axis. To allow for the variation of the angle of orientation, the charts presented in figures 4.2 and 4.3 show the percentage of variation of the initial irradiation load that is caused by changing the angle of orientation.

Modification of the irradiation load through other geometrical parameters such as the roof cover and the parapet height is extensively discussed in Chapter VI.

The approach of the study is a systematic one which aims at a clear understanding of the interaction between the parameters of the form and its thermal performance measured at the external surfaces of the form. The approach does not lead to one choice seen as the absolute optimum, but gives instead a range of possibilities corresponding to acceptable ranges of performance in relation to the thermal design criterion. It also shows how to change the value of one parameter to compensate for deviating from a desirable value of another parameter. This flexibility is needed in design situations.

The model developed in the study is seen as a part of a comprehensive model that can be developed to simulate the performance of the form in other respects. The performance of courtyard forms in relation to noise and to air flow are

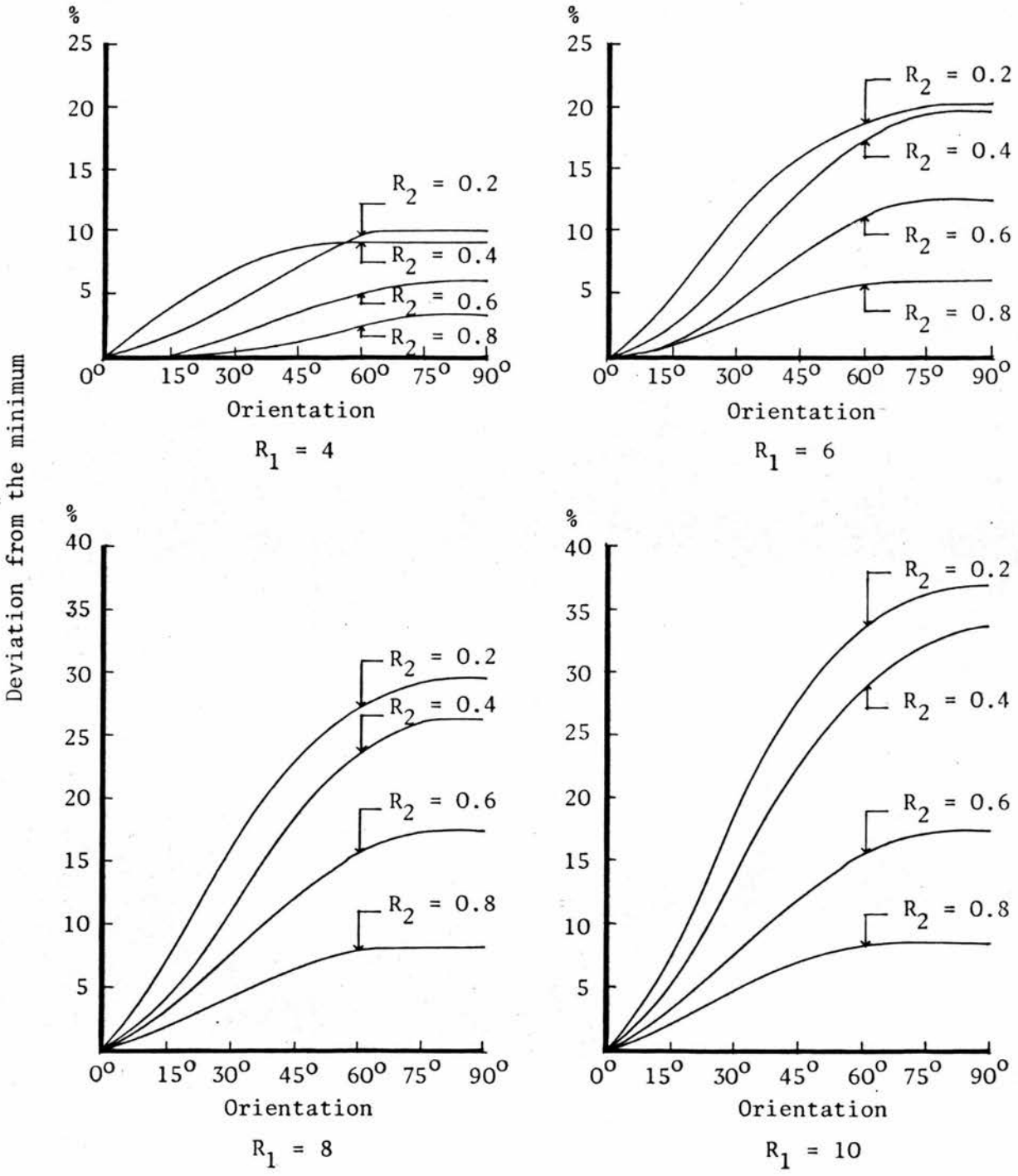

Figure 4.2 Effect of changing the orientation on the initial irradiation of the four walls in summer

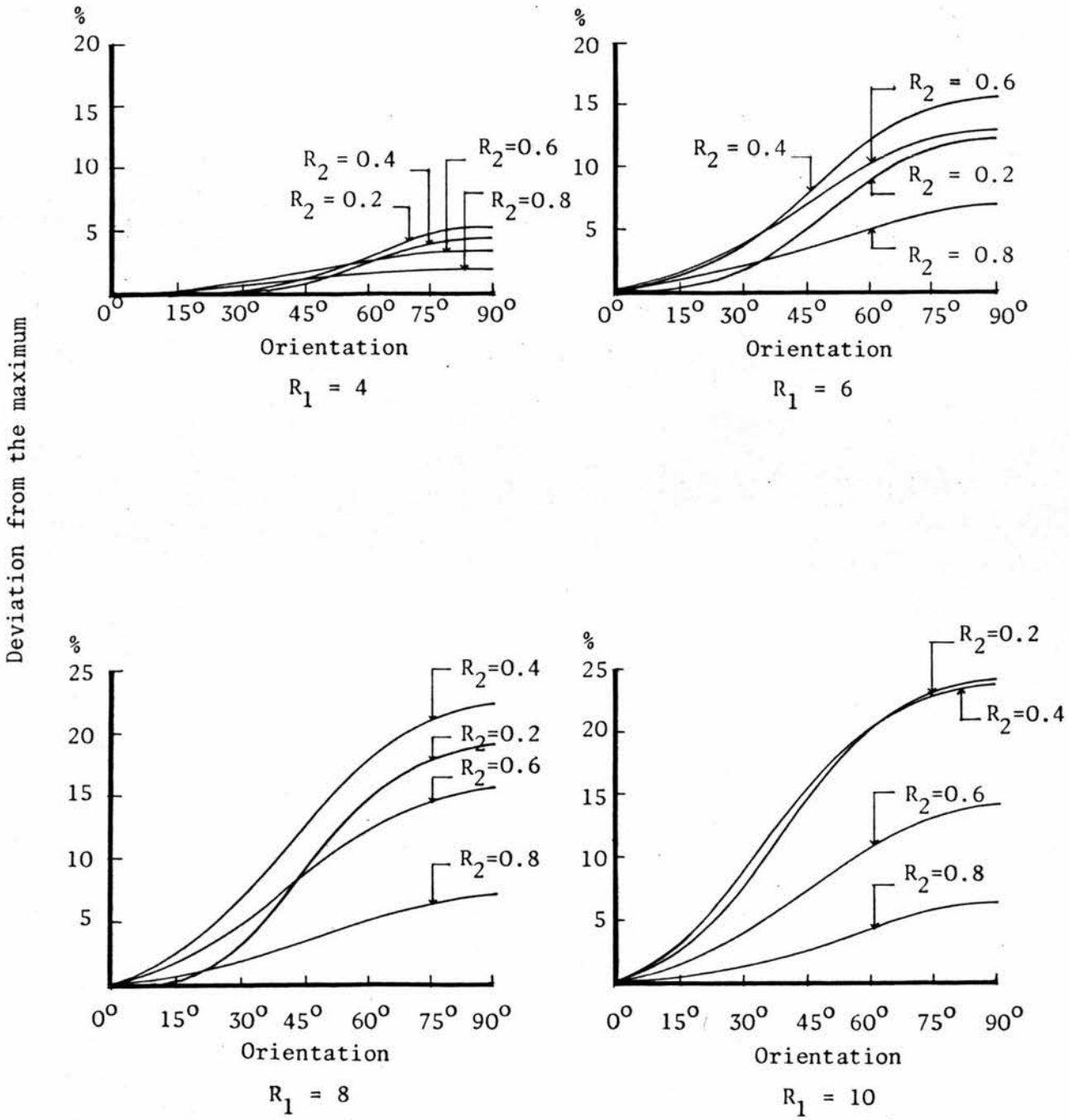

Figure 4.3 Effect of changing the orientation on the initial irradiation of the four walls in winter

examples. A further development of the model is needed to incorporate available knowledge concerning heat transfer through building materials in order to relate the thermal performance at the external surfaces of the form to the thermal performance of the indoor space.

APPENDIX 1

EVALUATION OF THE CONFIGURATION FACTORS

In a rectilinear enclosure two types of configurations may be identified :

(a) Two identical parallel directly opposed rectangles;

(b) Two rectangles with one common edge and perpendicular to each other.

Figure A 1.1 shows a courtyard form which it is assumed to have a hypothetical roof, R. The algebraic expressions presented below are given by Weibelt (1965), the configuration factors are given as functions of the two parameters m and n defined as follows : $m = \frac{y}{z}$ and $n = \frac{x}{z}$.

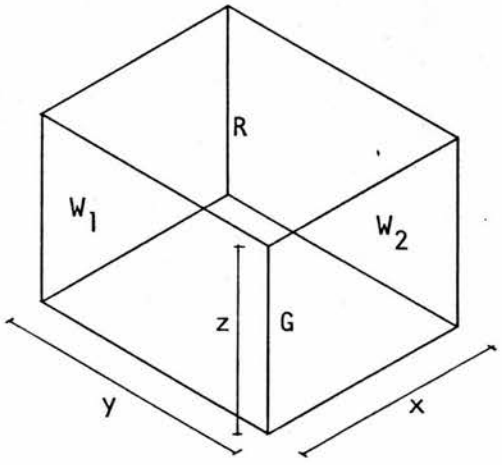

Figure A1.1 A courtyard form

$$F_{GR} = \frac{2}{\pi mn}\left\{\log_e\left[\frac{(1+m^2)(1+n^2)}{1+m^2+n^2}\right]^{\frac{1}{2}} + n\sqrt{1+m^2}\tan^{-1}\left(\frac{n}{\sqrt{1+m^2}}\right)\right.$$

$$\left. + m\sqrt{1+n^2}\tan^{-1}\left(\frac{m}{\sqrt{1+n^2}}\right) - n\tan^{-1}n - m\tan^{-1}m\right\}$$

A1.1

$$F_{W1W2} = \frac{1}{\pi m}\left(m\tan^{-1}\left(\frac{1}{m}\right) + n\tan^{-1}\left(\frac{1}{n}\right) - \sqrt{n^2+m^2}\tan^{-1}\left(\frac{1}{\sqrt{n^2+m^2}}\right)\right.$$

$$+ \tfrac{1}{4}\log_e\left\{\left[\frac{(1+m^2)(1+n^2)}{(1+m^2+n^2)}\right]\left[\frac{m^2(1+m^2+n^2)}{(1+m^2)(m^2+n^2)}\right]^{m^2}\right.$$

$$\left.\left. \times\left[\frac{n^2(1+m^2+n^2)}{(1+n^2)(m^2+n^2)}\right]^{n^2}\right\}\right)$$

A1.2

APPENDIX 2

THE MAIN FEATURES OF THE HOT-DRY CLIMATE

The hot-dry climate is one of the five principal types of climate according to Köppen's classification (Köppen and Geiger, 1936). It is characterized, in general, by the high capacity of the atmosphere to acquire evaporated water. Therefore, the amount of water vapour borne in the atmosphere represents only a small percentage of relative humidity. The predominance of clear skies provides an abundance of sunshine and permits a considerable amount of heat to be dissipated from the earth's surface at night. The high intensities of direct solar radiation coupled with high intensities of reflected solar radiation from the bare light-coloured ground and the wide range of daily temperatures are common features of this type of climate. Rain is scarce at any time, strong dry winds blow occasionally.

The seasonal variations are noticeable; two distinct seasons can be distinguished: a hot dry summer, a warm winter with little rain, and two transitional seasons. This type of climate prevails in a zone situated between 15^{o} and 30^{o} north and south. Within this zone, geographical and topographical conditions give rise to some regional modifications.

The climate of Egypt belongs to this type of climate since most of the country - known as Upper Egypt - lies south of 30^{o} north latitude. The northern part of the Nile delta and the northern coast - known as Lower Egypt - have a rather Mediterranean climate. Besides these, there are two secondary regions : the coastal regions of North Red Sea which has a hot but rather humid and rainless climate, and the mountains of Sinai which, because of their height, belong to the temperate climates (Soliman, 1972).

In the region of Upper Egypt, four seasons are experienced as follows (Soliman, 1972). In winter, the region has warm and sunny days but rather cool nights, rain is scarce. In spring, the air is hot and dry, the weather is very changeable, wind blows from south west frequently accompanied by sandstorms (known as Khamsin conditions). In summer, the weather becomes more stable, it is hot, very dry and rainless. Clear skies prevail, nights are cool. In autumn, the climatic conditions resemble those of the spring except that heat waves are less frequent and more mild.

Climatic data for the region of Upper Egypt are presented below.

Solar Radiation

The measurements of radiation were only recently begun in Egypt. There are two stations : Giza and Tahrir. The

global radiation (direct and sky radiation) is obtained from the records of a Robitzsch Actinograph which are regularly compared with the records of an Epply Pyrheliometer. When the difference is equal to or more than 5%, correction is carried out, but when it is less than 5%, the Robitzsch values are considered to be satisfactory and within the range of accuracy of the instrument (Meteorological Department, 1968). The monthly global radiations at Giza Station are shown in table A2.1.

	Jan.	Feb.	Mar.	Apr.	May	June
Mean	140	181	241	279	307	323
Max. Daily	202	247	320	349	364	360
Min. Daily	22	41	83	89	53	198

	July	Aug.	Sep.	Oct.	Nov.	Dec.
Mean	321	295	258	203	154	129
Max. Daily	363	346	306	263	198	177
Min. Daily	273	221	89	75	59	23

Table A2.1 Global radiation at Giza station in W/m^2 (ten years of record). After Soliman (1972)

Sunshine Duration

The actual duration of sunshine for a month is the sum of the actual daily sunshine durations. The total possible

duration for the month is the sum of the daily calculated periods between sunrise and sunset. The ratio between the two expresses the degree of clearness of the sky. The duration of sunshine is measured by Campbell Stokes sunshine recorders (Meteorological Department, 1968), Table A2.2 gives the monthly sunshine record in Giza station.

	Jan.	Feb.	Mar.	Apr.	May	June
Total Actual (hours)	216.3	227.3	275.8	293.0	338.3	361.1
Total Possible (hours)	324.4	311.7	371.9	387.2	423.5	421.4
Percentage	67	73	74	76	80	86

	July	Aug.	Sept.	Oct.	Nov.	Dec.	Annual Mean
Total Actual	369.4	350.4	309.2	289.1	249.8	222.4	291.8
Total Possible	430.0	409.6	370.5	355.0	319.8	317.8	370.2
Percentage	86	86	83	81	78	70	78

Table A2.2 Sunshine duration in hours and percentage of possible sunshine in Giza station. After Meteorological Department (1968).

Cloudiness

The monthly mean values of the total sky cover at the principal hours 6, 12 and 18 U.T. are computed from their routine values observed at these hours. The cloudiness reaches a minimum in summer and a maximum in winter, it is

greater by day than by night (Soliman, 1972). Table A2.3 gives the monthly total sky cover in Oktas for the three principal hours at Giza station.

Hour	Jan.	Feb.	Mar.	Apr.	May	June
6	3.3	3.1	2.9	2.8	2.5	1.8
12	3.8	3.7	3.3	2.5	2.4	0.4
18	2.0	1.9	1.8	1.1	1.3	0.1

Hour	July	Aug.	Sep.	Oct.	Nov.	Dec.	Annual Mean
6	2.5	3.1	2.6	2.4	2.9	3.8	2.8
12	0.3	0.2	0.9	2.1	3.0	4.0	2.2
18	0.0	0.0	0.3	0.9	1.7	2.1	1.1

Table A2.3 Total sky cover in Oktas in Giza station. (Averaged over 30 years of observation). After Meteorological Department (1968).

Air Temperature

In the 'Climatological Normals for Egypt' (Meteorological Department, 1968) data of air temperature are given in two forms : monthly mean values of maximum and minimum air temperature, and monthly mean values of dry and wet bulb air temperature at the principal hours 6, 12 and 18 U.T. The mercury and the alcohol thermometers, used for measuring

maximum and minimum temperatures respectively, are fixed freely exposed in the louvred screens with their bulbs at a height of 1.60 to 1.70 metres above the ground. For measuring dry and wet bulb temperatures, mercury thermometers are freely exposed in sloping double roofed louvred screens with their bulbs at a height of 1.40 to 1.50 metres.

Table A2.4 shows the monthly values of temperature recorded in Giza station.

Month	Max. Temp.	Min. Temp.	Mean of Day	Absolute Records		Dry Bulb Temp.		
				Max.	Min.	6	12	18
Jan.	20.2	6.1	13.2	29.3	-3.3	9.2	19.1	12.4
Feb.	21.7	6.6	14.2	34.7	-2.2	10.8	20.5	14.0
Mar.	24.4	8.7	16.2	38.6	1.2	14.4	23.3	16.9
Apr.	28.7	11.7	20.2	42.9	3.5	18.2	27.7	20.7
May	32.7	15.6	24.2	48.0	7.9	22.6	31.8	25.2
June	34.8	18.6	26.7	47.4	11.9	24.5	33.9	28.0
July	35.8	20.5	28.2	45.5	15.0	25.5	34.7	29.0
Aug.	35.0	20.5	27.8	40.8	15.3	25.3	34.0	28.5
Sept.	32.4	18.4	25.4	42.9	11.9	23.7	31.5	25.8
Oct.	30.6	16.1	23.4	44.5	9.2	21.2	29.7	23.3
Nov.	26.2	12.2	19.2	38.8	3.4	16.4	25.6	18.6
Dec.	21.6	8.1	14.8	33.6	-1.1	11.4	21.0	13.8
Annual Mean	28.7	13.6	21.2			18.6	27.7	21.3

Table A2.4 Monthly air temperature in ^{o}C in Giza station. (Average of 30 years of record). After Meteorological Department (1968).

From table A2.4, it is clear that the warmest months are July and August. However, May, June, September and October experience high temperatures which exceed 30°C. The coolest month is January with a mean temperature of about 13°C. The diurnal range of temperature is greater in April, May and June (about 17°C). It is relatively smaller in winter.

Relative Humidity

The data presented in the 'Climatological Normals for Egypt' are the monthly mean values at the principal hours, 6, 12 and 18 U.T. They are computed from the daily routine values derived from the dry and wet bulb thermometer readings using Jellink's Psychrometer Tables (Meteorological Department, 1968). An example is given in table A2.5.

Hour	Jan.	Feb.	Mar.	Apr.	May	June
6	80	78	72	70	66	67
12	43	38	34	28	25	29
18	72	64	58	49	42	42

Hour	July	Aug.	Sept.	Oct.	Nov.	Dec.	Annual Mean
6	67	66	69	73	76	80	72
12	30	35	40	38	43	46	36
18	47	54	60	63	77	75	59

Table A2.5 Monthly relative humidity (%) in Giza station. (Average of 30 years of record). After Meteorological Department (1968).

From the table, it is clear that the relative humidity decreases as the warmest months approach. The minimum is in May and June, and the maximum is in January.

Surface Wind

In winter, the prevailing directions are north and north west. In spring and autumn, the northerly winds prevail with few temporary interruptions. In summer, there is little interruption in the prevailing northerlies. At night, the wind is not so strong. It becomes stronger through the day until the afternoon and then dies down again. Observations of the surface wind are taken at the principal hours 6, 12 and 18 U.T. The monthly mean wind speed is the arithmetic mean of the speed observations at the three hours over a month (see table A2.6).

From the above discussion it is apparent that the main unfavourable factors of the climate of Egypt are the intense radiation of the sun in summer accompanying high air temperature and low humidity; and duststorms in the afternoons. Figure A2.1 is a summary of the data presented above.

Month	Mean Scalar Wind Speed in Knots	% Frequency of Surface Winds Blowing from the Following Directions								
		N	NE	E	SE	S	SW	W	NW	Calm*
Jan.	3.4	12.9	6.4	1.1	7.9	10.8	9.2	9.6	13.4	28.7
Feb.	3.8	15.9	6.2	1.0	6.3	10.2	9.4	10.7	16.8	23.5
Mar.	4.4	26.6	11.7	1.3	3.5	5.3	5.2	7.5	21.5	17.4
Apr.	4.8	32.2	14.7	1.2	3.0	3.0	3.0	5.4	24.0	13.5
May	5.0	35.3	17.2	2.0	1.3	1.4	1.8	3.3	23.0	14.7
June	4.7	40.9	13.1	1.4	0.5	0.4	0.7	2.0	30.5	10.5
July	4.5	39.5	8.1	0.7	0.1	0.1	0.2	3.0	37.4	10.9
Aug.	4.1	40.3	7.4	0.7	0.1	0.1	0.2	2.2	34.3	14.7
Sept.	4.0	41.8	9.7	0.2	0.2	0.3	0.5	1.2	29.9	16.2
Oct.	3.7	37.2	13.7	1.4	1.6	1.2	1.5	2.0	21.8	19.6
Nov.	3.5	26.9	11.8	1.1	2.9	4.6	4.2	4.5	17.4	26.6
Dec.	3.0	14.0	6.9	1.1	7.6	11.4	7.6	7.1	11.7	32.6
Annual Mean	4.1	30.3	10.6	1.1	2.9	4.0	3.6	4.9	23.5	19.1

Table A2.6 Surface wind speed in knots and the frequency of different directions measured at Giza station - period 1902-1956. After Meteorological Department (1968).
* Calm denotes wind speed less than one knot whatever its direction.

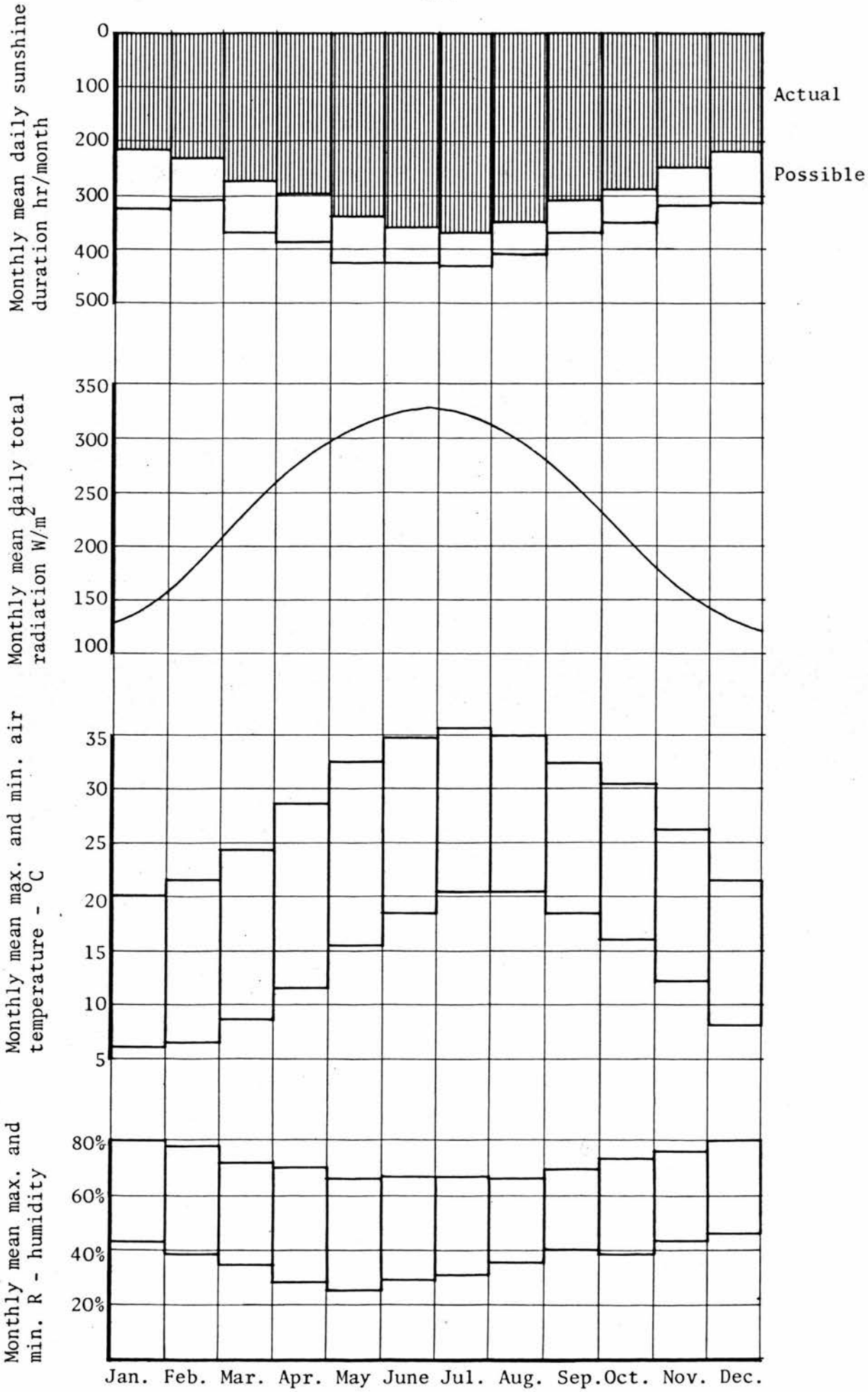

Figure A2.1 The climate of Egypt

APPENDIX 3

TRADITIONAL COURTYARD HOUSES IN EGYPT

A3.1 General

Traditional courtyard houses in Egypt date back to the seventh century when the Coptic architecture of the time was influenced by the Islamic conquest (Shafey, 1970). Traces of the houses built in the old capital El-Fustat show that, in spite of the variety of their plans, they share common characteristic features : a central courtyard either square or rectangular normally paved with limestone. On one side, there is a portico of three bays leading to a deep room, called Iwan, flanked by two smaller rooms. Smaller Iwans are arranged on the other sides of the courtyard and are flanked by niches or corridors leading to other parts of the house. A bent entrance leading to one corner of the courtyard does not allow a passer-by to see inside the house. A fountain is frequently located in the centre of the courtyard (Shafey, 1970), see figure A3.1.

Details of what the traditional courtyard house looks like can be gathered from the houses which belong to later eras than that of the city of El-Fustat. A consistency of approach to solve problems related to climate and social factors is strongly reflected in their designs. Examples of these houses still exist in the old districts of Cairo. A few of them are preserved in a good condition and have even been converted into museums.

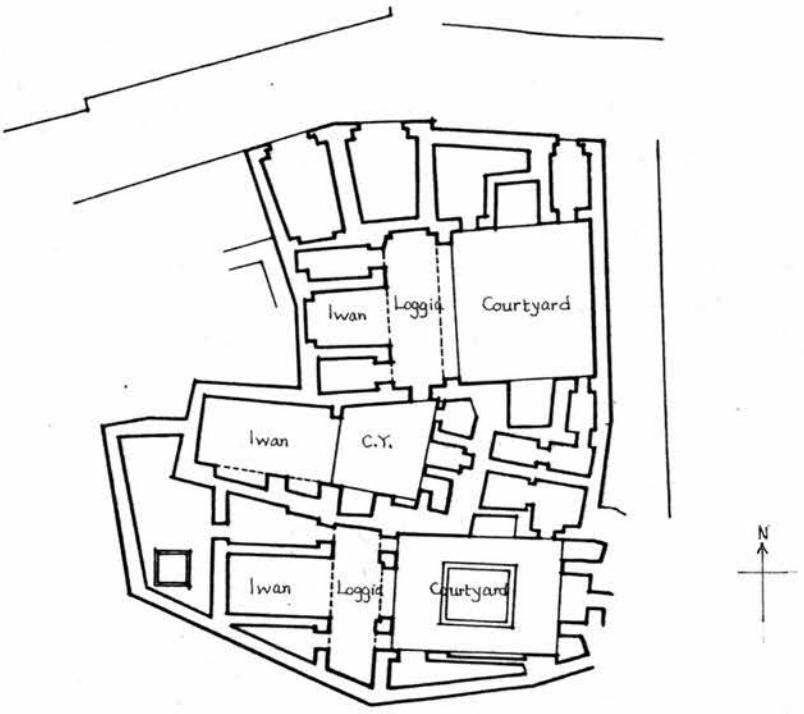

(a)

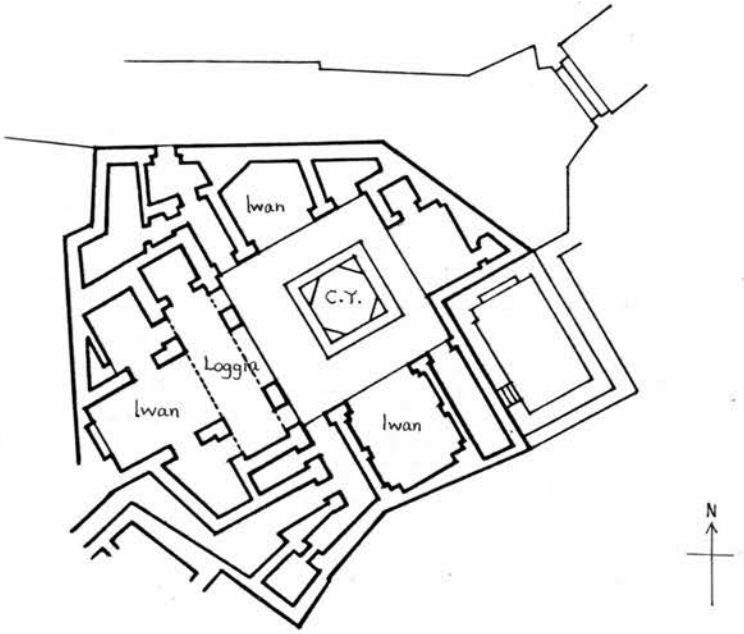

(b)

Figure A3.1 Examples of houses in El-Fustat

A3.2 Design Constraints

The design of the traditional courtyard houses is influenced by social as well as climatic considerations. The main social concern is to achieve privacy of the house from the street and to screen the women inside the house from strangers. The primary climatic consideration is to provide a variety of spaces which suit both the seasonal and the daily change of climate. The dominating hot arid climate calls for creating a rather humidified cool interior protected from the glare and sandstorms outside. Such social and climatic considerations are clearly manifested in the general concept of the house as well as in the details of its component elements.

A3.3 Design Concept

It is basically an inward looking house which has a central courtyard surrounded by other spaces. The house is usually attached to other houses on three sides and has one external facade looking over a narrow street (see figure A3.2). The main entrance to the house is made through a bent passage-way which keeps the inside unseen by outsiders. The passage-way leads to one corner of the courtyard which serves as a circulation space connecting the other spaces. A separate entrance is made for the women's quarters (see figure A3.3).

The size of the house varies according to the wealth and the social status of its occupants; however, a height of two

Figure A3.2 The houses are overlooking narrow streets

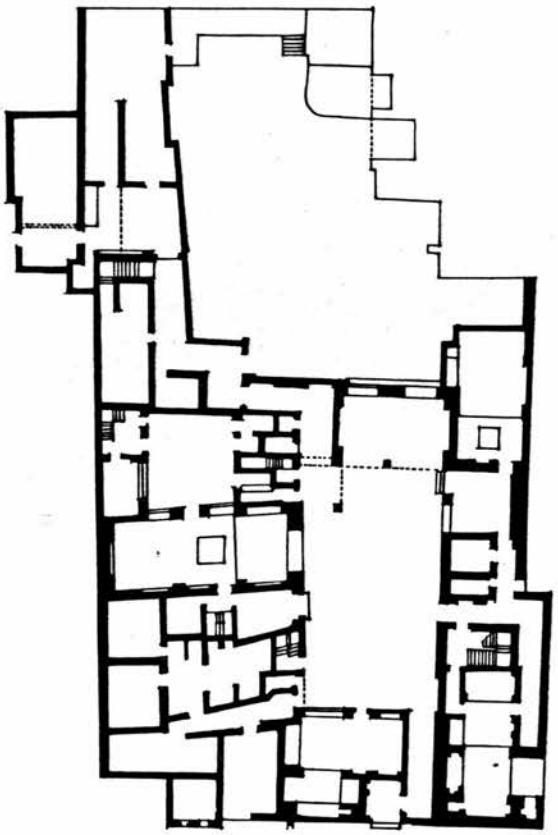

Figure A3.3 Plan of the ground floor of El-Sehimi house (17th century)

or three storeys is always retained. If a big house is required it is built around more than one courtyard: one for the reception of guests, one for the private use of the family, and probably a third one for the servants. Contrary to the deliberate attention to the enrichment of the interior with refined details, the external facades are left plain with the least amount of ornament, no symmetry or formal order is superimposed on it. The house contains a number of spaces which vary in their degree of closure and location in order to accommodate different activities and cope with the seasonal as well as the daily change of climatic conditions. Such spaces are as follows.

The Courtyard is a rectilinear open space in the centre of the house providing the main contact between the indoor of the house and the outside. It is generally paved,and in the middle of it there is usually a well or a fountain (see figure A3.4) which has the effects of humidifying the dry air and providing the sight of water which is very much appreciated in such arid conditions. A few plants or trees are found near the fountain. The night cool air is deposited in the courtyard space and flows into the house spaces. The coolness is conserved for some time during the day.

The Taktabosh is a square recess for sitting in summer, open to the courtyard from one side (usually north) and having large openings on the opposite side. It is one or two steps

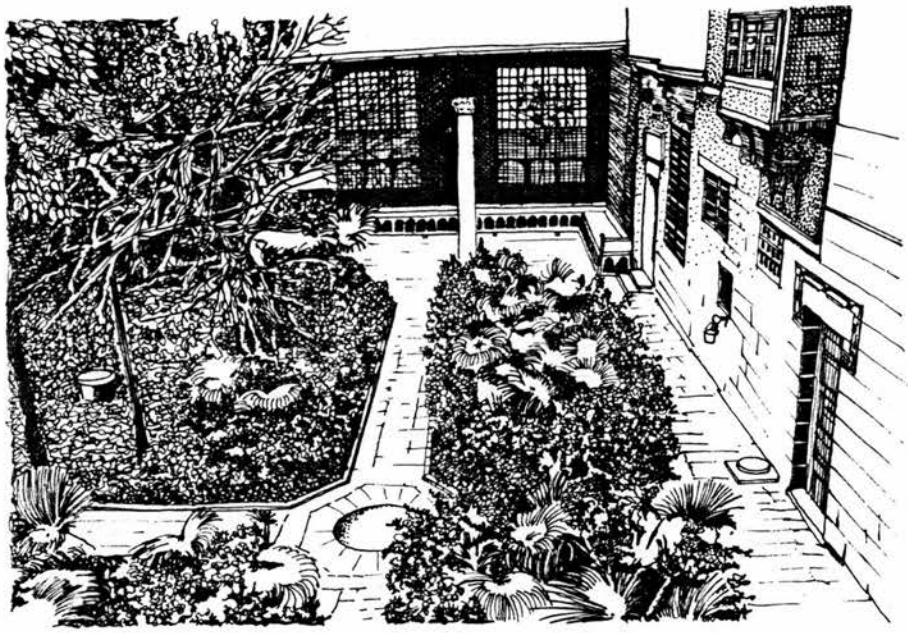

Figure A3.4 View of the courtyard of El-Sehimi house

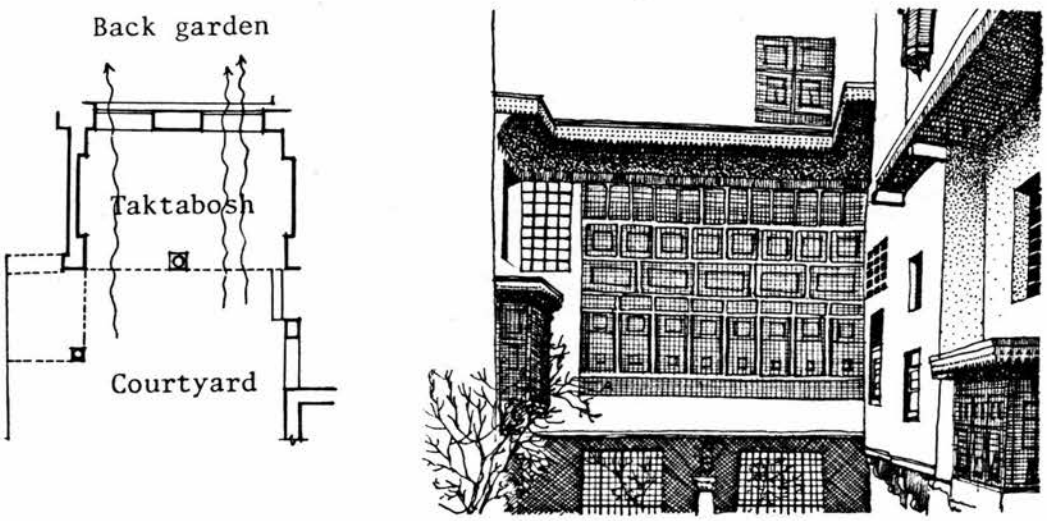

Figure A3.5 The Taktabosh in El-Sehimi house

above the level of the courtyard (see figure A3.5).

The Mandarah is the main room on the ground floor for receiving male visitors. It consists of two alcoves - called Iwans - surrounding a central space, two storeys high, called Dorqa'a. The floor of the iwans is raised one step from the floor of the Dorqa'a.

The Mak'ad is an open loggia in the first floor overlooking the courtyard through a pair of arches (see figures A3.6 and A3.7). It is used as a reception for male visitors in summer, it is reached directly from the courtyard by a staircase.

The Qa'a on the first floor, is the largest space in the house. Like the Mandarah, it has a central area (Dorqa'a) with two iwans leading off it. It is used for sitting in winter and as a celebration hall. The ceiling of the Dorqa'a is raised high above the rest of the house and is covered by a wooden lantern (Fathy, 1970). Its floor is paved with marble mosaics in decorative geometric pattern. The floor of the iwans is one step higher and is completely carpeted (see figures A3.8 and A3.9). The women's quarter (Hareem) is located in the upper floors overlooking the Qa'a through openings fitted with Mushrabeyas (lattice screens). It can be reached through a staircase from the courtyard.

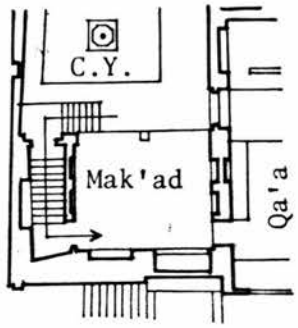

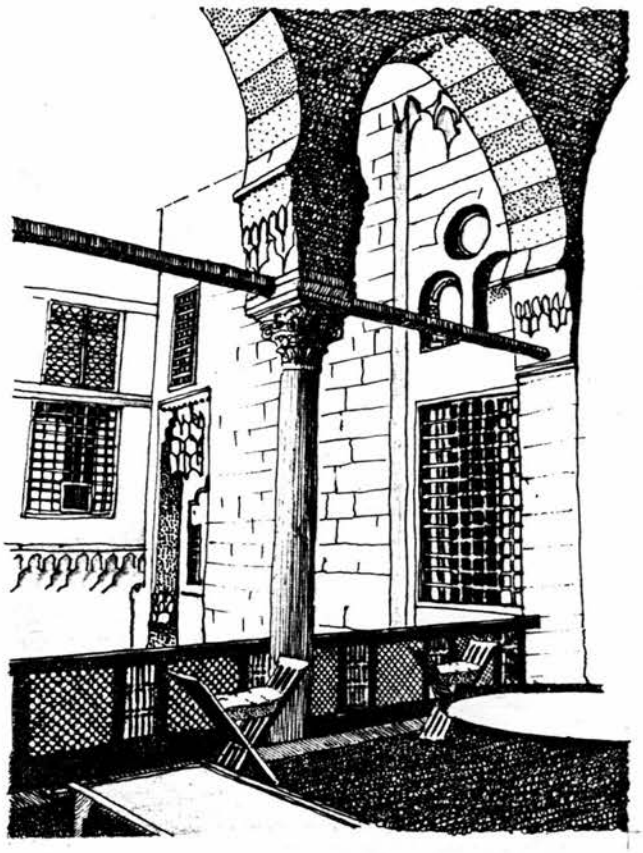

Figure A3.6 The Mak'ad (open loggia) of El-Kredleya house overlooking the courtyard

Figure A3.7 View of the Mak'ad of El-Kredleya house seen from the courtyard

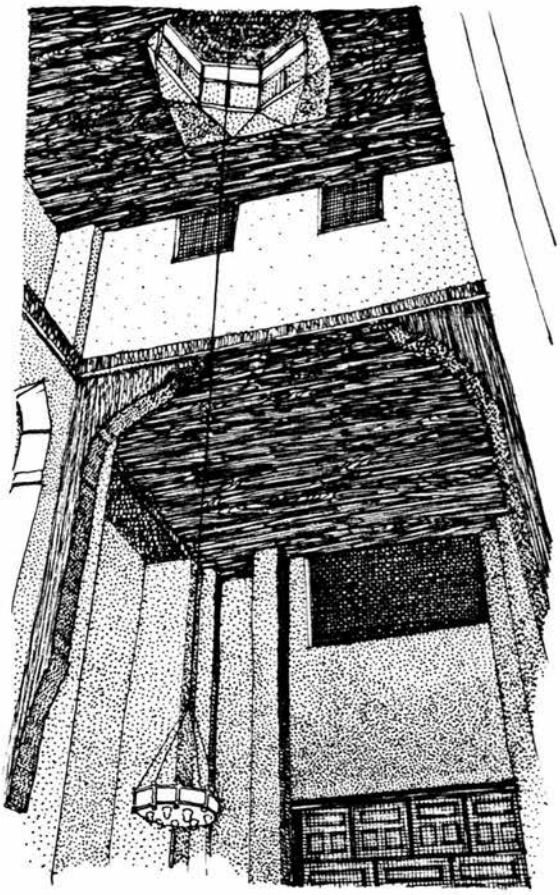

Figure A3.8 View of the roof of the Qa'a space in El-Sehimi house

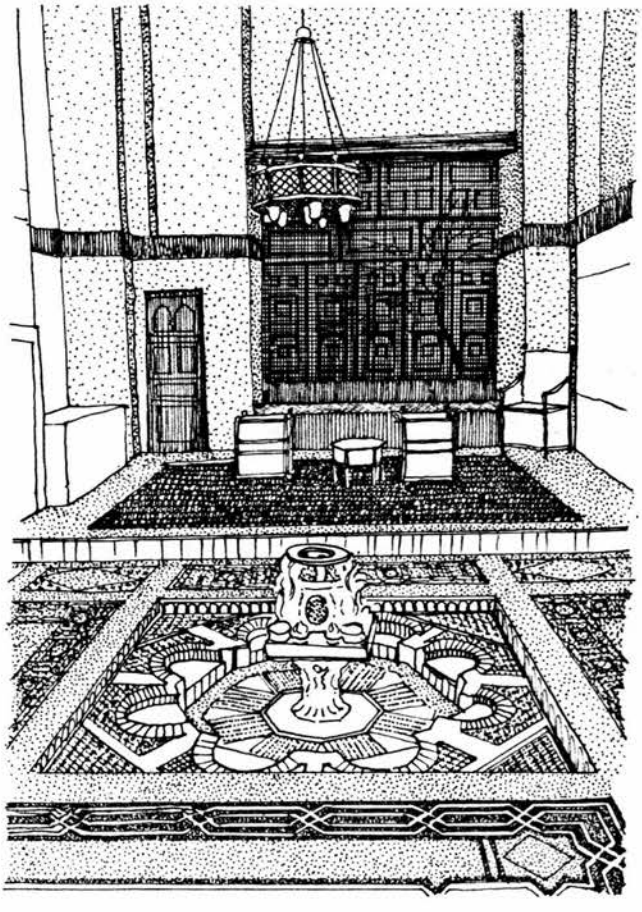

Figure A3.9 View of the Qa'a showing its floor paved with marble mosaics in decorative geometric patterns. A fountain is centrally located in the space.

Strong light and glare are characteristic features of the hot dry climate and they call for small openings placed high above eye level. On the other hand, ventilation requires larger openings placed at the level of sitting. This conflict of requirement was overcome by separating the functions of a window. Some openings were designed for viewing with reducing the glare effect, others for providing light, while a device called Malkaf (wind catcher) was introduced to meet the ventilation requirements, (see figures A3.10 - A3.13).

In the ground floor, windows which open to the street are few and are placed near to the roof to achieve the privacy of the inside. The privacy of the neighbouring houses is also attained by the careful location of the windows in the upper floors. A window is fitted with a wooden lattice screen called Mushrabeya which serves more than one function. The lower part of the Mushrabeya is composed of small wooden bars very close to each other. This part of the window allows the inhabitants to see what is taking place outside without being seen. These wooden bars as described by Fathy (1972) '... are circular in section, so that they have the effect of breaking up the light which falls on them; thus there are no sharp edges visible, nor is there any harsh contrast between the darkness of the lattice and the brightness of the light'. Another function is to allow fresh air to replace hot air in rooms where no Malkaf is provided. Above eye level, the

Figure A3.10 Windows overlooking the courtyard are fitted with Mushrabeya

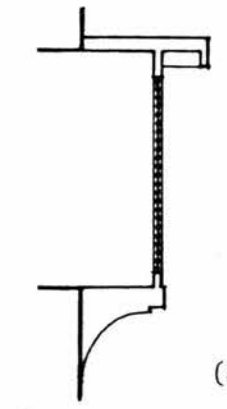

(a) Section in a Mushrabeya

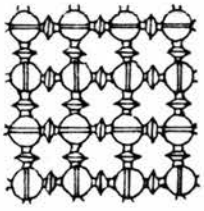

(b) The geometrical pattern of the Mushrabeya

Figure A3.11 Details of the Mushrabeya

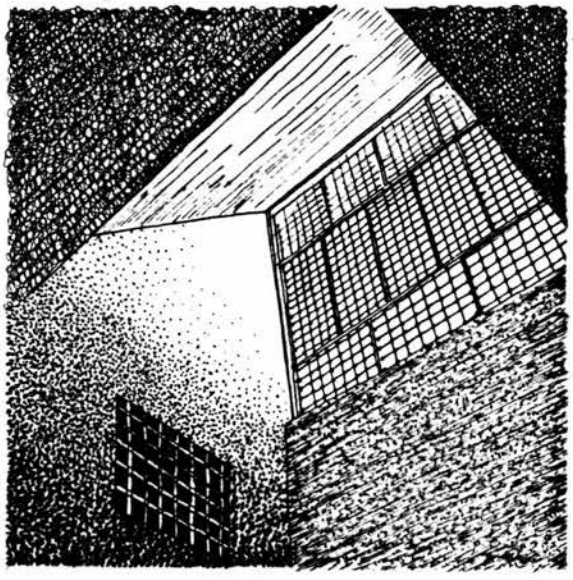

Figure A3.12 View of the Malkaf in El-Sehimi house

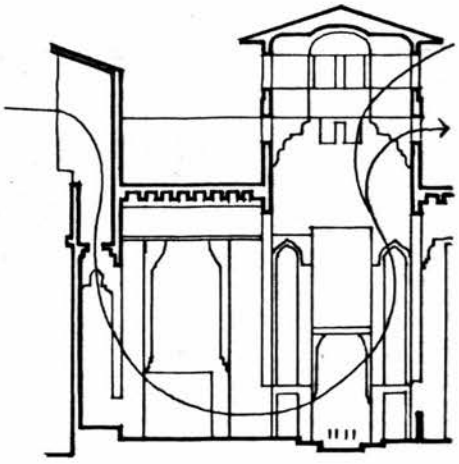

Figure A3.13 The thermal concept of the Malkalf

distances between the wooden bars of the Mushrabeya are made greater to provide light for the interior.

The Malkaf (wind catcher) is a shaft rising above the rest of the house spaces located on one side of the Qa'a. The upper end of it is left open from the north and west sides, the direction of the prevailing wind. As the air in the Qa'a gets hotter it rises up and escapes from the lantern on the top of the Dorqa'a. It is replaced by fresh air coming through the Malkaf creating a continuous flow of air inside the Qa'a even in the absence of winds. The air flow is not obstructed by any neighbouring house since the Malkaf is raised higher than the roof of houses.

A3.4 Construction and Materials

The walls of the ground floor are constructed of limestone (available in the hills near Cairo) of a thickness of at least 50 cm. In the upper floors, brickwork is used with wooden posts and the walls are thinner. The projection of the walls of the upper floors over the walls of the ground floor is made by means of stone corbels and wooden brackets. The structure of the roof is of wooden beams covered with cement and mud.

The structure of the whole house is heavy which delays the transmittance of the outdoor heat to the indoor spaces, with the result of keeping the indoor warm at night. However,

this slight disadvantage is overcome by providing good ventilation conditions through the Malkaf and the Mushrabeyas.

Windows are made of wooden frames fitted with Mushrabeyas, no glass is used. This results in a continuous air flow at night from the courtyard to the rooms. This is of great benefit in summer but it might be annoying in winter.

REFERENCES

Alcock, A. E. S. and Richard, H. M. (1960) How to Build for Climate, Longman, London.

ASHARE (1968) Handbook of Fundamentals, American Society of Heating, Refrigerating and Air Conditioning Engineers, New York.

Atkinson, G. A. (1950) Building in the Tropics, RIBA Journal, 57 (8), 313-320.

(1953) Building in Warm Climates, Proceedings of BRAB Conference, 'Housing and Building in Hot-Humid and Hot-Dry Climates', Report No. 5, Washington D.C.

Ballantyne, E. R. (1967) Solar Tables and Diagrams for Building Designers, Proceedings of CIE Intersessional Conference at University of Newcastle-upon-Tyne in April 1965, Bouwcentrum, Rotterdam.

(1973) Building Design and Solar Energy, Build. International, 6(5), 471-494.

British Admiralty (1957) The Nautical Almanac and Astronomical Ephemeris for the Year 1959, HMSO, London.

Buchberg, H. and Naruishi, J. (1967) On the Importance of Radiation Exchange in the Amelioration of Thermal Stress in Enclosures, International Journal of Biometeorology, 11 (1), 59-78.

Cain, A., Afshar, F. and Norton, J. (1975) Evolution of the Courtyard House, Architectural Design, 45 (4), 210-211.

Cornell, P. H. (1957) Architecture in the Tropics, Proceedings of the Symposium on 'Design for Tropical Living', Durban.

Danby, M. (1973) The Design of Buildings in Hot-Dry Climates and the Internal Environment, Build International, 6 (1), 55-76.

Deering, R. B. (1953) Technology of the Cooling Effect of Trees and Shrubs, Proceedings of BRAB Conference, 'Housing and Buildings in Hot-Humid and Hot-Dry Climates', Report No. 5, Washington D.C.

Degelman, L. O. (1966) The Development of a Mathematical Model for Predicting Solar Heat Gains Through Building Walls and Roofs, Better Building Report No. 6.

Department of Scientific and Industrial Research (1970) Some Principles of Design for Warm Climates, Overseas Building Notes No. 71.

Drysdale, J. W. (1953) Heat Capacity and Distribution of Mass in the Design of Buildings for Hot Climates, Proceedings of BRAB Conference, Report No. 5, Washington D.C.

Dunham, D. (1960) The Courtyard House as a Temperature Regulator, The New Scientist, 8 (199), 663-666.

El Dars, M. Z. and Said, S. Z. (1972) Libyan Court Houses, Bulletin of the Faculty of Engineering, University of Libya.

Fanger, P. O. (1973) Thermal Evironments Preferred by Man, Build International, 6 (1), 127-141.

Fathy, H. (1970) (Architecture in the Middle East : Past, Present and Future), A Lecture at the Beirut Arab University, Beirut, (Text in Arabic).

(1972) The Arab House in the Urban Setting : Past, Present and Future, The Fourth Carreras Arab Lecture of the University of Essex, Longman.

Fitch, J. M. (1972) American Building : The Environmental Forces that Shape It, Houghton Mufflin Company, Boston.

Gagge, A. P., Stolwijk, J. A. J. and Hardy, J. D. (1967) Comfort and Thermal Sensations and Associated Physiological Responses at Various Ambient Temperature, Environmental Research, 1 (1), 1-20.

Gagge, A. P. (1969) Man, His Environment and His Comfort, Heating, Piping and Air Conditioning Engineering, 41 (1).

Gebhart, B. (1959) A New Method for Calculating Radiant Exchanges, ASHRAE Transactions, 65, 321-332.

Givoni, B. (1969) Man, Climate and Architecture, Elsevier Publishing Company Limited, Amsterdam-London-New York.

(1974) Buildings for Hot Climates, Building Research and Practice, 2 (6), 336-343.

Gupta, C. L. (1970) Heat Transfer in Buildings - A Review, Architectural Science Review, 13 (1), 1-10.

Hardy, A. C. and O'Sullivan, P. E. (1967) The Building - A Climatic Modifier, Heating and Ventilating for a Human Environment, Institute of Mechanical Engineers, 182, paper 13, 40-46.

Heron, W. (1957) The Pathology of Boredom, Scientific American, 196 (1), 52-56.

Hopkinson, R. G. (1963) Architectural Physics : Lighting, HMSO, London.

Johnson, F. (1954) The Solar Constant, Journal of Meteorology, 11 (6), 431-439.

Koenigsberger, O. H., Ingersoll, T. G., Mayhew, A. and Szokolay, S. V. (1974), Manual of Tropical Housing and Building - Part One : Climatic Design, Longman.

Köppen, W. and Geiger, R. (1936) Handbuch der Klimatologie, Berlin.

Lippsmeier, G. (1969) Building in the Tropics, Verlag Georg D.W. Callwey, Munchen.

Liu, B. and Jordan, R. C. (1960) The Interrelationship and Characteristic Distribution of Direct, Diffuse and Total Solar Radiation, Solar Energy, 4 (3), 1-19.

Macintosh, D. (1973) The Modern Courtyard House, Lund Humphries, London.

Mahoney, C. T. (1969) The Application of Thermal Comfort Standards to a Building Programme, Proceedings of the Symposium on 'Environmental Physics as Applied to Buildings in the Tropics', Central Building Research Institute, Roorkee.

McHarg, I. L. (1957) The Court House Concept, Architectural Record, September , 193-201.

Meteorolgical Department (1968) Climatological Normals for United Arab Republic up to 1960, Ministry of Military Production, Cairo.

Moon, P. (1940) Proposed Standard Solar Radiation Curves for Engineering Use, Journal of Franklin Institute, 230 (5), 583-617.

Oakley, D. (1961) Tropical Houses : A Guide to their Design, B. T. Batsford Limited, London.

Olgyay, A. (1953) Solar Control and Orientation to Meet Bioclimatic Requirements, Proceedings of BRAB Conference, 'Housing and Building in Hot-Humid and Hot-Dry Climates', Report No. 5, Washington D.C.

Olgyay, V. (1962) Bioclimatic Evaluation Method for Architectural Application, Proceedings of the Second International Bioclimatological Congress at London in September 1960.

(1963) Design with Climate-Bioclimatic Approach to Architectural Regionalism, Princeton University Press.

(1967) Bioclimatic Orientation Method for Buildings, International Journal of Biometeorology, 11 (2), 163-174.

(1969) Solar Climate, Proceedings of the Symposium on 'Environmental Physics as Applied to Buildings in the Tropics', CBRIE, Roorkee.

Parmelee, G. V. (1954) Irradiation of Vertical and Horizontal Surfaces by Diffuse Solar Radiation from Cloudless Skies, ASHVE Transactions, 60, 341-358.

Porter, R. (1970) A School Course in Vectors, G. Bell and Sons Limited, London.

Rao, K. R. and Seshadri, T. N. (1961) Solar Insolation Curves, Indian Journal of Meteorology and Geophysics, 12 (2), 267-272.

Rapoport, A. (1969) House Form and Culture, Prentice Hall, New Jersey.

Rapp, G. M. (1953) Performance and Properties of Materials in Hot Climates, Proceedings of BRAB Conference 'Housing and Building in Hot-Humid and Hot-Dry Climates', Report No. 5, Washington D.C.

Raychaudhuri, B. C., Jain, S. P. and Yadva, K. G. (1964) Thermal Characteristics of Unconditioned Insulated Masonry Buildings in Hot Arid Regions, International Journal of Biometeorology, 8 (2), 137-145.

Richard, S. J. (1957) Climatic Control by Building Design, Proceedings of the Symposium on 'Design for Tropical Living', Durban.

Robinson, N. and Peleg, M. (1960) Direct Solar Radiation on and Inside Buildings, Proceedings of the 2nd International Bioclimatological Congress at London.

Robinson, N. (1966) (Editor) Solar Radiation, Elsevier Publishing Company, Amsterdam-London-New York.

Roux, A. J. A. (1951) A Method of Expressing Climatic Data and the Use of These Data in the Design of Buildings, Series D.R.093, NBRI, Pretoria.

Ryd, H. and Wyon, D. (1970) Methods of Evaluating Human Stress Due to Climate, Document D6, National Swedish Building Research, Stockholm.

Saini, B. S. (1962) Housing in the Hot Arid Tropics, Architectural Science Review, 5 (1), 3-12.

(1973) Building Environment - An Illustrated Analysis of Problems in Hot Dry Lands, Angus and Robertson, London.

Schoenauer, N. and Seeman, S. (1962) The Court-Garden House, McGill University Press, Montreal.

Shafey, F. (1970) (History of Islamic Architecture and Arts), Vol. 1, Cairo, (Text in Arabic).

Sharma, M. R. and Pal, R. S. (1965) Interrelationships between Total, Direct and Diffuse Solar Radiation in the Tropics, Solar Energy, 9 (4), 183-192.

Sparrow, E. M., Gregg, J. L., Szel, J. V. and Manos, P. (1961) Analysis, Results, and Interpretation for Radiation Between Some Simply-Arranged Gray Surfaces, Journal of Heat Transfer, Transactions of the ASME, 83C (2), 207-214.

Sparrow, E. M. (1963) A New and Simpler Formulation for Radiative Angle Factors, Journal of Heat Transfer, Transactions of the ASME, 85C (2), 81-88.

Soliman, K. H. (1972) The Climate of the United Arab Republic, In World Survey of Climatology, Vol. 10, Chapter 3, Elsevier Publishing Company, Amsterdam-London-New York.

Spencer, J. W. (1965 a) Calculation of Solar Position for Building Purposes, Technical Paper No. 14, Division of Building Research, CSIRO, Australia.

(1965 b) Estimation of Solar Radiation in Australasian Localities on Clear Days, Technical Paper No. 15, Division of Building Research, CSIRO, Australia.

Stephenson, D. G. (1965) Equations for Solar Heat Gain through Windows, Solar Energy, 9 (2), 81-86.

Threlkeld, J. L. and Jordan, R. C. (1958) Direct Solar Radiation Available on Clear Days, ASHAE Transactions, 64, 45-68.

(1963) Solar Irradiation of Surfaces on Clear Days, ASHRAE Transactions, 69, 24-36.

Tropical Advisory Service (1966) Climatic Design, Report prepared for the Ministry of Public Building and Works, London.

U.N. Department of Economic and Social Affairs (1971) Design of Low-Cost Housing and Community Facilities, Vol. 1 - Climate and House Design, U.N. Publication, New York.

Valko, P. (1968) Radiation Load on Buildings of Different Shape and Orientation Under Various Climatic Conditions, Proceedings of the WMO/WHO Symposium on Urban Climates and Building Climatology, Technical Note No. 109, Brussles.

(1972) The Effect of Shape and Orientation on the Radiation Impact on Buildings, Proceedings of the CIB/WMO Colloquium on Building Climatology, Vol. 3, Stockholm.

Van Deventer, E. N. and Dold, T. B. (1963) Some Initial Studies on Diffuse Sky and Ground Reflected Solar Radiation on Vertical Surfaces, Biometeorology II.

(1971) Climatic and Other Design Data for Evaluating Heating and Cooling Requirements of Buildings, CSIR Research Report 300, National Building Research Institute, Pretoria.

Van Straaten, J. F. and Van Deventer, E. N. (1964) The Functional Aspects of Building Design in Warm Climates with Particular Reference to Thermal Ventilation Considerations, International Journal of Biometeorology, 8 (2), 155-163.

Van Straaten, J. F., Lotz, F. J. and Van Deventer, E. N. (1969) The Sun and the Design of Buildings for Tropical Climates, Proceedings of the Symposium on Environmental Physics as Applied to Buildings in the Tropics, Vol. 2, CBRIE, Roorkee.

Wiebelt, J. (1965) Engineering Radiation Heat Transfer, Holt, Rinehart and Winston, New York-Chicago-San Francisco-Toronto-London.

Wyon, D. P. (1973) The Role of the Environment in Buildings Today : Thermal Aspects (Factors Affecting the Choice of a Suitable Room Temperature), Build International, 6 (1), 39-54.

(1974) Environmental Comfort - An Appraisal of Current Criteria and Future Trends, Proceedings of the Conference on Integrated Environment in Building Design, Nottingham.